Author:
Simpson, Anna

Title:
Glucose sensing and autonomic projections in Corticotrophin releasing neurons of the paraventricular hypothalamus

Glucose sensing and autonomic projections in Corticotrophin releasing hormone neurons of the paraventricular hypothalamus

Anna Katherine Simpson

A dissertation submitted to the University of Bristol in accordance with the requirements for award of the degree of PhD in the Faculty of Life Sciences

School of Physiology, Pharmacology and Neuroscience

Submitted September 2018 .

Word count 58,115

Abstract

Insulin induced hypoglycaemia is a significant cause of morbidity and mortality in people with diabetes, and commonly limits tight glycaemic control. An additional challenge is the loss of the normal counterregulatory response to hypoglycaemia over time in many patients, which reduces their ability to sense and respond to hypoglycaemia and can result in more frequent/severe hypoglycaemia. In addition, failure of the counterregulatory response is accelerated by recurrent hypoglycaemia. The mechanisms underlying this phenomenon remain incompletely understood, but one contributor is reduction of sympatho-adrenal responses to hypoglycaemia, originating in the central nervous system.

Novel techniques including the use of genetically modified mice now allow more detailed investigation of neuronal subtype connectivity and responses to hypoglycaemia. This thesis uses a mouse expressing Cre recombinase under the control of the corticotrophin releasing hormone (CRH) promoter to investigate the role of CRH PVN neurons in more detail. CRH neurons of the PVN are well placed to influence responses to hypoglycaemia, as they receive inputs from multiple central and peripheral centres providing information on glycaemic and overall metabolic state, and have outputs via the pituitary and (as shown in this thesis) the sympathetic outflow centres of the brainstem and spinal cord. In addition, data shown here presents the first evidence that a subset of CRH PVN neurons are able to directly sense changes in local glucose levels in the PVN, becoming activated when glucose levels fall. This represents a novel glucose sensing population of the CNS, which may have an important role to play in modulating the counterregulatory response to hypoglycaemia. Finally, data is presented of a model of recurrent hypoglycaemia resulting in an expansion of this glucose sensing CRH PVN population, which could represent a means by which these cells contribute to the development of counterregulatory failure following recurrent episodes of hypoglycaemia.

Dedication and Acknowledgements

This thesis is dedicated to my husband Charlie, and our sons Emrys and Gwion. Charlie has been incredibly supportive both emotionally and with helpful practical advice, tips and common sense. Emrys has provided a much appreciated alternative perspective on the world and a change of scene, and Gwion was the spur to getting this thesis submitted- shortly after his arrival!

I would also like to thank Tony Pickering, my supervisor for his patience and support, and especially for being so efficient and understanding of the need for rapid feedback whilst I was writing this. Thanks are also due to Nina Balthasar, who sadly was not able to continue to supervise me for the whole of this PhD, but who has continued to provide valuable advice and perspectives. Thanks also go to Mike Ashby for his generous donation of GCaMP6f mice, allowing me to use his calcium imaging system, and his time discussing the data obtained.

The whole membership of E27a office have leavened this experience with laughter, commiserated on the bad days and provided endless tea and biscuits. In particular I would like to mention Anna Sales for her much needed assistance in getting Matlab to do what I wanted, and Stefan Hirschberg for advice on all things involving histology and image processing.

I would like to thank my parents, my sister and my parents in law; Duncan, Caroline, Fiona, Christopher and Sarah for their generosity in helping out with life at home so that work could be done. It would have been impossible without you.

Author’s declaration

I declare that the work in this dissertation was carried out in accordance with the requirements of the University's Regulations and Code of Practice for Research Degree Programmes and that it has not been submitted for any other academic award. Except where indicated by specific reference in the text, the work is the candidate's own work. Work done in collaboration with, or with the assistance of, others, is indicated as such. Any views expressed in the dissertation are those of the author.

SIGNED: ….  ... DATE:.....14.09.2018.....

Table of Contents

List of Figures

List of Tables

List of Abbreviations

AC anterior commissure
aCSF artificial cerebrospinal fluid
ACTH adrenocorticotropic hormone
AgRP agouti related peptide
AMPA α-amino-3-hydroxy-5-methyl-4-isoxazolepropionic acid
AMPK AMP-kinase
AP action potential
AP-1 activator protein 1
ARC arcuate nucleus
ATP adenosine triphosphate
BAC bacterial artificial chromosome
BAPTA 1,2-bis(o-aminophenoxy)ethane-N,N,N’,N’-tetraacetic acid
BLA basolateral amygdaloid nucleus
BNST bed nucleus of the stria terminalis
CAM kinase IV
CCK cholecystokinin
CEA central amygdala
CFTR Cystic fibrosis transmembrane conductance regulator
cGMP cyclic GMP
CHAT Choline Acetyltransferase
CNQX cyanquixaline (6-cyano-7-nitroquinoxaline-2,3-dione)
CNS Central nervous system
CREB cAMP response element binding protein
CRH Corticotrophin releasing hormone
CRTC2 CREB regulated transcription coactivator 2
CT control
D-AP5 D-2-Amino-5-Phosphonovaleric acid
DAPI 2-(4-Amidinophenyl)-6-indolecarbamidine dihydrochloride
2-DG 2-deoxyglucose
DIO double floxed inverse orientation
DMN dorsomedial nucleus
DMX dorsal motor nucleus of the vagus
EDTA Ethylenediaminetetraacetic acid
EGFP green fluorescent protein
EGTA ethylene glycol-bis(β-aminoethyl ether)-N,N,N',N'-tetraacetic acid
EISB excitatory and inhibitory synaptic blockade
EPSC excitatory postsynaptic current
EPSP excitatory postsynaptic potential
ES embryonic stem
5HT serotonin
GABA gamma-aminobutyric acid
GE glucose excited
GECI glucose excited calcium indicator
GH growth hormone
GHRH growth hormone releasing hormone
GI glucose inhibited
GLUT-1 glucose transporter 1

GLUT-2 glucose transporter 2
GM genetically modified
GnRH gonadotrophin releasing hormone
HAAF Hypoglycaemia associated autonomic failure
HPA hypothalamo-pituitary axis
i.c.v intracerebroventricular
i.p intraperitoneal
i.v intravenous
IHC immunohistochemistry
IIH insulin induced hypoglycaemia
IPSC inhibitory postsynaptic current
IPSP inhibitory postsynaptic potential
ISH in situ hybridisation
ITT insulin tolerance test
KO knock out
LC locus coeruleus
LH lateral hypothalamus
MAP kinase mitogen-activated protein kinase
MCH melanin concentrating hormone
Mut mutant
NA numerical aperture
NAmb nucleus ambiguus
NaOH sodium hydroxide
NMDA N-Methyl-D-aspartic acid
NO nitric oxide
NPY neuropeptide Y
NR non-responsive
NTS Nucleus of the solitary tract
P2Y receptor purinergic 2Y receptor
PAG periaqueductal grey
PBN parabrachial nucleus
PCR polymerase chain reaction
PET positron emission tomography
PKA protein kinase A
PKC protein kinase C
PO preoptic area
POMC pro-opiomelanocortin
PSNS parasympathetic nervous system
PVN Paraventricular hypothalamus
RH recurrent hypoglycaemia
RIA radioimmunoassay
rTaq Taq polymerase
RVLM rostral ventrolateral medulla
s.c subcutaneous
SA spontaneously active
SF1 steroidogenic factor-1
SGLT sodium-glucose co-transporter
SH single hypoglycaemia
SNS sympathetic nervous system

SPN sympathetic pre ganglionic neuron
T1DM type 1 diabetes mellitus
T2DM type 2 diabetes mellitus
3V third ventricle
TH tyrosine hydroxylase
TRH thyrotropin releasing hormone
TrH tryptophan hydroxylase
TSH thyroid stimulating hormone
TTX tetrodotoxin
VMN ventromedial nucleus
VTA ventral tegmental area
WT wild type
YAC yeast artificial chromosome
ZI zona incerta

Chapter 1 Introduction

This thesis explores the role of corticotrophin hormone releasing (CRH) neurons of the paraventricular nucleus (PVN) in the context of their role in generating compensatory responses to hypoglycaemia and connections to autonomic outflow areas of the central nervous system. This chapter will set out the background underpinning the experiments carried out during this thesis. In particular, the clinical context of the work will be addressed. The physiology and pathophysiology of responses to hypoglycaemia will then be outlined. An overview of the role of the PVN and CRH neurons in particular will be presented, and the evidence for a role for CRH neurons in responses to hypoglycaemia will be assessed. An outline of some of the specific techniques employed in the thesis follows, focussing particularly on more recently developed experimental techniques including targeted genetic modifications. Following this review of the literature, the overall hypotheses and aims for this thesis will be presented.

1.1 Glycaemic control is essential for health

Glucose is essential for mammalian life, as the main fuel for respiration to provide energy for cells, and is obtained both directly from dietary intake and also synthesised from protein and fat. Storage of glucose as glycogen provides a rapidly released store of glucose in times of scarcity, and further synthesis from fat and protein can also be initiated. In health, the body maintains glucose levels within tight limits, with blood levels maintained at 4-5.9mmol/L in the pre-prandial state and less than 7.8mmol/L two hours after a meal. Glucose is an essential fuel for the body, and particularly the brain, which has a very limited capacity to utilise alternative sources of energy. The major regulatory hormones are insulin and glucagon released from the pancreas, with the sensitivity of peripheral tissues to insulin also playing an important role. Insufficient insulin release and/or insulin resistance leads to failure of glucose homeostasis (resulting in diabetes mellitus), causing significant morbidity and mortality in affected individuals.

The incidence of both type 1 diabetes (T1DM) and type 2 diabetes (T2DM) is increasing worldwide (Mathers and Loncar, 2006, Patterson et al., 2009). The prevalence of

diabetes in the UK in 2016-17 was almost 3.7 million (DiabetesUK, 2017) and is projected to rise above 5 million by 2025. Prevalence is increasing even more rapidly in low and middle income countries. The World Health Organisation predicts that diabetes will be the seventh leading cause of death worldwide by 2030 (Mathers and Loncar, 2006).

1.2 Hypoglycaemia- a common and significant complication of insulin administration in diabetes mellitus

Since the landmark discovery of insulin by Banting and Best (1922), huge steps have been made in improving the care of diabetic patients (Tibaldi, 2012). However, although insulin is life preserving, iatrogenic hypoglycaemia due to insulin remains an unresolved and significant adverse effect for many patients. Morbidity and mortality arising from hypoglycaemia is significant. A UK study of patients aged 20-49 with T1DM ascribed 18% (170/949) of male and 6% (57/949) of female deaths to severe hypoglycaemia over a 25 year period (Laing et al., 1999). It is a greatly feared complication for many patients, and frequently limits the degree of glycaemic control which can be achieved, leading to increased risks of long term diabetic complications. Whilst T1DM patients have always been at significant risk, the increasing use of insulin in T2DM (as well as the oral hypoglycaemic drugs- sulphonylureas and glinides), means that larger numbers of these patients are also at risk.

Hypoglycaemia can be divided into mild and severe episodes, where mild events can be self-treated by the patient, and severe events require assistance to resolve. Estimates of the incidence and prevalence of hypoglycaemic episodes in the literature vary widely depending on the method of data collection, the definitions used and the duration of the study. In general, an annual prevalence of 30–40% and an annual incidence of 1.0–1.7 episodes per diabetic patient per year are often quoted for T1DM (Frier, 2009). In a subsequent review, Frier (2014) summarised multiple studies between 1990 and 2014 examining the incidence of severe hypoglycaemia. The incidence of events ranged from 0.2-3.2 episodes per patient per year, with between 3 and 46% of patients being affected. For patients with T2DM, the incidence was 0.1-0.7 events per patient per years and 3-25% of patients were affected. It is important to realise that hypoglycaemic

episodes are not spread evenly across the whole population of patients with diabetes; the majority of events are experienced by a subset of patients (for example, 5% of patients experienced 54% of events (Pedersen-Bjergaard et al., 2004)). Hence any estimate of whole population incidence and prevalence will underestimate the effect on the lives of the individuals who do experience hypoglycaemic episodes (and overestimate it in the whole population).

The UK hypoglycaemia study group is of particular interest as it compared different subgroups of both T1DM and T2DM patients with respect to duration of treatment and treatment modality. Unsurprisingly, T1DM of longer duration (>15 years compared to <5 years) was associated with increased prevalence of hypoglycaemic events (3.2 vs 1.1) and a greater proportion of patients were affected (46% vs 22%). This also held true for T2DM, with patients on insulin >5years experiencing 0.7 severe hypoglycaemic events per patient per year with 25% of patients affected, compared to 0.2 and 7% for those on insulin for <2 years. Interestingly, sulphonylureas were also shown to cause a number of severe hypoglycaemic events in this study (0.1 events per patient per year, affecting 7% of patients) (U.K.HypoglycaemiaStudyGroup, 2007).

Collecting data on mild episodes is often less reliable as these are poorly recalled, and may not be recognised on every occasion on which they occur. Mild episodes have been reported as occurring around 1-2 times per week in T1DM and 0.3-0.7 times per week in insulin treated T2DM (Frier, 2014). Continuous glucose monitoring studies can give a more accurate indication of the overall frequency of hypoglycaemic episodes. Studies have revealed a much higher occurrence rate for nocturnal hypoglycaemic episodes than was previously recognised (Allen and Frier, 2003). Continuous glucose monitoring is also of value in patients who are unable to detect hypoglycaemic episodes (hypoglycaemia unawareness), both to gain accurate information about frequency of hypoglycaemic events and to assist in avoiding hypoglycaemia (Choudhary et al., 2013).

1.2.1 Risk factors for hypoglycaemia

Duration of insulin treatment is a key risk factor for hypoglycaemia as described above (U.K.HypoglycaemiaStudyGroup, 2007). Other risk factors include

- Greater stringency of control of blood sugars
- Extremes of age, both young and old
- Cognitive impairment (Feil and Pogach, 2014)
- Previous episodes of hypoglycaemia
- Renal impairment
- Hypoglycaemia unawareness and autonomic failure
- Absence of c-peptide indicating absolute loss of pancreatic insulin

(Morales and Schneider, 2014, Frier, 2014)

The increasing incidence of diabetes and exogenous insulin use worldwide is certainly leading to increasing issues related to hypoglycaemia and its consequences.

1.2.2 Sequelae of hypoglycaemia

1.2.2.1 Physiological

The effects of hypoglycaemia can be divided into those directly arising from the low blood sugar (neuroglycopenic symptoms and signs), and those resulting from the physiological response to hypoglycaemia (autonomic). Neuroglycopenic symptoms include cognitive impairment, confusion, drowsiness, odd behaviours, seizures and loss of consciousness. Autonomic effects include sweating, palpitations, shaking and hunger.

Cardiac events are of particular concern with regard to morbidity and mortality. In particular arrhythmias associated with hypoglycaemic episodes have been linked to 'dead in bed' syndrome (Tattersall and Gill, 1991). The mechanisms underlying this are thought to include a reduction of plasma potassium levels secondary to increased epinephrine levels. ECG changes associated with hypoglycaemia include prolonged QT interval, which predisposes to tachyarrythmias which may be fatal (Robinson et al., 2003). ST and T wave changes, and symptoms of cardiac ischaemia have also been associated with hypoglycaemia (Desouza et al., 2003). Furthermore, autonomic activation will increase the likelihood of tachycardia and hypertension, reducing coronary perfusion, and this may lead to ischaemia, especially in the context of pre-existing coronary artery disease.

Coma associated with hypoglycaemia is thought to occur in up to 25% of severe hypoglycaemic episodes (Frier, 2014). Seizures and coma are fortunately fully reversible if treated promptly, and are not believed to be associated with longer term sequelae. A lesser degree of acute cognitive impairment during the hypoglycaemic episode is more common and insidious. This effect has been extensively studied. In general, patients appear to suffer from reduced speed at performing tasks before accuracy is lost (Warren and Frier, 2005). Multitasking and complex decision making are amongst the earliest domains to be affected. It is important to note that full return of cognitive function may be delayed by up to an hour and a half after restoration of normoglycaemia (Zammitt et al., 2008). In addition, with increasing age, the gap between onset of warning symptoms and onset of cognitive impairment narrows, and this can significantly impact on the ability of an individual to recognise and self-treat the episode (Matyka et al., 1997). Links have been made between hypoglycaemia and longer term impairment of cognitive function in the very young (<5 years) and the very elderly (Asvold et al., 2010, Feinkohl et al., 2014). Deliberate insulin overdose or very protracted hypoglycaemia can result in irreversible neurological damage and death at any age.

Other neurological sequelae, including impairment of normal vision, balance, and coordination can lead to falls and injuries and other accidents. Drivers experiencing hypoglycaemia are of particular concern (Inkster and Frier, 2013).

1.2.2.2 Psychological

Fear of hypoglycaemia is a common issue for patients and their relatives and can significantly impact their ability to achieve good glycaemic control (Wild et al., 2007). Patients experiencing hypoglycaemic episodes tend to report poor quality of life, greater anxiety about their condition and poorer general health (Lundkvist et al., 2005, Alvarez-Guisasola et al., 2010). Hypoglycaemic episodes can also have a direct adverse effect on mood (McCrimmon et al., 1999).

1.3 The normal physiological response to hypoglycaemia

The normal counter-regulatory response to hypoglycaemia involves ceasing insulin secretion, release of glucagon, autonomic activation and cortisol and growth hormone secretion all leading to the liberation of glucose from tissues (Figure 1.1). There is no

direct glucose detection system mediating conscious awareness of hypoglycaemia. Awareness of hypoglycaemia is dependent on autonomic activation and the symptoms caused by this, and promotes food seeking. These compensatory systems involve a significant degree of redundancy, which is protective in the event of failure of any single part of the physiological response.

It is important to note that hypoglycaemia is only very rarely seen in healthy individuals in the absence of therapeutic insulin use. Insulinoma is probably the most common example which would be found spontaneously (incidence 4 per million per year (Service et al., 1991)). Other candidates in a healthy individual include drugs, factitious disorders, extreme exercise and ketosis (Service, 1995). The physiological systems responding to insulin induced hypoglycaemia have therefore evolved to respond to slower falls in glucose, for example in the context of fasting, extreme exercise, starvation and severe infection, and are not necessarily best suited to responding to rapid falls in glucose due to excess exogenous insulin.

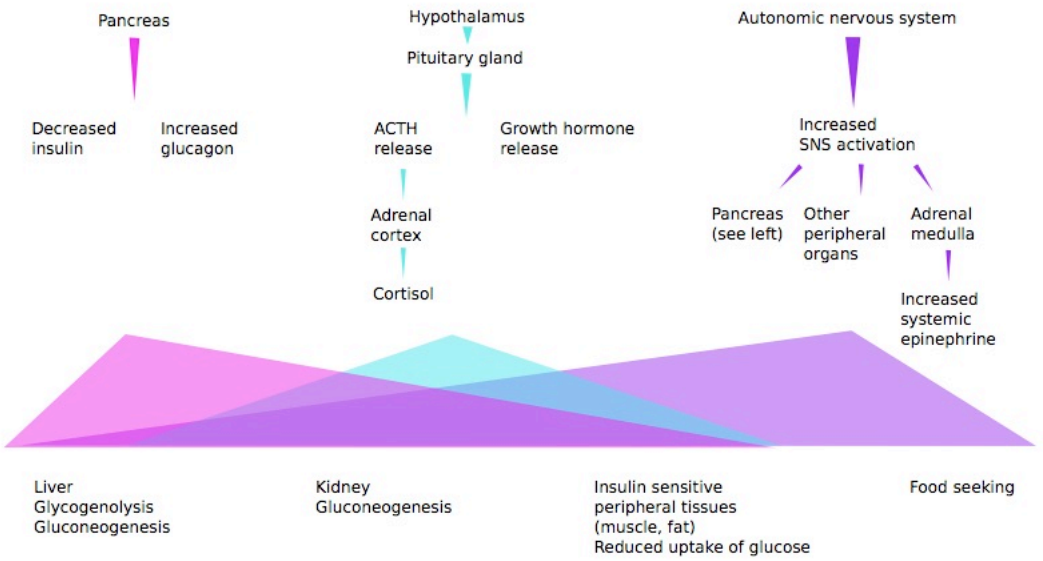

Figure 1.1 The counterregulatory response to hypoglycaemia

As discussed in the text, these is considerable redundancy in the system, with the final effects of falling insulin, rising glucagon, cortisol, growth hormone and epinephrine/norepinephrine all leading to liberation of glucose from the liver, gluconeogenesis in liver and kidney, and reduced uptake in peripheral tissues. Sympathetic autonomic activation, both cholinergic and adrenergic, also contributes to these effects. Food seeking is triggered by the SNS and epinephrine release, but not by other mechanisms illustrated here.

Patients become aware of hypoglycaemia due to sympathetic/adrenal activation (adrenergic-tachycardia, tremor, anxiety; cholinergic-sweating, paraesthesia, hunger) and seek food to restore glucose levels (Cryer, 2005, Towler et al., 1993). In a study on healthy human volunteers, autonomic blockade reduced the hypoglycaemic symptoms experienced by 70%, suggesting that the first signs of hypoglycaemia awareness are via this pathway (Towler et al., 1993). Interestingly, bilateral adrenalectomy does not abolish hypoglycaemia awareness due to autonomic symptoms, suggesting that the main pathway is neural rather than due to circulating epinephrine and norepinephrine (DeRosa and Cryer, 2004). In the absence of a response from the sympathetic nervous system and/or epinephrine release from the adrenal medulla, patients lose their early warning of hypoglycaemia, until neuroglycopenic symptoms commence.

The triggering of the various counterregulatory responses occurs at differing degrees of severity of hypoglycaemia, as illustrated in table 1.1. The glucose values quoted are not absolute, but context dependent and subject to being reset. For example, a subject with very poor glycaemic control may reset the values quoted to higher levels (Boyle et al., 1988), and very tight glycaemic control can lower the glucose level at which counterregulation occurs (Amiel et al., 1988).

Table 1.1: Triggers to counterregulatory hormone release adapted from Cryer (1997a)

Blood glucose (mmol/L) for a healthy volunteer	**Compensatory mechanism**	**Effects**
4.5	Insulin no longer released Parasympathetic nervous system activation Glucagon levels start to rise in response to PSNS activation and loss of inhibition by glucose	Increased glucose production- hepatic and renal Reduced uptake of glucose by insulin sensitive tissues- muscle, fat
3.6-3.8	Increased glucagon secretion Sympathetic nervous system activation Epinephrine/norepinephrine secretion (act within minutes) Cortisol and growth hormone secretion (act over hours)	Glycogenolysis, Gluconeogenesis- hepatic and renal Reduced uptake of glucose in periphery- muscle, fat Alternative fuel generation- ketones, alanine, glutamine Conscious awareness of symptoms from sympathetic activation promotes food seeking
3	Early neuroglycopenic symptoms	Food seeking
2.6	Impaired cognition	Impairs ability to self-treat

1.4 Pathophysiology of hypoglycaemia associated autonomic failure (HAAF)

Recurrent episodes of hypoglycaemia can cause failure of the counter-regulatory response, defined as hypoglycaemia associated autonomic failure (McCrimmon, 2009). The ability of a diabetic patient to respond to hypoglycaemia is already, by definition, impaired due to their (absolute or relative) lack of endogenous insulin. If the amount of insulin (absolute or relative) in the body is low, then there will be no benefit in attempting to reduce levels (floor effect), which impairs counter-regulation from the very beginning. Subsequently, there is an incremental loss of the ability to release glucagon from the pancreas, which typically develops within 5 years of commencing insulin treatment in TIDM (Mokan et al., 1994). The underlying cause of the loss of glucagon release remains somewhat unclear, but is thought to be related to the loss of local insulin signalling from the beta cells of the pancreas which tonically inhibits glucagon release from the alpha cells in health (Banarer et al., 2002, Cryer, 2005). This leaves patients dependent on the remaining counterregulatory hormones, especially epinephrine and norepinephrine from the sympatho-adrenal system. However, the sympatho-adrenal response is also impaired in many diabetic patients, especially with longer durations of disease (Cryer, 1997a, Cryer, 2005). The reduction or loss of the sympatho-adrenal response to hypoglycaemia is functional rather than absolute, and is not directly linked to autonomic neuropathy per se. It appears that the plasma glucose level for sympatho-adrenal activation is context dependent, and prior episodes of hypoglycaemia can reset the threshold to lower levels of plasma glucose (Amiel et al., 1988, Dagogo-Jack et al., 1993).

In summary, the hormonal profile of a patient with fully developed HAAF will exhibit absent or reduced insulin, glucagon, cortisol, growth hormone, epinephrine and norepinephrine responses to hypoglycaemia. Such patients, with impairment of all the major counterregulatory systems will have both an inability to liberate glucose effectively from peripheral stores, and in addition lack of triggering of warning symptoms which would otherwise promote food intake and resolution of hypoglycaemia. HAAF therefore puts patients at risk of severe and unpredictable episodes of hypoglycaemia. A vicious cycle of worsening hypoglycaemic events can arise

(Cryer, 2005). This effect can be at least partially reversed by relaxation of glycaemic control, but this comes at a cost in the long term related to the complications of hyperglycaemia (Cryer et al., 2003, Dagogo-Jack et al., 1994, Leelarathna et al., 2013)

The concept of HAAF was initially developed from studies in healthy volunteers. A very small number of hypoglycaemic episodes (just one in some cases) are required to recreate the hormonal profile seen in HAAF (Heller and Cryer, 1991, Davis and Shamoon, 1991). Further work has expanded and placed this work in a clinical context. The finding that recent episodes of hypoglycaemia alter the glycaemic threshold at which autonomic activation occurs (such that a lower glucose level is required for activation), and in addition reduce the glucose level at which patients are symptomatically aware of hypoglycaemia, is supportive of this hypothesis (Amiel et al., 1988). In addition, the previously mentioned phenomenon of resolution of HAAF with scrupulous avoidance of hypoglycaemia is highly persuasive (Cryer, 2005). These effects all appear to occur via the restoration of the sympatho-adrenal system because the glucagon responses are not restored in studies in diabetic patients (Cryer, 2001).

1.5 Glucose sensing in the peripheral and central nervous system

In order to effect a response to hypoglycaemia, low glucose levels must first be detected. As for the effector pathways, there is a redundancy in the sensing system, with both peripheral and central sensing of glucose occurring. Peripheral sensors almost all convey information to the central nervous system to engage motor responses. It is likely that the sensing systems developed for different reasons, and are triggered in differing ways.

1.5.1 Role of the peripheral glucose sensors

1.5.1.1 Pancreas

In a healthy individual, the pancreas is a key glucose sensor, with the beta cell long identified as the classical K_{ATP} mediated glucose sensing cell (Figure 1.2), responding to rises in glucose with increased secretion of insulin and to decreases in glucose with a fall in insulin release (Ashcroft and Rorsman, 2004). However, due to beta cell loss, this

system is impaired in all forms of diabetes, and absent in fully developed T1DM and long standing T2DM.

The alpha cells of the pancreas, which are responsible for glucagon release during hypoglycaemia, are also thought to exhibit intrinsic glucose sensing. Glucose inhibition of glucagon release has been suggested to be mediated by voltage *inactivation* of calcium channels during membrane depolarisation due to K_{ATP} channel closure when glucose levels rise (Walker et al., 2011). However, mechanisms which are not intrinsic to alpha cells are probably of greater importance, in particular, sympatho-adrenal activation of the alpha cells is important for glucagon release during hypoglycaemia. The paracrine inhibitory effect of insulin is also of key importance to the glucagon response to hypoglycaemia, and as stated previously, the glucagon response is lost over time in diabetes mellitus patients (Banarer et al., 2002).

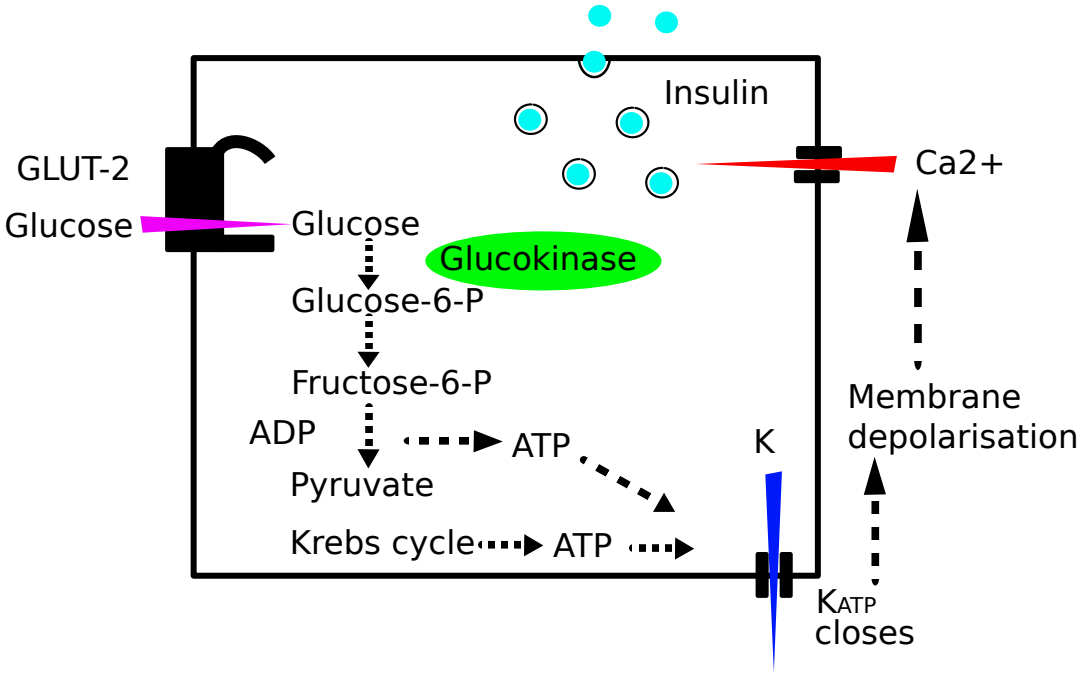

Figure 1.2 K_{ATP} channel dependent glucose sensing in pancreatic beta cell
Glucose enters via GLUT-2 and is metabolised to produce ATP. Increased levels of ATP close K_{ATP} channels, depolarising the cell. Depolarisation opens voltage gated calcium channels. Calcium influx signals exocytosis of insulin.

1.5.1.2 Hepatic portal vein

The portal vein glucose sensors are also important in the detection of hypoglycaemia. Extensive animal work has demonstrated that perfusion of the hepatic portal vein with glucose during whole animal hypoglycaemia significantly decreases epinephrine and norepinephrine responses (42-73% suppression of epinephrine, 42-67% suppression in norepinephrine reported (Hevener et al., 1997, Donovan and Watts, 2014)). This effect is even more pronounced when the superior mesenteric vein is included with suppression of 91% of epinephrine response reported (Saberi et al., 2008). The converse experiment- perfusion of this system with low glucose in a euglycaemic animal, is able to elevate epinephrine and norepinephrine levels (Lamarche et al., 1996). Detection of low glucose appears to require GLUT-2 transport (Burcelin et al., 2000). Experiments perfusing the system with lactate and pyruvate have demonstrated that, similarly to the pancreatic beta cell, metabolism of glucose is necessary for glucose sensing in the portal system (Matveyenko and Donovan, 2006). Sodium-glucose co-transporters have also been demonstrated to be involved in the signalling of satiety by the portal vein glucose sensors, and have been suggested to be important for detection of small changes in glucose levels (<1mM) (Delaere et al., 2012). SGLTs have not so far been investigated for a role in detection of hypoglycaemia. The rate of fall of glucose has been shown to be of importance for portal glucose sensing. In rats with ablation of the portal mesenteric sensors there was no response to a slow fall in glucose, whilst responses to a rapid fall were preserved (Saberi et al., 2008).

The signalling pathway for hypoglycaemia from portal and mesenteric veins appears to be via spinal afferents, and not via the vagus nerve as originally thought (Fujita and Donovan, 2005, Fujita et al., 2007, Barja and Mathison, 1984). The spinal afferents pass via the coeliac/superior mesenteric ganglia to the lower thoracic spinal cord (Barja and Mathison, 1984). Signals are transmitted to the central nervous system via the nucleus of the solitary tract (Adachi et al., 1984) to the lateral hypothalamic area (Shimizu et al., 1983). Vagal signalling does appear to play a role in glucose sensing from the hepatic portal vein, but it appears to be involved in signalling rises in glucose (Niijima, 1989).

1.5.1.3 Carotid body glucose sensors

The carotid body has been suggested as a potential further site of peripheral glucose sensing. Studies in vitro in carotid body slices or cultured cells appear to demonstrate responses to low glucose (Nurse, 2005). However, work in a whole carotid body preparation could not replicate this, and it has been suggested that low glucose in fact sensitises the response of the carotid body to CO_2 (Bin-Jaliah et al., 2004). In vivo studies have also proved inconclusive thus far and the role of the carotid body remains unclear.

1.5.2 Role of the central glucose sensors

The concept of the brain sensing glucose was first put forward in the 1950s (Mayer, 1955). Early work to establish the importance of the CNS in sensing glucose involved perfusion of the whole brain with glucose in a hypoglycaemic whole animal preparation. The counterregulatory response was decreased under these conditions (Biggers et al., 1989). Further infusion or microdialysis experiments targeting specific brain regions were also able to show effects on the whole animal response to hypoglycaemia, for example the infusion of 2-deoxyglucose to the ventromedial nucleus (VMN), which mimics hypoglycaemia, caused activation of the counterregulatory response (Borg et al., 1995). In contrast, application of glucose to the same area in a hypoglycaemic animal blunted counterregulation (Borg et al., 1997).

When considering central glucose sensing, the importance of the blood brain barrier must be taken into account. The microvasculature of the central nervous system is a significant barrier to almost all molecules which would otherwise freely pass between the blood and brain interstitium. The blood brain barrier is protective as it prevents exposure of the brain to potential toxins, cytokines, drugs and infectious agents and in addition aids the maintenance of a more stable interstitial milieu compared to that of blood. The structure of the endothelial cells of brain capillaries, with their tight junctions and additional contributions from pericytes, astrocytes and the basement membrane all create a barrier to free movement of the vast majority of molecules which would otherwise freely diffuse (Abbott et al., 2010). The only molecules which pass freely by diffusion are small gaseous molecule (oxygen, carbon dioxide), and small lipophilic molecules which are not transported back into the blood by active transport

(examples include caffeine and ethanol). All other molecules, including water, ions and nutrients are transported or conducted via specific proteins and channels. The major glucose transporter across the blood brain barrier is GLUT-1, with SGLT-1 also playing a role on the interstitial side of the endothelial cells (Patching, 2017). Therefore most glucose is moved by facilitated diffusion down its concentration gradient (via GLUT1) with a small contribution from secondary active transport (SGLT1). The glucose levels experienced by the majority of CNS cells is lower than those observed in the periphery, and subject to smaller variations when glucose in the blood increases or decreases (Silver and Erecinska, 1994b).

In general, it is thought that most CNS glucose sensors must be able to sense changes in glucose levels which are observed in the CNS interstitium. However, there are a few 'privileged' areas of the brain in which the blood brain barrier is deficient. In these regions, neurons may be exposed to blood glucose levels and so respond to a wider range of levels of glucose. Such areas include the area postrema, the subfornical organ, and the median eminence. In addition, some cells within the CNS are directly apposed to the ventricles, and therefore can respond to CSF glucose levels in a similar fashion. An example would be the tanycytes of the third ventricle (Frayling et al., 2011).

Central glucose sensors are likely to be important for several different functions. The brain is largely reliant on glucose as a metabolic fuel with a respiratory quotient very close to 1.0, and thus accounts for a large proportion of whole body glucose consumption (Cryer, 1997b). In a fasted individual at rest, the brain uses around 60% of the total glucose consumed (Wasserman, 2009). The ability of the brain to use fuels other than glucose is extremely limited. Therefore it is likely that central glucose sensing is designed to act in a protective fashion for the brain to preserve its glucose supply. In addition, the central nervous system plays an important role in many aspects of the counterregulatory response to hypoglycaemia as previously outlined in section 1.3. Finally, information about the overall metabolic status of the body is of importance in the longer term for a wide range of physiological functions, for example fertility (GnRH), thyroid function and circadian rhythms (Burdakov et al., 2005b).

1.5.2.1 Hypothalamus

The hypothalamus was the first CNS area to be identified to contain glucose sensing cells (Oomura et al., 1969). These neurons exhibited distinct responses to increases in glucose levels e.g. glucose-excited neurons increase their firing rate, while glucose inhibited neurons are silenced. Glucose-sensing neurons have subsequently been identified in multiple distinct regions of the hypothalamus, including the arcuate and ventromedial nuclei (Kang et al., 2006, Kang et al., 2004), paraventricular hypothalamus (Melnick et al., 2011) and lateral hypothalamic area (Marston et al., 2011). A degree of heterogeneity in what is defined as a glucose sensitive neuron exists, with criteria for identification including changes in resting potential, action potential frequency, input resistance, calcium levels and combinations of these factors. The glucose concentrations used also vary considerably between studies. In some cases, the response observed appears to follow a dose response curve (Wang et al., 2004), in other cases only a binary response is reported (Melnick et al., 2011). Plasticity has been reported in neuronal responses to glucose with changing environment, e.g. lowered glucose thresholds with recurrent hypoglycaemia in VMN (Song and Routh, 2006).

The mechanisms underlying glucose sensing in the CNS are the subject of much interest. Parallels have been drawn between the pancreatic beta cell and glucose excited neurons (Ashford et al., 1990a, Ashford et al., 1990b). The mechanisms underlying activation of some glucose inhibited neurons have been suggested to involve AMPK, cGMP, and chloride channels (Kang et al., 2004, Murphy et al., 2009a). However, the genetic and molecular mechanisms determining the characteristics of the neuronal glucose-response phenotype remain incompletely understood despite extensive investigations. Further discussion of specific glucose sensing mechanisms and neuronal subtypes will be addressed in Chapter 4, section 4.1.1 and 4.1.4 and Chapter 5, section 5.1.

1.5.2.2 Hindbrain

The hindbrain is the other major area which has been identified in the CNS as being important in sensing and responding to hypoglycaemia. Early work established that the hindbrain can to some extent operate independently of the mid- and fore-brain, by demonstrating that a decerebrate rat preparation, which also removed the hypothalamus, can still mount an effective counterregulatory response to

hypoglycaemia (DiRocco and Grill, 1979). In addition, work by Ritter and colleagues, which involved microdialysis of multiple hypothalamic and hindbrain sites with 5-thioglucose (which mimics hypoglycaemia in a similar fashion to 2-deoxyglucose), showed that hindbrain but not hypothalamic applications were effective in increasing glucose levels and eliciting feeding behaviours (Ritter et al., 2000).

Glucose sensing neurons have been identified in the area postrema (Funahashi and Adachi, 1993), dorsal motor nucleus of the vagus (Kobashi and Adachi, 1995, Balfour et al., 2006), nucleus of the solitary tract (Balfour et al., 2006, Mimee and Ferguson, 2015) and lateral parabrachial nucleus (Flak et al., 2014, Garfield et al., 2014). The precise role of each of these areas is not well understood. However, recent work on the glucose sensitive neurons of the lateral parabrachial nucleus suggests that activation of a subset of these cells, which express cholecystokinin, can cause activation of the counterregulatory response (Garfield et al., 2014). The rostral ventrolateral medulla (RVLM) has also been shown to play a role in activating the counterregulatory response (Ritter et al., 2001, Madden et al., 2006).

1.5.2.3 Non neuronal cells as glucose sensors

It is increasingly appreciated that the glial cells, astrocytes and other 'support' cells of the central nervous system also have important signalling roles to play (Araque et al., 2001). One clear example of this is the restoration of glucagon responses to hypoglycaemia in global GLUT-2 knock out mice which have had GLUT-2 re-expressed only in astrocytes (Marty et al., 2005). The proposed mechanism involves metabolic coupling between these astrocytes and neurons in the NTS/DMX leading to restoration of the ability to sense hypoglycaemia in these regions and alter the autonomic outflow from NTS/DMX to the alpha cells of the pancreas. Both astrocytes and tanycytes have been shown to express many of the key proteins implicated in glucose sensing, including GLUT-2, glucokinase, K_{ATP} channels and the sodium glucose co-transporter type 1 (Steinbusch et al., 2015, Leloup et al., 2016). Glucose sensing also has been demonstrated in tanycytes surrounding the third ventricle (Frayling et al., 2011) and in some astrocyte populations (Lee et al., 2016, McDougal et al., 2013). Tanycytes represent an interesting population as they are situated in close apposition to the ventricular surface, and therefore access the CSF glucose levels, as opposed to that of

the extracellular fluid. These cells also have processes that extend into hypothalamic areas, creating potential anatomical sites for communication with neurons (Elizondo-Vega et al., 2015). The sweet taste receptor has recently been implicated in tanycyte glucose sensing (Benford et al., 2017).

Potential mechanisms by which tanycytes could communicate with neurons include ATP release to act on P2Y receptors (Frayling et al., 2011) and lactate, which can be taken up by neurons using monocarboxylate transporter 2 (Elizondo-Vega et al., 2015, Weightman Potter et al., 2018). The lactate shuttle hypothesis, which suggests that astrocytes supply lactate to neurons, both as a fuel and as a means of signalling energy status, is a long established theory for astrocytic signalling (Pellerin and Magistretti, 1994). In addition, other peptides, for example the endozapines have also been suggested as signalling molecules mediating glucose signalling between astrocytes and neurons (Tonon et al., 2013).

1.6 Putative mechanisms underlying HAAF

1.6.1 Loss of hypoglycaemia awareness

As discussed in section 1.3, awareness of hypoglycaemia appears to derive largely from neurogenic symptoms secondary to cholinergic and adrenergic signalling by the SNS. The evidence for this comes from studies in healthy volunteers. The early symptoms of hypoglycaemia were all suggestive of SNS activation (Towler et al., 1993). Adrenergic blockade alone using phentolamine and propranolol did not alter symptoms. Pan-autonomic blockade using phentolamine, propranolol and atropine reduced the hypoglycaemic symptoms experienced by 70% (Towler et al., 1993). The remaining hypoglycaemic symptoms may, therefore, be due to neuroglycopenia, but could also be residual SNS symptoms due to incomplete blockade. In a further study, evidence that the main pathway is due to activation of the sympathetic nervous system rather than due to circulating epinephrine and norepinephrine is presented, as patients with prior bilateral adrenalectomy can still demonstrate hypoglycaemia awareness due to neurogenic symptoms (DeRosa and Cryer, 2004).

1.6.2 Reduced counterregulatory response to hypoglycaemia

The reasons underlying loss of the insulin and glucagon responses to hypoglycaemia have already been covered in section 1.4. The mechanisms which underlie the failure of the sympatho-adrenal, cortisol and growth hormone response are much less well understood. Whilst a range of mechanisms have been proposed, no single hypothesis has yet emerged with compelling evidence.

1.6.2.1 CNS versus peripheral mechanisms

Given that the effector response is mediated by the CNS for both the sympatho-adrenal and cortisol responses to HAAF, it is clear that the CNS must play some role in failure of these aspects of the counterregulatory response. However, it is possible that the main point of failure could be downstream of these effectors. Interest has focused on the possible role of the adrenal medulla, with reports of reduced epinephrine stores (De Galan et al., 2004), and reduced levels of mRNA for key enzymes involved in epinephrine synthesis (tyrosine hydroxylase and phenylethanolamine N -methyltransferase (Inouye et al., 2005)) after hypoglycaemia, which could result in the observed reduction in epinephrine release. However, it is also entirely possible that all of these effects could be due to reduced activation of the adrenal medulla per se, rather than the cause of the observed effects. This hypothesis cannot explain the observed reductions in sympathetic neural activation or cortisol levels. Overall, it seems more likely that a change within the CNS is responsible for the change in thresholds observed during failure of sympatho-adrenal and cortisol counterregulatory responses.

1.6.2.2 Systemic cortisol elevations as potential causative agents in HAAF

A further hypothesis that has been advanced is that the rise in systemic cortisol which is observed during hypoglycaemia drives the subsequent development of HAAF. This is based upon the finding that cortisol infusion or stimulation of endogenous cortisol with infused ACTH can reduce the sympatho-adrenal response to subsequent hypoglycaemia (Davis et al., 1996). Infusion of $\alpha_{1\text{-}24}$ACTH to stimulate a cortisol rise has a similar effect (McGregor et al., 2002). In addition, patients with primary adrenocortical failure do not appear to develop HAAF (Davis et al., 1997).

However, the levels of cortisol which were required to cause the observed effects have been called into question as being rather higher than observed during cortisol rises due to hypoglycaemia (32-45µg/dL (cortisol or ACTH infusion) versus 26µg/dL (hypoglycaemia)). When healthy volunteers received cortisol infusions designed to reproduce levels comparable to those measured during hypoglycaemia, there was no effect on the sympatho-adrenal response to subsequent hypoglycaemia (Raju et al., 2003). However, this study actually infused cortisol at rather higher levels than originally planned, achieving peak concentrations of ~31 and ~34µg/dL in 2 sets of infusions, and in many ways is therefore comparable to Davis et al. (1996) where the peak plasma concentration of cortisol was 33µg/dL. There were differences between studies with regard to the rapidity of infusion of cortisol and indeed the speed at which hypoglycaemia was induced (both more rapid in the Davis study), which might contribute to the observed differences.

Further evidence that contradicts this hypothesis relates to sleep and hypoglycaemia. It is recognised that hypoglycaemia during sleep contributes to development of HAAF, and it is also known that cortisol responses to hypoglycaemia in sleep are blunted (Cryer, 2005, Cryer, 2004).

1.6.2.3 Increased endogenous beta endorphins

Beta endorphins are known to be released in response to stressful stimuli (Nakao et al., 1979). Investigations in both healthy volunteers (Caprio et al., 1991, Vele et al., 2011) and patients with type 1 diabetes (Caprio et al., 1991, Leu et al., 2009) have shown amelioration of HAAF following delivery of naloxone (opioid antagonist) during a prior episode of hypoglycaemia. This suggests that the development of some components of HAAF could be mediated by an opioid related mechanism. However, a study using naltrexone (a longer acting, orally delivered opioid antagonist) alongside an initial episode of hypoglycaemia caused only a modest increase in epinephrine response to subsequent hypoglycaemia and no effect on other hormones (Naik et al., 2017). Work by Carey and colleagues (2017) examined the effect of an infusion of morphine (or saline control) on day 1 on the response to a stepped hypoglycaemic clamp on day 2. They report a 30% reduction in the epinephrine response to hypoglycaemia after morphine compared to a saline infusion, and a reduction in hypoglycaemia symptoms score. There

was no difference in the glucagon or norepinephrine response between the 2 groups in this study. Taken together, these data are suggestive of a contributory role of opioids in the development of HAAF.

It is not clear from these studies whether opioids acting centrally or peripherally are responsible for the observed effects, or what the underlying mechanism might be. Peripherally, the adrenal medulla secretes beta endorphin as well as epinephrine/norepinephrine (Cheng et al., 2001). Infusion of beta endorphin in streptozotocin induced diabetic rats has been shown to directly increase peripheral glucose uptake and reduce hepatic gluconeogenesis, which would exacerbate hypoglycaemia (Cheng et al., 2002). A negative feedback action of beta endorphin to reduce epinephrine release from the adrenal medulla has also been proposed (Dermitzaki et al., 2001). However, there was no change in beta endorphin levels during naloxone infusion in the studies above, which does not support a negative feedback role (Leu et al., 2009, Vele et al., 2011, McCrimmon, 2011). In addition, morphine infusion had no direct effect on glucose levels and effects were only observed during subsequent hypoglycaemia (Carey et al., 2017).

With regard to the CNS, naloxone and morphine both readily cross the blood brain barrier. Opioid receptors have been reported to be expressed widely in both the hindbrain and hypothalamus (Zhang et al., 1996, Zheng et al., 2005, Mansour et al., 1994). Neurons in the VMN are inhibited by opioids (Zhang et al., 1996). In addition, Suda and colleagues report a reduction in CRH mRNA expression and ACTH secretion in response to hypoglycaemia, when beta endorphin is delivered i.c.v (Suda et al., 1992). Further studies are needed to better identify potential mechanisms by which opioids could act centrally at these and other sites in the context of HAAF.

1.6.2.4 Increased availability of glucose or alternative fuels in the brain

A further alternative hypothesis is that prior episodes of hypoglycaemia alter glucose uptake to the central nervous system, making transport more efficient and/or increasing glycogen stores. This would improve the glucose supply to the brain, which would improve energy supplies in the face of future hypoglycaemia, but would also reduce the threshold for sympatho-adrenal activation. It is known that long term hypoglycaemia in

rats (days rather than hours) results in increased GLUT-1 (glucose transporter) expression in cells of the blood-brain barrier (Kumagai et al., 1995). Preserved glucose uptake to the brain in the face of prolonged, between meal, hypoglycaemia has been reported in healthy volunteers and type 1 diabetics (Boyle et al., 1995, Boyle et al., 1994). In these studies, whole brain glucose uptake was calculated from the arteriovenous difference across the brain and cerebral blood flow using the Ketty Schmidt method. However, this evidence does not appear to translate to the acute episodes of hypoglycaemia experienced in diabetic patients. Glucose uptake imaging studies using radiolabelled PET and acute hypoglycaemia have not so far proven supportive of this theory, at least when global uptake of glucose is examined (Segel et al., 2001, de Vries et al., 2003). It is possible that regional changes in glucose uptake could still play a role, but this has not yet been shown.

Alternative fuels for the brain include lactate and acetate (De Feyter et al., 2013, Mason et al., 2006). The concept of the astrocyte-neuron lactate shuttle has been described (Pellerin and Magistretti, 2012), with metabolism of glucose to lactate taking place in astrocytes, which then make lactate available to neurons for ongoing metabolism. Boumezbeur and colleagues (2010) showed that approximately 10% of the brain's metabolic needs could be provided by lactate. Infusion of lactate was observed to cause attenuation of counterregulatory responses and hypoglycaemic awareness in healthy volunteers and patients with type 1 diabetes (Veneman et al., 1994, Maran et al., 2000). A period of exercise to increase lactate levels followed by a hypoglycaemic clamp resulted in increased lactate uptake and oxidation by the brain in type 1 diabetic patients with impaired hypoglycaemia awareness when compared to healthy controls and patients with type 1 diabetes who did not have impaired hypoglycaemia awareness (Wiegers et al., 2017). In an earlier study on patients with type 1 diabetes, De Feyter et al. (2013) found that lactate uptake was increased during hypoglycaemia 5-fold in subjects with type 1 diabetes compared to control subjects, but without increased oxidation. It is thought that increased use of lactate as a fuel source for the brain can be protective in hypoglycaemic conditions, but can also impair the ability of the brain to sense and respond to hypoglycaemia.

Glycogen stores have been shown to increase in the CNS following hypoglycaemia, and 'glycogen supercompensation' has been suggested as a further mediator of reduced counterregulation and delayed detection of hypoglycaemia. Astrocytes are the main source of glycogen within the brain (Brown, 2004), and it is thought that metabolism to lactate within astrocytes may provide fuel to neurons when glucose levels fall. Choi et al (2003) induced hypoglycaemia in anaesthetised rats and measured brain glycogen levels. They showed that glycogen fell during hypoglycaemia, but during the recovery phase glycogen levels were higher than those measured prior to the hypoglycaemic event, i.e supercompensation. Suh et al. (2007) showed that increased levels of glycogen in astrocytes of rats resulted in increased neuronal survival following hypoglycaemia. Therefore, increased availability of glycogen due to supercompensation after hypoglycaemia could contribute to HAAF. However, the total available glycogen store in the CNS is still very small compared to liver or muscle, and increased glycogen levels return to baseline well before resolution of HAAF is observed (Herzog et al., 2008).

1.6.2.5 Changes in metabolism/glucose sensing within the CNS

The overall concept is that alterations in the ability of small groups of glucose sensitive neurons to sense and respond to hypoglycaemia could contribute to failure of the sympatho-adrenal and other counterregulatory responses. Table 1.2 summarises some of the potential contributors. Multiple mechanisms are likely to contribute to this system. This is a broad topic, and there is limited evidence for any single mechanism operating in isolation. Much of the work has focused on the ventromedial nucleus of the hypothalamus (VMN), but it is clear that this is not the only region of the CNS which contributes to the counterregulatory response. Other regions which have been implicated in counter-regulation, and could showed altered responsiveness contributing to HAAF include the parabrachial nucleus, lateral hypothalamus, paraventricular nucleus, arcuate nucleus, and indeed the portal and mesenteric vein glucose sensors (Beall et al., 2012a, Cryer, 2005)

Table 1.2 Putative mechanisms causing changes in metabolism/glucose sensing in the CNS

Mechanism	References
Globally in CNS	
Reduced insulin signalling	(Fisher SJ, 2005)
Increased GABA release	(Klement et al., 2014)
Increased circulating CRH levels	(Flanagan et al., 2003)
VMN	
Increased glucokinase activity	(Dunn-Meynell et al., 2002, Routh, 2003)
Reduced AMPK activity	(McCrimmon et al., 2004)
K_{ATP} channel closure	(Evans et al., 2004, McCrimmon et al., 2005, McCrimmon et al., 2004)
Urocortin release	((McCrimmon et al., 2006, McCrimmon RJ, 2005))
PVN	
Reduced PVN activation	(Sanders and Ritter, 2000, Evans et al., 2001, Evans et al., 2003)

VNM ventromedial nucleus, K_{ATP} ATP sensitive potassium channel

1.7 The hypothalamus as a key player in the integration of glycaemic control

Significant elements of the response to hypoglycaemia are mediated via the central nervous system, (CNS), which integrates peripheral and central information about physiological state (Beall et al., 2012a). Indeed, the first clues that the brain is important for whole body glucose levels were presented over 160 years ago, when Bernard stimulated the floor of the 4th ventricle and observed a rise in blood glucose (Bernard and Tripier, 1858). As discussed in the review by Watts and Donovan (2010), the classical view of a sensory, integrative and output system can be applied to the glucose homeostatic system, but is a significant simplification of the actual process. Any one anatomical region may exhibit overlapping functions- for example the lateral hypothalamus receives inputs from peripheral glucose sensors, contains directly glucose sensing cells, has outflow to autonomic areas of the brainstem and also contains gonadotrophin releasing hormone (GnRH) neurons which release GnRH into the pituitary portal circulation and alter their output depending on metabolic context.

Multiple nuclei of the hypothalamus have been identified as playing a role in the response to hypoglycaemia. Figure 1.3 summarises the major connections and roles ascribed to various hypothalamic nuclei in this context. Glucose sensing populations within the hypothalamus include the arcuate, VMN, LH and possibly the PVN as previously mentioned in section 1.6.2.5. In addition to the ability of these nuclei to respond to changes in glucose, their response can also be modulated by sensing and responding to other signals indicating the overall status of the body, with examples including insulin, ghrelin, leptin, free fatty acids, oestrogen and androgens and angiotensin (Canabal et al., 2007b, Jordan et al., 2010, Santiago et al., 2016, Roland and Moenter, 2011).

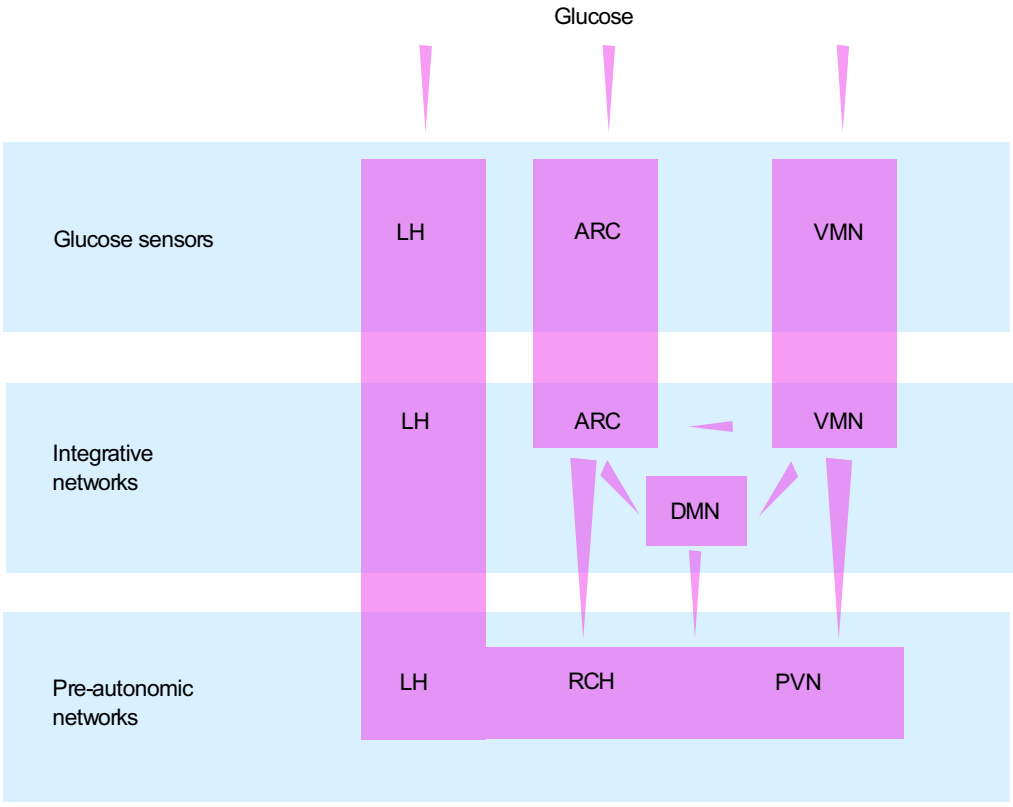

Figure 1.3 Elements of the hypothalamic network sensing and responding to glucose. Adapted from Watts and Donovan (2010)
Several nuclei have more than one function. The PVN also has a role in activation of the hypothalamo-pituitary axis leading to glucocorticoid rises.
LH Lateral hypothalamic area, ARC Arcuate nucleus, VMN Ventromedial nucleus, DMN dorsomedial nucleus, RCH retrochiasmatic hypothalamus, PVN paraventricular nucleus

However, much of what we know is incomplete. A major challenge is that in many cases, neuronal subtyping within the hypothalamus does not readily identify populations with single functions. For example, consider the pro-opiomelanocortin (POMC) and agouti related peptide/neuropeptide Y (AgRP/NPY) neurons within the arcuate nucleus, one of the better characterised areas of the hypothalamus. The generally accepted roles of these neurons are related to control of food intake and energy expenditure, with AgRP/NPY neurons being activated when food/energy stores are less available, promoting food seeking and reducing energy expenditure via projections to the PVN, whilst POMC neurons are activated when energy stores and food are abundant, opposing these effects. However, some NPY neurons in the ARC have been shown to be inhibited by glucose, but by no means all (Murphy et al., 2009b). In addition, not all POMC neurons project to the PVN, which is thought to be their main site of action to mediate food intake and energy expenditure (King and Hentges, 2011).

The hypothalamus contains a wide range of specialised cell types, often spatially intermingled, and their anatomical location and connectivity is not precisely conserved between species. In addition, much previous work has relied on immunohistochemistry to identify neuronal subtypes and try to connect structure and function. Technical advances over the last 10-15 years have greatly increased the ability to dissect out different subsets of neurons in vitro and in vivo and this has improved the understanding of this complex anatomical area.

1.8 The paraventricular nucleus- more than just an effector nucleus

The PVN is situated dorsally within the medial hypothalamus, on either side of the third ventricle. It is best known for its role at the apex of the hypothalamo-pituitary axis, with large numbers of neurons projecting to both the anterior and posterior pituitary originating here. It is an area with multiple roles, including regulation of stress responses, body temperature, circadian rhythms, food intake and energy expenditure. Historically the PVN was largely thought to be an output (effector) nucleus, responsible for enacting motor responses subsequent to integration of signals in other areas of the brain.

With regard to its outflow, the classical pathway from the PVN is to the median eminence, with major projections to both posterior and anterior pituitary. The PVN also has a significant outflow to autonomic areas of the brainstem, and also receives significant inputs from multiple brainstem areas. This reciprocal innervation places it in a key position with regard to coordination of autonomic and hypophyseal outflow (Hosoya et al., 1991, Geerling et al., 2010, Sawchenko and Swanson, 1985, Saper et al., 1976). The output effects of the different divisions of the PVN are summarised in Figure 1.4. The classical view of the PVN was that its functions were compartmentalised, in particular by neuronal subtype, and that there was relatively little cross talk between the various areas.

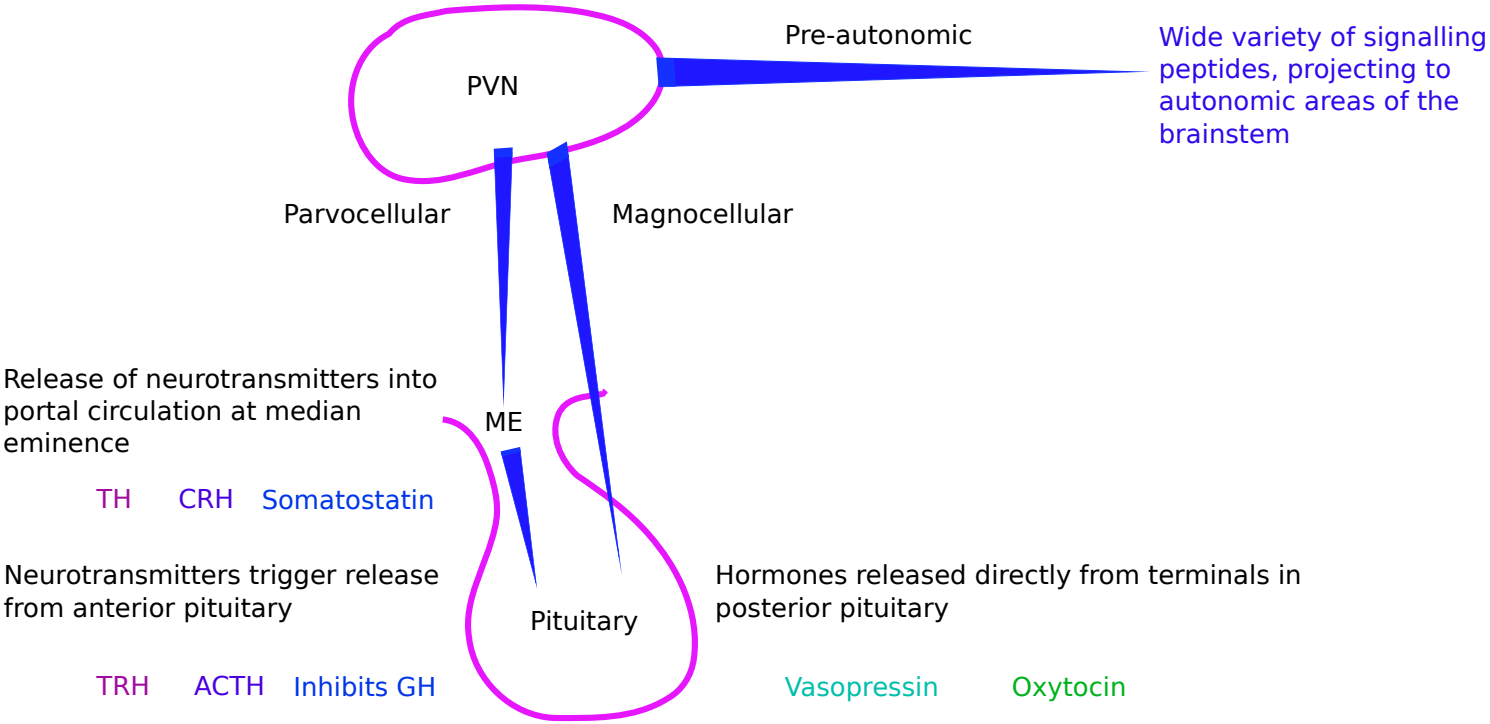

Figure 1.4 Schematic to illustrate the major outputs of the PVN

TH Thyrotropin releasing hormone, CRH corticotropin releasing hormone, TRH thyroid releasing hormone, ACTH adrenocorticotrophin releasing hormone, GH growth hormone

1.8.1 Neuronal subtypes in the PVN

The PVN contains specialised neuronal subtypes (Figure 1.4). Broadly, neurons can be classified as magnocellular or parvocellular, based on their morphology and projection patterns. Magnocellular neurons are larger, contain oxytocin or vasopressin, and project to the posterior pituitary where they release these hormones directly into the circulation to act peripherally. Parvocellular neurons are smaller, contain CRH, thyrothropin releasing hormone or somatostatin, and project to the median eminence where they release peptides into the hypophyseal portal circulation, causing release of downstream hormones (ACTH, TRH) from the anterior pituitary gland into the bloodstream. While this partitioned cell class model has stood the test of time there is evidence for a degree of overlap between cell types and co-expression of signalling molecules in some cases. Perhaps the clearest example of this is the co-release of vasopressin and CRH from parvocellular CRH neurons after acute stressful stimuli (Swanson et al., 1986, Sawchenko and Swanson, 1985).

A third group of pre-autonomic neurons has also been identified within the PVN. These were initially identified by neuronal tracing studies, demonstrating 1) that not all PVN neurons project to the median eminence (Simmons and Swanson, 2009, Swanson et al., 1983, Sawchenko and Swanson, 1982), and 2) that retrograde tracing from the brainstem identifies a subgroup of neurons situated caudally in the PVN (Geerling et al., 2010, Biag et al., 2012). In addition, pre-autonomic neurons exhibit a characteristic electrophysiological profile, at least in rat studies (Luther et al., 2002, Tasker and Dudek, 1991). Pre-autonomic neurons identified by neuronal tracing studies express a wide range of neurotransmitters including oxytocin, vasopressin, 5HT, dopamine, TRH, CRH and enkephalins, as well as glutamate (Sawchenko and Swanson, 1982, Biag et al., 2012, Simmons and Swanson, 2009, Zhao et al., 2017). With regard to GABA, one paper used retrograde tracing, either with fluorogold from the thoracic spinal cord, or GFP tagged herpes simplex virus from the adrenal medulla, with additional GABA immunohistochemistry, but was unable to show any evidence of GABA expression in pre-autonomic PVN neurons (Watkins et al., 2009).

In the rat, neuronal subtypes are clearly anatomically delineated on the basis of their size, morphology and peptide expression, and up to 10 subdivisions of the rat PVN have

been described (Simmons and Swanson, 2009). However, this is not the case in the mouse, where a much higher degree of intermingling of neuronal subtypes occurs (Biag et al., 2012). The human PVN appears to exhibit a degree of homology with the rat PVN, albeit with a smaller number of subdivisions being identified (Koutcherov et al., 2000). The overall topography of the human PVN is also somewhat different to that in rodents, largely due to the fornix which compresses the anterior PVN into a more vertical structure, with a significant caudal extension behind the fornix.

1.8.2 Overall connectivity of the PVN

The PVN receives inputs from a very wide range of structures, both local and distant. From within the hypothalamus, significant inputs are received from the VMN, ARC, LH, DMN and preoptic area (Larsen et al., 1994). Projections are also received from brainstem nuclei; from the NTS (in particular the C2/A2 catecholaminergic group), the ventral medulla, as well as the parabrachial nucleus, the periaqueductal grey and the raphe nuclei (Cunningham and Sawchenko, 1988, Sawchenko et al., 1983, Krukoff et al., 1993, Floyd et al., 1996). In addition, the lamina terminalis group of nuclei, which lies outside the blood brain barrier, has significant connections to the PVN, including from the subfornical organ, the median pre-optic nucleus and the vascular organ of the lamina terminalis (Sawchenko and Swanson, 1983). The forebrain, notably the hippocampus, prefrontal cortex and amygdala also provide some inputs to the PVN, but these are largely indirect, via the bed nucleus of the stria terminalis or the brainstem (Sawchenko and Swanson, 1983).

Traditionally, the roles of different areas of the PVN were thought to be segregated, and this was partly due to the very clear sub-divisions of the PVN observed in the rat. However, it is increasingly clear that this view of the PVN should be modified, with more recent work expanding the concept of its role to include the collation of multiple inputs and balancing information to effect a coordinated output. Overall, the PVN is of key importance to effect homeostatic responses, and this is known to involve activation of multiple outflows in a coordinated manner. For example, consider the response to acute severe haemorrhage. Release of vasopressin from the posterior pituitary, ACTH from the anterior pituitary, catecholamines from the adrenal medulla and loss of sympathetic vasoconstriction all occur simultaneously (Schadt and Ludbrook, 1991).

Given the close proximity of the magnocellular, parvocellular and pre-autonomic parts of the PVN, it seems likely that cross talk is occurring between these areas (the alternative being segregated inputs targeted to each individual output region). Signalling via dendrites within the PVN has been suggested as likely to contribute to co-ordinating responses (van den Pol, 1982, Rho and Swanson, 1989, Herman et al., 2003, Stern, 2015). Paracrine signalling may also play a role, for example, both nitric oxide and CO have been shown to be released within the PVN and to alter neuropeptide release (Rivier, 2001, Rivier, 2002). The PVN has also been shown to have an important role in feeding back upon itself, with a shell of inhibitory terminals and GABAergic interneurons surrounding the more closely packed cell bodies in the main PVN (Biag et al., 2012, Roland and Sawchenko, 1993). Indeed, many inputs to the PVN have been shown to synapse onto this shell, rather than entering the body of the PVN, and this has been suggested as an important gating mechanism for altering PVN neuronal activity (Herman et al., 2003).

1.8.3 Glucose homeostasis and the PVN

The PVN is reported to have important roles maintaining glucose homeostasis (Hill, 2012). Connections to both the pituitary axis and the autonomic system are well established, and these are two systems that are key for counter-regulation (Herman et al., 2003, Hosoya et al., 1991). The PVN has an established role in the regulation of appetite and energy homeostasis, with inputs from the POMC and AgRP neurons of the ARC, as well as other well established centres signalling the availability of food and energy status. In terms of PVN outflows, autonomic projections provide routes by which the PVN can potentially communicate with organs including the pancreas, liver, stomach and adipose tissue, and in addition, via the neuro-hypophyseal route, cortisol and thyroid hormone both play important roles in adaptation of metabolic state to the environment.

With specific regard to the response to hypoglycaemia, the PVN is recognised as having a role to play. Hypoglycaemia is a trigger of the stress response, and the PVN is a key component of the generic response to any stressor, as opposed to specifically responding to hypoglycaemia per se. PVN neurons are activated by systemic hypoglycaemia as evidenced by cfos expression (Evans et al., 2001, Al-Noori et al., 2008)

and PVN inactivation using lignocaine causes defective counter-regulation (Evans et al., 2003). The specific potential of CRH neurons as effectors of the counterregulatory response to hypoglycaemia will be discussed in more detail in the next section.

1.9 CRH neurons

1.9.1 Identification of CRH and early studies

The concept of substances arising in the brain which could stimulate the release of hormones from the pituitary gland had existed since the 1930s, and a focus on the hypothalamus as the source of such substances was developed by, amongst others, Geoffrey Harris in the 1950s (Harris, 1955). Validation of this concept came with the identification of TRH in 1969 by Guilleman and colleagues (Burgus 1969). However, it was not until 1981 that Wylie Vale and colleagues identified a 41 amino acid peptide responsible for simulating secretion of ACTH- namely CRH (Vale et al., 1981). The development of the CRH antibody and subsequent immunohistochemical studies revealed the dense group of CRH neurons within the paraventricular nucleus as the apex of the HPA axis signalling cortisol release (Bloom et al., 1982), as well as a much wider network of CRH neurons throughout the brain (Swanson et al., 1983).

It is clear from immunohistochemical studies that CRH neurons are not confined to the PVN, although that is an area with one of the highest densities of CRH neurons. Other areas with significant concentrations of CRH neurons include the central amygdala, bed nucleus of the stria terminalis, Barrington's nucleus and inferior olivary complex (Swanson et al., 1983). Many of the areas in which CRH neurons are found have been implicated in responses to stress. In addition, small CRH-positive GABAergic interneurons are found scattered throughout the cortex (Taniguchi et al., 2011). These additional CRH expressing areas have not been implicated in glucose sensing and will not be considered further in this introduction.

1.9.2 CRH PVN neuron anatomy and physiology

There are thought to be approximately 2000 CRH neurons in the PVN in the rat (Swanson et al., 1983). CRH neurons are concentrated in the PVN, and in particular in the parvocellular part, with at least 90% of CRH neurons being reported to be found in

this region in mice (Biag et al., 2012). Rat and mouse anatomy are not identical, with CRH neurons being found in more dorsal and lateral part of the parvocellular PVN in the mouse compared to the rat. Additional CRH neurons have been reported in more posterior areas, and some have been demonstrated to be pre-autonomic (Sawchenko, 1987b).

CRH neurons of the PVN can co-express a range of additional neurotransmitters, including glutamate, vasopressin, enkephalins, CCK and angiotensin II (Sawchenko et al., 1984b, Sawchenko et al., 1984a, Dabrowska et al., 2013). Basal CRH levels exhibit circadian rhythms, and are driven by inputs from the suprachiasmatic nucleus (Ixart et al., 1993). The level of CRH mRNA within PVN neurons is relatively high, and so variations in CRH levels in the portal circulation are likely to be due to variation in release, rather than transcription (Watts et al., 2004). Indeed, CRH mRNA levels rise at times of low ACTH levels, and this is likely to be due to the need to replace CRH peptide already released from pools at terminals (Watts et al., 2004). Acutely stressful stimuli cause rapid rises in CRH release from CRH neurons over minutes, followed by an increase in CRH translation and transcription over the next 2 hours. This response appears to be attenuated in some forms of chronic stress, such as cold or restraint (Grissom and Bhatnagar, 2009, Kant et al., 1983, Keim and Sigg, 1976). However, many other stressors show no attenuation with repeated application, for example foot shock(Kant et al., 1983, Grissom and Bhatnagar, 2009). Chronic stress has been shown to increase the responsiveness of CRH neurons to a different stressor, regardless of the response to the chronic stimulus, suggesting sensitisation and plasticity in CRH responses (Herman and Cullinan, 1997).

Interestingly, evidence has also been presented that responses to CRH in the brain are different for an acute infusion of CRH compared to chronic or repeated exposure. In particular, whilst cortisol, epinephrine and norepinephrine release are all stimulated by acute exogenous CRH administration, longer term administration tends to reduce responsiveness (Cunningham et al., 1988, Flanagan et al., 2003). This effect is not thought to be via the HPA axis, as ACTH or corticosterone infusion had the opposite effect to CRH infusion (Flanagan et al., 2003). In addition, CRH infusion intravenously was still able to cause an acute rise in ACTH and cortisol in animals after chronic CRH

infusion intracerebroventricularly (i.c.v) had caused attenuation of the normal response, again suggesting a central mechanism of action (Cunningham et al., 1988).

Inputs to the CRH PVN neurons are diverse. Table 1.3 is a summary of known inputs. In addition, it is not entirely clear where such inputs are targeted in all cases. For example, the BNST neurons are primarily GABAergic, but a proportion of BNST effects on CRH neurons are excitatory. This is thought to be mediated by BNST synapses onto GABAergic interneurons in the shell surrounding the PVN. It is also thought that the mediators of responses observed from many neurons identified by neuropeptide expression are in fact GABA or glutamate which are co-released or indeed released independently from terminals.

Table 1.3: Identified neurotransmitter phenotypes of neurons signalling to CRH neurons of the PVN, and their effects (derived from Herman et al. (2003) and Aguilera and Liu (2012))

Nuclei	Neurotransmitters	Effect
All hypothalamic nuclei with direct connections to PVN	GABA Glutamate	Inhibitory via $GABA_A$ Excitatory
ARC	AgRP, NPY, CART, αMSH	Can all cause CRH release
PVN	CRH, oxytocin, vasopressin	Inhibitory
LH	Orexins	Excitatory
BNST	GABA Glutamate	Inhibitory, also excitatory via interneurons Excitatory
NTS	Epinephrine/norepinephrine GLP-1 Substance P Glutamate	Excitatory via α_1 Possible indirect inhibitory effect via β Excitatory Inhibitory, likely indirect effect Excitatory
RVLM	Epinephrine/norepinephrine	Excitatory via α_2 Possible indirect inhibitory effect via β
Raphe	5HT	Excitatory, direct and via interneurons
PBN	Glutamate	Excitatory

In addition to neuronal inputs CRH neurons can also respond to a range of signals from the periphery conveyed via the PVN microvasculature (substances that can cross the blood brain barrier, e.g. steroids and cytokines) or via signals from circumventricular organs, particularly the subfornical organ and organum vasculosum of the lamina terminalis, where the blood brain barrier is deficient. Circulating plasma levels of glucocorticoids, sex steroids, cytokines, angiotensin II, prolactin and leptin have all been shown to modulate CRH neuronal responsiveness (Aguilera and Liu, 2012).

1.9.3 Evidence for specific involvement of CRH PVN neurons in responses to hypoglycaemia and development of HAAF

CRH expressing neurons in the PVN project to the median eminence (Swanson et al., 1983) and also connect with autonomic areas (Simmons and Swanson, 2009, Sawchenko, 1987b). They are therefore a key element of the hypothalamic-pituitary-adrenal axis and the sympatho-adrenal outflow, important components of the counterregulatory response to hypoglycaemia. Data in rats show that the transcription factor ΔfosB accumulates in the PVN in recurrent hypoglycaemia and this is co-localised with corticotrophin releasing hormone (CRH) (Al-Noori et al., 2008). ΔfosB is a member of the immediate early gene family, which includes cfos and is thought to exhibit raised levels following neuronal activation (McClung et al., 2004). Acute i.c.v infusion of CRH in the rat results in hyperglycaemia with increases in epinephrine, norepinephrine and glucagon. Adrenalectomy and hypophysectomy do not prevent this effect, suggesting that it is mediated via the sympathetic nervous system (Brown et al., 1982).

CRH activation as part of the counter-regulatory response would be expected to reduce the requirement for exogenous glucose as it liberates glucose from tissues. Therefore it is interesting to examine the effect of CRH knockout on responses to a hypoglycaemic insulin clamp- it would be expected that CRH KO mice would have a higher requirement for exogenous glucose. Jacobson and colleagues (2006b) examined the effect of hypoglycaemia on CRH knockout mice. They found that CRH KO mice did indeed have higher glucose requirements in response to the *initial* hypoglycaemic event, and that this was unchanged during a second hypoglycaemic challenge. In comparison, WT mice showed an increase in glucose requirements only *after* previous exposure to

hypoglycaemia. This might imply that failure of activation of CRH neurons contributes to HAAF.

However, the effects were complex and difficult to interpret, in particular as CRH KO mice have a very different basal hormonal profile when compared to WT mice, with extremely low levels of corticosterone, lower levels of insulin and increased levels of norepinephrine. This makes interpretation of the responses to hypoglycaemia challenging. The profile of all the hormones measured (epinephrine, norepinephrine, glucagon and corticosterone) were comparable in CRH KO mice to WT once the changes in basal levels were considered, and suggested that CRH KO mice can still exhibit elements of HAAF. The basal levels of corticosterone are dramatically reduced in a CRH knockout mouse throughout development, and it is likely that the development of other elements of the counterregulatory response were also affected by CRH KO. Candidates include effects on glycogen storage and insulin sensitivity related to long term deficits in corticosterone levels and in addition alteration of the sympatho-adrenal response acting via neuronal synaptic transmission rather than mass release of epinephrine/norepinephrine.

Davis et al. carried out studies in healthy human volunteers as mentioned in section 1.6.2.2, which showed that cortisol infusion can reproduce the effect of prior hypoglycaemia in generating a HAAF hormonal profile on exposure to subsequent hypoglycaemia (Davis et al., 1996). A further study showed that patients with primary adrenocortical failure were not able to develop HAAF (Davis et al., 1997).

Work by Flanagan and colleagues (2003), using a rat model of hypoglycaemia, expanded and developed this line of enquiry. They found that prior CRH infusion or insulin induced hypoglycaemia could both elicit a hormonal profile consistent with HAAF on subsequent induction of hypoglycaemia. However, this was not true of either antecedent ACTH or corticosterone infusion, so the results appear somewhat conflicting. Persuasively, the addition of a CRH receptor antagonist (antalarmin) to CRH infusion abolished the HAAF like effect seen on subsequent insulin-induced hypoglycaemia. An explanation that would account for all of the results would be that the effect is

mediated by CRH acting on CRH type 1 receptors via sympatho-adrenal outflow, rather than via the HPA axis.

Overall, the evidence suggests an effect related to CRH, perhaps mediated primarily via the sympatho-adrenal response rather than the HPA axis. Unpicking the effects of different groups of CRH neurons, in particular the pre-autonomic versus the neuroendocrine populations has been a significant barrier to further investigation of this area.

1.9.4 Challenges to the study of CRH neurons

A major limitation to the study of CRH neurons has been the difficulties in identifying this specific neuronal subtype amongst the wide range of different neurons present in the PVN. As a result of this, previous studies have not been able to demonstrate that CRH neurons are necessary and sufficient to mediate counterregulation, or indeed to demonstrate definitively whether CRH neurons of the PVN are glucose sensing. Although immunocytochemistry was effective in fixed tissues, there was no readily available method to identify or isolate these neurons in live cells. Essentially, many studies were carried out which could only identify CRH neurons after the event, either by immunohistochemistry or using single cell PCR. The advent of genetically modified mice, and in particular the use of the Cre-loxP system has revolutionised the study of neuronal subtypes in all parts of the brain, and this is certainly true for CRH neurons (McLellan et al., 2017, Albanese et al., 2002).

1.10 Development of techniques allowing neuronal subtyping

1.10.1 Genetically modified rodent models

The CRH KO mouse has already been mentioned, and indeed knock out mice were the earliest genetically modified mice used to examine the effect of individual neuronal subtypes. This provided valuable information about functionality in some cases, for example, the POMC knock out mouse was hyperphagic and obese (Coll et al., 2004). However, in many cases the effects were unpredictable, due to compensation during development, and also because the knockout affected the whole animal. More precise techniques were therefore required.

The use of genetic modification to label cell subtypes of interest with reporter proteins (often fluorescent), has been of enormous value in opening up new possibilities for investigation of specific cell types, in particular in the central nervous system, where it has often proved impossible to identify subtypes in living cells by other means. The additional flexibility conveyed by conditional targeting systems, which will be discussed in more detail below, has further enabled studies in this area.

1.10.1.1 Transgenic versus knock in genetically modified mice

Initial genetic modifications to allow identification of specific neuronal subtypes involved injection of DNA into the male pronucleus of a fertilised egg to introduce the DNA encoding the desired protein into the genome. This generates a transgenic mouse, with random incorporation of the genetic material into the genome, at an unknown number of sites (from one to many). Construction of larger bacterial and yeast artificial chromosomes (BACs and YACs), allowed more complex DNA constructs to be introduced in a similar manner. This methodology is simple and effective, but can be unreliable. Three main problems were observed. Firstly, the presumed promotor sequence included in the transgene construct was not always comprehensive, as upstream promotor effects can extend a much longer distance away from the gene of interest than was initially appreciated. This could lead to patterns of expression that differed from the endogenous gene of interest. Secondly, the random incorporation of the construct into the genome could result in its integration at sites with either very high or very low levels of transcription, and this could circumvent the specificity of the promotor sequence included in the construct, leading to off target effects or indeed under-reporting. Finally, the presence of an unknown number of copies of the same construct makes spontaneous recombination events more likely, and this could result in genetic instability in the genetically modified mouse line, most commonly with loss of the introduced DNA, but also potentially disruption of other genes (producing an unintended phenotype unrelated to the introduced transgene).

Gene targeting techniques, initially developed to produce knockout mice by excising specific sections of the genome, were subsequently expanded to generate knock in mice, with new genetic material being introduced at a specific point in the genome. This method targets a specific sequence of genetic material to introduce the DNA of interest

into embryonic stem (ES) cells. Although the desired insertion event occurs at very low frequency, successful insertion can be screened for by including a gene conveying antibiotic resistance in the DNA to be inserted. Only ES cells with successful DNA insertion will grow in the presence of the drug, and these can then be inserted into early embryos to produce chimeric mice. Subsequent breeding of the chimeric mice will produce mice with the desired mutation expressed in all cells (Doyle et al., 2012). This method results in targeted mutations at a single known point in the genome. This is advantageous as, for example, genes can be inserted directly downstream of the promotor of interest, allowing near identical control of the endogenous gene and the new genetic material. All of the mice used in this thesis were developed using the knock in technique.

1.10.2 Cre-loxP and FLP-FRT systems

The development of the Cre-loxP and FLP-FRT systems was complimentary to the development of knock in or transgenic mice, as it allowed significantly more flexibility in the use of the same mouse line for a wide variety of purposes (Albanese et al., 2002). These techniques exploit the ability of enzymes from bacterial phages (Cre recombinase) or eukaryotes including yeasts (FLP) to edit their genomes, targeting excision and recombination events to specific short DNA sequences designated loxP and FRT respectively. The enzyme will have no effect on the cell until the relevant DNA sequence is present. Therefore, two mutations are required to generate an effect in any one cell. The first is the expression of the enzyme, usually under the control of a specific promoter (Figure 1.5A). The CRH Cre mouse used throughout this thesis expresses Cre recombinase under the control of the endogenous CRH promotor and is referred to as the CRH-ires-Cre mouse (Taniguchi et al., 2011). The second mutation is a DNA sequence of interest, flanked by the targeting sequences required by the enzyme (LoxP for Cre recombinase, FRT for FLP). This could be a fluorescent reporter gene, a section of DNA to be excised or indeed a functional gene to be expressed such as an ion channel (Figure 1.5B, 1.6). Only when the enzyme and the relevant DNA targeting sequences are both present in the same cell will recombination occur and the effect of the second mutation be observed.

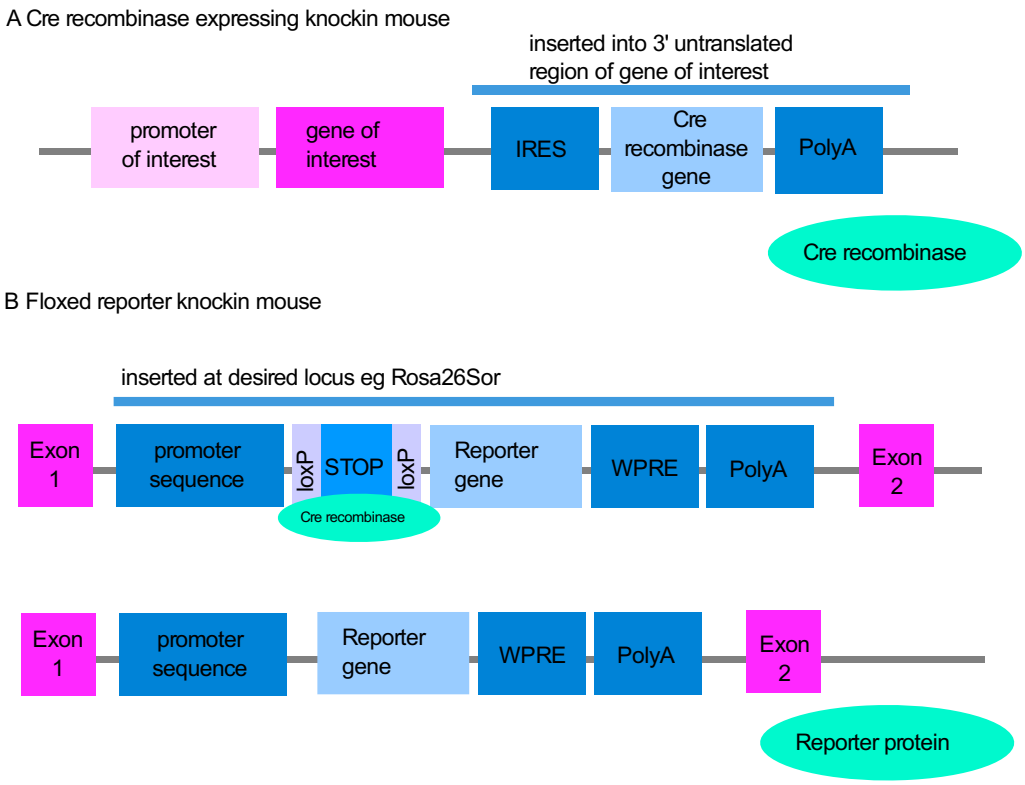

Figure 1.5 Illustration of Cre-loxP system
A Cre recombinase enzyme is expressed under the control of the desired promoter
B A reporter protein with a loxP flanked STOP codon preceding it is introduced, either via a viral vector or crossing a Cre mouse line with a floxed reporter mouse line. In cells expressing Cre recombinase, the DNA between the loxP sites is excised, removing the STOP codon and leading to expression of the reporter protein.

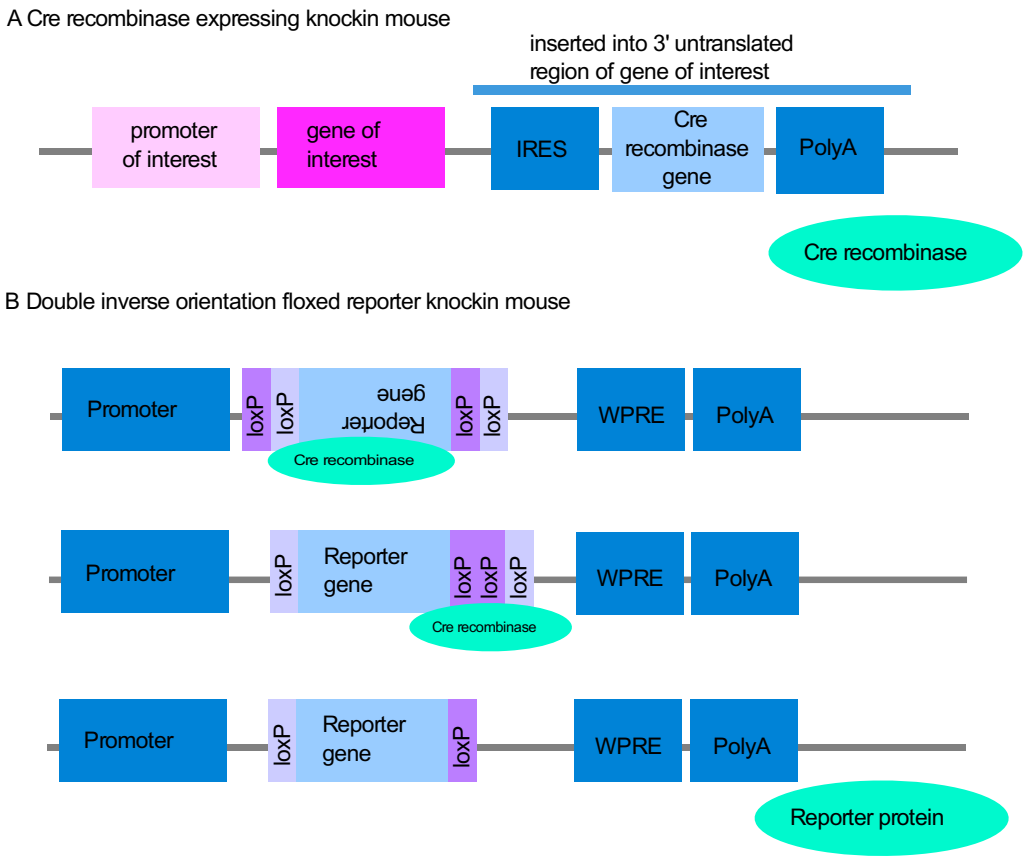

Figure 1.6 Illustration of Double floxed Inverse Orientation (DIO) version of the loxP system

A Cre recombinase is expressed under the control of the desired promoter

B The reporter protein is engineered to be in reverse orientation, such that it will not be transcribed, flanked by two sets of loxP sequences, in pairs. Cre recombinase will firstly reverse the orientation of the DNA between one pair of loxP sequences. It will then excise DNA to remove 2 loxP sites, leaving the reporter DNA intact and now in the correct orientation for transcription.

The introduction of conditionality in this fashion allows a wide range of genetic effects to be produced in a cell specific manner, without needing to specifically generate a new transgenic or knock in mouse line in each case. In this thesis, two loxP 'reporter' mouse lines are crossed with the CRH-ires-Cre mice, to produce mice expressing TdTomato (Madisen et al., 2010) or GCaMP6f (Madisen et al., 2015). An alternative method of introducing loxP targeted DNA is to use a viral vector containing a loxP flanked reporter protein to express the reporter protein only in Cre recombinase expressing neurons, and only in the anatomical area targeted by the virus (Figure 1.6) (Wang et al., 1996, Albanese et al., 2002). The utility of the Cre-lox system to allow investigation of specific neuronal subtypes has been of great value in allowing more detailed investigation of the CNS. Development of repositories of genetically modified mouse lines, for example Jackson Laboratories, such that they are commercially available, has improved access to a wide range of GM lines for the use of the whole scientific community.

The range of reporter or effector genes which can be activated using Cre-recombinase is very broad, and encompasses a wide range of techniques, as briefly summarised below.

Simple fluorescent reporter genes for identification of neuronal subtypes in vivo and in vitro are perhaps the most widely used. Neuroanatomy can be elucidated without the need for complex immunohistochemical techniques, especially where the peptide of interest is expressed at low levels. This also removes the need for pharmacological treatments such as colchicine, previously used to increase sensitivity of staining for neuropeptides such as CRH in neuronal somata by inhibiting microtubule transport of such neuropeptides to terminals for release. Additionally, by introducing the reporter gene via a viral vector, or using a time locked gene (tamoxifen or tetracycline dependent as well as Cre recombinase dependent), still greater precision can be achieved in which neurons are identified. This technique minimises the effects of changes in patterns of gene expression during development. The choice of viral vector can also allow tracing of neuronal projections both anterograde and retrograde; this topic will be discussed in more detail in section 3.1.6. Pre identification of neurons of interest can also direct functional investigation, for example using electrophysiology. The molecular profiles of specific neuronal subtypes could also be investigated, for example using fluorescence activated cell sorting followed by quantitative PCR.

Genetically encoded calcium indicators (and indeed voltage indicators) can be expressed in specific neuronal subtypes for non-invasive, functional imaging of neuronal activation, in vitro and in vivo (Paredes et al., 2008). Technical advances in imaging such as gradient refraction index lenses and 2-photon microscopy have increased the breadth of application of these techniques.

Finally, the fields of optogenetics and pharmacogenetics allow investigation of the effects of functional activation or inhibition of specific neuronal populations, either in vitro, or in a whole animal model (Fenno et al., 2011, Sternson and Roth, 2014). This ability to target specific populations in the context of well characterised mouse models of disease has greatly increased the precision with which experiments can be designed and carried out.

1.11 Summary

This introductory chapter has outlined the clinical context underpinning this thesis; in particular the increasing incidence and prevalence of diabetes mellitus worldwide, and associated with this the increasing frequency of hypoglycaemia associated autonomic failure due to insulin use. In order to better understand the potential causes of HAAF, a better understanding of the physiological and pathophysiological response to hypoglycaemia is required. A summary of the known physiological response to hypoglycaemia has been presented, and it is clear from this that the loss of the sympatho-adrenal response to hypoglycaemia is key to the development of HAAF in diabetic patients. Having outlined some of the potential mechanisms underlying the development of HAAF a wide range of potential avenues present themselves for further investigation.

Focusing in on the CRH neurons of the PVN, it is clear that there are a number of known features of this neuronal population which makes them an attractive target for a potential role in the development of HAAF. In particular, the role of these neurons at the top of both the hypothalamo-pituitary-adrenal axis and their potential pre-autonomic connections to the brainstem situate them such that they can influence both aspects of the sympatho-adrenal response to hypoglycaemia. Those experiments involving infusions of CRH with observed alterations in the response to hypoglycaemia

are also suggestive of an important role for these neurons. Currently, there are some important gaps in the knowledge of this system, and recent technical developments now allow these questions to be effectively addressed.

- The specific targets of CRH PVN pre-autonomic neurons have not been fully described, and would provide valuable indications of the potential effector targets of CRH PVN neurons in the brainstem, in particular the sympathetic outflow
- Glucose sensing has been described in PVN putative pre-autonomic neurons in the rat, but not at physiological glucose levels, and glucose sensing in CRH PVN neurons has not been investigated
- Whilst the PVN as a whole has been shown to be activated by hypoglycaemia as evidenced by cfos, this has not been investigated for CRH neurons, particularly in the mouse.
- Models of recurrent hypoglycaemia and HAAF in the mouse are currently still being optimised, and would be of great value in further investigating the role of neuronal subtypes in development of HAAF using the wide range of GM mice available.
- The availability of mice expressing Cre recombinase under the control of a wide range of specific promoters facilitates the investigation of neuronal subtypes including CRH
- Cre dependent reporter genes including simple fluorescent proteins and genetically encoded calcium indicators allow investigation of both the anatomy and function of specific neurons, especially when combined with differing methods of introducing these genes

This thesis will therefore aim to use the CRH-ires-Cre mouse in combination with floxed reporter mice (TdTomato and GCaMP6f) and viral vectors including floxed mCherry to investigate the neuroanatomy and glucose responsiveness of the CRH PVN neurons. The hypotheses and aims are outlined in detail below.

1.12 Hypotheses

CRH PVN neurons:

- make direct connections to autonomic areas of the brainstem
    - including the nucleus of the solitary tract, dorsal motor nucleus of the vagus and ventrolateral medulla
- are intrinsically glucose sensing
- include a subpopulation that are activated by hypoglycaemia
- exhibit altered responses to glucose following exposure to recurrent hypoglycaemia

1.13 Aims

- Use anterograde and retrograde viral tracing techniques to investigate the autonomic areas of the brainstem which have direct synaptic connections from CRH PVN neurons
- Use electrophysiology and calcium imaging to seek evidence of glucose sensing in CRH PVN neurons
- Investigate whether glucose sensing in the PVN requires metabolism of glucose
- Use a mouse model of single hypoglycaemia and cfos immunohistochemistry to demonstrate neuronal activation of CRH PVN neurons by hypoglycaemia
- Develop a mouse model of recurrent hypoglycaemia, seek evidence of HAAF as indicated by corticosterone and glucagon levels, and examine the effect of recurrent hypoglycaemia on glucose sensing

Chapter 2 Methods

This chapter describes in detail the methods used for data collection and analysis throughout this thesis, including relevant negative and positive controls. Specific experiments using the methods described are outlined in the relevant sections.

Overall the thesis chapters contain data from experiments using:

- All chapters contain data collected using genetically modified mice.
- Chapter 3 uses injection of viral vectors for neuronal tracing and immunohistochemistry/microscopy.
- Chapters 4 and 5 use in vitro slice preparations for electrophysiology and calcium imaging.
- Chapter 6 uses in vivo mouse models of hypoglycaemia, immunohistochemistry (IHC), radioimmunoassays (RIA) and calcium imaging.

2.1 Genetically modified mice

The mouse lines chosen for use in this thesis were based on an examination of the literature to find what had been used successfully in the past. Several strains of mice have been developed to identify CRH neurons, some using direct expression of a reporter protein under the control of the CRH promoter (Alon et al., 2009), and others using the Cre-lox system (Taniguchi et al., 2011). The Cre-lox mouse was preferred for two main reasons. Firstly, it recapitulates the known expression pattern for CRH neurons more accurately than some other strains (Chen et al., 2015). Secondly, the use of Cre recombinase increased the flexibility of the system, as genes with different functions could be introduced into CRH neurons, either by crossing with floxed mouse strains or using floxed viral vectors.

The CRH-ires-Cre mouse used throughout this thesis expresses Cre recombinase under the control of the endogenous CRH promotor, as illustrated in Figure 2.1A (Taniguchi et al., 2011). Two loxP mouse lines are crossed with the CRH-ires-Cre mice, to produce mice expressing TdTomato (Madisen et al., 2010) or GCaMP6f (Madisen et al., 2015)

specifically in CRH neurons (Figure 2.1B, C). TdTomato was chosen on the basis that it is a very bright fluorescent protein which does not in general require amplification using immunohistochemistry, and has previously been combined successfully with the CRH-ires-Cre mouse strain (Wamsteeker Cusulin et al., 2013). GCaMP6f is a genetically encoded calcium indicator (GECI) with rapid kinetics and good signal to noise ratio. More detailed discussion of GECIs can be found in Chapter 4, section 4.2.

Mice from genetically modified lines were obtained from Jackson Laboratories as shown in Table 2.1. The experiments performed in each chapter and which mouse strain was used is summarised in Table 2.2.

Mice were maintained on a 12-h light/dark cycle with temperature and humidity control and free access to water and mouse chow. Studies were carried out in accordance with the UK Animals (Scientific Procedures) Act and with the approval of the local AWERB.

.

Table 2.1: Genetically modified mouse lines used in this thesis

Name	Jax ref.	Promoter	What expressed	Hetero or homozygous	Used for
CRH-ires-Cre	012704	Endogenous CRH promoter	Cre Recombinase in CRH expressing neurons	Homozygous	Founder line breeding, for F1 crosses CRH-ires-Cre used with viral vectors for neuronal tracing
TdTomato	007914	ROSA promoter	Conditional expression of TdTomato (Floxed stop codon before TdTomato gene)	Homozygous	
GCaMP6f	028865	ROSA promoter	Conditional expression of GCaMP6f (Floxed stop codon before GCaMP6f gene)	Heterozygous	
CRH x Td	n/a	See above	TdTomato, potentially in all neurons which ever expressed CRH at any developmental point. Cre recombinase in any neurons in which CRH is currently expressed	Heterozygous	Identify CRH neurons by TdTomato (red) fluorescence for IHC, ISH and electrophysiology
CRH x GCaMP6f	n/a	See above	GCaMP6f in all neurons which ever expressed CRH at any developmental point. Cre recombinase in any neurons in which CRH is currently being expressed	Heterozygous for both genes	Calcium imaging in CRH neurons
CRH x GCaMP6f x Td	n/a	See above	TdTomato and GCaMP6f in all neurons which ever expressed CRH at any developmental point. Cre recombinase in any neurons in which CRH is currently being expressed	Heterozygous for all 3 genes	Calcium imaging with pre-identification of CRH neurons using TdTomato

All mice are bred on background strain C57Bl6J

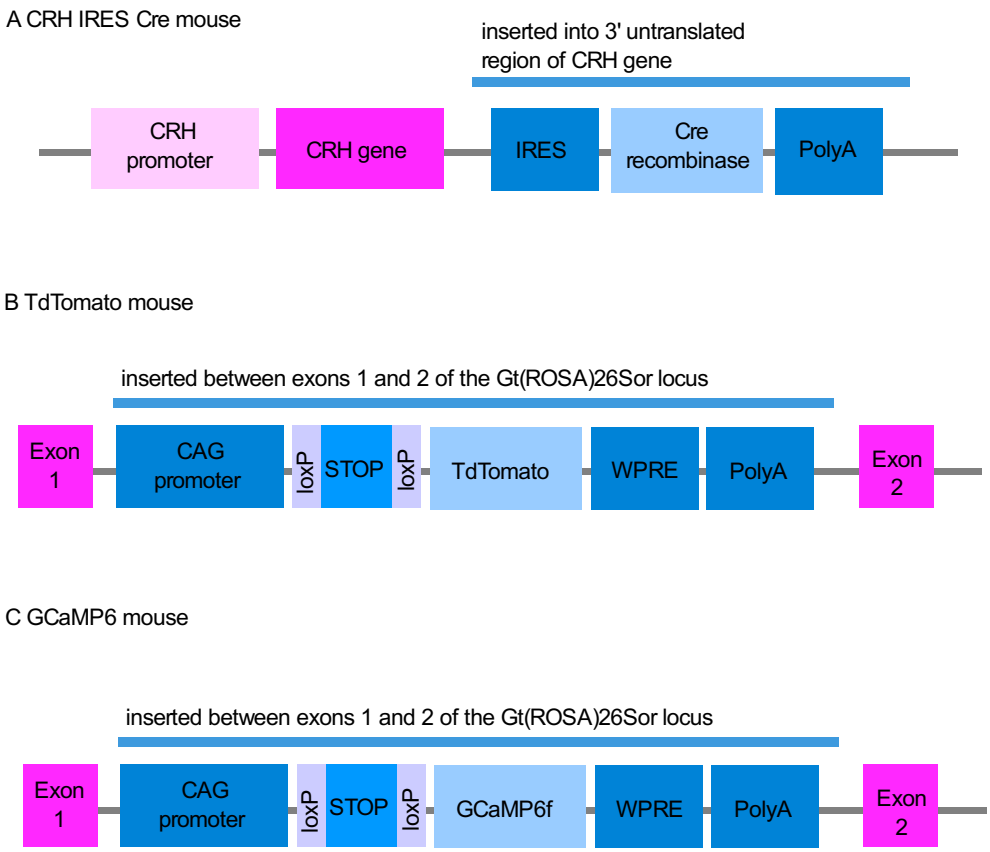

Figure 2.1 Diagrams to illustrate the genetic modifications introduced in the 3 mouse strains used in this thesis

Introduced elements in blue/purple, native elements in pink, CRH corticotropin releasing hormone, IRES- internal ribosome entry site, PolyA- to maintain stability of transcribed mRNA, CAG promoter- a Cytomegalovirus early enhancer element/chicken beta-actin/rabbit beta-globin hybrid promoter, loxP- target sites for Cre recombinase to act on, STOP- a sequence containing STOP codons in all three reading frames, WPRE- woodchuck hepatitis virus post-transcriptional regulatory element to enhance mRNA transcript stability

Table 2.2 Overall characteristics of mice used for each experiment

Chapter	Experiment	Mouse line	Sex	Age (weeks)
3	Anterograde tract tracing	CRH x Td	Both	6-20
	Retrograde tract tracing	CHR-ires-Cre	Both	6-20
	In situ hybridisation	CRH x Td	Male	6-8
4	Electrophysiology	CRH x Td	Both	6-12
	Calcium imaging	CRH x GCaMP6f x Td	Both	6-12
		CRH x GCaMP6f	Both	6-12
5	Calcium imaging	CRH x GCaMP6f	Female	6-12
6	IHC (cfos)	CRH x Td	Male	6-8
	RIA (glucagon, cortisol)	C57Bl6J	Male	12-20
	Calcium imaging	CRH x GCaMP6f	Female	6-9

2.2 Genotyping

Mice were genotyped by polymerase chain reaction analysis from DNA extracted from ear notches. DNA was extracted from the ear notch using 30µl of 0.2mM EDTA/25mM NaOH solution, heated to 98°C for 30minutes, followed by physical disruption of tissue by pipetting. The digestion was neutralised using 30µl 40mM TrisHCl, pH7.4.

The DNA obtained from this method was input to a master mix for PCR (Table 2.3):

Table 2.3 PCR master mix

	Volume (µl) for one reaction tube
10X PCR buffer	2
Deoxynucleotides	2
Primers (100mmol each)	1 x number of primers
rTaq	0.2
DNA	1
To total volume with distilled water	20

rTaq, 10X PCR buffer and deoxynucleotides supplied as a kit R001A, TaKaRa Taq™ (Takara BIO, USA)

Table 2.4 contains a summary of the primers used in each case. PCR programs are summarised in table 2.5.

Table 2.4 Primer details for each mouse strain genotyped

Strain	Primer A (Forward WT)	Primer B (Reverse WT)	Primer C (Forward Mutant)	Primer D (Reverse mutant)
CRH-ires-Cre Mut 468bp WT 676bp	CAC GAG CAG GCT GCG GCT AAC	CTT ACA CAT TTC GTC CTA GCC	CAA TGT ATC TTA TCA TGT CTG GAT CC	As Primer B (common reverse primer)
TdTomato Mut 196bp WT 297bp	AAG GGA GCT GCA GTG GAG TA	CCC AAA ATC TGT GGG AAG TC	CTG TTC CTG TAC GGC ATG G	GGC ATT AAA GCA GCG TAT CC
GCaMP6f Mut 450bp WT 297bp	AAG GGA GCT GCA GTG GAG TA	CCG AAA ATC TGT GGG AAG TC	ACG AGT CGG ATC TCC CTT TG	As Primer B (common reverse primer)

Primers obtained from Eurofins (UK)

Table 2.5 PCR programs for each mouse strain genotyped

Strain	Initial denature (°C, time)	Cycling denature (°C, time)	Anneal (°C, time)	Amplifi-cation (°C, time)	Final amplification (°C, time)	Hold (°C)
CRH-ires-Cre	94 3min	94 30s	66 60s	72 60s	72 2min	4
TdTomato	95 2min	95 30s	57 45s	72 60s	72 5min	4
GCaMP6f	95 2min	94 30s	64 reducing 0.5 per cycle, to 55, continue at 55 30s	72 45s	72 2min	4

Each cycle (shaded boxes) performed 35 times for each reaction

The PCR product was pipetted into a 2% agar gel with 0.01% ethidium bromide in TAE buffer (40mMTris, 20mM acetic acid and 1mM EDTA) and electrophoresed to allow identification of bands of interest. Example gels are shown in Figure 2.2

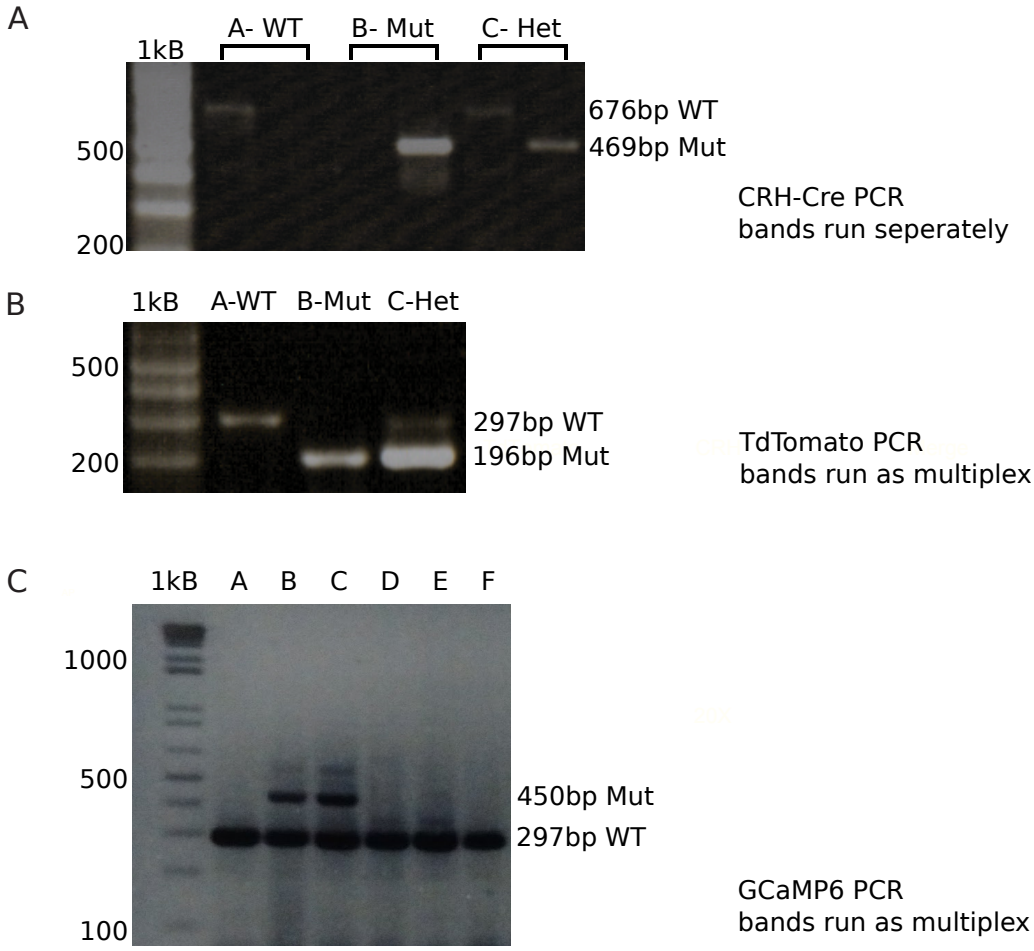

Figure 2.2 PCR results for CRH Cre, TdTomato and GCaMP6f genotyping
Left hand lane is a 1kb ladder in all gels
A CRH Cre PCR-results for 3 mice shown. PCR for wild type (WT) and mutant (Mut) bands are carried out separately such that there are 2 lanes for each mouse genotyped, left lane is WT band, right lane is CRH Cre band. Mouse A is a WT, B is homozygous for CRH Cre and C is heterozygous (Het). Mutant band is 469bp, wild type 676bp.
B TdTomato- results for 3 mice as for CRH, Mut band 196bp, WT 297bp. Here, a multiplex PCR was run, so bands are visible in a single lane
C GCaMP6f, genotyping a litter of 6 mice, of which 2 are heterozygous for GCaMP6f (mice B and C), and the rest are all wild types, Mut band 450bp, WT 297bp

As most breeding strategies used homozygous parents, routine genotyping was not required once the colonies were established. The exception was the CRH x GCaMP6f line, which used a heterozygous GCaMP6f parent, and therefore genotyping of all offspring for GcaMP6f was required to identify offspring with the desired mutation. The reason for using a heterozygous GCaMP6f parent was two-fold- firstly this was expedient for obtaining litters with the relevant mutation rapidly, as homozygous GCaMP6f animals were not initially available. Secondly, there is evidence that some homozygous GCaMP strains have a tendency to epileptiform activity (Steinmetz et al., 2017). There were no obvious behavioural or physiological phenotypes in any of the mouse lines maintained for this study. CRH-ires-Cre homozygous mice in general had smaller litters than observed in the TdTomato strain or crosses between strains.

2.3 Viral vectors

For retrograde tracing studies, a canine adenovirus type 2 expressing GFP under the CMV promoter (CAV-CMV-eGFP) was obtained from E. Kremer (Institut de Génétique Moléculaire de Montpellier, CNRS-Universities of Montpellier I and II, Montpellier, France.)(Bru et al., 2010). The titre was $4.8X10^{12}$particles/ml. The virus was not diluted for injection into the brain. This virus was used for retrograde tracing of neurons projecting to the nucleus of the solitary tract (NTS) from the PVN. Virus was injected into the NTS of CRH x TdTomato mice where it will be taken up into any axonal terminals, dendrites and soma. CAV-2 viruses specifically transduce neurons, and not glial cells (Junyent and Kremer, 2015). This means that distant neurons with projections to the NTS will be transduced, resulting in GFP signal in the soma of these neurons (in this case the PVN). Local cell bodies will also be transduced, as will cells projecting to the NTS from other areas. The genetic modifications introduced using this virus are summarised in Figure 2.3B.

Adeno-associated viral vector (serotype 2), DIO-mCherry (AAV_DIO-mCherry) was obtained from Carolina Vector Core Services (originator Karl Deisseroth lab, Stanford,USA, now available (plasmid#20297) via Addgene, MA, USA)(Cerritelli et al., 2016). The titre was $6X10^{12}$particles/ml, the virus was not diluted for injection. The genetic modifications included in the virus are summarised in Figure 2.3A. This vector

was used for anterograde tracing, and does not travel retrogradely. It was injected into the PVN of CRH-ires-Cre mice to express mCherry only in CRH neurons, and only in the anatomical area targeted by the virus.

Both viruses were used in the autonomic tracing experiments in chapter 3. In addition, the CAV-CMV-eGFP virus was injected into some mice used in chapter 4 for electrophysiology.

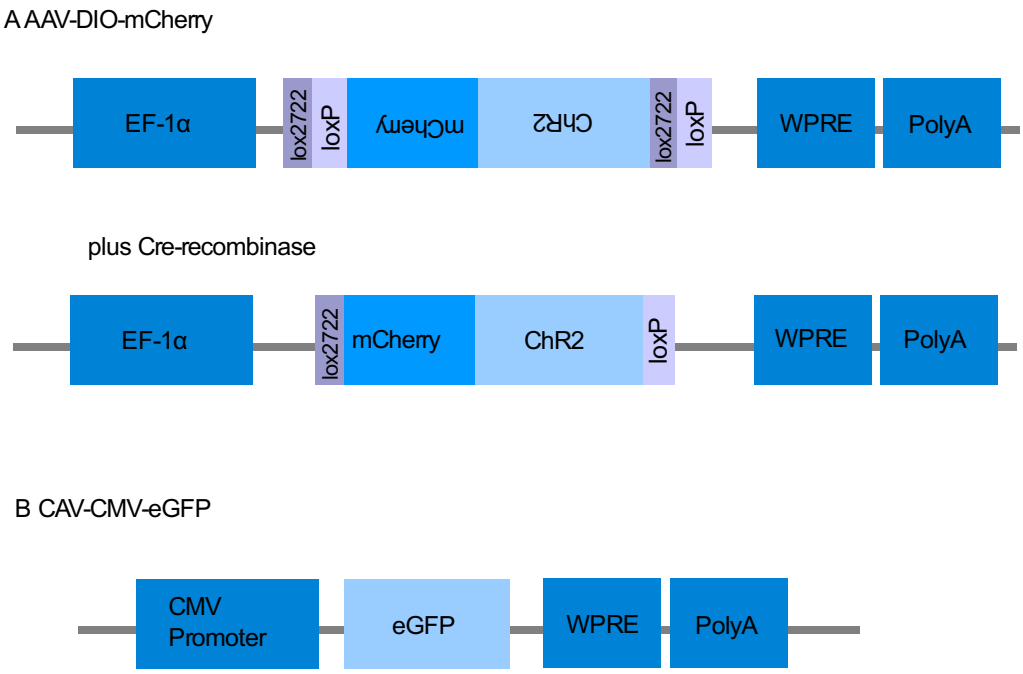

Figure 2.3 Diagrams to illustrate the genetic modifications introduced in the 2 viruses used in this thesis

AAV- adeno associated virus, CAV- canine adeno virus, EF-1α- human elongation factor 1-alpha is a constitutive promoter which can be used to drive ectopic gene expression, LoxP or lox2722- target sequences for Cre recombinase, DIO- Double-floxed Inverse Orientation-two sets of loxP sequence are inserted, cre recombinase will firstly switch the orientation of the DNA between loxP-loxP or lox2722-lox2722 and then excise one set of loxP to leave DNA in the correct orientation for transcription and translation, mCherry- fluorescent red protein, ChR2- channel rhodopsin; a light activated ion channel (not used functionally in this thesis), WPRE- woodchuck hepatitis virus post-transcriptional regulatory element to enhance, mRNA transcript stability, PolyA- to maintain stability of transcribed mRNA, CMV promoter- human cytomegalovirus early promoter; causes high levels of transient downstream gene expression, eGFP- enhanced green fluorescent protein

2.4 Surgery – stereotaxic vector injections

Mice were anesthetized with intraperitoneal ketamine (70mg/kg, Vetalar; Pharmacia) and medetomidine (0.5mg/kg, Domitor; Pfizer) until loss of the hindpaw withdrawal reflex. The area to be operated on was shaved and cleaned with iodine. Lacrilube was applied to the corneas to prevent drying. The animal was placed in a stereotaxic frame (David Kopf Instruments, CA, USA) and core temperature was maintained using a heat pad. Aseptic surgical techniques were used throughout.

Injections were made using a micropipette pulled to ~20μm diameter tip, using a vertical puller (Harvard Apparatus, UK). 2 types of microcapillary glass were used. For NTS injections, microcapillary glass with 1μL calibration was used (P0549, Sigma, USA). For PVN injection, microcapillary glass with external diameter 1.14mm, internal diameter 0.53mm, was used (3-000-203-G/X, Drummond Scientific, USA). The pipette was attached to two different systems. Experiments involving injection of virus into the NTS used a 25μL Hamilton syringe (Hamilton, UK) in a Genie RS232 pump (Kent Scientific Corp, Torrington, CT USA), attached via polyethylene tubing to the pipette using polyethylene silicon tubing. Polyethylene silicon tubing expands in ethyl ether and then contracts to form a tight seal around the connections once removed from the solvent. Experiments injecting virus into the PVN used a syringe injector system directly connected to the pipette (Nano-W Wireless capillary nanoinjector, Neurostar, Germany). In both cases, the tubing and micropipette were firstly filled with mineral oil, and virus then back filled into the pipette tip. Injections were made at a rate of 0.2μl/min, with the pipette being kept in place for one minute after each injection before moving to the next point of injection.

2.4.1 NTS injection

The head was flexed by means of inverting the bite bar and gently pushing the end of the bite bar against the animal's snout. An incision was made over the occiput extending to the nape of the neck. Muscles were removed from their attachments to the occiput. A 27G needle was used to incise the dura (atlanto-occipital membrane) to enable visualisation of calamus scriptorius (caudal tip of area postrema) on the dorsal surface of the medulla. The most caudal point of calamus scriptorius was identified and

used as a reference point to delineate the midline and rostro-caudal targeting of injections.

Stereotaxic injections of CAV-CMV-eGFP were made into the nucleus of the solitary tract/dorsal motor nucleus of the vagus using a similar approach to that described in (Cerritelli et al., 2016). Vector injections were made unilaterally at the following coordinates: From the reference of calamus scriptorius, lateral 0.2 mm, 0.3–1.0 mm deep from brain surface with a 35° rostral angulation. 3 viral injections (210 nL) at 0.35mm intervals were performed (1.0mm, 0.65mm, 0.3mm). Bilateral NTS injections were performed for mice used subsequently for electrophysiological recordings. Muscles and skin were sutured in two layers, and antibacterial powder applied to the wound.

2.4.2 PVN Injection

An incision was made over the dorsum of the skull, bregma was identified and used to delineate the midline and rostro-caudal targeting of injections. A burr hole was drilled unilaterally allowing access at the following coordinates: bregma -0.94mm, 1mm lateral, for injection from a pipette with 10˚ angle from vertical, aiming towards the midline in a coronal plane, 4.5-5.1mm deep. A total of 4 injections (100nl) were performed at 0.2mm intervals (5.1mm, 4.9mm, 4.7mm, 4.5mm). The skin was then sutured, and wound powder applied.

A vertical approach at 0.2mm lateral was initially employed (bregma -0.94mm, lateral 0.2mm, 5.1mm deep), but it proved difficult to avoid the central sinus and resultant bleeding (and also the 3rd ventricle), and therefore the 10˚ angle and more lateral entry point were used subsequently.

2.4.3 Recovery from surgery

At the end of stereotaxic surgery, anaesthesia was reversed with atipamezole (Antisedan, 1mg/kg, i.p; Pfizer) and buprenorphine was given for pain relief (Temgesic, 0.1mg/kg, s.c; Schering-Plough). Animals typically showed a rapid functional recovery from anaesthesia and surgery. Welfare scoring was used to monitor animal's recovery.

2.5 Solutions and chemicals

All chemicals used in this thesis were obtained from Sigma, UK unless otherwise stated.

2.6 Tissue Fixation and imaging

These techniques were used as follows:

- This chapter uses ISH to validate CRH x Td mice as identifying CRH neurons
- Chapter 3 uses immunohistochemistry to amplify transfected viral fluorescence- eGFP and mCherry, double immunohistochemistry to label autonomic neuronal subtypes in addition to mCherry.
- Chapter 6 uses immunohistochemistry for cfos and oxytocin.

2.6.1 Solutions

Solutions used for tissue fixation and immunohistochemistry were as summarised in table 2.6

Table 2.6 Solutions used for tissue fixation and immunohistochemistry

Solution	Abbreviation	Volume	Solvent	Solutes	pH
10% neutral buffered formalin	N/A- purchased ready to use				
0.1M Phosphate buffer	PB	1L	Distilled water	NaH2PO4 3.2g, Na2HPO4 10.9g	7.4
0.1M Phosphate buffer with azide	PB azide	1L	PB	Sodium azide 0.2g	7.4
0.1M Phosphate buffer with 0.3% triton X-100	PBT	1L	PB	Triton X-100 0.3ml	7.4

2.6.2 Histology

2.6.2.1 Perfusion/fixation

Mice were terminally anesthetized with intraperitoneal injection of pentobarbitone (100mg/kg) and perfused trans-cardially with 25 ml of 10% neutral buffered formalin. Brains were removed, stored in the same fixative for 12 hours at 4°C and then immersed

in 20% sucrose in PB, pH 7.4, at 4°C overnight for cryoprotection prior to cutting on a freezing microtome.

2.6.2.2 Slice preparation

Coronal sections of brain, brainstem and spinal cord were cut of 30µm thickness into 1:4 equal series on a freezing microtome. Sagittal sections were cut of 30µm thickness into 1:3 equal series in the same manner. Sections were stored at 4°C in PB azide for use in the next 2 weeks, or at -20°C in a cryoprotectant solution (2:3:5 glycerol:ethylene glycol:PB) for long term storage.

2.6.3 Immunohistochemistry:

2.6.3.1 Free floating sections

This method was used for the majority of immunohistochemistry experiments.

Sections were washed 3 times for 10 minutes, in PB (6 times if taken from storage in cryoprotectant). Sections were then incubated in 50% ethanol in distilled H_2O for 30 minutes to permeabilise cell membranes and facilitate antibody entry into cells. They were subsequently incubated overnight at room temperature in primary antibody in PBT and 3% donkey serum (NDS). After washing 3 times in PB, sections were incubated in secondary antibody in PBT plus NDS 2% for 3 hours at room temperature. Brain sections were mounted onto electrostatically charged slides (Superfrost plus slides, Menzel-Glaser, Fisher Scientific, UK) using fluorsave medium (FluorSave, Merck Millipore, Germany) and stored at 4°C. See tables 2 and 3 for antibodies and concentrations used.

2.6.3.2 On slide immunohistochemistry

This was performed for parasagittal brainstem sections.

Sections were mounted immediately after cutting onto electrostatically charged slides and dried overnight (or in an oven at 30°C for 2 hours). 3 washes of the slides with PB were performed, and they were subsequently blocked for 30 minutes in 5% normal donkey serum in PBT. Primary antibody in PBT and 5% donkey serum was added and left overnight at room temperature. After washing in PB, slides were incubated in secondary antibody in PBT plus NDS 2% for 4 hours at room temperature. Slides were

then washed 3 times and cover-slipped using fluorsave mounting medium before viewing/for storage at 4°C. The same antibody concentrations were used as for free floating immunohistochemistry.

2.6.3.3 DAPI counterstaining

In some cases, DAPI (2-(4-Amidinophenyl)-6-indolecarbamidine dihydrochloride) at 1:10,000 was applied to stain nuclei at the end of the IHC process. 5 minutes of incubation at room temperature was used. Sections were then washed and mounted/cover-slipped as described above.

2.6.3.4 Double immunohistochemistry

Where 2 antibodies were employed, both primaries were added to the slices at the same time in the concentrations described in table 2. Both secondaries were also added at the same time at the concentrations described in table 3. Care was taken in the choice of primary and secondary antibodies to avoid cross reactions.

2.6.3.5 Controls and need for amplification of native fluorescence

Primary antibody was omitted from negative control slides during immunohistochemistry, for example during cfos staining to test the specificity of any fluorescence. Most antibodies used in this study have been widely validated by the group in previous work, and therefore positive controls were not repeated (Cerritelli et al., 2016, Hickey et al., 2014, Li et al., 2016). The antibodies which had not been previously validated by the group were the rabbit anti oxytocin antibody (T4084 Peninsula) and the sheep anti tyrosine hydroxylase antibody (Millipore).

The oxytocin antibody has been previously used in a range of publications including (Mecawi et al., 2011, Sutton et al., 2014, Griffin et al., 2010). Immunoreactivity was not observed in oxytocin knock out mice or following a pre-absorption control (Griffin et al., 2010). The distribution of positive signal in the PVN was as previously reported for oxytocin neurons.

The tyrosine hydroxylase antibody was observed in areas known to have tyrosine hydroxylase activity, including locus coeruleus, A1/C1 and A2/C2. This antibody was

validated by the manufacturer using Western blotting, and reported to have positive staining in corpus striatum and adrenal medulla, but not liver. It has been reported in a range of publications including (Koblinger et al., 2014, Tsai et al., 2014).

The fluorescence signal from native TdTomato was very bright and was not enhanced using IHC at any point in the data presented here. IHC was performed to enhance intrinsic fluorescence from mCherry and eGFP where viral vectors were used for neuronal tracing. This was particularly of value for highlighting axonal terminals, which were challenging to visualise without amplification given their small size and distance from the soma.

Table 2.7 Primary antibodies used in this thesis

Antigen	Raised in	Concentration used	Company	Name/ catalogue no	Poly or monoclonal
Green Fluorescent Protein	Chicken	1:5000	Abcam	AB13970	Polyclonal
mCherry	Goat	1:2000	Biovision	5993-100	Polyclonal
Choline Acetyltransferase (ChAT)	Goat	1:200	Chemicon	AB144P	Polyclonal
Tryptophan Hydroxylase (TrH)	Mouse	1:300	Sigma	T0678	Monoclonal
Tyrosine Hydroxylase (TH)	Sheep	1:1000	Millipore	AB1542	Polyclonal
cfos	Rabbit	1:200	Santa Cruz	Sc-52	Polyclonal
cfos	Goat	1:200	Santa Cruz	Sc-52g	Polyclonal
Oxytocin	Rabbit	1:2500	Peninsula	T-4084	Polyclonal

Table 2.8: Secondary antibodies used in this thesis

Anti-	Raised in	Concentration used	Company	Name/ catalogue no	Alexa
Chicken	Donkey	1:1000	Jackson	703-545-155	488
Sheep	Donkey	1:200	Jackson	713-545-003	488
Goat	Donkey	1:1000	Molecular Probes	A11055	488
Rabbit	Donkey	1:500	Life technologies	A21207	594
Goat	Donkey	1:1000	Invitrogen	A11055	594
Rabbit	Donkey	1:1000	Abcam	Ab175651	405
Mouse	Goat	1:1000	Life technologies	A11001	488
Rabbit	Goat	1:1000	Invitrogen	A11012	594

2.6.4 In situ hybridization for validation of the CRH x Td mouse.

2.6.4.1 Rationale for experiment

As discussed in the introduction, using a Cre-lox system with a genetically modified reporter mouse line to identify a neuronal subtype, in this case CRH neurons, is in principle a simple, reliable and repeatable system. The major concern is that some neurons may have expressed CRH in development and no longer do so, but remain fluorescent as they have activated transcription of the gene for the fluorescent reporter protein (Schmidt-Supprian and Rajewsky, 2007). The gold standard for validation would be IHC for CRH and TdTomato protein, which has been reported by two different groups for this mouse line. Wamsteeker et al. (2013) have previously characterised the CRH x Td mouse line and report that 80.5+/-1.1% of PVH TdTomato neurons stain positive for CRH after colchicine treatment (2013). Chen et al. (2015) report even better co-localisation, without the use of colchicine (93.3 +/-1.2% of TdTomato neurons stain for CRH). Colchicine has been widely used in the past to allow visualization of CRH (as well as many other neuropeptides) in cell bodies (Rho and Swanson, 1989, Sawchenko and Swanson, 1985, Sawchenko et al., 1984a), due to its inhibition of microtubules, preventing axonal transport (Paulson and McClure, 1975). The possibility of repeating CRH IHC in-house was investigated, however it was anticipated that without colchicine treatment results would be unreliable at best, as the sensitivity of CRH IHC in this instance is greatly reduced (Prof S. Lightman, personal communication).

Therefore an alternative approach, using ISH, was used to examine co-localisation of CRH and TdTomato mRNA. The main area of interest for this thesis is CRH expression in the PVN, therefore PVN CRH and TdTomato expression was examined in this region and adjacent territories.

2.6.4.2 Method

The RNAscope®_2.0 Assay kit (Wang et al., 2012)(ACD-Biotechne, USA) was used for in situ hybridization, according to the manufacturer's instructions (Protocols 320535 and 320393).

As the native TdTomato fluorescence is exceptionally strong, some experiments were carried out with the aim of preserving this fluorescence and only probing for CRH mRNA.

Pretreatment 4 involved proteases, and this step was shortened on the manufacturers advice to try to preserve TdTomato. A further series used the standard protocol with fluorescent probes for both TdTomato and CRH mRNA.

Briefly, 2 CRH x Td mice were perfused with 4% paraformaldehyde (otherwise treated as for all mice undergoing perfusion), and tissue post-fixed in 4% paraformaldehyde overnight. A further 24 hours of incubation in 20% sucrose in PB then followed. 22μm slices in a 1:4 equal series through the PVN were obtained as before on a freezing microtome. 4 series were mounted onto superfrost plus slides and dried.

Pretreat 2 (Antigen retrieval) was applied at a low boil, after which 2 washes in distilled water were carried out, followed by a wash in 100% ethanol. The slides were then dried overnight. Pretreat 4 (Protease reagent) was applied for different lengths of time, as there was a possibility of preserving the native TdTomato fluorescence with a shorter treatment, which would mean that only one probe (for CRH mRNA) would be needed. The standard duration of 30 minutes was used for the multiplex CRH and TdTomato ISH and for controls. Incubation with pretreat 4 was performed at 40°C, and 2 washes in distilled water followed.

Table 2.9 summarises the timings of pretreat 4 and the experiments performed.

Table 2.9 Tissue used for ISH

CRH probe only (to compare with native TdTomato fluorescence)	**CRH probe plus TdTomato probe**	**Positive control probe**	**Negative control probe**
1 series for short pretreat 4 protocol (10minutes) 1 series for longer pretreat 4 protocol (20minutes)	1 series, standard pretreat 4 protocol (30 minutes)	1 series shared, standard pretreat 4 protocol (30 minutes)	

Probes and amplification treatments were then applied as summarised below:

- Probes applied for 2 hours at 40°C
- Wash 2X 2minutes in kit Wash Buffer
- Apply AMP 1-FL solution for 30 minutes at 40°C
- Wash 2X 2minutes in kit Wash Buffer
- Apply AMP 2-FL solution for 15 minutes at 40°C
- Wash 2X 2minutes in kit Wash Buffer
- Apply AMP 3-FL solution for 30 minutes at 40°C
- Wash 2X 2minutes in kit Wash Buffer
- Apply AMP 4-FL solution for 15 minutes at 40°C
- Wash 2X 2minutes in kit Wash Buffer
- Apply kit DAPI for 30 seconds at room temperature
- Mount and coverslip
- Stored at 4°C

2.6.4.3 Results and conclusion

The CRH TdTomato multiplex slides resulted in clear, bright co-localisation of red (TdTomato) and green (CRH) fluorescence (Figure 2.4).

Quality control (Figure 2.5A)

- the negative control probe was negative
- the positive control probe revealed scattered fluorescent puncta throughout the section

This suggests that the assay was performing as expected by the manufacturer, and that there is a low likelihood of false positive/negative signal.

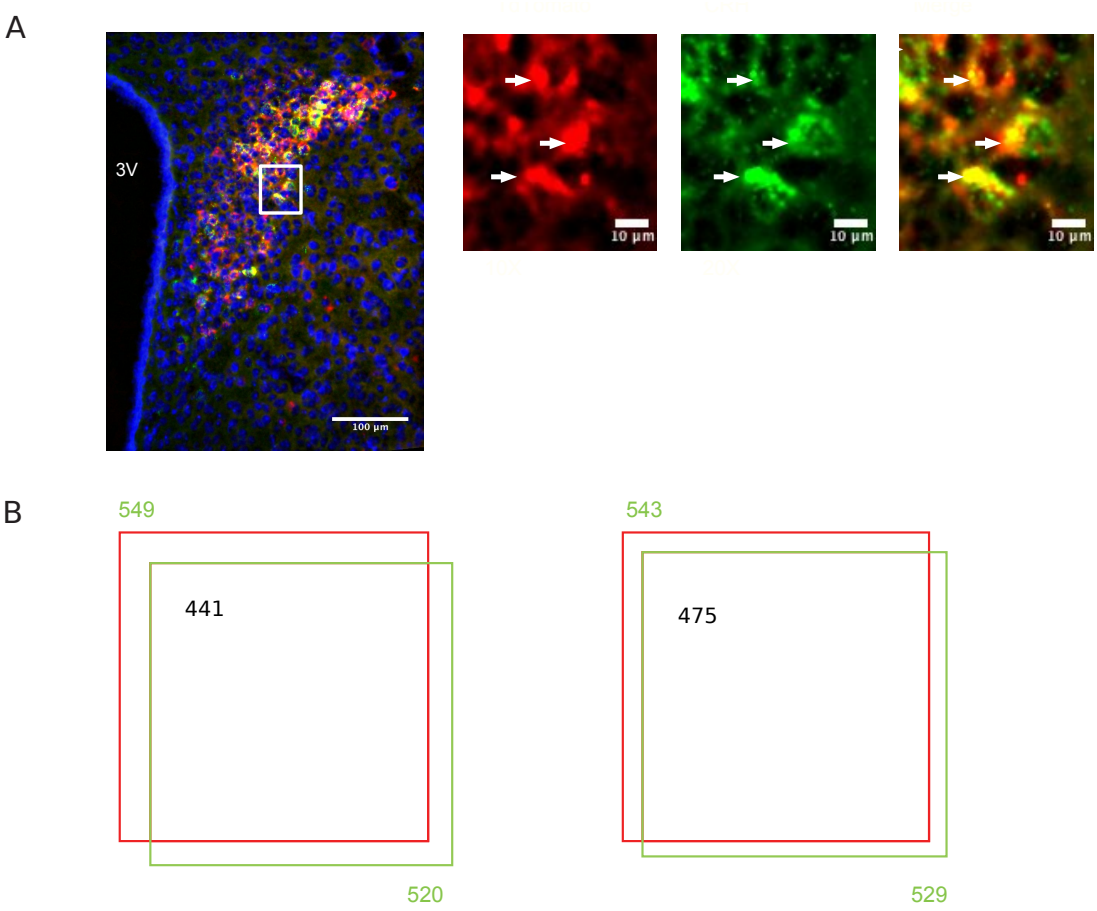

Figure 2.4 Results from multiplex ISH show co-localisation of CRH and TdTomato mRNA in the PVN

A Low power image of PVN after multiplex ISH, with DAPI (blue), TdTomato (red) and CRH (green). White square shows location of higher power images shown to right. Arrows indicate co-localisation of mRNA

B Diagrammatic representation of co-localisation for cells counted in 2 separate animals. Numbers are for total cells counted for TdTomato (red), CRH (green) and both (black)

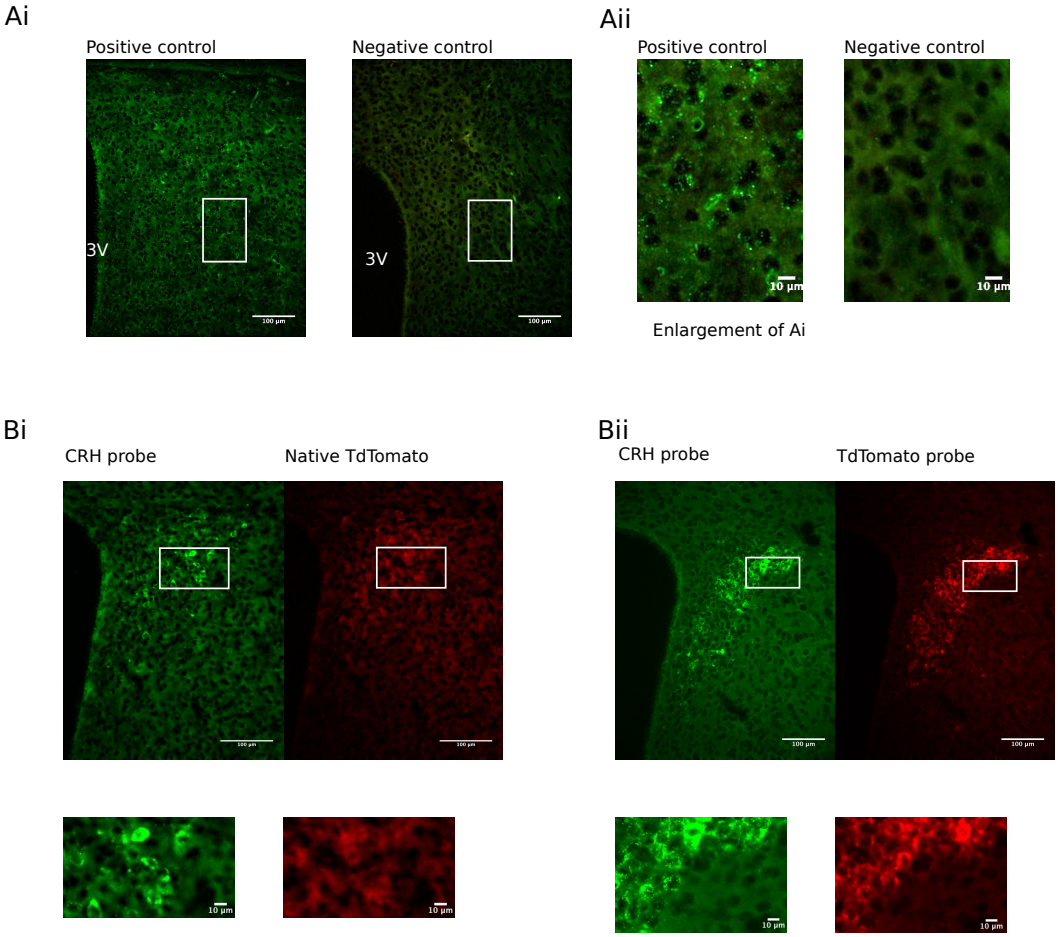

Figure 2.5 In situ hybridisation controls and comparison of probes
Ai Positive and negative control probes, ii zoomed in
Bi CRH probe (green) with partially preserved native TdTomato protein fluorescence (red).
ii Multiplex with CRH (green) and TdTomato (red) probes showing much clearer TdTomato signal.
Zoomed in images shown below main images. White square=zoomed in area, 3V=3rd ventricle

The slides in which native TdTomato fluorescence were to be preserved did not successfully preserve signal in either pre-treatment condition (only one shown). The fluorescence was much reduced compared to freshly mounted sections. Therefore as multiplex images were much clearer they were used for interpretation (Figure 2.5B shows comparison).

In sections from both of the mice, co-localisation of CRH mRNA (green fluorescence) and TdTomato mRNA (red fluorescence) was observed in most neurons visualised in the PVN (Figure 2.5). 87.5% and 80.3% of TdTomato neurons co-expressed CRH in the 2 animals.

This approach has now been published for these mice, (Harris et al., 2014), available as part of the Allen Mouse Brain Connectivity Atlas and the data presented here falls broadly in line with that report. The large majority of the TdTomato neurons seen in CRH x Td mice in the PVN are indeed CRH expressing neurons. A small number of false positive and negatives were observed. These cells may indeed express both CRH and TdTomato mRNA, but at levels which are not sufficient to be detected by IHC. Alternatively, these neurons may have expressed CRH at some point in their development, but not currently (false positives).

To be even more confident that all neurons identified were currently expressing CRH, an alternative strategy, for example, using injections of a Cre dependent viral vector in a CRH-Cre mouse could be used. Indeed, this strategy is employed for neuronal tracing studies (see chapter 3).

2.6.5 Microscopy and image processing

2.6.5.1 Conventional light microscopy

Histological sections were initially viewed on a Zeiss Axioskop 2 microscope (Oberkochen, Germany) and images captured using an AxioCam (Zeiss, UK) and the Axiovision 4.7 software (Zeiss, UK), using X10 and X20 objectives. The light source was a pE-2 LED excitation system (Cool LED, UK). Excitation and emission spectra are summarised in table 6.

Table 2.10 Axioskop excitation and emission wavelengths

Fluorophore/colour	Excitation LED	Filter sets nm
mCherry or TdTomato/Red	565nm	Excitation 560/40 Dichroic 585 Emission 630/75
eGFP / Green	490nm	Filter cube #10 (Zeiss)
DAPI / Blue	365nm	Filter cube #02 (Zeiss)

Tile scanning was performed using a widefield Leica DM1600 inverted epifluorescence microscope in the Wolfson Bioimaging facility. The camera was a Leica DFC365FX monochrome CCD. Images were acquired using a 20x objective with NA 0.4. The filter sets were as follows:

Table 2.11 DM1600 excitation and emission wavelengths

Fluorophore/colour	Filter sets nm
mCherry or TdTomato/Red	Excitation 560/40 Dichroic 595 Emission 645/76
eGFP/Green	Excitation 480/40 Dichroic 505 Emission 527/30
DAPI/Blue	Excitation 350/50 Dichroic 400 Emission 460/50

2.6.5.2 Confocal scanning microscopy

Confocal imaging was also carried out on some sections for confirmation of co-localisation. A Leica SP5-AOBS confocal scanning microscope (Leica, UK) was used (Wolfson Bioimaging facility). eGFP or Alexa488 (green) was imaged using a 100mW Argon laser, whilst TdTomato, mCherry or Alexa 594 (red) used a 2mW HeNe 594nm laser. A line average of 2 was used to reduce noise. Z stacks 0.5µm apart were obtained using the x40 oil immersion objective (NA 1.25), or x20 oil objective (NA 0.7) for analysis of co-localisation in cell bodies. Individual z planes were examined for evidence of co-localisation of red and green pixels. Where the confocal microscope is used, this is

stated in the figure legend. All other images were generated by conventional microscopy.

Software for image acquisition on all Wolfson Bioimaging microscopes was Leica-LASX.

2.6.5.3 Image processing and analysis

All files were saved in the .TIFF format and processed using FIJI software (Version 1.0 (Schneider et al., 2012, Schindelin et al., 2012)). All comparative images taken from a single experiment were acquired with the same exposure times and using identical filter and laser settings where applicable. Any adjustments to brightness and contrast from within FIJI were also applied to all comparable images.

Quantitative analysis of cell bodies largely involved manual counting of all visualised cells in a defined area. A particle counting plugin provided by FIJI was used to quantify cfos expression in the PVN from 20X widefield images. For this, thresholding was first performed using the Otsu algorithm. The thresholded, binarized image was processed by the FIJI particle counter. The same parameters were applied to all images counted in this way.

Mapping of mCherry fibres was performed after amplification of the signal using immunohistochemistry. Images were captured using the widefield tile scanning microscope and a X20 objective. The density of labelled fibres was assigned a value of 0, +, ++, +++, ++++ (from zero to maximal expression as observed in the NTS) for each area of interest and mapped onto the mouse brain atlas (Franklin and Paxinos, 2007) as colour coded shading. Quantification of fibre density was performed comparing the DMN, NTS and hypoglossal nuclei in the same slice in 3 mice. 2 parasagittal sections were imaged for each mouse, at lateral 0.04 and 0.24mm from the midline. 6 100x100micron boxes were placed evenly rostral to caudal within each nucleus and fibre counts determined within each box. Fibres were only counted if they were clearly linear structures, with length at least 5µm. Puncta were not counted for this analysis. These values were then summed for each mouse.

2.7 In vitro hypothalamic slicing and recording

These methods were employed throughout chapters 4 and 5

2.7.1 PVN Slices

Hypothalamic slices were prepared from mice at 6-12weeks, which were schedule 1 culled by cervical dislocation followed by decapitation. The brain was removed and bathed in ice-cold artificial CSF (aCSF, see below). A coronal block containing the hypothalamus was glued to the vibratome stage, caudal surface down, and 300µm thick coronal slices were cut using a vibratome (Dosaka LinearslicePro 7; DSK, Japan) in cold (4°C) aCSF. Slices were incubated at 37°C in carbogenated aCSF for 20 minutes to remove/reduce dead surface cells. Slices were then kept at room temperature in carbogenated aCSF for at least 1 hour before recording.

2.7.2 Electrophysiology

Slices were transferred into the recording chamber of an upright fluorescence microscope (Eclipse E600FA, Nikon, Japan), superfused with aCSF containing the following (mM): NaCl 127, KH_2PO_4 1.2, KCl 1.9, $NaHCO_3$ 26, $MgCl_2$ 1.3, $CaCl_2$ 2.4, and d-Glucose 10, saturated with 95% O2/5% CO2, pH 7.3, 36.5°C at a rate of 2–3ml/min. aCSF containing lower glucose (2.5mM and 0.5mM) used mannitol substitution to compensate osmolarity (300-310mosm). Patch pipettes (4–7 MΩ) were pulled from borosilicate glass (GC120, Harvard Apparatus, UK) and filled with internal solution containing the following (mM): K-gluconate 140, KCl 10, Na-HEPES 10, NaATP 2, EGTA 1, KOH 4, Sucrose 4. All membrane potentials were corrected for junction potential of 15 mV.

Fluorescent CRH neurons (TdTomato) were firstly identified using epifluorescent illumination and then the soma identified using DIC contrast with a 40X water immersion objective (Nikon, Japan, NA 0.8). A MP225 manipulator (Sutter, CA, USA) was used to manoeuvre the patch pipette to the cells. Recordings were made in current-clamp mode in the whole cell configuration. Current pulses were injected to examine the current-voltage and current-spike frequency relationships (Multiclamp 700A amplifier; Molecular Devices). The signal was filtered at 3 kHz, digitized at 10 kHz

(micro1401, Cambridge Electronic Design, UK), and stored using Spike 2 software (Cambridge Electronic Design, UK).

The threshold for action potential discharge was determined as the point at which the rate of change of membrane potential exceeded 7.5 V/s and all spike parameters were measured with reference to this point (using a custom Spike2 script).

2.7.3 Calcium imaging

Calcium imaging experiments used hypothalamic slices prepared from CRH x GCaMP6f mice (cutting protocol as above). Slices were transferred into the recording chamber of the 2-photon microscope (Prairie Technologies) and perfused with aCSF as for electrophysiology. A 16X water immersion objective (NA=0.8, Nikon) was used throughout. Fluorescent CRH neurons expressing native GCaMP6f (and in some cases additional native TdTomato) were identified in the PVN using direct epifluorescence (LED) prior to switching to 2-photon mode. GCaMP6f was excited using a tuneable Ti:Sapphire pulsed laser (~100 fs pulse width, MaiTai HP, SpectraPhysics) at 940nm, and a XY plane was delineated containing a hemi-PVN to one side of the third ventricle. The depth of field of view in focus was 1-2µm. The zoom required to encompass a hemi PVN ranged from 1 to 1.6X. Data was collected using PrairieView acquisition software at a rate of between 0.4 and 0.5Hz (slight variation due to differences in zoom used altering the time taken to acquire each image). Resolution was 1024 X 1024 pixels, and data was collected using a high sensitivity photon detector (GAASP PMT) and a GFP filter at 525/70nm, with a dichroic at 565nm. The TdTomato filter, where used, was 595/50nm. File sizes were around 2-3GB for an experiment lasting 20minutes. Longer recording times were avoided as they were prone to data loss due to errors in processing and conversion of files at the end of acquisition. For this reason, in most cases the recording was split into 2 parts (each of 20minutes) to allow experiments lasting ~40minutes to be carried out.

As discussed in the introduction, the fluorescence signal from GCaMP6f at basal levels of calcium is low- which is an advantage of the dye in terms of dynamic range. However, this made it impossible to confidently localise the non-activated CRH cells in the slice in any experiments. In order to clearly identify all the GCaMP6f cells which were present in

the slice, aCSF with 40mM potassium was applied at the end of each experiment, depolarising cells and raising their calcium levels, making all of the CRH neurons fluoresce.

Table 2.12 Drugs used in electrophysiology and calcium imaging.

Drug	Catalogue no	Stock concentration	Concentration in bath
Tetrodotoxin (TTX)	1078	1mM	500nM
D-AP5	0106	50mM	50μM
CNQX	1045	10mM	10mμM
Picrotoxin	1128	50mM (DMSO)	100μM

All drugs were obtained from Tocris (Biotechne)

2.8 Pipeline for processing of calcium imaging data

All initial analysis was performed in FIJI

- Data saved as .tiff uploaded to FIJI. Image series, (typically 1200 images for one experiment) concatenated to make a single file using FIJI.
- Registration to align all images and correct for movement in xy carried out using the template matching plugin (FIJI, (Tseng et al., 2012)). The region of interest to register outlined as a rectangular region encompassing PVN.
- Maximum projection over time and standard deviation of images over time generated in FIJI.
- Regions of interest drawn manually using these maximum projection images to identify cells, many of which only became visible for short periods or during application of high potassium.
- Background subtraction process applied to the registered file with using the FIJI standard background subtraction process, with a 50-pixel rolling ball. This is a widely used method to remove uneven background signal. Objects smaller than the ball (here 50 pixels, ~22microns, which is approximately 2 times the size of a neuronal soma) are counted as foreground and preserved.

- FIJI Multimeasure function applied to subtracted image series to generate a mean pixel value for each region of interest for each image in the series. Result saved as .csv
- Imported into Matlab for next steps in analysis.
- Convert data into $\Delta F/Fo$ format for each ROI, where the baseline (Fo) is the mean of the lowest 5% of values for that ROI, as measured over the entire time series.

A visual example of the effect of registration and background subtraction is provided in Figure 2.6

- Data thresholding (see also figure 2.7).
    - For glucose excited cells (GE), find mean and standard deviation of baseline $\Delta F/Fo$ (last 100s (50 values) before change to low glucose solution).
    - Find mean of final 100s (50 values) in low glucose solution (response). If response >3SD below baseline mean, consider as GE.
    - Exclude if falling baseline (and no sign of a washout), no response to K, or random events visible in trace.
    - For glucose inhibited cells (GI), plot mean of baseline $\Delta F/Fo$+3SD. If > 2 values above this line in low glucose period, consider as candidate GI cell. Then exclude as above, in particular, if spontaneous activity at the same level or greater is seen in the control period.

2.8.1 Measuring size of response to low glucose in GE cells

These cells exhibited a relatively consistent profile of response, examples of which are shown in Figure 2.7. The size of response was assessed using the raw fluorescence data. This was preferred to the $\Delta F/Fo$ as it compared the absolute change in fluorescence, rather than the relative change. The relative change is highly useful for identifying events within a single trace, but less so when comparing responses between different cells as it is dependent on the maximum and minimum observed responses within a

trace, which are not consistent between cells. A rolling mean with a timeframe of 40 seconds (20 images) was calculated in Matlab. From this, the highest value in the timeframe prior to change of solution (x) and the lowest value during the response period at the end of perfusion with low glucose solution (y) were obtained using peak and trough functions in Matlab. Peak and trough levels were preferred to simply fixing a time point to measure the response, as not every trace showed a maximum or minimum at the same time point, leading to underestimates of the size of response in some cells. The normalised value x-y/x was then calculated. See Figure 2.8 for a visual summary.

2.8.2 Measuring size of response to low glucose in GI cells

The profiles of the responses in these cells was much more heterogenous both within and between experimental conditions (Figure 2.9). The combination of some spiking cells and others with slower response profiles was a challenge, as a mean or peak measurement as used for GE cells did not accurately represent all of the data. Area under the curve was also unsatisfactory as spiking cells were not well represented. The method which seemed best able to detect both spiking and slow rising responses was a measure of the amount of time spent with calcium levels >3standard deviations above the mean of the baseline (with the maximum possible time set as 450seconds). A maximum time was set as there is a small amount of variation in the duration of time it takes to capture one image, depending on the degree of zoom, and this standardised all of the data to include the same number of data points. Having plotted a series of mean GI response traces to assess the time course of GI responses, the response period was measured from +100 images (~200s) after onset of low glucose to +300 images (~600s), as this contained the maximal response in most cells. See Figure 2.9 for a visual summary of this measure.

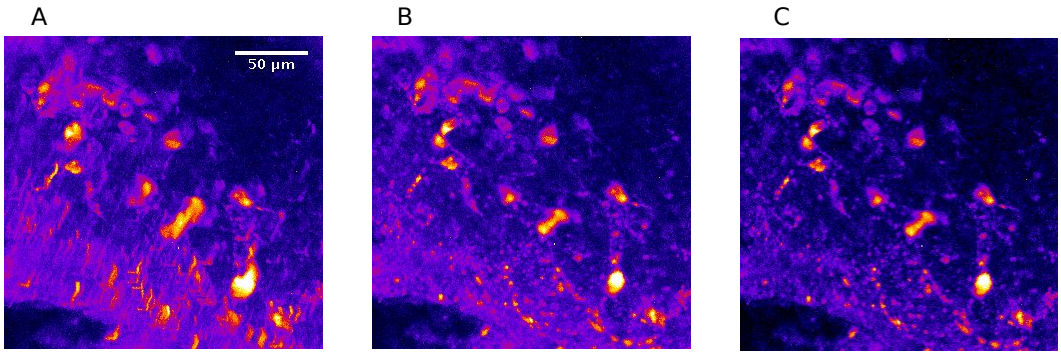

Figure 2.6 Effects of processing in FIJI on calcium images
A Projection of maximum fluorescence over time using raw images (with false colour). Note 'smearing' of cell outlines due to movement in xy over time
B Same projection after application of the template matching registration algorithm. xy movement largely corrected
C Same projection after background subtraction.

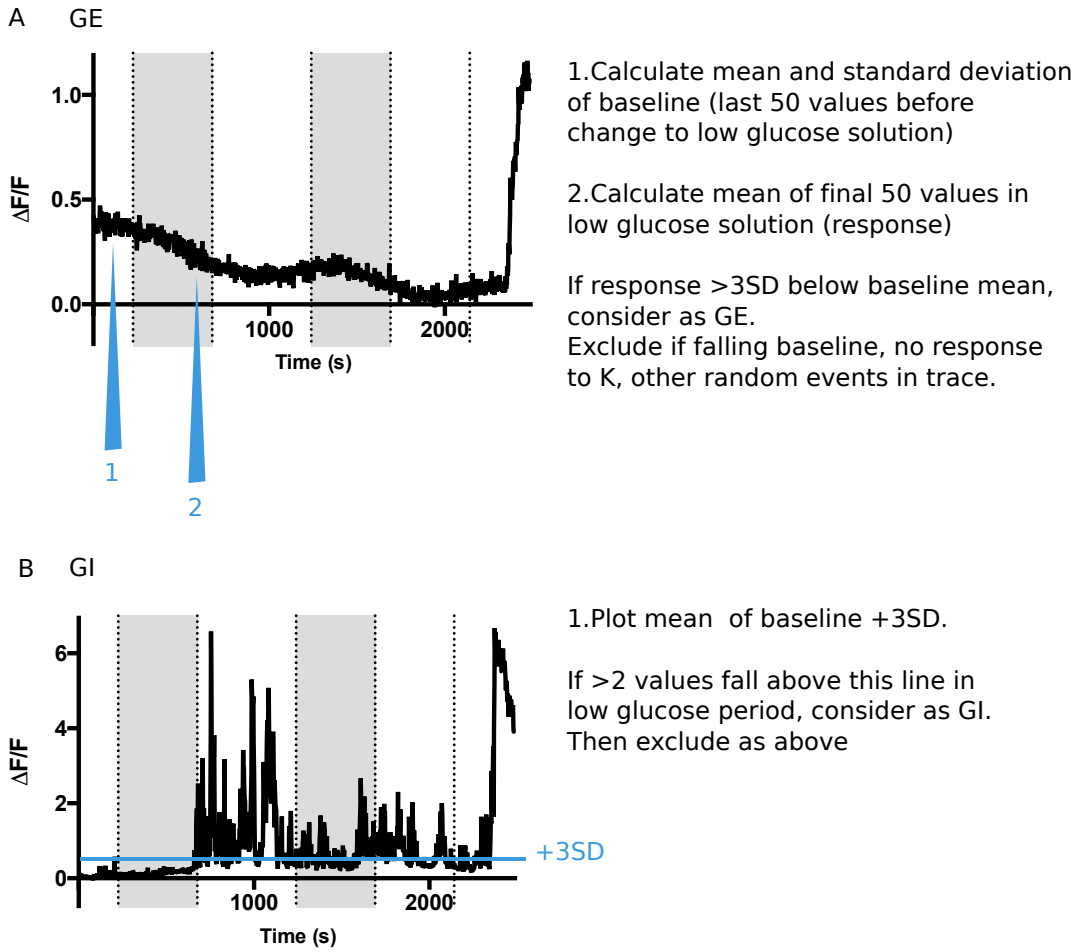

Figure 2.7 Data processing pipeline for calcium imaging data
A GE
B GI

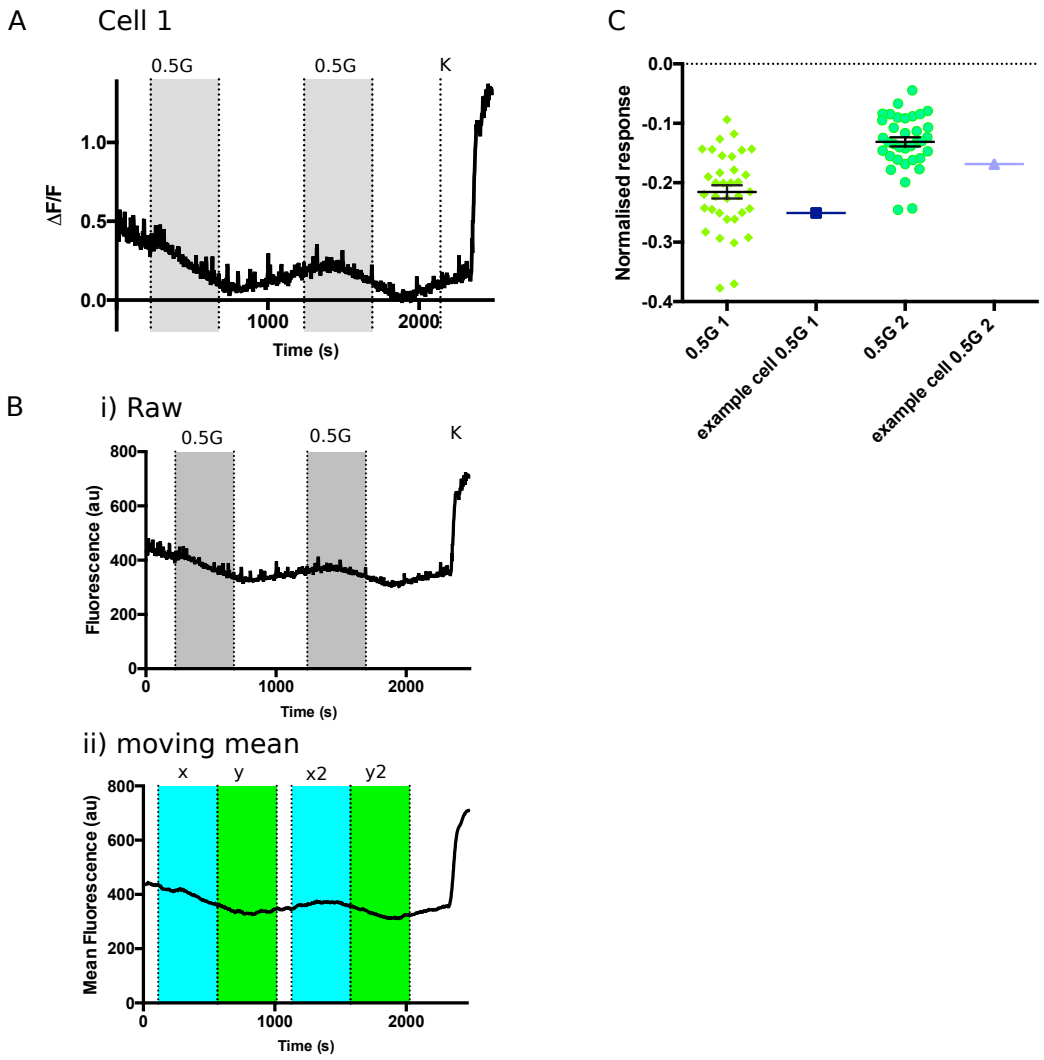

Figure 2.8 Illustrating calculation of effect size for GE cells
A Example of GE cell, normalised trace.
B Cell from A redrawn using i) raw data, ii) following application of moving mean
blue shaded area=period from which mean for baseline (peak) is obtained, green shaded area=period from which mean for response (trough) is obtained. Normalised value calculated as (y-x)/x
C Data for a set of GE cells obtained as illustrated in B. Example cell shows where Cell 1 falls in this dataset.

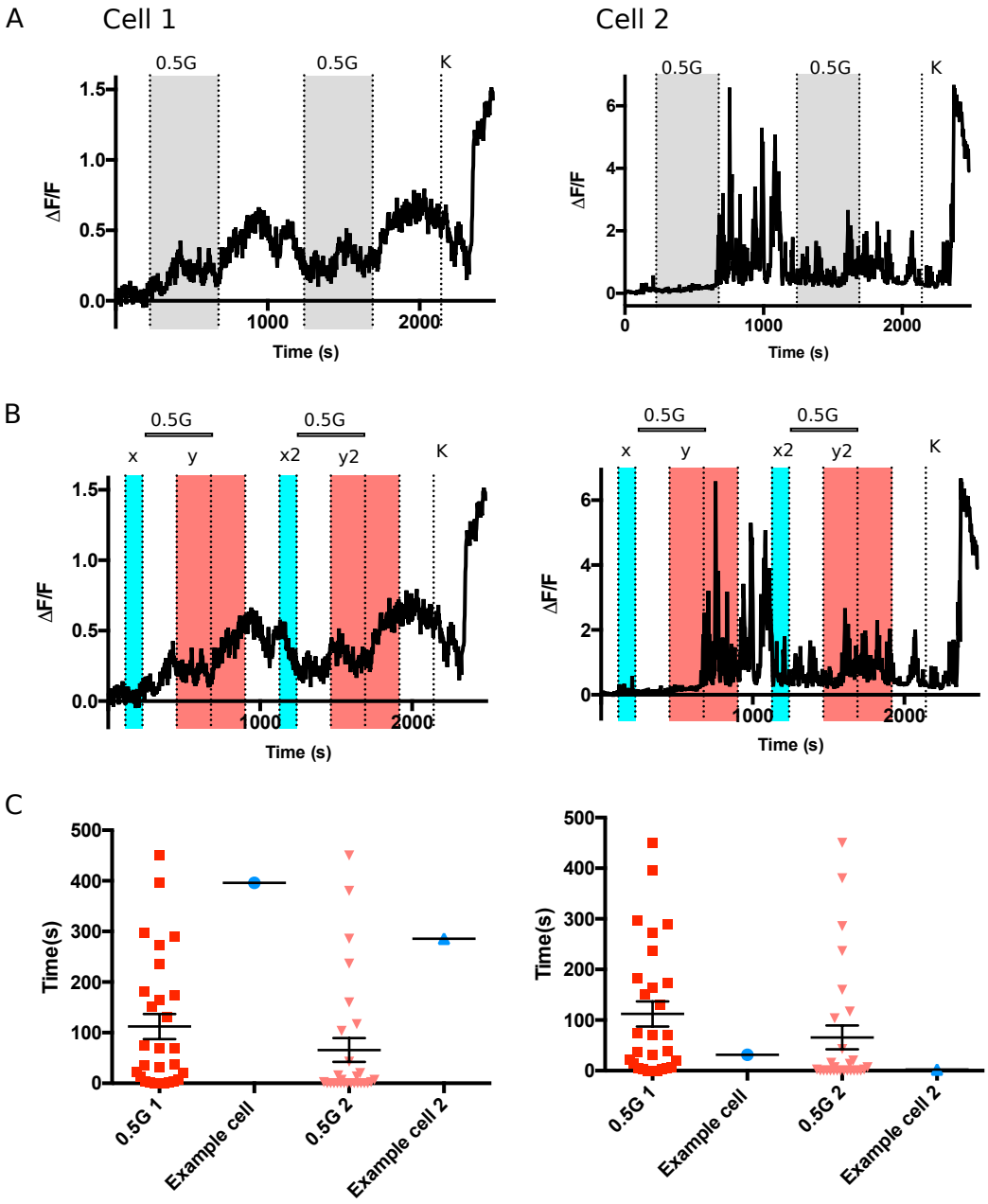

Figure 2.9 Illustrating calculation of effect size for GI cells
A 2 examples of GI cells, normalised traces, one slow rising, one spiking.
B Cells from A redrawn, blue shaded area=area to obtain mean and standard deviation for baseline, red shaded area=area to obtain number of points greater than 3 standard deviations above the mean of the baseline.
C Data for a set of GI cells including these examples. Example cell shows where cells shown here fall in this dataset.

2.9 Hypoglycaemic models

Please see Chapter 6 section 6.1 for a detailed discussion of models of hypoglycaemia and HAAF in human, rat and mouse studies.

2.9.1 Mouse model of single hypoglycaemia

After acclimatization to handling and daily i.p injection (with saline 50µl per day for 7 days), mice were injected with short acting insulin i.p (2.5U/kg, Humulin S, Lilly, USA) and confirmed to have blood glucose <4mmol/L at 30 minutes from a tail tip blood sample using a handheld glucometer (Onetouch, Lifescan, UK). A control group received saline injections in place of insulin.

Following the completion of the protocol, mice were terminally anaesthetised and perfused/fixed as described in section 2.6.2.1 for immunohistochemistry.

2.9.2 Mouse model of recurrent hypoglycaemia

Mice fasted for 2 hours, and then were injected i.p with rapid acting insulin (2U/kg, Lispro (Humalog), Lilly, USA). Fasting was used in this protocol as it allowed a lower insulin dose to be used, but with reliable development of hypoglycaemia. The insulin used here is more rapid acting than that used for single hypoglycaemia, with the aim of achieving rapid development of hypoglycaemia at lower dose, followed by reliable recovery. Mice were confirmed to have blood glucose <4mmol/L, 30 minutes after each i.p injection using a handheld glucometer (Onetouch, Lifescan, UK). This was repeated a total of 4 times over a 48 hour period. Figure 2.10 is a summary. Control groups received saline injections in place of insulin (CT), or saline followed by a final single insulin injection (SH).

Following the completion of the protocol, mice were either terminally anaesthetised and decapitated for collection of truncal blood for radioimmunoassays, or kept until the following day to obtain brain slices for calcium imaging.

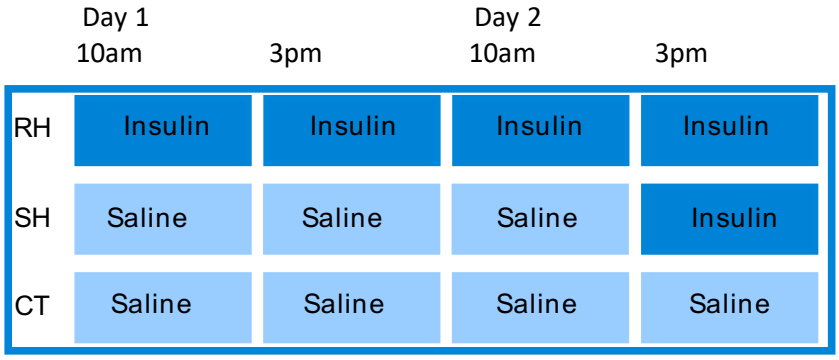

Figure 2.10 Injection schedule for mice in 3 groups
RH (Recurrent hypoglycaemia), SH (Single hypoglycaemia), and CT (control saline injected).

2.10 Radioimmunoassays

These assays were used in chapter 6.

2.10.1 Truncal blood collection

Samples for use in RIAs were collected onto ice from truncal blood, with 0.5M EDTA, 100µL/mL added to prevent clotting and 1mg/mL aprotinin, 50µL/mL added to inhibit protease activity. Plasma was obtained by centrifuging samples for 15minutes at 3000rpm at 4 ˚C and collecting the supernatant into 100µL aliquots. These were stored at -80˚C.

2.10.2 Glucagon RIA

2.10.2.1 Experimental procedure

A glucagon RIA kit (GL-32K, Merck Millipore, Germany) was used according to the manufacturer's instructions. The kit uses iodine-125 as the tracer, with gamma radiation measured using a gamma counter (NE1600, Nuclear Enterprises, Edinburgh UK). This is a competitive binding assay, using a known, limited concentration of glucagon antibody to bind an unknown amount of glucagon in the sample, which is in competition with a quantity of radioactive tracer glucagon. As the amount of glucagon present in the unknown sample increases, the amount of radioactive tracer bound glucagon which can bind to the antibody will decrease and thus the gamma radiation count will decrease.

Briefly, a standard curve was prepared using serial dilution of glucagon (400pg/mL) supplied in the kit to obtain standards of 25, 50, 100, 200 and 400pg/mL. Standards, quality controls and samples were all pipetted in duplicate. 50µL of each sample was used rather than the 100µL samples suggested in the assay. This was because all of the mice had undergone some degree of fasting, and the SH and RH mice were all hypoglycaemic at the time of blood collecting. Therefore, many of the glucagon levels were expected to read higher than the fed or baseline range.

- Each tube was incubated with 100µL glucagon antibody at 4˚C overnight.
- 100µL glucagon I-125 tracer was then added to each tube and incubated at 4˚C overnight.
- Precipitating reagent was then added for 20minutes, after which each tube was vortexed at 2000xg for 20 minutes at 4°C.
- The supernatant was then decanted and discarded and the remaining radioactivity in the pellet counted using a gamma counter.

2.10.2.2 Analysis

A number of definitions were assigned:

Total binding: maximum possible binding of tracer to antibody. Tubes containing glucagon antibody, tracer and no sample or standard.

Non-specific binding: Count due to binding of tracer to substances other than the antibody- e.g. interior of assay tube, assay buffer. Tubes where glucagon tracer with no antibody was added.

The **mean count** was calculated for each duplicated pair of results. The count reflecting non-specific binding was subtracted from all other results.

The % total binding was then calculated for each standard and each sample as follows:

(Sample or standard/Total binding)x100

The standard curve % total binding was plotted against the known standard concentrations and the line of best fit determined.

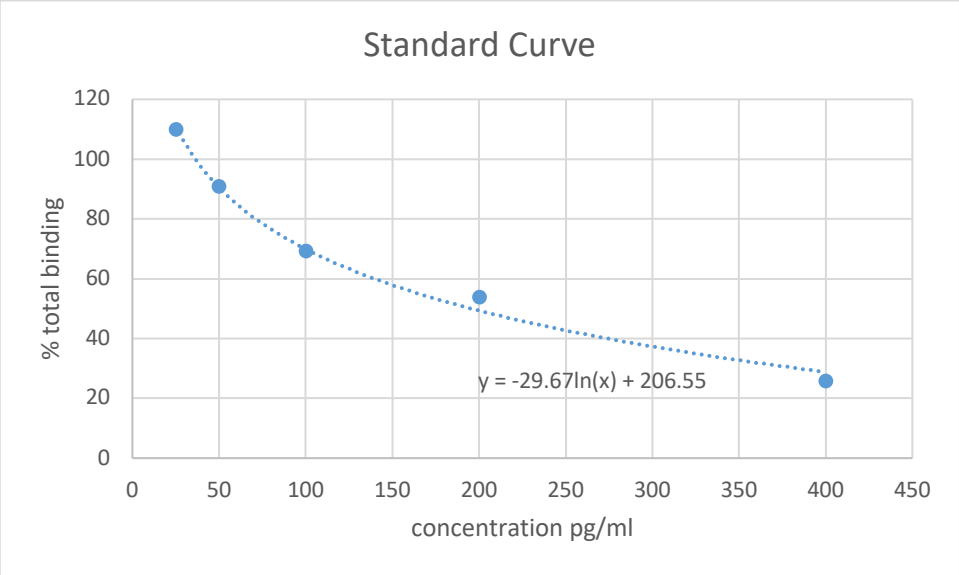

Figure 2.11 Standard curve and line of best fit for glucagon assay.

Internal quality controls were then calculated from the line of best fit equation as follows:

QC1 48.9pg/mL at start of assay, 58.2pg/mL at end (acceptable range 35-73pg/mL)

QC2 106.8pg/mL (acceptable range 98-205pg/mL)

The assay was therefore accepted as valid.

The results for the samples were calculated and corrected for a dilution factor of 2 (50µL input rather than 100µL). The normal fasting range is 50-150pg/mL. The values obtained for samples from the RH protocol ranged from 43.8 to 693.8pg/mL.

2.10.3 Corticosterone RIA

This assay was kindly carried out by Mrs Yvonne Kershaw in the Dorothy Hodgkin building according to their standard protocol for corticosterone assays. This is a competitive binding RIA using corticosterone bound I-125.

Solutions:

- *B Buffer* 7.3g Tri-sodium citrate [$HOC(COONa)(CH_2COONa)_2$], 6.9g Sodium dihydrogen orthophosphate [NaH_2PO_4], 1g BSA in 1L H_2O, pH 3 with HCl
- *Charcoal solution* 0.5g Dextran T70, 5g Charcoal in 1L B Buffer
- *Tracer* I-125 Corticosterone (cat no IRC-123 Izotop, Institute of Isotopes, Hungary), diluted to give 3500-4000 CPMs per 50µL
- *Antibody* Donation from Gabor Makara, Hungary, diluted 1:50
- *Stock standard* (10ng/100µL), serially diluted with 100µL of B buffer (C2505, Sigma, UK)
- *Quality controls* QC20 & QC100 (Sigma, UK)

Construct the assay as shown below (all volumes are in µL)

Table 2.13 Corticosterone RIA construction

Tube no.	Description	B Buffer	Sample	Ab	Tracer
1-3	Total (T)	0	0	0	50
4-6	B0	100	0	0	50
7-28	Standards	100	0	50	50
29	QC20	0	100	50	50
30	QC100	0	100	50	50
31-174	Samples	50	50	50	50

- Shake/vortex for ~5 seconds
- Incubate overnight at 4°C
- Add 500µl of charcoal solution to each tube except T (totals) and gently shake/vortex.
- Centrifuge for 15 minutes at 4000RPM and 4°C

- Aspirate off supernatant immediately
- Count tubes using gamma counter.

Data was provided in the form of the raw counts, standard curve and final calculated values. Quality controls were in range according to the acceptable limits used routinely by the lab.

2.11 Statistical analysis:

Data were analysed in GraphPad Prism. A D'Agostino-Pearson omnibus normality test was used to test for normal distribution of data. Results are displayed as mean ± standard error unless otherwise stated. Comparison of normally distributed groups of data is performed using Student's *t*-test or one way ANOVA with Sidak's multiple comparisons test for parametric data. Non-normally distributed data is analysed using Mann-Whitney or Kruskal Wallis with Dunn's multiple comparisons and displayed as median ± interquartile range (IQR). Categorical data is analysed using Chi-square. The statistical tests used in each case are described in detail in the relevant results chapter and/or figure legend.

Chapter 3 CRH neurons in the paraventricular hypothalamus project widely to autonomic areas of the brainstem

3.1 Introduction

Projections to autonomic areas of the brainstem from CRH neurons are an important alternative means by which these neurons could effect responses to hypoglycaemia, by activation of neurons contributing to sympathetic outflow. This chapter firstly discusses what is known about the projections of CRH PVN neurons to destinations other than the median eminence and pituitary gland. Reports from non-neuronal subtype specific studies of PVN projections are also presented. Most work examining projections from the PVN and indeed CRH neurons has been carried out in rats, and the differences between mouse and rat PVN anatomy is briefly discussed. The advantages of viral vector neuronal tracing techniques for more detailed study of neuroanatomy are considered. Results are then presented for retrograde and anterograde tracing experiments to demonstrate projections from CRH PVN neurons to specific autonomic brainstem areas.

3.1.1 Initial identification of CRH neurons and early tracing experiments (rat)

Following the identification of CRH expressing neurons by Bloom and colleagues (1982) further work identified a wide range of other sites where CRH positive cells and their projections could be found (Swanson et al., 1983). Adrenalectomy and colchicine were both shown to increase CRH signal, colchicine throughout the brain, adrenalectomy solely in cells of the PVN. However, it was difficult at that time to unpick which groups of neurons were projecting to which areas, as immunohistochemistry could only determine whether a cell body or terminal expressed CRH, but not where terminals originated. In addition, not all axons were visible under these conditions.

A large body of early work was performed in rats. In particular Swanson et al. (1983) and Simmonds and Swanson (2009) extensively investigated PVN neuronal populations and their projections. These studies used injection of fast blue into the bloodstream to identify neuroendocrine neurons, which will stain positive for fast blue as their terminals lie in the median eminence, which is outside the blood brain barrier. This has been

shown to identify at least 98% of neuroendocrine neurons (Markakis and Swanson, 1997). Non-neuroendocrine cells will not stain positive as they have no direct connection to the circulatory system. Simmons and Swanson (2009) largely focussed on identifying the anatomical location of different neuronal subtypes within the PVN. They show that fewer than 1:10 CRH neurons are non-neuroendocrine, and that in the rat these neurons are scattered rostro-caudally throughout the PVN, although interestingly they do not appear within the central core of the neuroendocrine CRH population. The earliest demonstration of CRH neurons projecting to the brainstem and spinal cord was performed by Sawchenko (1987b). Fast blue dye was injected into the area postrema/NTS/DMX of a group of rats, and a second set of experiments injected fast blue into the thoracic spinal cord. The fixed brains were then stained for both vasopressin and CRH and examined for colocalization with fast blue in cell soma in the PVN. Colchicine was used in a subgroup of animals and was shown to be required to allow identification of CRH neurons. In both the brainstem and spinally injected animals, CRH colocalization was demonstrated with fast blue, indicating a population of CRH neurons projecting to the brainstem and spinal cord. Sawchenko suggested that around 5.5% of the CRH neurons of the PVN could be pre-autonomic. This pre-autonomic population has frequently been disregarded when considering the CRH neuronal population. However, given that there are thought to be 2000 CRH neurons in rat PVN, even 5-10% of this number would still represent around 100-200 neurons.

In addition to examining the location of different neuronal subtypes within the PVN, further work has examined the projections of neurons of the PVN to brainstem centres. Projections of neurons in the PVN to brainstem autonomic areas have been widely described in the rat, with areas including NTS, DMX, RVLM, locus coeruleus, and nucleus ambiguus (Swanson et al., 1987, Sawchenko and Swanson, 1982, Swanson et al., 1986). These are all important contributors to sympathetic outflow, and a CRH projection to these areas would certainly be a potential means to modulate SNS activation. A particularly detailed and comprehensive study was performed by Geerling et al. (2010) which used phaseolus vulgaris leucoagglutinin (PHAL) injected into the PVN as an anterograde tracer to identify a wide range of PVN terminals in the areas summarised in table 3.1. This work was all performed examining the projections of all neurons, rather than describing what the individual neuronal subtypes do (i.e. CRH). The most extensive

projection to the brainstem of PVN terminals, observed in the majority of reported studies, is the nucleus of the solitary tract, a significant autonomic relay area.

Table 3.1 PVN Projection targets in the brainstem courtesy of Geerling et al. (2010)

Midbrain	Ventral tegmental area Edinger-Westphal nucleus Ventrolateral periaqueductal gray matter Reticular formation Pedunculopontine tegmental nucleus Dorsal raphe nucleus
Dorsal pons	Pre-locus coeruleus Viscerosensory subregions of the parabrachial nucleus.
Ventral medulla	Superior salivatory nucleus Retrotrapezoid nucleus Compact and external formations of the nucleus ambiguous A1 and caudal C1 catecholamine neurons Caudal pressor area
Dorsal Medulla	Medial nucleus of the solitary tract (including A2 neurons) Dorsal vagal nucleus Area postrema

3.1.2 CRH specific projections to autonomic areas of the brainstem

Whilst the reports presented thus far provide evidence that some CRH neurons are indeed pre-autonomic, the destination of these autonomic projections had not been extensively investigated in detail, and until very recently no studies had been carried out in the mouse. Indeed, in many cases all that can really be stated with confidence is that these neurons are not projecting to the median eminence. More recent retrograde studies have demonstrated some further specific CRH connections via the brainstem. Work by Stanley and colleagues using pseudorabies virus injections in mice demonstrated connections from white adipose tissue and the liver to the PVN, possibly via the DMX and pontine reticular nucleus (Stanley et al., 2010). Co-localisation was demonstrated with both oxytocin and CRH. A similar study by Jansen et al. (1995) used pseudorabies viral tracing in rats to demonstrate a connection between the stellate ganglion and the PVN, with 5% of the neurons identified reported to express CRH.

However, in both cases the study could not specifically identify the CRH pathway to the brainstem, as it was a multi-synaptic tracing study carried out over time.

3.1.3 Anatomy of the PVN in the mouse

Whilst PVN neuroanatomy has been extensively investigated in the rat, much less work has been done in the mouse. Similar cell groups and functions are ascribed to the PVN, but it is clear that even at a superficial level, there are significant differences in the neuroanatomy of the two species. Whilst the rat PVN exhibits closely packed neurons, and a clear delineation between magnocellular and parvocellular compartments, in the mouse the neuronal subtypes are much more mixed, and the limits of the rostral and caudal PVN are much less easy to delineate using Nissl staining (Biag et al., 2012). One publication which sought to address this examined neuropeptide expression and autonomic projections in the mouse PVN (Biag et al., 2012). They examined the distribution of neuronal subtypes within the PVN using fast blue and fluorogold in a similar fashion to that described above using fast blue in the rat. In addition to labelling neurons with projections to the median eminence, they also injected labels into the spinal cord and DMX/NTS to identify neurons projecting to brainstem autonomic centres. It is clear that the majority of pre-autonomic neurons identified in this study are located caudally within the PVN. The minority which are more rostral are present along the ventral border of the PVN. Biag and colleagues did not go on to examine whether any of their pre-autonomic neurons expressed neuropeptides other than oxytocin and vasopressin.

3.1.4 Colchicine treatment to facilitate neuropeptide immunohistochemistry

One of the challenges of identifying CRH neurons in all the work described above has been the need for colchicine treatment in most IHC studies, to retain CRH in cell somata and allow their identification. This problem is not limited to CRH neurons and affects a large number of peptidergic neuronal subtypes. Colchicine acts to inhibit microtubule activity, preventing transport of neuropeptides to terminals and therefore concentrating them in the cell somata (Paulson and McClure, 1975). Colchicine treatment is in itself a stressful experience for the animal, and we know that such stress can alter neuropeptide expression in the PVN (Swanson et al., 1986). In addition, colchicine has

been observed to alter neuronal morphology (Rho and Swanson, 1989, Berkenbosch and Tilders, 1988).

3.1.5 CRH neuronal subtype specific investigation

Genetic modification ± viral tracing techniques have enabled the use of reporter molecules in mice to visualize CRH neurons without the need for colchicine treatment (Wamsteeker Cusulin et al., 2013, Alon et al., 2009, Taniguchi et al., 2011). These gene-reporter systems have been validated using fluorogold and CRH in the PVN, showing that the fluorescently labelled neurons do indeed express CRH. The evidence for this and an in-house validation using ISH are covered in detail in Chapter 2, section 2.6.4.

3.1.6 Advantages of viral tracing techniques

The advent of viral vectors carrying reporter proteins has allowed investigation of neuroanatomy with greater precision and sensitivity than earlier techniques (Kantor et al., 2014). In particular, use of the cre-lox system makes it possible to examine the connections made by a specific sub-population of neurons, delineated in time, space and by their neuronal subtype marker. The choice of viral vector allows tracing to be carried out in an anterograde or retrograde direction or indeed across multiple synapses. A wide range of viral subtypes have been used for research purposes (Nassi et al., 2015). Some commonly used viral vectors used in the CNS are summarised in table 3.2. Of note, the choice of vector can determine whether the virus transduces cell soma at the injection site, axon terminals, or both. This will affect whether anterograde or retrograde tracing is carried out. In addition, some viruses can replicate and cross synapses.

Table 3.2 Properties of various viral vectors used for gene transduction into the CNS (Kantor et al., 2014, Bru et al., 2010, Nassi et al., 2015)

Virus	Genetic material	Integration and stability	Anterograde or retrograde
Parvoviridae e.g. adeno-associated viruses	ssDNA, ~4.7kb	Not integrated at high levels, stable over many years in non-dividing cells	Most anterograde Serotypes 6,8,9 retrograde
Retroviridae e.g. lentiviruses	ssRNA, ~9-12kb	Integrated, stable	Anterograde
Adenoviridae e.g. canine adenoviruses (CAV2) e.g. human adenoviruses (HAV5)	dsDNA, ~35kb	Not integrated, stable >1year Not integrated, not always stable	Both
Herpesviridae e.g. pseudorabies virus	dsDNA, ~144kb	Not integrated	Transynaptic, retrograde
Rhabdoviridae e.g. rabies virus	ssRNA ~12kb NB cannot use Cre/FRT as no DNA phase in life cycle	Not integrated	Transynaptic, retrograde.

The viral vectors used in this chapter were chosen to allow anterograde tracing (AAV2 vector) and retrograde tracing (CAV2 vector), without any trans-synaptic travel. This will identify primary neurons only.

The use of a viral vector in combination with the Cre-lox system is especially attractive as it removes any concerns regarding transient expression of Cre recombinase during development (Padilla et al., 2012). Only neurons expressing Cre recombinase at the time of viral injection will be able to recombine a floxed vector and lead to the expression of a reporter protein. In addition, the use of a reporter protein allows clear visualisation of a neuron and its processes without the use of inhibitors of protein trafficking such as colchicine.

Potential disadvantages include problems that are experienced with any use of the Cre-recombinase system. Off target Cre-recombinase expression in the mouse line can occur, and the vector itself can exhibit non-specific or leaky expression. In addition, problems with inbred mouse strains can arise. A further issue could be considered to be that the reporter protein is not expressed or trafficked under the same regulatory elements as the native protein of interest. This may lead to over or under amplification of signal compared to the native protein. However, in general, these issues are outweighed by the benefits of a highly sensitive system.

3.1.7 Evidence from electrophysiological studies with subsequent neuronal subtyping

Neuronal populations in the rat PVN can be identified by their electrophysiological properties as either neuro-secretory, pre-autonomic, or magnocellular (Luther et al., 2002). Pre-autonomic neurons of the PVN have been shown to exhibit a distinct profile in response to a depolarising current step, with low threshold spiking and t-type calcium currents. Having identified the different cell types electrophysiologically, the peptide profile of putative pre-autonomic neurons was then identified using IHC after the recording (Melnick et al., 2007). Almost half of the PVN neuro-secretory neurons (47/95) were found to be positive for CRH. Interestingly, 35/74 pre-autonomic neurons, thought to project to the brainstem, were also found to contain CRH. This is a higher proportion than might have been expected from the previous neuroanatomical studies.

Differences could be explained by the differing methods of identifying pre-autonomic neurons, or indeed by a bias towards patch clamping CRH neurons compared to other neuronal subtypes.

3.2 Hypotheses

- A specific subpopulation of CRH neurons arising in the PVN will target brainstem autonomic areas
- These neurons are located laterally and caudally within the PVN- known pre-autonomic areas

3.3 Aims

- Use retrograde tracing from the brainstem to investigate the anatomy of pre-autonomic CRH cell bodies in the PVN
- Use anterograde tracing from the PVN to delineate and describe the projections of CRH PVN neurons

3.4 Results

3.4.1 TdTomato fluorescence was readily observed in sections from CRH x Td mice

The mice used in the experiments described in this chapter were CRH x Td and CRH-ires-Cre. CRH x Td mice were generated by crossing CRH-ires-Cre males with TdTomato females. Expression of TdTomato in areas previously reported to express CRH (including the PVN, median eminence, amygdala, bed nucleus of the stria terminalis, Barrington's nucleus and scattered cortical interneurons) was observed on fluorescent microscopy (Figure 3.1). No amplification of the native TdTomato signal was needed to enable visualisation of presumed CRH neurons.

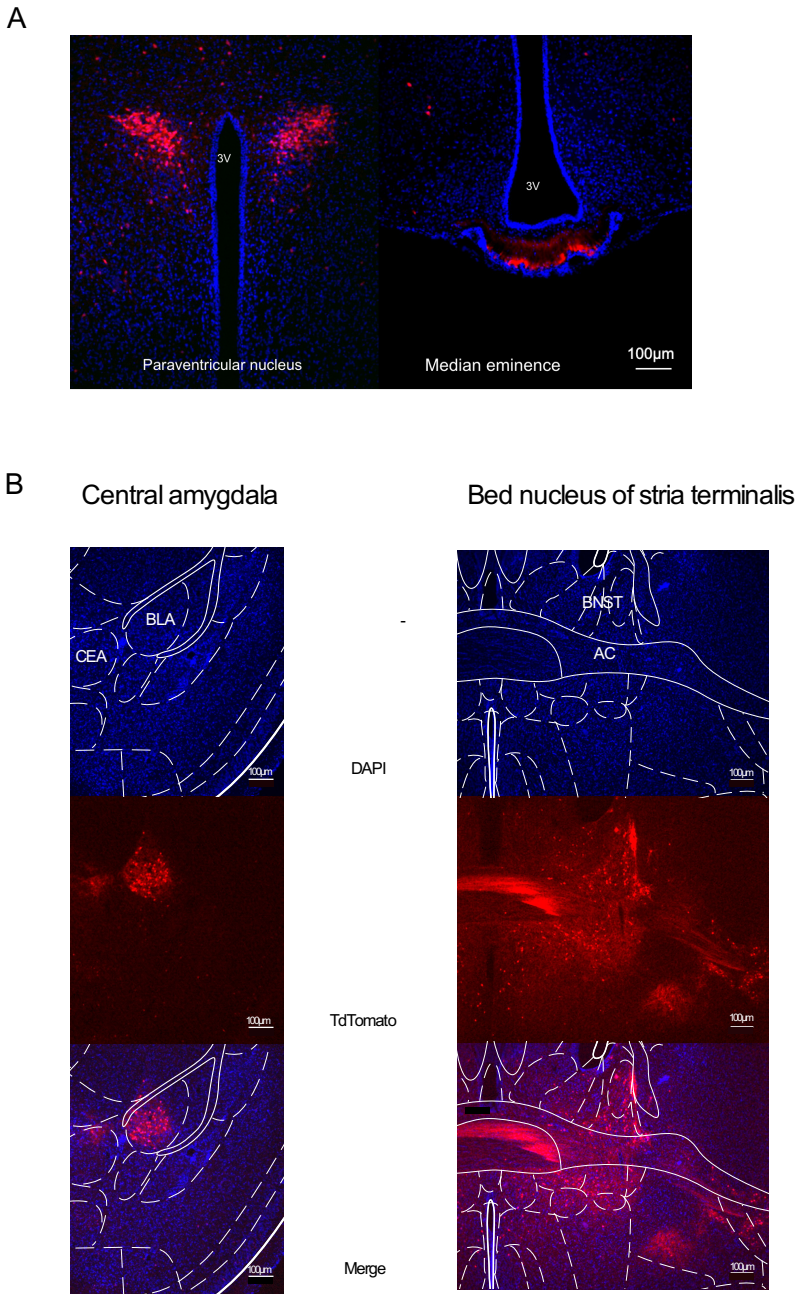

Figure 3.1 TdTomato expression in sections from a CRH x Tdtomato mouse in areas known to express CRH

A PVN and median eminence, merged images with DAPI and TdTomato
B Central amygdala and bed nucleus of the stria terminalis
3V Third ventricle, CEA- central amygdala, BLA- basolateral amygdaloid nucleus, AC anterior commissure, BNST- bed nucleus of the stria terminalis

3.4.2 Anterograde tracing

3.4.2.1 Injection sites

8 homozygous CRH-ires-Cre mice were unilaterally injected with AAV_DIO-mCherry adenovirus to the mid PVN (see Methods section 2.3 for details of this virus). Mouse characteristics are summarised in table 3.3

Table 3.3 Characteristics of mice having injections of AAV_DIO-mCherry to PVN

ID	Sex	Age at surgery (weeks)	Incubation period (weeks)	Injection Site sections	Brainstem sections	Spinal Cord sections
42624	M	6	2	Coronal	Transverse	n/a
42623	M	6	2	Coronal	Transverse	n/a
41067	F	6	2	Coronal	Transverse	n/a
43825	F	11	4	Coronal	Parasagittal	n/a
43824	F	11	4	Coronal	Parasagittal	n/a
43823	F	11	4	Coronal	Parasagittal	n/a
45937	F	10	4	Parasagittal	Parasagittal	Transverse
47832	M	12	4	Parasagittal	Parasagittal	Transverse

Transduction at the site of injection was confirmed in all 8 mice by histology and microscopy of the injection site. Examples of injection sites from sections cut coronally and parasagittally are shown in Figure 3.2.

There is a small amount of spread across the midline to transduce cell somata visible in some transverse sections, but the injection was largely confined to a unilateral site.

Longer incubation following injection appeared to result in more readily visible terminals in the brainstem, but did not greatly affect the number of cells visibly transduced in PVN. No differences in the numbers of transduced cells or projection patterns were observed between males and females.

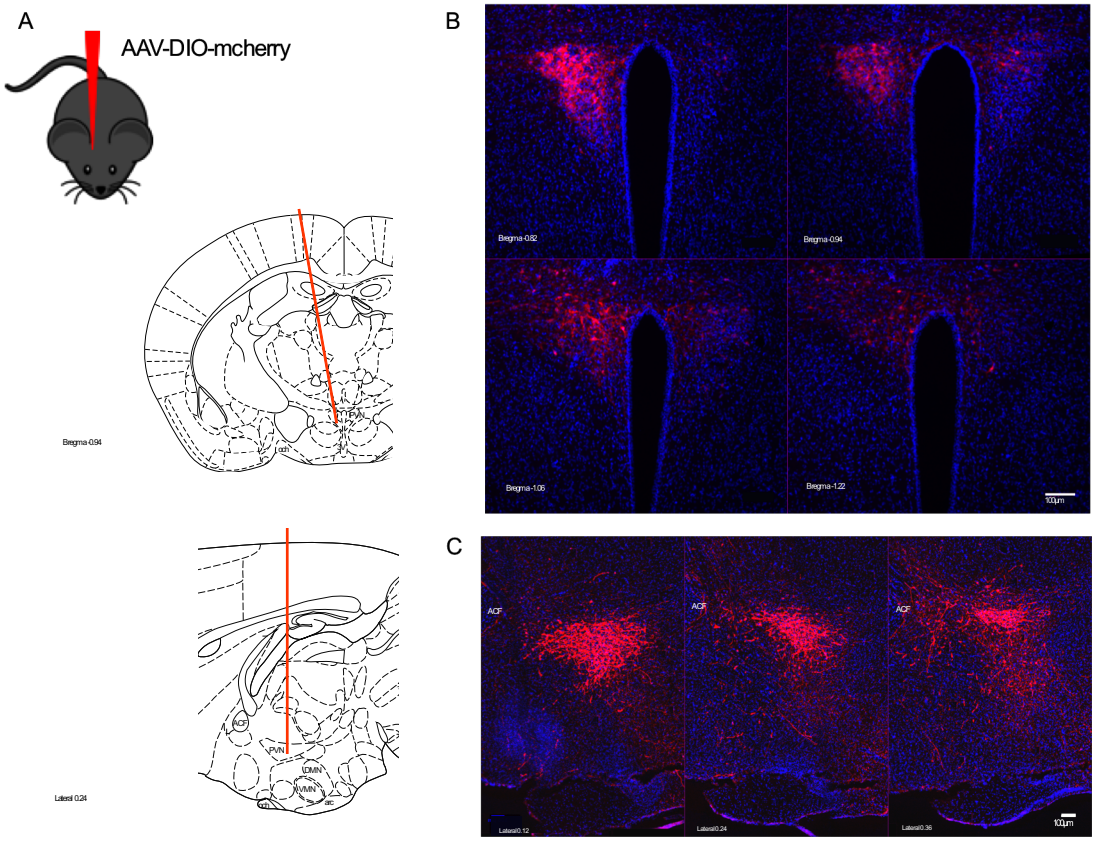

Figure 3.2 Injection sites in the PVN

A CRH-Cre mice were injected with AAV-DIO mCherry to the PVN. Diagram shows the planned coordinates

B Example of viral transduction within PVN, coronal slices. Immunohistochemistry used to enhance mCherry fluorescence. Red; Alexa 594 in CRH neurons expressing mCherry. Blue; DAPI

C Further example as above but sliced parasagitally.

3V- third ventricle

3.4.2.2 Localised projections

The main projection within the hypothalamus was to median eminence, as illustrated in figure 3.3A. The tracts ending in the median eminence passed laterally and then medially around the periphery of the hypothalamus.

Sparse terminals were observed in other areas of the hypothalamus. Very few terminals were observed in the arcuate nucleus (Figure 3.3A). The VMN received a moderate innervation whilst the DMN and lateral hypothalamus were sparsely innervated (Figure 3.3B).

3.4.2.3 CRH neuronal axonal tracts to brainstem

Two major tracts were observed running from the CRH PVN neurons and descending to brainstem. The first runs below the fornix and then into the PAG before entering the brainstem and travelling laterally to join the more ventral tract. The second runs more laterally into the ventral medulla. These pathways are illustrated in figure 3.4. Very few fibres were observed to travel to other areas, in particular no major forebrain projections were identified in the cortex, amygdala, BNST or hippocampus.

3.4.2.4 CRH neuronal terminals in the midbrain

Terminals with varicosities as well as fibres of passage were observed within the PAG (Figure 3.5 A,B). A similar picture was observed for the ventral tegmental area (Figure 3.5 C).

3.4.2.5 Terminals in the pons

The locus coeruleus received sparse innervation, with terminals more readily visible in the adjacent medial and lateral areas (pre-locus coeruleus) (Figure 3.6A). The parabrachial nucleus, both the medial and lateral parts, received moderate inputs from CRH terminals (Figure 3.6 A and B). The dorsal raphe also received sparse innervation (Figure 3.7).

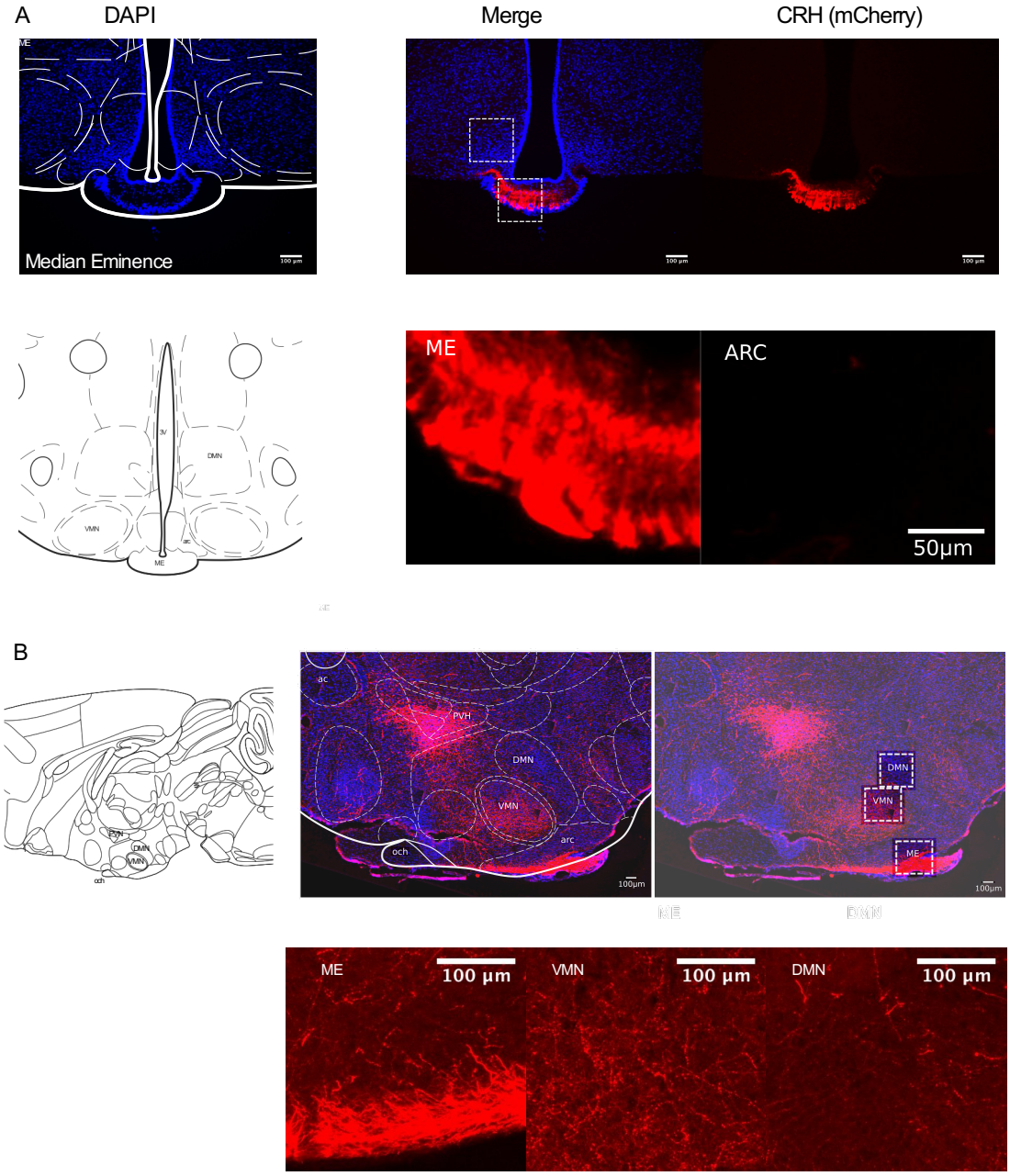

Figure 3.3 Local projections of CRH neurons within the PVN
A Dense projection to median eminence compared to absence of fibres in arcuate nucleus. Red; Alexa 594 enhanced CRH-Cre mCherry fibres. Blue; DAPI
B Moderate density of fibres seen in VMN and sparse fibres in DMN when compared to median eminence in sagittal sections
ME- median eminence, ARC- arcuate nucleus, VMN- ventromedial nucleus, DMN- dorsomedial nucleus

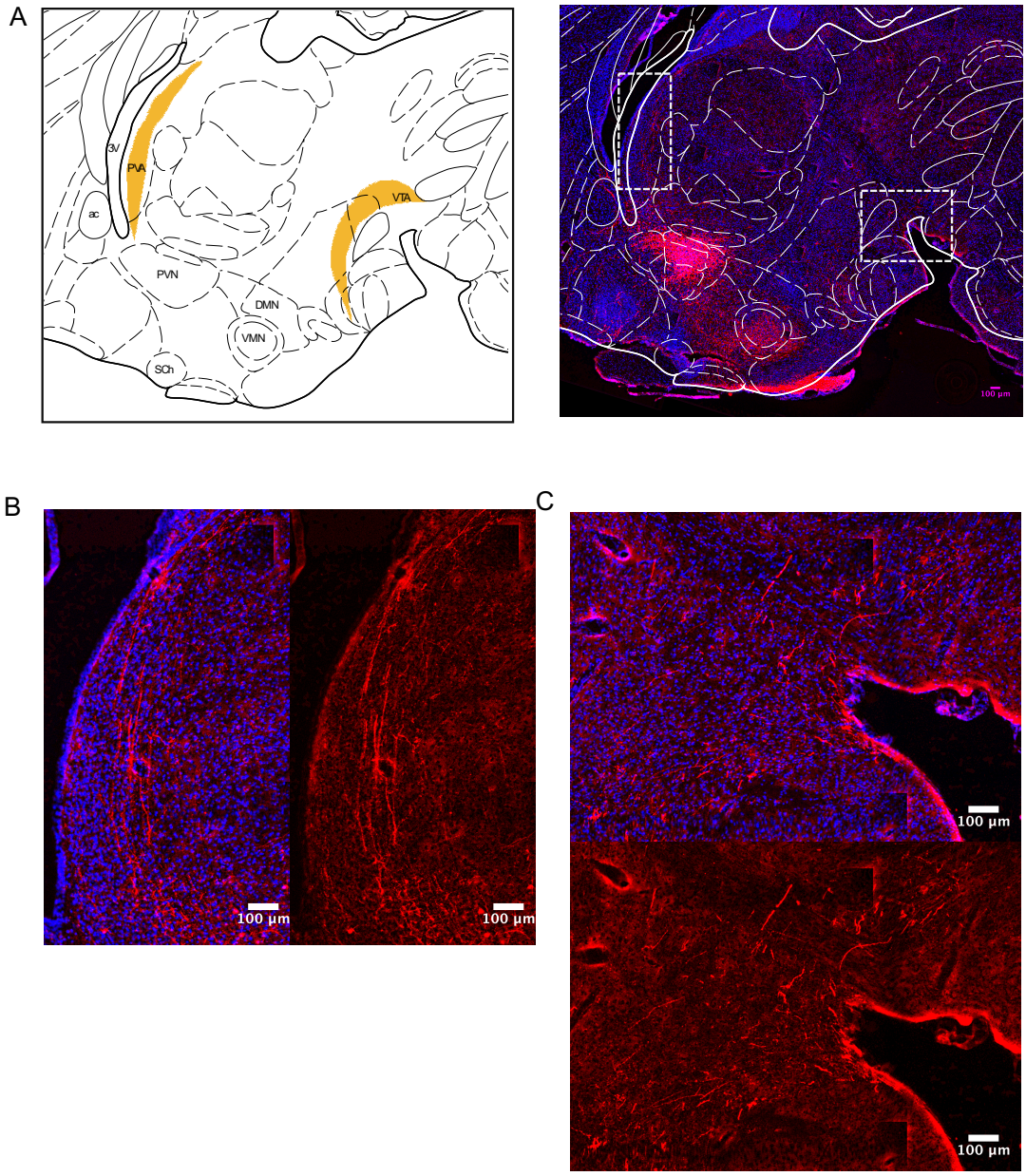

Figure 3.4 Two main tracts of CRH fibres projecting from PVN to mid and hindbrain
A Diagram and widefield image to illustrate both periventricular and ventromedial tracts running close to midline in a sagittal section. Red; Alexa 594 enhanced mCherry in CRH neurons. Blue; DAPI
B Fibres running in the periventricular tract.
C Fibres running through the ventral tegmental area in the ventromedial tract.

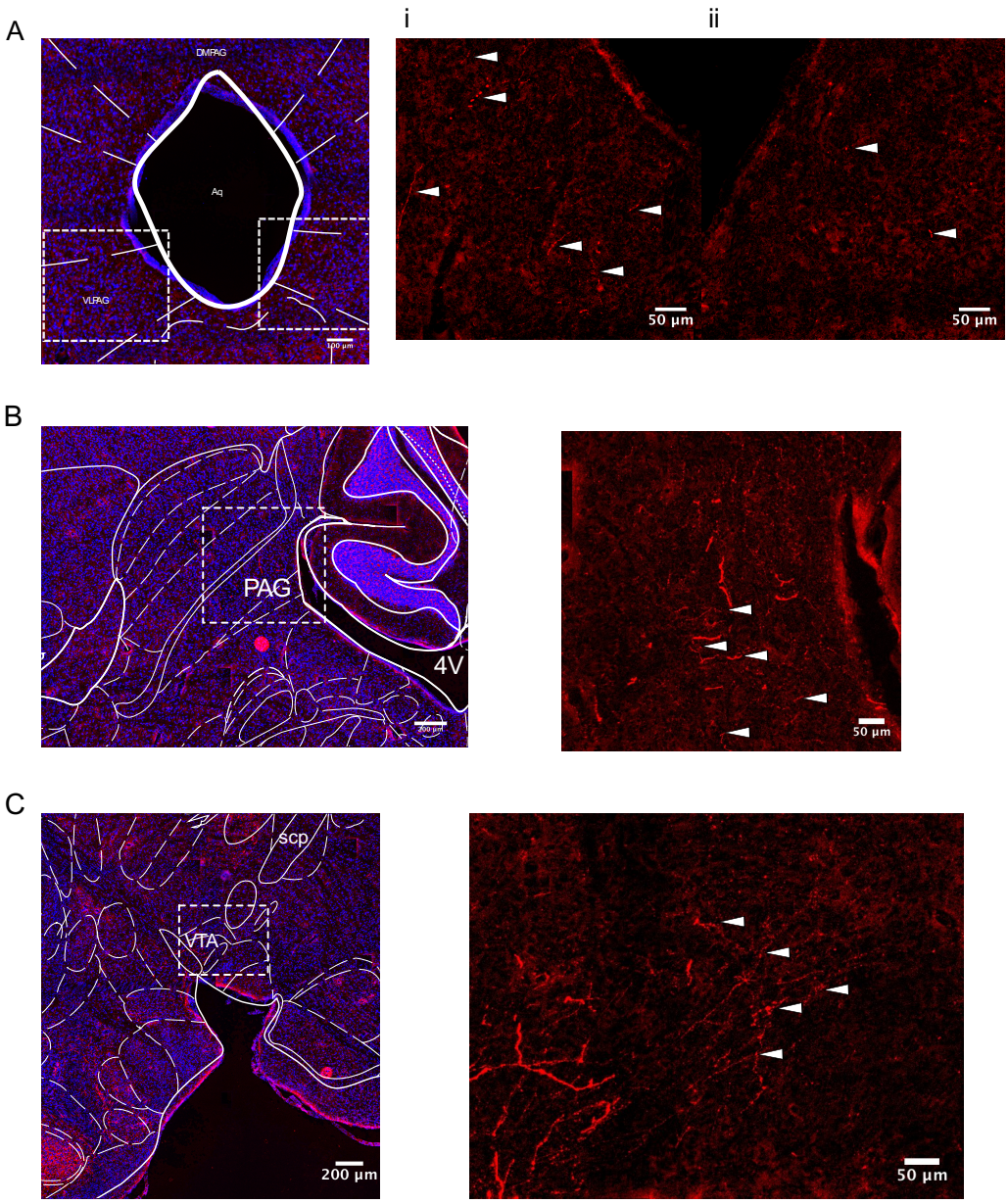

Figure 3.5 Fibres from CRH PVN neurons in the periaqueductal grey and ventral tegmental area.

A Images to show lateralisation of fibres in the mid brain- fibres visible in left ventrolateral PAG (i), not in right (ii). Fibres indicated by arrows

B Sagittal section showing fibres running in ventrolateral PAG (white arrows)

C Sagittal section showing fibres in the VTA, some fibres of passage and others with varicosities suggestive of terminals (white arrows)

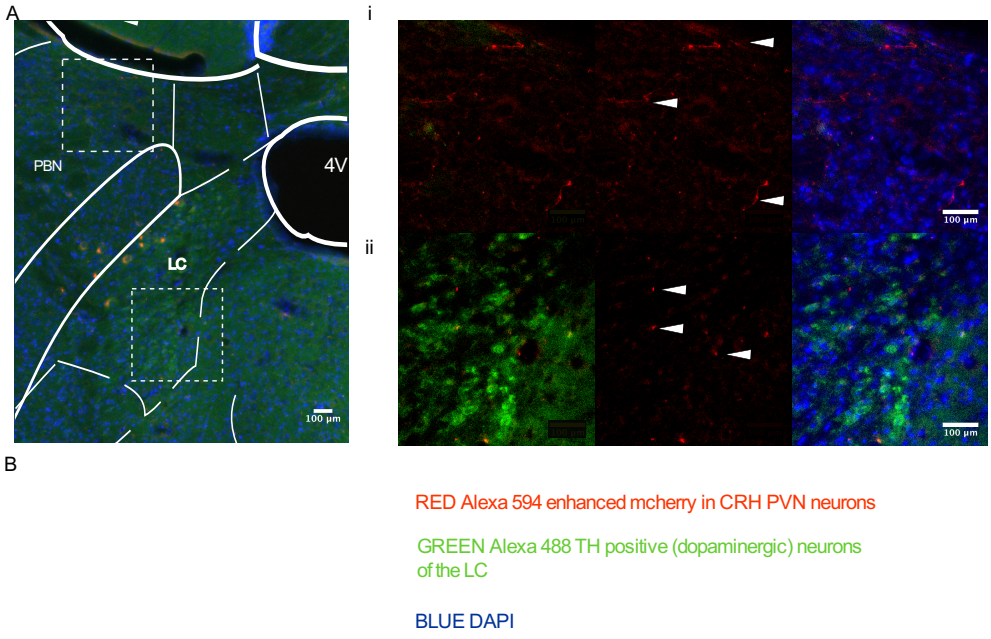

Figure 3.6 Projections to locus coeruleus and parabrachial nucleus
CRH PVN fibres were observed in lateral and medial parabrachial nuclei, very limited evidence of fibres in locus coeruleus
A Sagittal section showing CRH PVN fibres in PBN (i), with limited puncta of uncertain significance in the LC (ii).
B Transverse section showing CRH PVN fibres in both the lateral and medial parabrachial nuclei (white arrows)

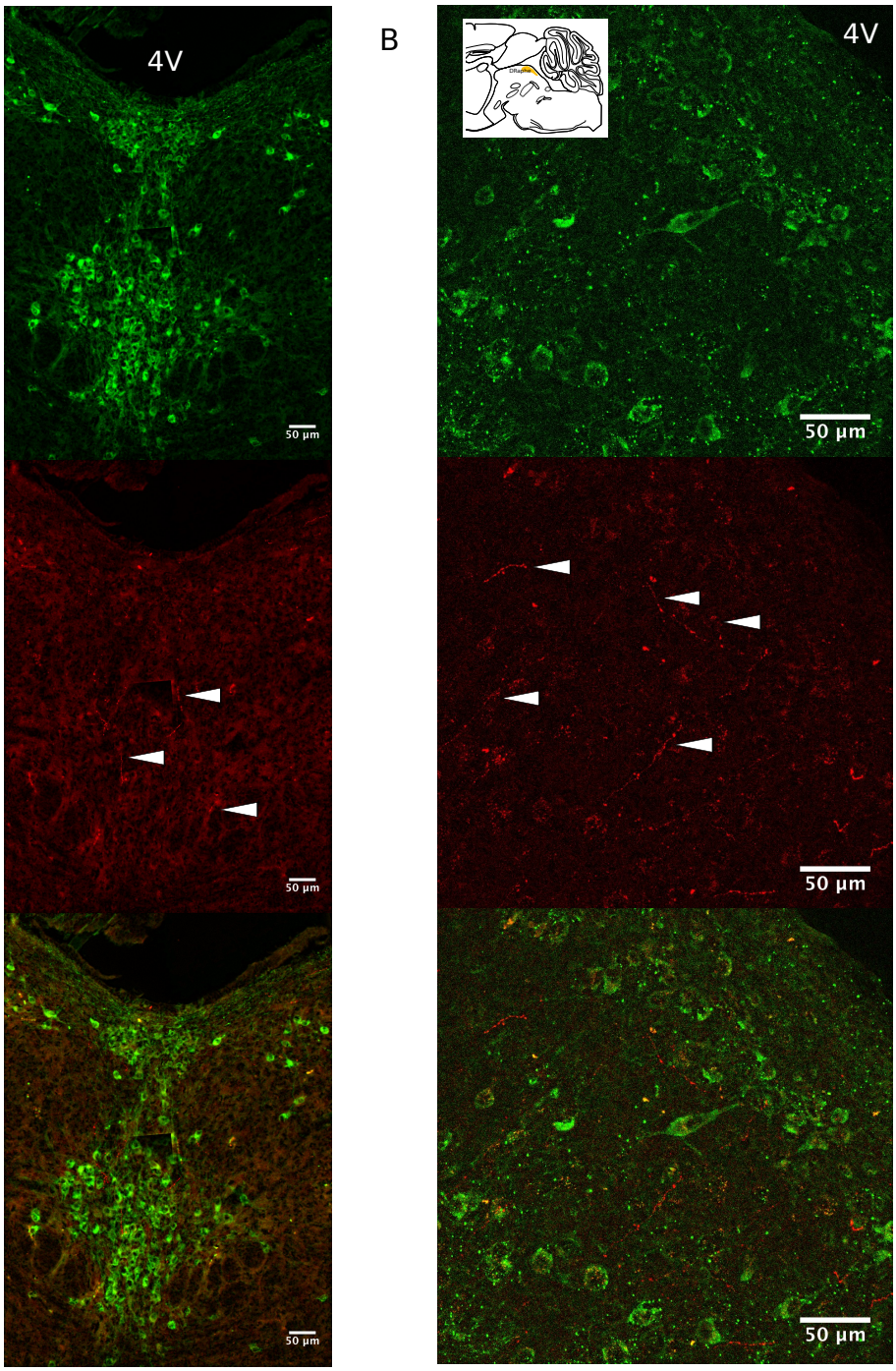

Figure 3.7 CRH PVN fibres in the dorsal raphe
Green neurons are stained for TrH to identify serotoninergic neurons of the dorsal raphe. Red is mCherry from CRH PVN fibres
A Transverse section
B Sagittal section. Inset schematic to show location of dorsal raphe (DRaphe, orange)
CRH PVN fibres indicated by white arrows

3.4.2.6 Terminals in the medulla

The nucleus of the solitary tract received the densest innervation from CRH neuronal terminals, the dorsal motor nucleus of the vagus received a moderate input whilst the hypoglossal nucleus received few or no terminals (Figure 3.8). It was possible to quantitate innervation to these three structures as they were all visible in the same images, and the results are summarised in figure 3.9. Fibres were only counted if they were clearly linear structures, >5µm long. More detail regarding quantification can be found in methods section 2.6.5.3.

CRH terminals with varicosities were observed in close apposition to A2 cell bodies in the NTS, and similarly varicosities in close apposition to cholinergic neuronal cell bodies were observed in the DMX (Figure 3.10).

Moderate innervation was observed in the ventral raphe (Figure 3.11) and the RVLM (Figure 3.12). The nucleus ambiguus received a very sparse innervation, although more terminals were seen in the area around the NAmb, which includes the C1/A1 neurons (Figure 3.12).

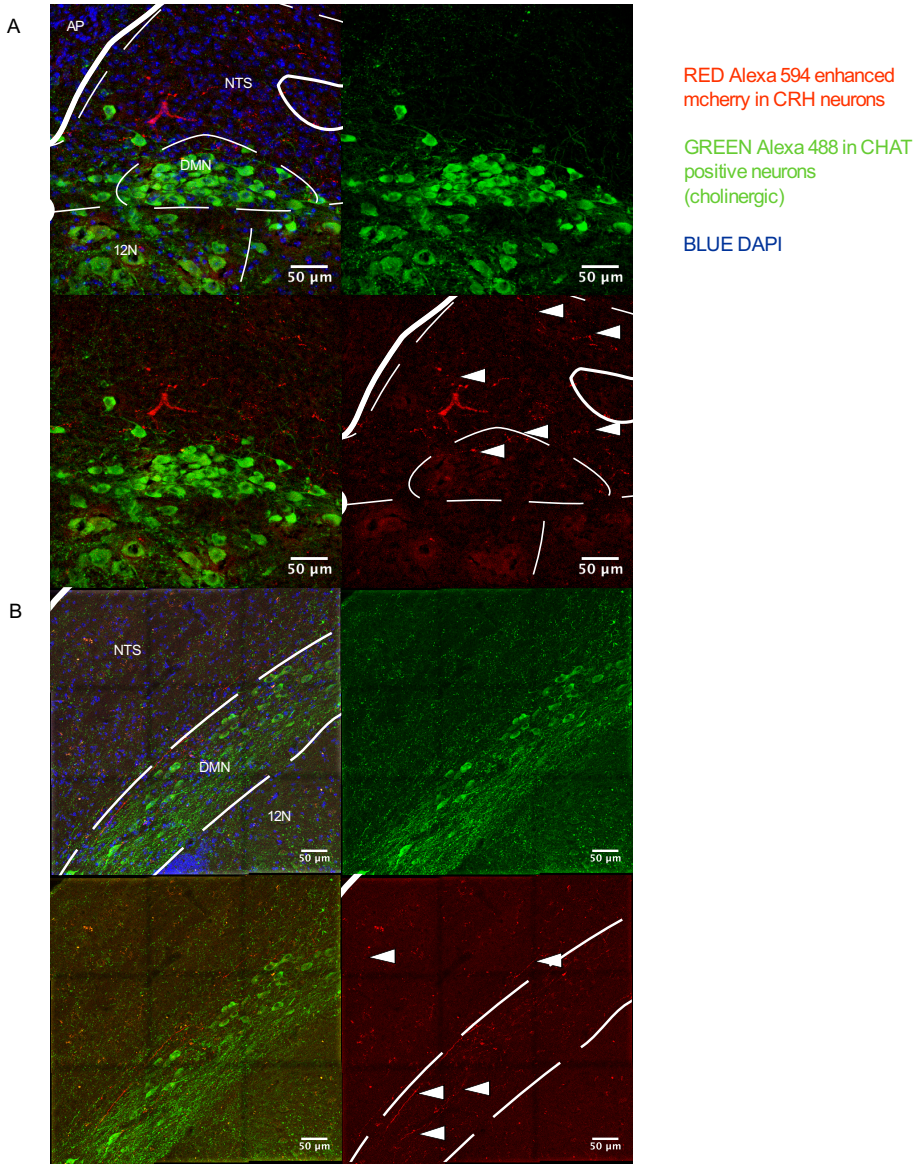

Figure 3.8 CRH PVN fibres in NTS and DMX
A Transverse section with CHAT staining to identify cholinergic neurons of the DMX. CRH fibres clearly visible in NTS and DMX (white arrows)
B Sagittal section as above, again fibres indicated by white arrows

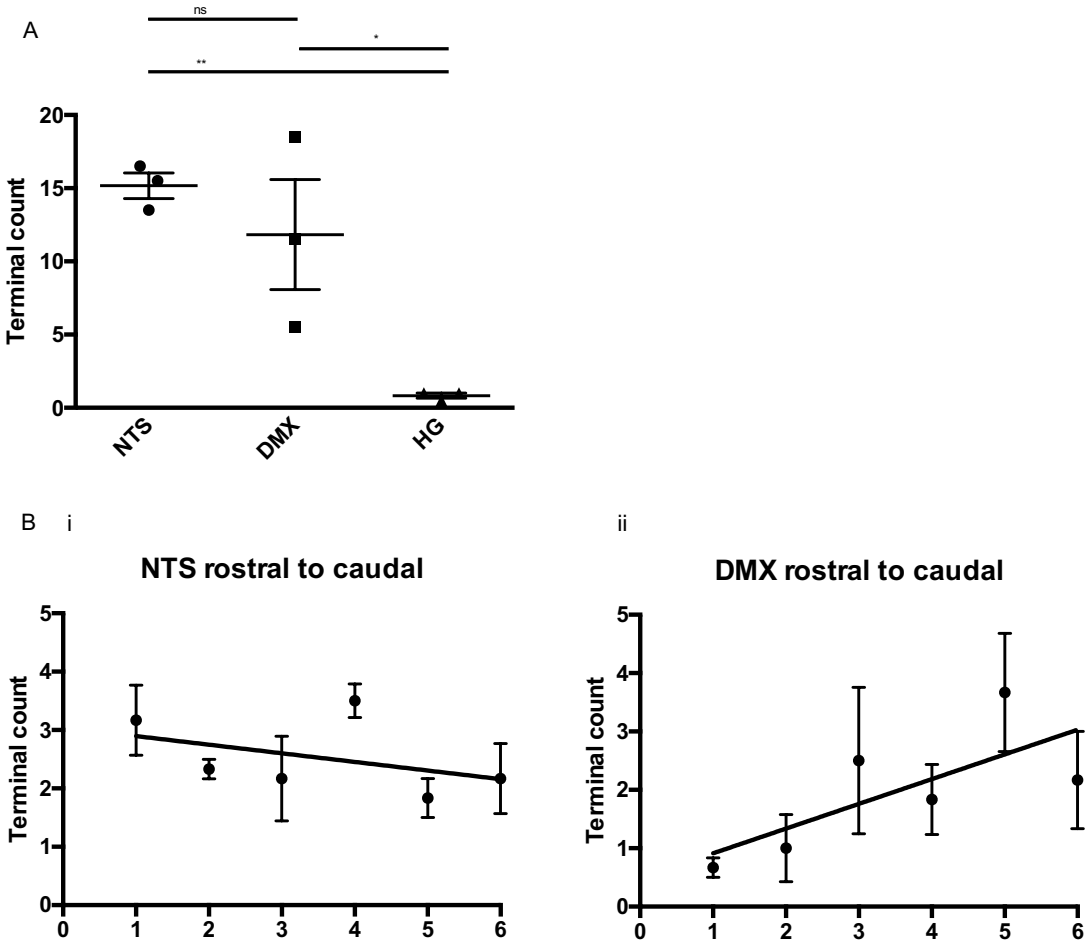

Figure 3.9 Quantification of terminals in the nucleus of the solitary tract, dorsal motor nucleus of the vagus and hypoglossal nucleus

A Terminal counts are higher in the DMX and NTS compared to the HG. Data shown as mean ± SEM. One way ANOVA with multiple comparisons, p=0.0092. NTS vs HG 95% CI 4.6-24.0 (**), DMX vs HG 95% CI 1.3-20.7 (*), NTS vs DMX 95% CI -6.3-13 (ns).

B Comparison of terminal counts at 6 levels rostral to caudal along a longitudinal section of i) NTS and ii) DMX, with superimposed lines of best fit. No significant trend in regression for NTS (R square= 0.075). Significant trend to increased terminal counts in more caudal areas for DMX (R square=0.23)

A

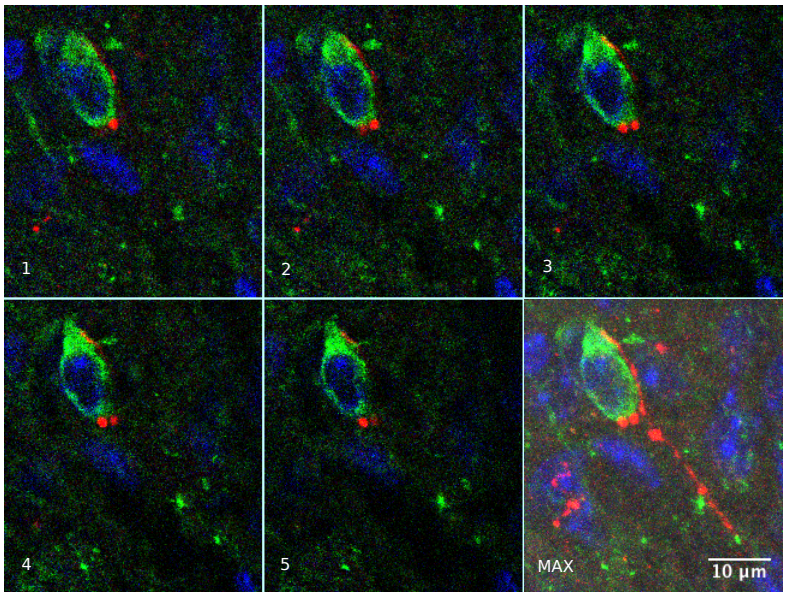

RED mCherry-
CRH PVN fibre
GREEN TH- A2 neuron
BLUE DAPI

B

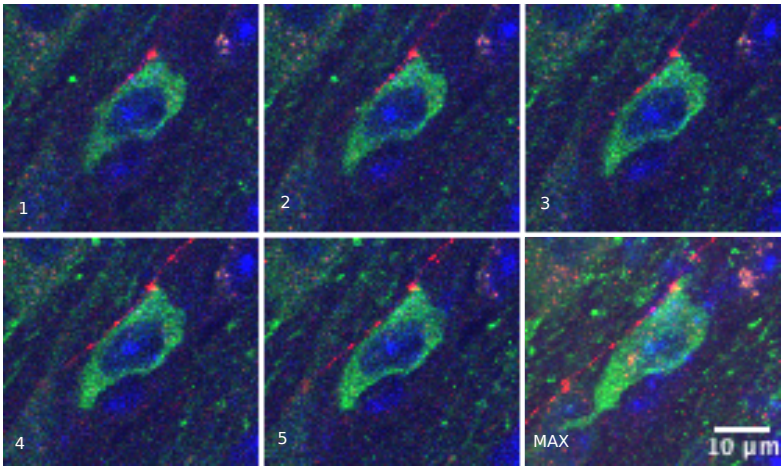

RED mCherry-
CRH PVN fibre
GREEN CHAT-
cholinergic neuron
BLUE DAPI

Figure 3.10 CRH PVN fibres in close proximity to autonomic neuronal cell bodies in the brainstem

A Confocal images of an A2 neuron within the NTS, with CRH fibres in close proximity. 1-5 are sequential z planes at 0.5micron intervals. MAX is a maximal projection of entire 21 slice z stack

B Confocal images of a cholinergic neuron within the DMX with closely apposed CRH fibre. Details as for A

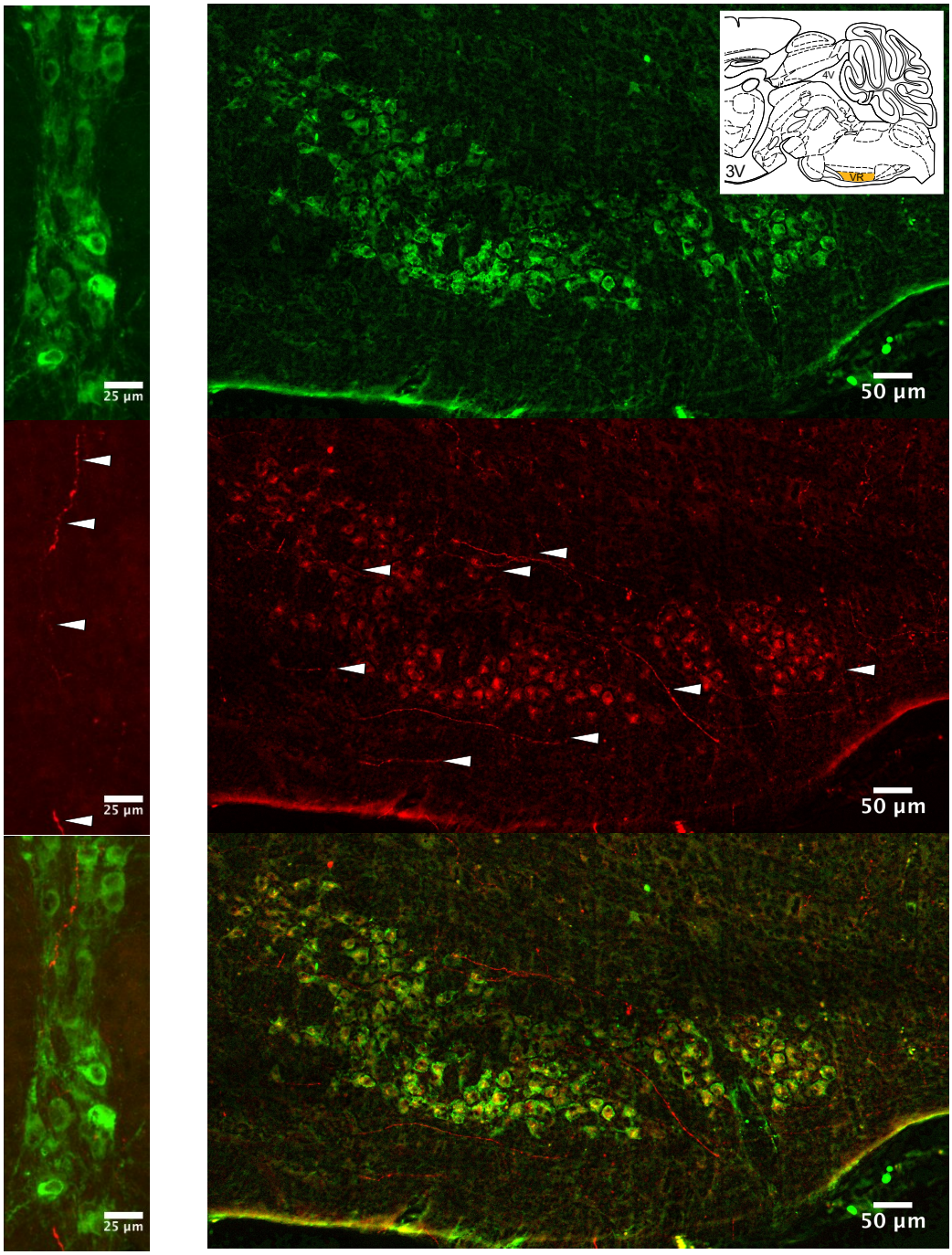

Figure 3.11 CRH PVN fibres within the ventral raphe
Green neurons are stained for TrH to identify serotoninergic neurons of the ventral raphe
Inset diagram top right to illustrate anatomical location of ventral raphe (orange, VR) 3V third ventricle, 4V fourth ventricle
Left panel- transverse section
Right panel- parasagittal section.
CRH PVN fibres indicated by white arrows

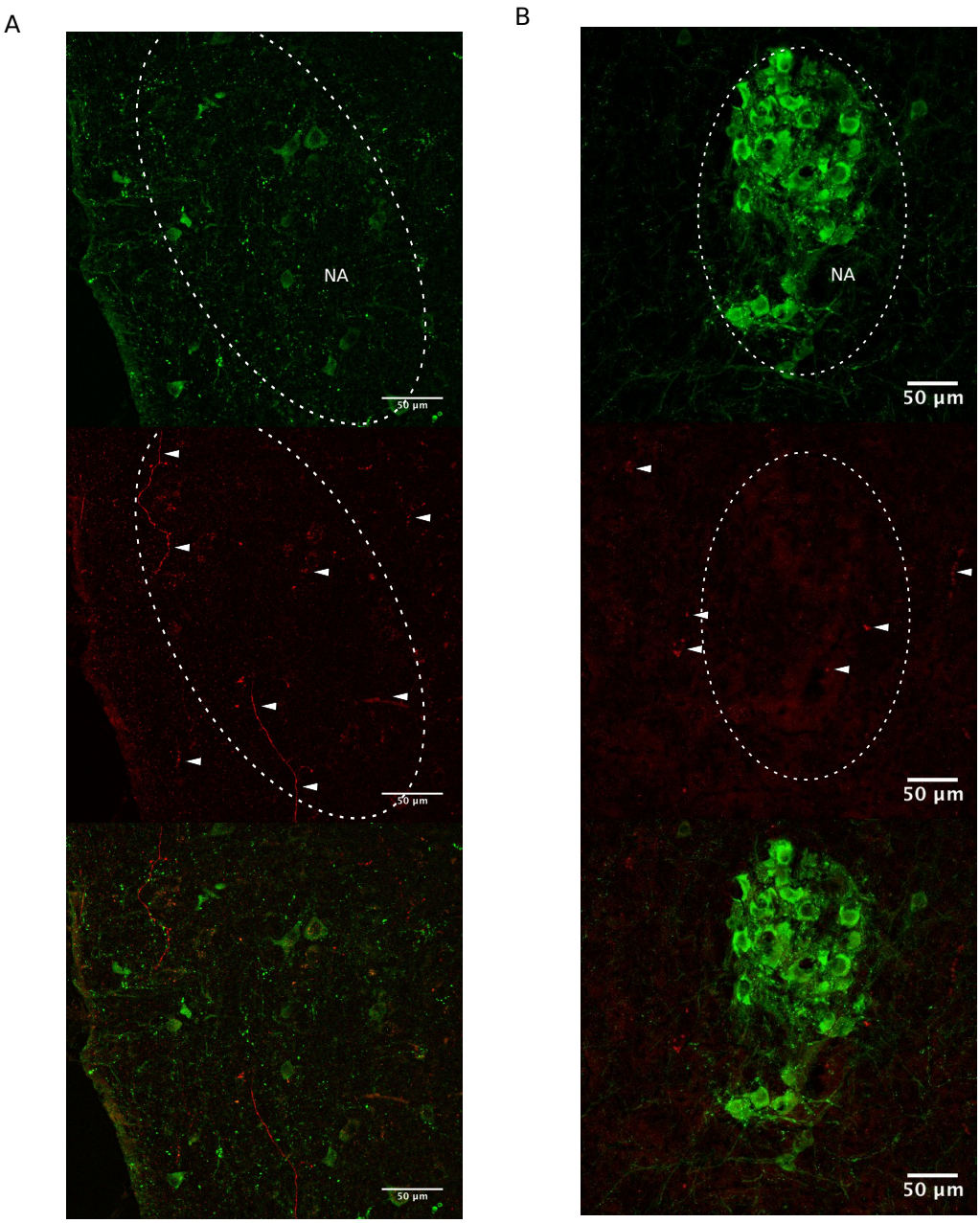

Figure 3.12 Sparse CRH PVN fibres around the nucleus ambiguus, with relative sparing of the compact NA

A Sagittal section showing CHAT positive neurons within the NAmb and more ventrally C1 in green, and CRH PVN fibres in red. CRH PVN fibres are largely seen running longitudinally.

B Transverse section through NAmb showing fibres in the surrounding areas, likely C1/A1/RVLM, but sparing the compact part of the NAmb

Table 3.4 Summary of CRH innervation density

	Nucleus	Fibre density
Midbrain	Ventral Tegmental Area	++
	Edinger-Westphal nucleus	0
	Ventrolateral periaqueductal gray	+
	Dorsal raphe nucleus	+
Dorsal pons	Locus coeruleus	0/+
	Pre-locus coeruleus	+
	Medial parabrachial nucleus	++
	Lateral parabrachial nucleus	++
Ventral medulla	Nucleus ambiguus	
	Compact	0
	external	+
	A1 and caudal C1 catecholamine neurons	+
	RVLM	+
	Ventral raphe	++
Dorsal medulla	Nucleus of the solitary tract (including A2 neurons)	++++
	Dorsal vagal nucleus	+++

A map of these projections is contained in Figure 3.13

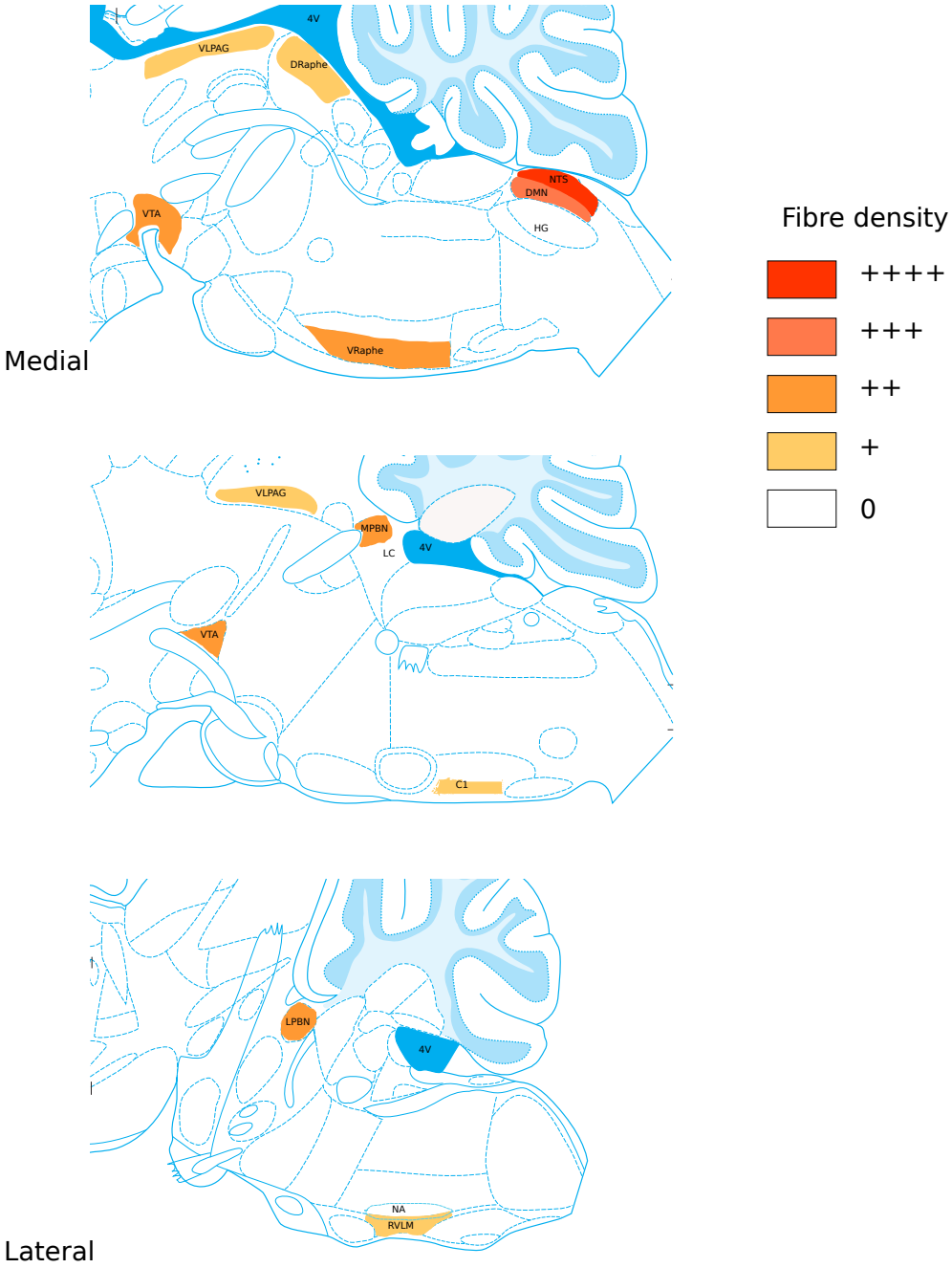

Figure 3.13 Map to illustrate relative density of innervation of various autonomic areas by CRH PVN neurons

4V; Fourth Ventricle, VLPAG; ventrolateral periaqueductal gray, DRaphe; dorsal raphe, NTS; Nucleus of the solitary tract, DMX; dorsal motor nucleus of the vagus, VRaphe; ventral raphe, VTA; ventral tegmental area, MPBN; medial parabrachial nucleus, C1/A1; C1/A1 catecholaminergic neurons, LPBN; lateral parabrachial nucleus, NAmb; nucleus ambiguus, RVLM; rostral ventrolateral medulla

3.4.2.7 Spinal cord projections

Coronal spinal cord sections from mid thoracic cord showed evidence of a tract running in the lateral funiculus, and terminal varicosities in the region of the sympathetic preganglionic cell bodies as identified by CHAT positive staining (Figure 3.14).

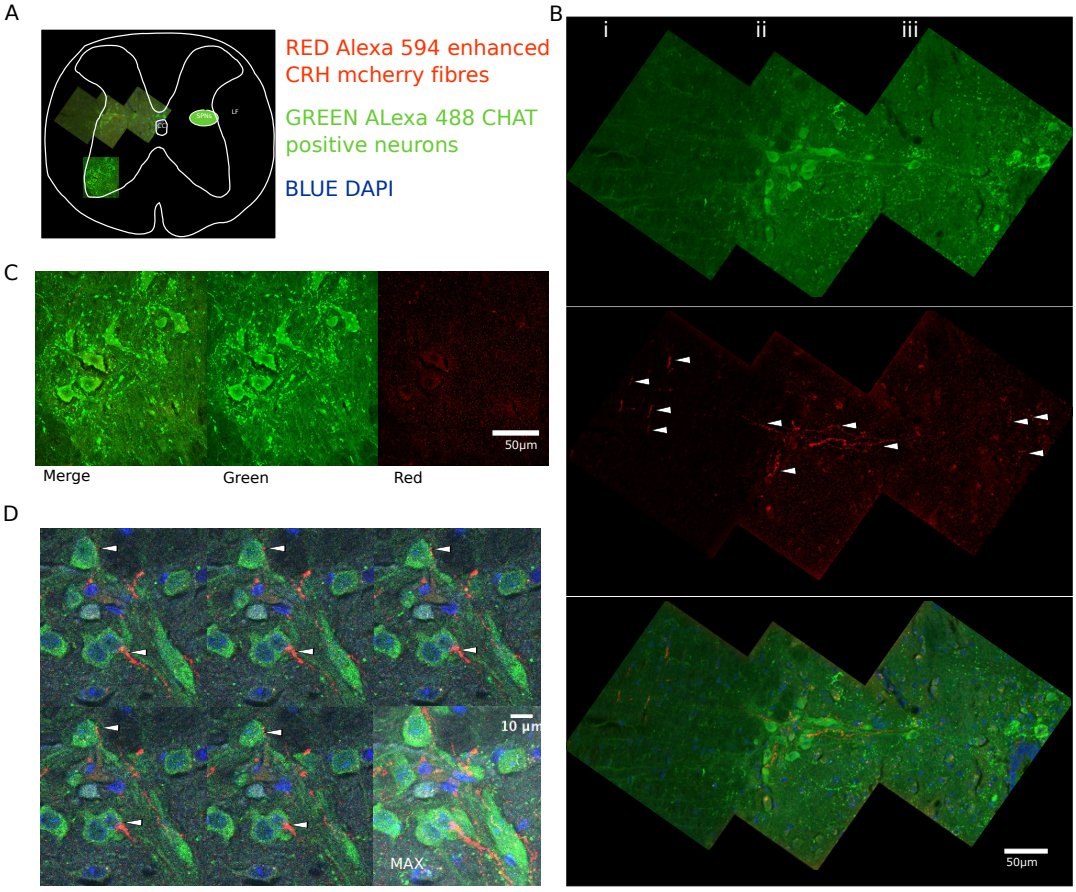

Figure 3.14 Projections of CRH PVN neurons to sympathetic pre-ganglionic neurons of the mid thoracic spinal cord

A Diagram of transverse section of mid thoracic spinal cord to show location of sympathetic pre ganglionic neurons (SPNs) and location of images.
B Maximal projections of a 21 plane z stack from confocal microscopy to show (i) fibres running in the tracts of the lateral fasiculus, (ii) fibres apposing SPNs and (iii) fibres extending from SPNs towards the central canal. Arrows in white indicate fibres
C Control area- CHAT positive neurons from the ventral horn with no CRH fibres seen
D CRH PVN fibres in close proximity to CHAT stained SPNs. 5 sequential z planes at 0.5micron intervals. MAX is the projection of the entire 21 plane z stack. White arrows indicate fibres apposed to CHAT neuronal cell bodies

3.4.3 Retrograde tracing of pre-autonomic neurons projecting to the NTS/DMX

The NTS/DMX was chosen as the best site for injections for retrograde tracing because it was the site of the densest projections and has previously been shown to be a target of the PVN. Successful targeting of CAV-CMV-eGFP viral injection to the NTS/DMX was confirmed in 4 animals with IHC for eGFP (Figure 3.15). Their characteristics are summarised in table 3.5. This virus primarily acts as a retrograde tracer, but does also transduce neurons locally and the reporter protein (eGFP) fills the cell projection tree. CAV viruses do not cross synapses. The CMV promoter is a non-specific promoter, so will express eGFP in all transfected neurons.

Table 3.5 Characteristics of mice having injections of CAV-CMV-eGFP to NTS/DMX

ID	Sex	Age at surgery (weeks)	Incubation period (weeks)	Injection Site sections	Brainstem sections
C	F	11	2	Transverse	Transverse
D	F	11	2	Transverse	Transverse
E	F	11	3.5	Transverse	Transverse
G	F	11	3.5	Transverse	Transverse

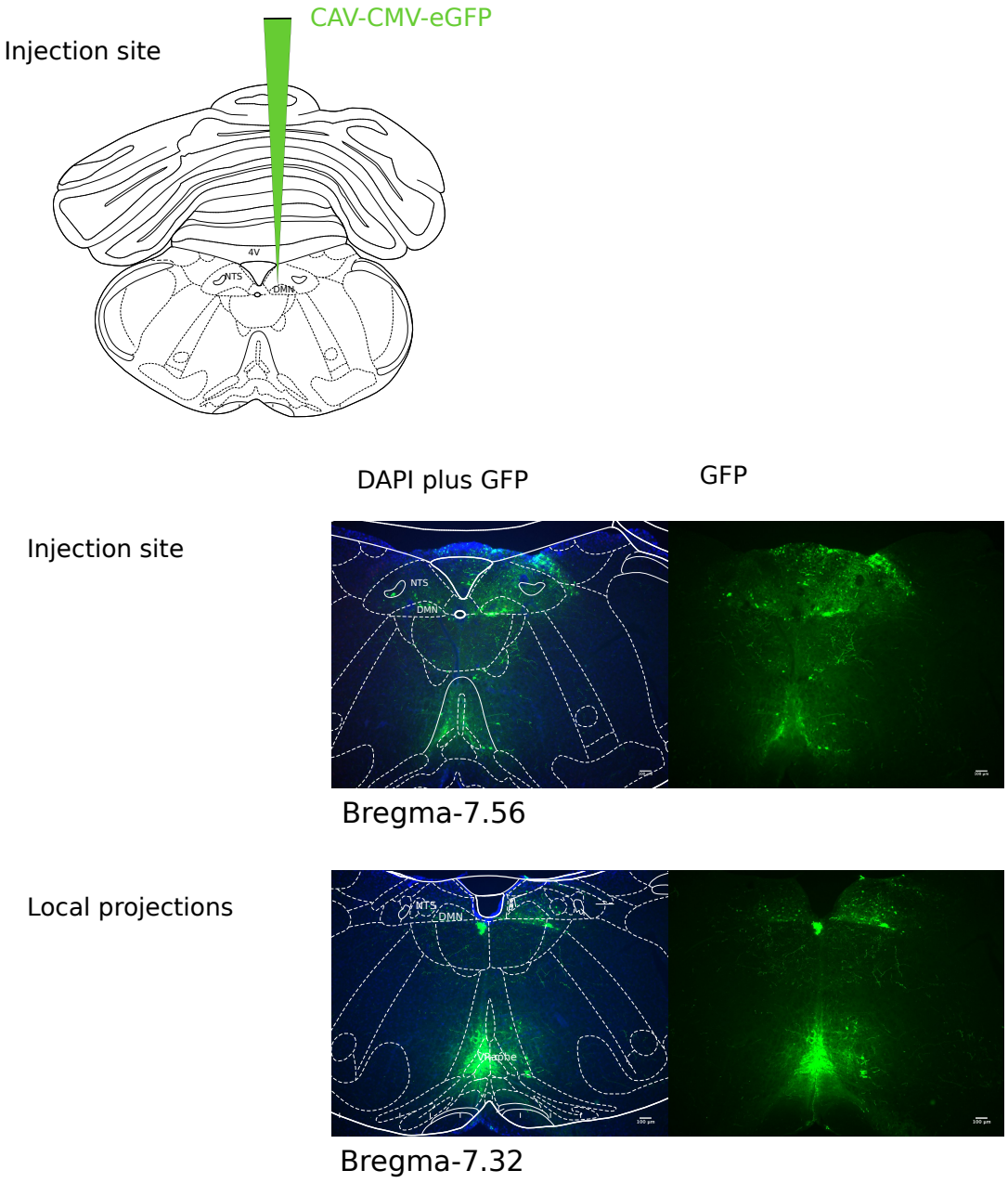

Figure 3.15 Injection site in NTS/DMX
Top: Injection schematic
Below: Injection site and local projections to contralateral NTS and ventral raphe

3.4.3.1 eGFP positive cell bodies in the hypothalamus

eGFP cell bodies (retrograde) and fibres (anterograde fills) were identified in the PVN, indicating that the PVN both projects to and receives projections from the NTS/DMX, as previously reported (Biag et al., 2012). eGFP positive cell bodies are retrogradely transduced cells sending fibres to the NTS/DMX. Cell bodies were seen in the caudal PVN, LH and Zona incerta (ZI) which connects PVN and LH (Figure 3.16 and table 3.6). This corresponds with previous reports of the locations of pre-autonomic neurons within the PVN in mice (Biag et al., 2012). 38.6% of the pre-autonomic neurons identified in each mouse were also positive for TdTomato, indicating that a substantial proportion of these pre-autonomic neurons express CRH.

Table 3.6 Counts for cell bodies in 3 hypothalamic nuclei, after eGFP immunohistochemistry

	Pre-autonomic neurons (eGFP+)	**CRH pre-autonomic neurons (eGFP+TdTom+)**	**% of pre-autonomic neurons identified which are CRH+**
Paraventricular hypothalamus	30 ±3	9 ±2	30 ±3
Lateral hypothalamus	32 ±12	17 ±11	32 ±12
Zona incerta	8 ±2	1 ±0	12.5

n=4 mice, 1:4 series

The data from all 4 animals was collated to generate a map of CRH positive cells projecting to the NTS, as shown in Figure 3.17.

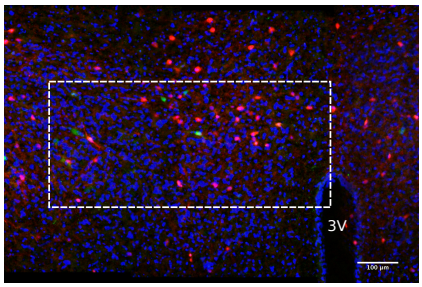

Green: Retrogradely labelled cell bodies with terminals in NTS/DMN- Alexa 488 enhanced GFP

Red: CRH neurons expressing Tdtomato

Blue: DAPI

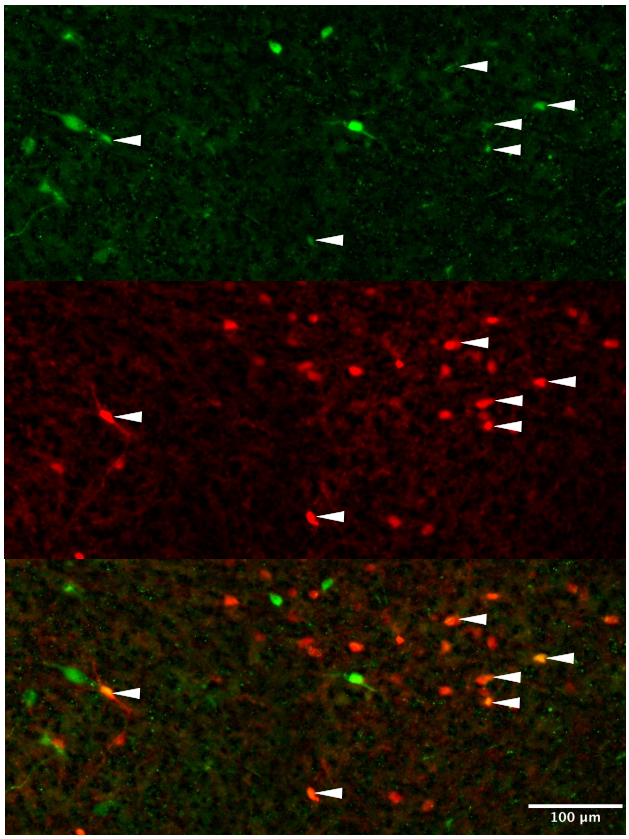

Figure 3.16 A subset of CRH neurons project to the NTS/DMX as evidenced by retrograde labelling

Co-labelling of neurons for CRH (red, Tdtomato), and retrogradely transported GFP from NTS/DMX. White arrows indicate cell bodies with both Tdtomato and GFP

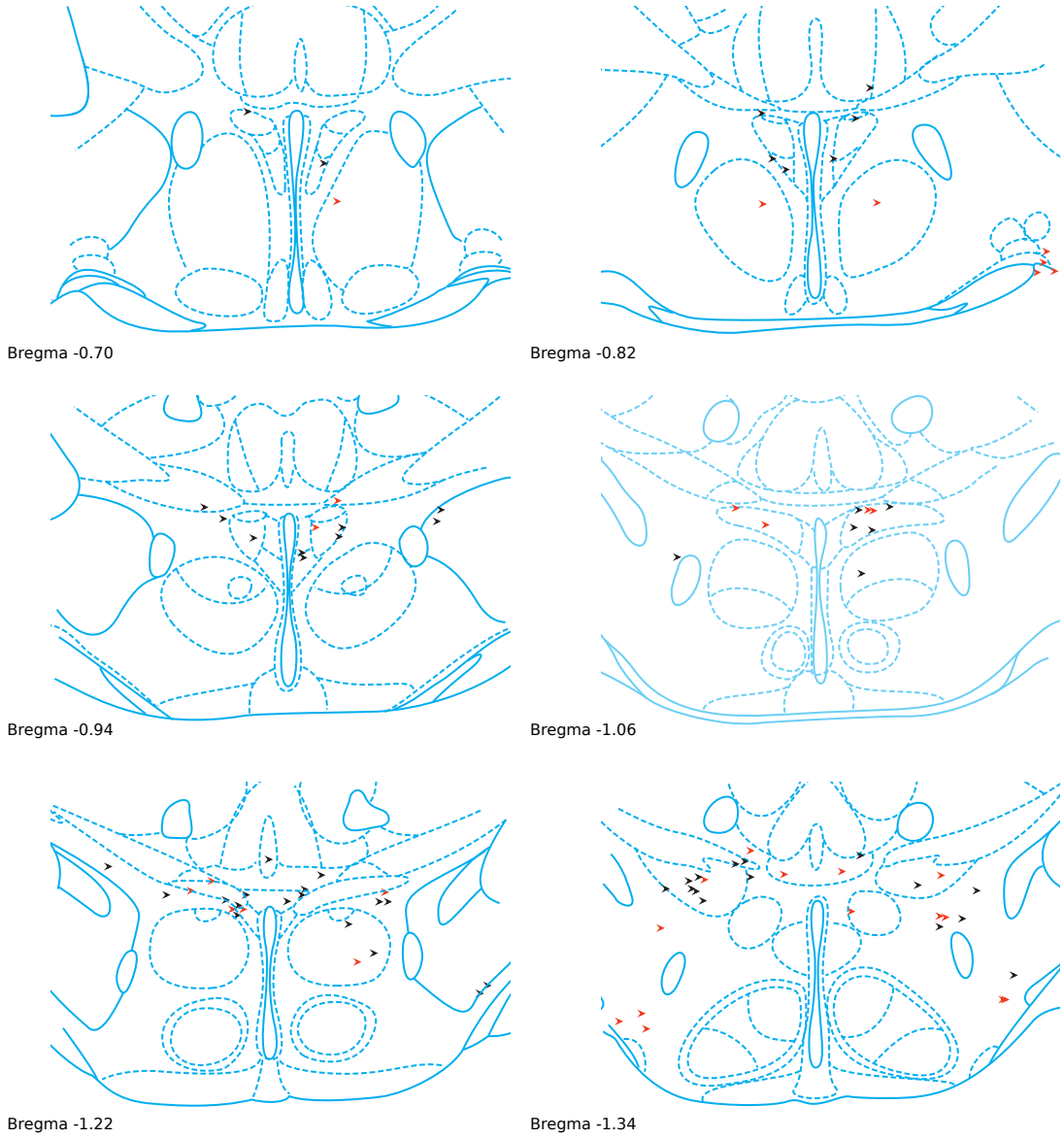

Figure 3.17 Map of PVN neurons retrogradely transduced from the NTS
Unilateral NTS injection in one representative mouse (Mouse C)
Black arrow; pre-autonomic neuron
Red arrow; pre-autonomic neuron co-expressing CRH

3.5 Discussion

This is the first demonstration of a CRH PVN pre-autonomic pathway in the mouse. This PVN-brainstem tract has previously been identified in mice, but neuronal subtypes were not investigated (Biag et al., 2012). These data also provide more details regarding the targets of these neurons when compared to previous studies in the rat (Sawchenko, 1987b, Simmons and Swanson, 2009). In rats, evidence had been presented that some PVN neurons are CRH expressing but do not belong to the neuroendocrine population (projecting to the pituitary gland), and these were hypothesised to have autonomic projections (Swanson et al., 1983, Simmons and Swanson, 2009, Sawchenko, 1987b). Up until this thesis, the sole area of the brainstem that had been clearly demonstrated to receive CRH PVN terminals was the NTS/DMX. Investigations regarding which other areas of the brainstem such neurons would project to have not previously been carried out, although reports of multi-synaptic connections to via brainstem outflow tracts to downstream autonomic targets had been published (Jansen et al., 1995, Stanley et al., 2010). There were no other reports regarding CRH expression in pre-autonomic neurons of the PVN in mice at the time that this study was carried out. However, a subsequent very similar experiment has been carried out as part of the Allen Mouse Brain Atlas connectivity project, experiment 266840498 (Oh et al., 2014, Atlas, 2011). In this experiment, an AAV encoding floxed EGFP was injected into the PVN of a CRH-ires-Cre mouse of an alternative strain, developed by Lowell and colleagues (Kong et al., 2012). Data in the study is presented visually and also as a total projection volume for each area of the brain. It is not clear whether terminal projecting fibres were differentiated from fibres of passage or puncta. The results are broadly comparable to those presented here, with particular enrichment of terminals in the NTS, DMX, reticular nuclei, and raphe magnus in the medulla, the parabrachial nucleus in the pons and the PAG in the midbrain. Within the hypothalamus itself, increased local terminals are reported in the periventricular nucleus, ARC, DMN, medial preoptic area, sub paraventricular zone, anterior hypothalamic nucleus, LH, posterior hypothalamic nucleus, parasubthalamic nucleus, perifornical nucleus, retrochiasmatic nucleus, tuberal nucleus and ZI, as well as the ME. The VMN does not appear to receive as many fibres in this study. The study also reports a significant projection to the thalamus, but on examining the images, much of this appears to be due to transduction of cells dorsal to

the PVN in the path of the injection. Projections to forebrain structures are also described, but because they are presented as total volume rather than density of projection, they appear more substantial in numerical values than when viewing the fibres, as the total area of the forebrain is much larger. Indeed, only the BNST and central amygdala appear to have increased density of fibres when the sections are inspected visually.

The existence of a CRH expressing population of autonomic projecting neurons is of particular interest in the context of the counterregulatory response to hypoglycaemia, as the autonomic component of this response is more rapidly activated than the HPA axis, and is key to maintaining effective counter-regulation and hypoglycaemia awareness, as discussed in sections 1.4 and 1.6 of the introduction. This therefore strengthens the case for a role for CRH PVN neurons in this scenario.

3.5.1 Local projections

Projections within the hypothalamus are dominated by the major projection to the median eminence, a finding in alignment with previous descriptions of non-subtype specific projections within the hypothalamus (Geerling et al., 2010). Interestingly, it is also clear that there are extensive CRH dendritic networks within the PVN itself. It was not clear from the experiments reported here whether these fibres originated from neuroendocrine or pre-autonomic cells. However, this effect has previously been reported in the mouse for pre-autonomic, non-subtype specific PVN neurons, with dendritic networks essentially extending to form a shell around the whole neuroendocrine PVN (Biag et al., 2012). Liposits et al. (1985) used electron microscopy and immunohistochemistry to examine local CRH circuits in the PVN. They report extensive connections between CRH neuronal axons and CRH as well as non CRH containing neuronal soma and dendrites of the PVN. These connections may represent a means by which neurons can feedback directly via local networks and has been suggested to provide a means of ultrashort negative feedback (Liposits et al., 1985, Herman et al., 2003).

Fibres are seen within the bounds of the VMN (and to a lesset extent the DMN), but these are sparse in comparison to the main tracts. Interestingly, the VMN is known to

contain CRH/urocortin receptors, and CRH/urocortin have been reported as modulating glucose sensing in this nucleus (McCrimmon et al., 2006, McCrimmon RJ, 2005). Few or no fibres were seen within the arcuate nucleus. In general, this fits with the hypothesis that whilst the PVN receives extensive inputs from other areas of the hypothalamus, its own outflow is not predominantly to these same areas.

3.5.2 Tracts to brainstem

CRH neuronal fibres travel in two major tracts towards the brainstem, again closely matching descriptions of generalised PVN projections from anterograde studies (Saper et al., 1976, Luiten et al., 1985). There appears to be a degree of lateralisation in these fibre tracts in their early course, and at the level of the PAG, but beyond the midbrain the innervations of centres in the brainstem appeared to be bilateral. It is likely that a bilateral injection to the PVN would result in a larger number of visible fibres.

Previous evidence from the literature suggests that the ventral tract is the main source of innervation for the hindbrain and spinal cord, and that the dorsal tract does not continue significantly beyond the midbrain as a separate entity; the remaining fibres from the dorsal tract travel laterally to join the ventral tract (Luiten et al., 1985).

3.5.3 Targets in the mid brain

Both the PAG and VTA received projections from the CRH PVN neurons, in addition to fibres passing through these regions. The ventrolateral PAG, where most terminals were observed, is a centre with known projections to the raphe magnus and RVLM, and is thought to be of importance in coordinating the behavioural, autonomic and antinociceptive responses to stressful stimuli (Behbehani, 1995). The VTA contains multiple dopaminergic neurons and is a key area for motivation, reward or aversion. It has many connections to the forebrain, unlike most of the projections of the CRH PVN neurons. VTA activity measured by BOLD fMRI signal in humans has been shown to be altered by hyper-insulinaemia, which tends to depress VTA activation and reduce the palatability scores of foods. This effect is lost in insulin resistant individuals (Tiedemann et al., 2017). A further study using fMRI in healthy human subjects showed VTA activation during mild hypoglycaemia in obese individuals (Page et al., 2011). This

suggests that the VTA may be implicated in food seeking behaviour during hypoglycaemia.

3.5.4 Autonomic targets in the pons and medulla

A wide range of autonomic targets were identified throughout the brainstem. The NTS received by far the densest innervation in these studies. This is of interest as this is a key autonomic relay area, and has previously been identified as playing a role in the counter-regulatory response to hypoglycaemia (Lamy et al., 2014, Marty et al., 2005, Ritter et al., 2000). In addition, the NTS has previously been shown to directly and indirectly respond to hypoglycaemia (Adachi et al., 1984, Balfour et al., 2006).

Other areas of particular interest include the RVLM, which has recently been implicated in stress induced hypoglycaemia (Zhao et al., 2017), with a necessary input from the PVN. It is tempting to speculate that the pathway identified here could contribute the response described, in the context of hypoglycaemia, with activation of CRH PVN neurons in response to hypoglycaemia contributing to activation of catecholaminergic RVLM neurons, which in turn can clearly act to increase glucose levels via descending projections to the spinal cord.

The lateral parabrachial nucleus also received a significant input from the CRH PVN neurons. Again, this is a nucleus that has been shown to be important for counter-regulation to hypoglycaemia, and indeed can also sense changes in glucose (Flak et al., 2014, Garfield et al., 2014). Interestingly, the effect of the PBN to effect counter-regulation was upstream to the ventromedial hypothalamus in this study, rather than via activation of the sympathetic nervous system. Given the known projections from VMN to PVN, it is possible that these anatomical connections could represent a closed feedback loop important in the counter-regulatory response.

In general, the areas with fibres closely followed those previously identified in non-subtype specific tracing experiments in the rat (Geerling et al., 2010, Luiten et al., 1985). There were some significant differences, however. Of particular note, the NAmb does not appear to receive a significant input from CRH neurons of the PVN. The compact part of the NAmb has primarily been identified as important for swallowing and

laryngeal control. The external formation of the NAmb is important for parasympathetic cholinergic outflow to the heart, and has previously been demonstrated to have innervation from vasopressin and oxytocinergic neurons of the PVN modulating this outflow (Buijs, 1978). Given that CRH neurons appear to have a greater role in sympathetic outflow, it is perhaps less surprising that they do not appear to have a major projection to the compact NAmb.

The locus coeruleus also exhibited a paucity of terminals from the PVN CRH neurons. This fits with previous reports that much of the CRH input to the LC comes from the central amygdala (McCall et al., 2015). Geerling and colleagues also described minimal projections from non-specific PVN neurons to the LC, and similarly to here, saw more terminals in the pre-LC (Geerling et al., 2010).

Interestingly, the sympathetic preganglionic neurons of the thoracic spinal cord also clearly received CRH PVN innervation. This is a new finding and represents a further direct means by which these neurons could modulate the known counter-regulatory response to hypoglycaemia. The sections in which the SPN/CRH terminals were observed were from the mid thoracic regions, which are known to supply the abdominal viscera via the coeliac and superior mesenteric ganglia, which includes innervation to the pancreas and adrenal glands, areas which are clearly relevant to the counterregulatory response to hypoglycaemia. A previous tracing experiment had demonstrated a connection between the CRH PVN neurons and the cervical spinal cord in rats, but this was a retrograde study, and so did not examine specific spinal cord targets, and aimed to label all fibres of passage passing through the cervical spinal cord (Sawchenko, 1987a).

3.5.5 Retrograde tracing

The second experiment carried out here explored the location of CRH neurons within the PVN with projections specifically to the NTS/DMX. As would have been predicted from earlier work, these neurons were located primarily in the caudal part of the PVN and extending into the zona incerta and lateral hypothalamus- this area has been described as a continuation of the caudal PVN in the mouse (Biag et al., 2012). Whilst the rat is thought to have around 2000 CRH PVN neurons, work by Biag et al. (2012)

suggest the mouse has a smaller population; ~1650 (n=3). Wamsteeker et al. (2013) used fluorogold to identify the neuroendocrine population and suggested that ~86% of CRH neurons in their model were neuroendocrine (so a maximum of 14.1% could be pre-autonomic), whilst previous work in rats suggested that a figure of 5-10% might be pre-autonomic (Sawchenko, 1987b). Extrapolating from these figures, we might estimate that a maximum of 82-230 neurons might be pre-autonomic (5-14% of 1646 neurons). We here counted a mean of 9 CRH PVN neurons to be pre-autonomic with projections to the NTS/DMN, in a 1:4 series. The total number including zona incerta and lateral hypothalamus CRH neurons was 27. If these figures are multiplied up and an Abercrombie correction applied, the value achieved for the PVN CRH neurons is 30, a rather smaller number than extrapolated here. For the ZI plus LH plus PVN, the value is 90, which falls within the estimated number mentioned above. This work was based on a unilateral injection at one level of NTS/DMX. We might expect somewhat larger numbers of neurons to be labelled with a bilateral injection, or indeed with injection at multiple levels of the NTS. In addition, further neurons might project only to other nuclei within the brainstem.

3.5.6 Summary

This chapter expands and develops previous work examining the projections of CRH PVN neurons to autonomic areas of the brainstem. In particular, the mapping of detailed CRH PVN outflow to the brainstem and spinal cord in the mouse is novel and useful. In the context of hypoglycaemia and HAAF, the sympathetic outflow of the brainstem is of particular interest. Key brainstem areas involved in sympathetic outflow include the RVLM, caudal ventrolateral medulla and the NTS, with inputs from higher centres including circumventricular organs and the paraventricular nucleus. The data presented here confirm that CRH PVN neurons project to all three of the major centres in the medulla oblongata, as well as further down to the sympathetic preganglionic neurons of the spinal cord. This provides clear neuroanatomical routes by which these neurons might modulate the response to hypoglycaemia.

The question of what signalling molecules might be released by these pre-autonomic CRH neurons has been addressed in previous work. It is known that pre-autonomic PVN neurons express a wide range of peptides including CRH and glutamate, but not GABA.

CRH PVN neurons in rats have been previously shown to express glutamate transporters (VGLUT2) using immunofluorescence and single cell RT-PCR (Dabrowska et al., 2013). Similar work has not been performed in the mouse. CRH receptors are expressed in certain brainstem areas, including the NTS, PAG, VTA, LC and raphe nuclei (Henckens et al., 2016), but are not expressed in all of the areas that CRH neurons of the PVN appear to project to, and therefore it seems likely that additional signalling molecules, for example glutamate, are also likely to be employed.

With regard to the retrograde tracing study presented here, it is clear from work in other areas of neuroscience that even a small population of neurons can have a significant effect on physiology, if they are placed at a pivotal point in a circuit. A recent example would be the identification of a small population (~30 neurons) of parvocellular oxytocin neurons in the PVN which, when activated, can cause significant functional analgesia in a model of inflammatory pain (Eliava et al., 2016). The population identified here certainly appear to be ideally suited anatomically to collate information about whole body homeostasis and effect/modulate responses throughout the autonomic system.

Chapter 4 Evidence for glucose sensitivity in PVN CRH neurons

4.1 Introduction

This chapter sets out the background to what is known about glucose sensing within the CNS, and in particular the hypothalamus. The proposed mechanisms underlying glucose sensing in the CNS will be discussed in Chapter 5 and are not covered here. New evidence for glucose sensitivity in CRH PVN cells is then presented, using both electrophysiological recordings and calcium imaging in vitro.

4.1.1 Glucose sensing by specific neurons within the central nervous system.

Glucose sensing neurons within the central nervous system were first described by Oomura and colleagues (1969, 1964) and Anand and colleagues (1964). In these studies, extracellular recordings in vivo were made from the ventromedial nucleus of the hypothalamus in anaesthetised cats and dogs, and responses to intravenous infusion of glucose and/or insulin were recorded. Glucose sensing neurons exhibit distinct responses to increases in glucose levels; glucose-excited neurons increase their firing rate, while glucose inhibited neurons are silenced. This effect is independent of changes in osmolarity. Hypoglycaemia can cause more generalised reductions in neuronal activity due to reductions in energy supply, but the response of the glucose sensing populations was distinct in that reversible increases and decreases in activity were seen in direct response to changes in glucose levels (Mobbs et al., 2001). Other neurons within the CNS show responses to changes in glucose due to alterations in synaptic inputs, but true glucose sensing is direct/intrinsic i.e. persists in the presence of synaptic blockade (Fioramonti et al., 2017).

4.1.2 Defining electrophysiological responses to glucose

A wide variety of electrophysiological methods have been used to identify and categorise neurons as GI, GE or non-responsive. Depolarisation and hyperpolarisation as measured in current clamp are commonly used measures of response, often in combination with changes in action potential frequency (Fioramonti et al., 2007, Fioramonti et al., 2004, Garfield et al., 2014, Gonzalez et al., 2008). Changes in

membrane resistance in response to current steps, indicative of ion channels opening or closing, are also commonly used (Burdakov et al., 2005a, Fioramonti et al., 2007, Gonzalez et al., 2008). In addition, the tendency of a given cell to fire in response to a current step has also been used as evidence of increased or decreased excitability (Burdakov et al., 2005a). Relatively few papers list absolute thresholds above or below which a cell is defined to be a responder, most commonly the group of cells deemed to be GE or GI are presented as having a statistically significant change in, for example resting potential. Comparable data is sometimes available for non-responsive neurons but not in all cases. This can present problems in interpreting the statistical significance of the effects seen due to selection bias. For example, if the only data presented is from 10% of cells, which show a depolarisation in response to a glucose step, whilst the other 90% are not discussed, then the question arises as to why that threshold was set, and how the other cells responded. If they all, in fact, depolarised to a much lesser extent, that would be very different from if they behaved in a heterogeneous fashion, or did not change their activity at all. Care should therefore be taken in interpreting results.

4.1.3 Physiological glucose levels within the central nervous system

Initial descriptions of glucose sensing neurons within the CNS used steps in glucose to/from 10mM, in vivo as intravenous infusions (Oomura et al., 1964, Oomura et al., 1969, Anand et al., 1964). With the development of acute slicing and recording techniques, an arbitrary choice of glucose level to use in the slices was made. Therefore early in vitro recordings also used steps from 10mM glucose (Ashford et al., 1990a, Ashford et al., 1990b). This would be a relatively high plasma glucose level in the fed state, and it is known that the CNS is not as a whole exposed to plasma levels of many substances due to the presence of the blood brain barrier. The major transporter for glucose across the blood brain barrier is GLUT-1, a high affinity glucose transporter, which is essential to maintain CNS glucose levels (Mueckler and Thorens, 2013, Simpson et al., 1994). Indeed, cerebrospinal fluid contains much lower levels of glucose than plasma- generally around 30% of the blood level. This raises the question as to whether the cells being identified in the initial in vitro studies were in fact ever likely to be exposed in vivo to the glucose levels being used.

Subsequent studies have demonstrated that interstitial CNS glucose levels are indeed much lower. Silver and Erecinska (1994a), performed early work in the anaesthetised rat, and this has been followed up by microdialysis experiments in awake animals (Dunn-Meynell et al., 2009, de Vries et al., 2003, McNay and Gold, 2001). Table 4.1 summarises some of these findings. Overall, the summary of this work is that in the fed state, a rat is likely to have a CNS glucose level of 2-2.5mM, and that this level will fall to 0.2-0.5mM after induction of hypoglycaemia. The maximum level recorded during pathological hyperglycaemia might be as high as 4.5mM. Therefore, one might consider these to be more physiological levels to apply in vitro.

Table 4.1 Studies comparing CNS glucose levels to blood levels in rats

Study	Blood glucose mM	CNS glucose mM	Preparation
Silver and Erecinska (1994b)	7.6 2.8 15	2.4 0.16 4.5	Anaesthetised animals, glucose sensitive microelectrodes
De Vries et al. (2003)	7.7 3.8	1.4 0.2	Microdialysis of VMH
McNay and Gold (2001)	Not measured, fed	1-1.2	Microdialysis of hippocampus
Dunn-Meynell et al. (2009)	6.7 3.1	1 0.5	Microdialysis of VMH
Van den Top et al. (2017)	6.5	4	CSF samples, anaesthetised

There are a few areas of the CNS, the circumventricular organs, where the blood-brain barrier is deficient, and here cells could be exposed to higher (plasma) levels of glucose via fenestrated capillary networks. Examples include the arcuate nucleus of the hypothalamus and the area postrema in the brainstem, as well as the subfornical organ. The PVN is not considered to be a circumventricular organ, although it does receive projections from these areas. Interestingly, it has been shown that within the hypothalamus, neurons which respond to higher levels of glucose (above 2.5mM) are only found in the arcuate nucleus, a circumventricular organ, whilst GI and GE neurons

in other areas of the hypothalamus respond to changes below 2.5mM (Fioramonti et al., 2004).

4.1.4 Cell subtypes of interest in glucose sensing

The hypothalamus is a key CNS area sensing and integrating information on glycaemic state, with specialized glucose-sensing neurons in distinct regions, including the arcuate and ventromedial nuclei (Kang et al., 2006, Kang et al., 2004), dorsomedial nucleus (Otgon-Uul et al., 2016), paraventricular hypothalamus (Melnick et al., 2011) and lateral hypothalamic area (Marston et al., 2011). Anteriorly, the preoptic area has also been reported to contain GnRH neurons which are glucose excited (Beall et al., 2012a, Roland and Moenter, 2011). Plasticity has been reported in neuronal responses to glucose with changing environment, e.g. lowered glucose thresholds with recurrent hypoglycaemia in VMN (Song and Routh, 2006). Changes have also been reported related to age and exposure to high fat diet (van den Top et al., 2017). In addition, van den Top et al. describe glucose sensing neurons which behave in an adaptive fashion, altering their responses to glucose depending on the context of the whole animal's energy state.

Other areas of the brain have also been identified as playing a role in glucose sensing. In particular, the brainstem has been identified as a further important area. Areas in the brainstem which have been implicated as having intrinsic glucose sensing include the nucleus of the solitary tract ((Balfour et al., 2006, Mimee and Ferguson, 2015); Mimee and Ferguson did not examine intrinsic glucose sensing), dorsal motor nucleus of the vagus (Balfour et al., 2006), and area postrema (Funahashi and Adachi, 1993). The lateral parabrachial nucleus has recently been the focus of interest. A group of cholecystokinin expressing neurons, a proportion of which also express the leptin receptor, within the lateral parabrachial nucleus have been shown to be intrinsically glucose inhibited and to be involved in the counterregulatory response to hypoglycaemia (Flak et al., 2014, Garfield et al., 2014).

Table 4.2 Hypothalamic glucose sensing areas and neuronal subtypes (after Fioramonti et al. (2017))

Area	GE	GI
Arcuate	POMC (Parton et al., 2007) unclear if direct glucose sensing Unknown additional subtypes (Fioramonti et al., 2007)	NPY (Muroya et al., 1999, Fioramonti et al., 2007, Murphy et al., 2009b) GHRH (Stanley et al., 2013) unclear if direct glucose sensing
VMN	SF1(Toda et al., 2016) Unknown additional subtypes (Fioramonti et al., 2004, Wang et al., 2004)	SF1 (Toda et al., 2016) Unknown additional subtypes (Wang et al., 2004, Fioramonti et al., 2004)
DMN	GABA (Otgon-Uul et al., 2016)	GABA (Otgon-Uul et al., 2016)
LH	MCH (Burdakov et al., 2005a)	Orexin (Burdakov et al., 2005a) NPY (Marston et al., 2011) GABA (Karnani et al., 2013)
PVN	Unknown subtypes (Melnick et al., 2011)	Unknown subtypes (Melnick et al., 2011)
PO	GnRH (Roland and Moenter, 2011, Beall et al., 2012a)	None found

PO- preoptic area, POMC- pro-opiomelanocortin, NPY- neuropeptide Y, GHRH- growth hormone releasing hormone, SF1-steroidogenic factor-1 , MCH-melanin concentrating hormone, GnRH- gonadotrophin releasing hormone

4.1.5 Evidence for glucose sensing in the PVN

The PVN is believed to have a role to play in glucose homeostasis and in particular the response to hypoglycaemia, as discussed in the introduction, section 1.8.3. There is a small body of existing evidence for glucose sensing in the PVN. One electrophysiological paper using acute slices has been published in rats, which suggests that some putative pre-autonomic neurons (defined by their response to a depolarising current step, see also section 4.2.5 below) may be glucose excited (~24% of neurons), some may be glucose inhibited (~26%), and that these responses persist in the presence of TTX (Melnick et al., 2011). Putative neurosecretory neurons were not shown to be glucose responsive.

Prior to this, a publication performing extracellular recordings in anaesthetised rats reported that 12/92 cells in the PVN behaved in a GI fashion in one experiment, and a further 4/40 in a second experiment (Shiraishi et al., 2000). No GE neurons were reported in this study. A more recent paper using extracellular recordings in

anaesthetised rats demonstrated both GE (27) and GI (20) cells in the PVN, in response to microinjections of 5mM glucose (Guan et al., 2017). No statement is made as to how many non-responsive neurons were observed in the PVN in this paper. The authors report that 'changes in neuronal firing frequencies were considered to be responses if they were statistically significant ($p < 0.05$) and exceeded 20%'. GE neurons increased their firing rate from 3.34 ± 0.65 Hz to 6.12 ± 0.94 Hz, no data is provided for the magnitude of response of GI neurons. In addition, it does not appear that any control was made for the osmotic effect of microinjecting 5mM glucose in this study.

As previously discussed, the PVN contains a wide range of differing neuronal subtypes, and little or no work has been done to examine subtype specific responses. One review paper (Fioramonti et al., 2017), suggests that there is evidence that some PVN GE neurons are nesfatin-1 expressing cells (Sedbazar et al., 2014). However, on closer examination of the original paper, mention is made in the text of calcium rises in the presence of 5mM glucose in dissociated neurons in culture, but not what the previous glucose level was or whether there was any change. No other evidence is presented regarding the glucose sensitivity of these cells, and the paper focuses on their responses to NPY and alpha-MSH in the presence of 5mM glucose.

4.1.6 The electrophysiological properties of CRH neurons of the PVN

Most work has focused on the differences between broad subtypes within the PVN, in particular seeking to identify electrophysiological differences between parvocellular, magnocellular and pre-autonomic neurons (Tasker and Dudek, 1991, Luther et al., 2002). As is the case for other techniques, it is also true here that most studies have been performed in slices from rats, and there is relatively little mouse data available. It is clear that there are differences between the broad subtypes of neurons present in the rat PVN. Putative neurosecretory neurons, which project to the anterior pituitary gland, exhibit brisk firing in response to a depolarising current injection, whilst pre-autonomic neurons are seen to fire in bursts. In addition, the bursting activity seen in pre-autonomic neurons is often superimposed on a slow depolarisation, mediated by T-type calcium currents (Luther et al., 2002, Melnick et al., 2007).

Wamsteeker and colleagues (2013), published a paper which briefly describes the electrophysiological properties of CRH neurons in mice, as identified using the fluorescent reporter gene TdTomato. This is the same CRH-ires-Cre strain of mice, developed by Huang and colleagues (Taniguchi et al., 2011) used for electrophysiology reported in this thesis and therefore direct comparisons will be made with their results. Wamsteeker et al. patched neurons (n=23) in the mid PVN, and reported these as a single group of neurons, with properties similar to the rat putative neurosecretory cells. No low threshold spiking activity indicative of putative pre-autonomic neurons was observed in this mid PVN population, such as was described in rat putative pre-autonomic neurons. Wamsteeker et al. report relatively high input resistance (933MΩ) and a near linear current-voltage relationship over the range -20pA to +20pA from a holding potential of -80mV. It is not clear whether the resting potential of these cells is -80mV or whether they were held at this level. The current: action potential frequency relationship is also near linear with injections of current up to +60pA from a holding potential of -80mV. This paper also presents evidence for inputs onto these neurons which are NMDA, AMPA and $GABA_A$ mediated, using a combination of pharmacological antagonists and assessment of reversal potentials to identify the nature of the conductances mediating the synaptic events.

4.1.7 Other techniques used to identify glucose sensing neurons in the CNS

Although electrophysiology remains the gold standard for the identification of glucose sensing neurons in the CNS, a range of other techniques have been employed. The use of extracellular recordings in in vivo has already been described (Guan et al., 2017, Shiraishi et al., 2000, Oomura et al., 1964, Oomura et al., 1969, Anand et al., 1964). Voltage sensitive fluorescent signals have also been used to investigate glucose sensing (Vazirani et al., 2013, Murphy et al., 2009b, Murphy et al., 2009a, Canabal et al., 2007a, Canabal et al., 2007b), largely in dissociated adult hypothalamic neurons in culture. A similar approach in dissociated cells using fura-2 calcium imaging has also been employed (Kang et al., 2004, O'Malley et al., 2006, Dunn-Meynell et al., 2002). These techniques have not been employed in acute slices or in vivo in the glucose sensing field up to this point, perhaps largely due to technical considerations such as the challenge of loading neurons evenly with dye, and time constraints on experiments following loading.

There are clear limitations to primary cell culture of neurons, in particular, the normal connectivity of these neurons is disrupted, and they will also lack the broader supportive network of astrocytes, glia and other non-neuronal cells. It is also challenging to identify which type of neuron is present in the culture, in particular in a very heterogeneous brain area such as the hypothalamus where many neuronal subtypes are found in close proximity.

4.1.8 Beyond electrophysiology- GECIs and potential for neuronal subtype specific calcium imaging

The recent advent of GCaMP6f and similar calcium sensitive fluorescent indicators (GECIs) (Grienberger and Konnerth, 2012), which can expressed in specific cell subtypes, has the potential to offer further avenues of investigation of glucose sensing. This technique has not thus far been used in glucose sensing work, but has been used in the related field of feeding signals in vivo in the arcuate hypothalamus, examining responses of AgRP neurons to feeding compared to sham feed (Betley et al., 2015). The potential for expressing GECIs in specific cell subtypes, and indeed imaging in vivo makes this an appealing technique for further development.

Successful calcium imaging requires two main technologies acting in synergy, firstly the ability to signal calcium levels, which has largely relied on development of fluorescent calcium dependent molecules, and secondly the ability to image the fluorescence with appropriate spatial and temporal accuracy. This section will firstly consider the signalling molecules before briefly covering recent advances in imaging techniques.

4.1.8.1 History of calcium indicators

The initial development of calcium indicators involved the development of small molecules or proteins combining some form of binding of calcium with the ability to fluoresce at a specific wavelength. Aqueorins (bioluminescent photoproteins), and arsenazo III, a synthetic compound which altered its light absorption when bound to calcium, were among the earliest calcium sensors. However, the major problem with these indicators lay in getting them into cells. The development of the next generation of calcium sensors by Tsien and colleagues (Tsien, 1980) significantly advanced the field. These compounds combined calcium chelators such as EGTA or BAPTA with a

fluorescent chromophore. Fura-2 was the most widely adopted of these molecules and has been very widely used in a range of cell types, both neuronal and non-neuronal (Grynkiewicz et al., 1985). Fura-2 was particularly useful as it fluoresces at 340 and 380nm, and alters the ratio on binding calcium. Ratiometric comparison of the 2 wavelengths allows more accurate calcium measurements (Neher, 1995). Further small molecule calcium sensors were developed, with improved signal to noise properties and photostability, including Oregon Green BAPTA and fluo-4 (Paredes et al., 2008).

The disadvantages of all the small molecule calcium sensors lay in their lack of cell subtype specificity. They could also be problematic in terms of the need to load cells with dye, which could lead to variability in loading, increased background signal from dye not loaded into cells and dye failing to remain in cells for more than 2-3 hours. They were thus unsuitable for chronic imaging.

The advent of genetically encoded calcium indicators (GECIs), again by Tsien and colleagues (Miyawaki et al., 1997) resolved many of these problems. These indicators use a calmodulin binding protein fused with a fluorescent protein (initially GFP) to create a molecule which alters its fluorescence on binding calcium. Initially these indicators were less appealing due to poor signal: noise ratios and slow kinetics, limiting the time course over which they could detect events. However, newer GECIs have largely surmounted these early problems, such that specific subtype cells of interest can now be transduced to express a calcium indicator and imaged readily.

Two major groups are currently in widespread use. The first, the FRET group (e.g. yellow cameleon (Nagai et al., 2004), use a conformational change on binding calcium to bring two flourophores close enough together that Forster resonance energy transfer can occur, with reduction in the fluorescence signal of one (the donor) and increase in the second (acceptor). This results in a ratiometric change in fluorescence. The second group, of which the GCaMP family are excellent examples, are single fluorophore molecules, again undergoing conformational changes on binding calcium to a calmodulin element, in this case acting to increase overall fluorescence. The GCaMP molecules initially had less favourable signal to noise ratios and kinetics, but newer generations have resolved both problems, for example comparing GCaMP3 and the GCaMP6 family,

the signal to noise ratio is 6-11 fold improved for GCaMP6 family members, and the rise time for GCaMP6f is ~80ms compared to ~137ms for GCaMP3 (Chen et al., 2013, Ye et al., 2017). Figure 4.1 illustrates calcium sensing in a GCaMP molecule.

It is important to remember that all calcium sensors are only able to provide an indication of free calcium levels within a cell, and also that they are effectively acting as an additional calcium buffer within cells. Those with low affinity calcium binding, such as GCaMP2 will have less of a buffering effect than the high affinity molecules such as Fura-2 and Oregon Green BAPTA-1, but they will all have some effect. In addition, the higher the concentration of the indicator in the cell, the greater the buffering effect. This factor is not always readily under the control of the investigator, particularly when expressing a GECI using a viral vector or genetically modified mouse line (Grienberger and Konnerth, 2012).

GCaMP6f, the GECI used in this thesis, is a highly useful, fast responding GECI, with rapid on and off kinetics (tau 74ms on, 400ms off), which has a linear signal response over small numbers of action potentials (1 action potential~120% increase in signal, 8 action potentials~870%) (Chen et al., 2013). Additionally, GCaMP6f has been reported to allow identification of neurons without the addition of a co-expressed fluorescent molecule, at low levels of calcium (typical resting calcium ~0.1µM in cytoplasm). The dynamic range of fluorescence for this GECI in vitro is wider than its predecessors. Overall, these properties result in a signal which is dim but still visible in quiescent cells, good temporal resolution and a bright signal in response to activity dependent increases in calcium.

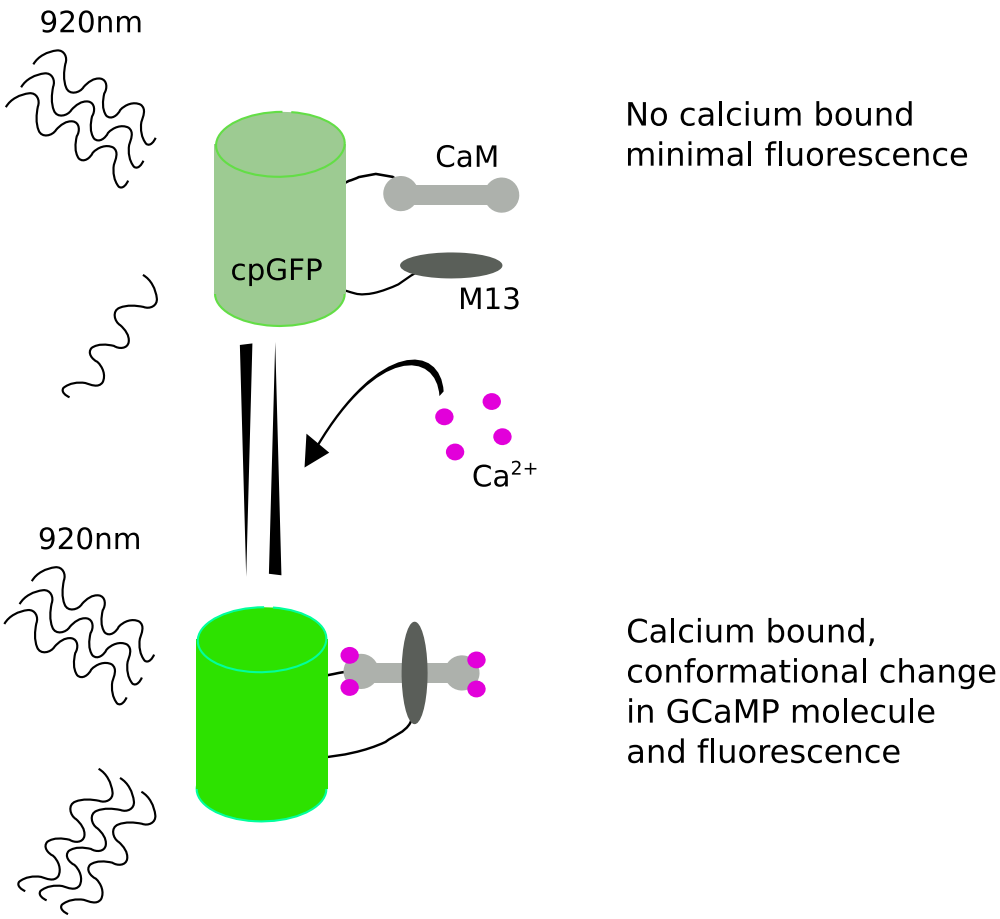

Figure 4.1 Schematic to illustrate calcium sensitive fluorescence in GCaMP family of genetically encoded calcium indicators
Upon binding calcium (4 binding sites), GCaMP undergoes a conformational change which results in greatly increased GFP fluorescence.

4.1.8.2 2-photon imaging in vitro and in vivo

The development of 2-photon imaging techniques has greatly expanded the potential uses of GECIs, particularly in vivo (for a detailed minireview, see (Svoboda and Yasuda, 2006). The principles underlying 2-photon imaging as compared to confocal imaging are summarised in Figure 4.2. Essentially, the key advantage of the technique over conventional widefield microscopy lies in the ability to image at deeper levels within tissues. The tissue penetration of near red and infrared wavelengths used in 2-photon microscopy is greater and causes less tissue damage. Traditional confocal imaging is able to image at depth, but causes much greater damage and bleaching effects, both in the plane of imaging and above and below, compared to 2-photon. Particular advantages are gained for in vivo studies, but even in slices, the ability to image a z-plane below the surface is of great value, as it enables imaging of a plane of healthy neurons, whilst neurons on the surface of a slice often exhibit very bright signals, due to cell damage in the slicing process.

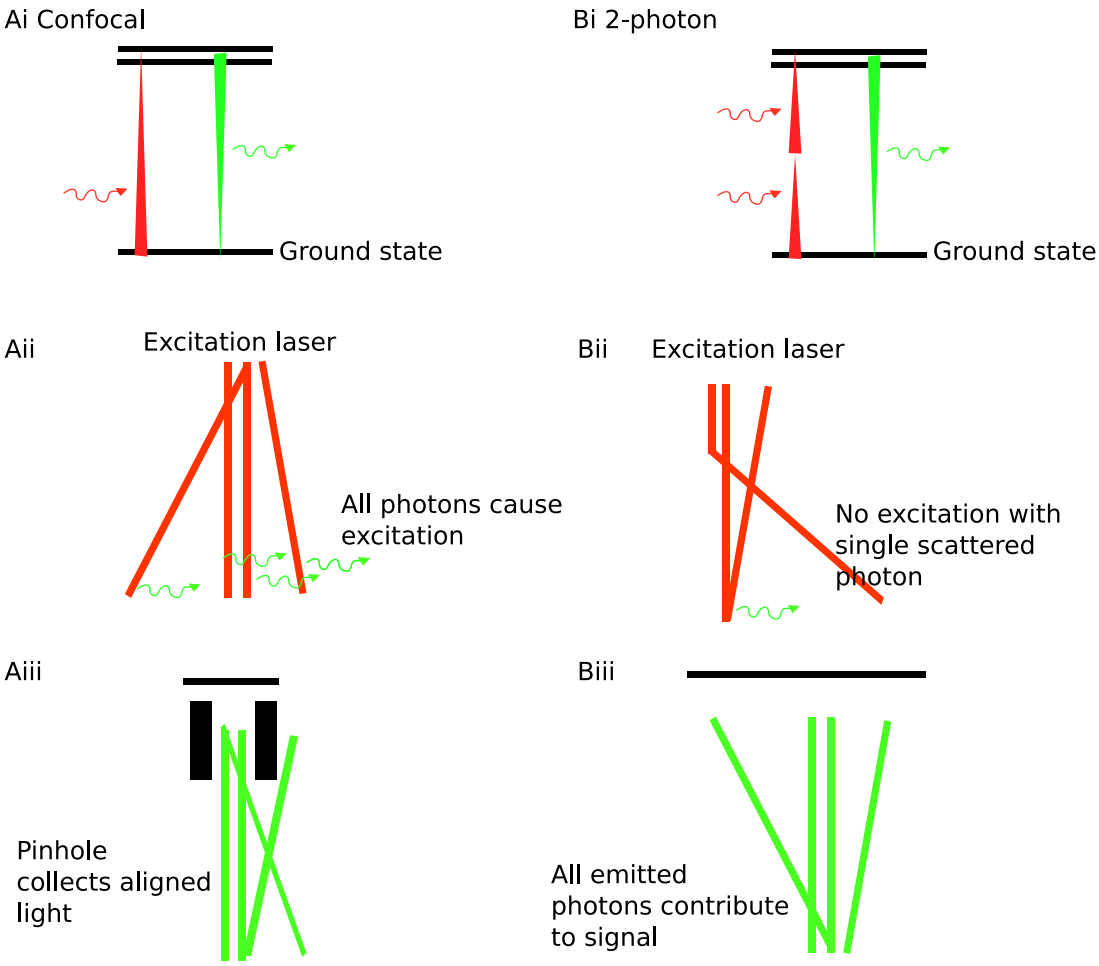

Figure 4.2 Schematic to illustrate principles of 2-photon compared to confocal microscopy

Ai Confocal microscopy- a single high energy photon excites a fluorescent protein which emits fluorescence on returning to ground state.

ii Excitation can occur wherever a high energy photon is found, including all photons which are scattered.

iii A pinhole is needed to collect emitted fluorescence from a focused area which means that only aligned photon emissions contributed to signal- scattered emitted photons contribute to noise.

Bi 2-photon microscopy; 2 low energy photons (infrared or near infrared) act cooperatively to excite a fluorescent molecule, which then emits a single high energy photon on returning to its ground state. The excitation by 2 photons is a non-linear process, and is therefore confined to a very small focal area.

ii Single scattered photons cause no excitation, reducing noise from out of focus tissue.

iii In addition, because excitation only occurs in a focused area, all emitted light contributes to signal, whether or not it is scattered; there is no need for a pinhole for emission fluorescence.

4.2 Hypotheses

- CRH PVN neurons show altered activity with reductions in extracellular glucose
    - seen with steps from high and physiological baseline glucose

4.3 Aims

- Investigate electrophysiological properties of CRH neurons *in vitro*
- Characterise their responses to a fall in perfused glucose from 10mM
- Develop a calcium imaging approach and analysis pipeline using CRH x GCaMP6f mice
- Examine the effect of steps from a physiological glucose concentration of 2.5mM

4.4 Results

4.4.1 Initial electrophysiological characterisation of CRH neurons in the PVN

4.4.1.1 Baseline electrophysiological characteristics of CRH PVN neurons

In the whole cell current clamp configuration, baseline current voltage relationships (n=13) and action potential firing frequencies were recorded (n=22). Initial data were obtained in 10mM glucose, to enable comparison of properties with those previously reported for this neuronal population (Wamsteeker Cusulin et al., 2013). Some of the CRH neuronal properties reported here appear comparable to those reported previously (shown in Table 4.3 and Figure 4.3) and additional features were also observed. This was a spontaneously active neuronal population, with a brisk baseline firing frequency of 6.9±0.7Hz from a resting potential of -52±0.9mV (Table 4.4). Many cells were tonically active, whilst 10.2% (6/59) showed bursting patterns of activity (Figure 4.4). In addition, these neurons showed synaptic drive from elsewhere in the slice with multiple EPSPs and IPSPs visible when hyperpolarised below the action potential threshold (Figure 4.4C). Wamsteeker et al. did not comment on the intrinsic firing rate or resting potential of their neuronal population. Input resistance was significantly lower than that described by Wamsteeker et al. (751±50.1 MΩ here, 933±19.8 MΩ for Wamsteeker, unpaired t-test p=0.0024). This could be due to a number of reasons. Wamsteeker et al. in general used younger animals (4-6 weeks) and recorded at a lower temperature (30-32°C). They also patched solely in the mid PVN, whilst the results here are from the entire length of the PVN. In addition, it is not entirely clear what potential Wamsteeker et al. held their cells at to measure input resistance.

Table 4.3 Comparison of CRH neuronal properties here with Wamsteeker Cusulin et al. (2013)

Reported property	Wamsteeker	Simpson
Input resistance	933±19.8 MΩ	751+/-50.1 MΩ
Current- membrane potential relationship	Near linear over range -20 to + 20pA from holding potential of -80mV	Held to -70mV. Similar over relationship over -20 to +20pA range, above this linearity lost as cell nears action potential threshold
Current- action potential frequency relationship	Near linear over range +10 to +60pA from -80mV	Held to -70mV, steeper increase in AP frequency seen
EPSCs	Present- combination of NMDA and AMPA	Present
IPSCs	Present, $GABA_A$	Present
Intrinsic properties	Not reported	See Table 4.4

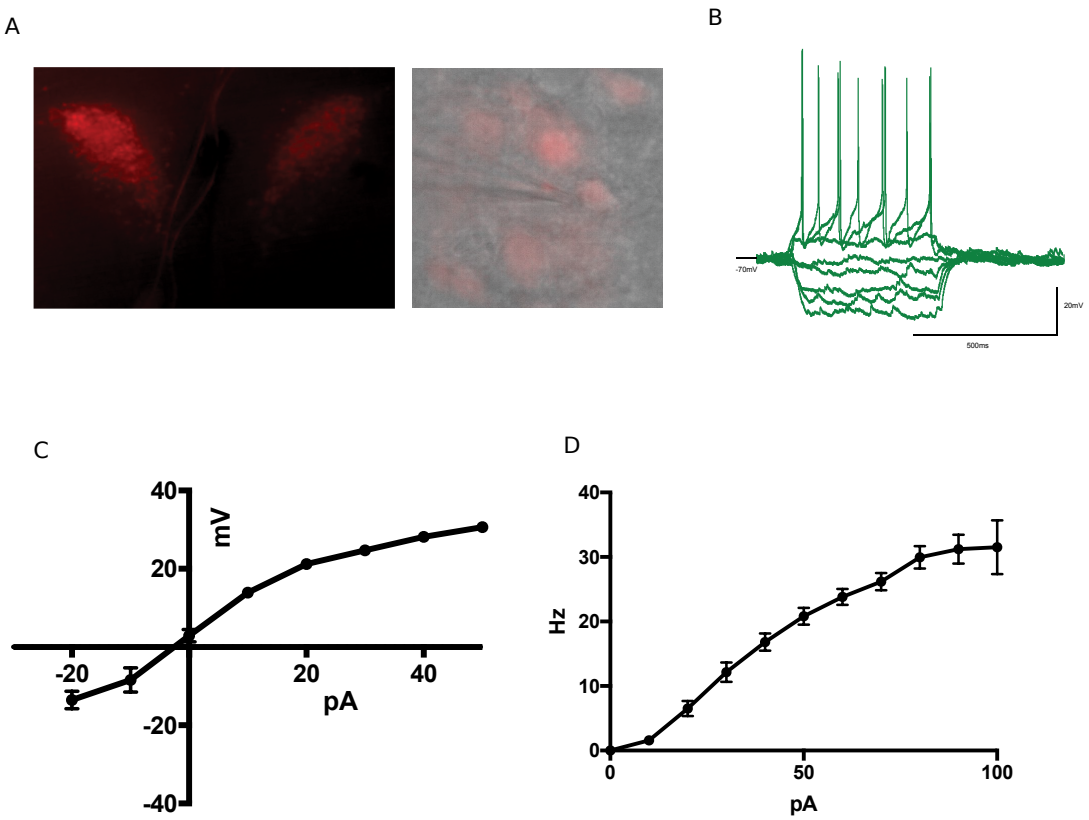

Figure 4.3 Baseline electrophysiological properties of CRH-Cre x TdTomato expressing neurons in 10mM glucose

A Example images of fluorescent neurons seen under 5X (left) and 40X objectives. 40X fluorescence image (red) superimposed onto image from infrared camera (greyscale), with pipette visible touching cell membrane

B Example whole cell recording showing voltage response to current steps from -40 to +30pA with cell held at -70mV between steps

C Current voltage relationship from cells patched in 10mM glucose (n=13)

D Action potential frequencies in response to incremental current steps from -70mV (n=22)

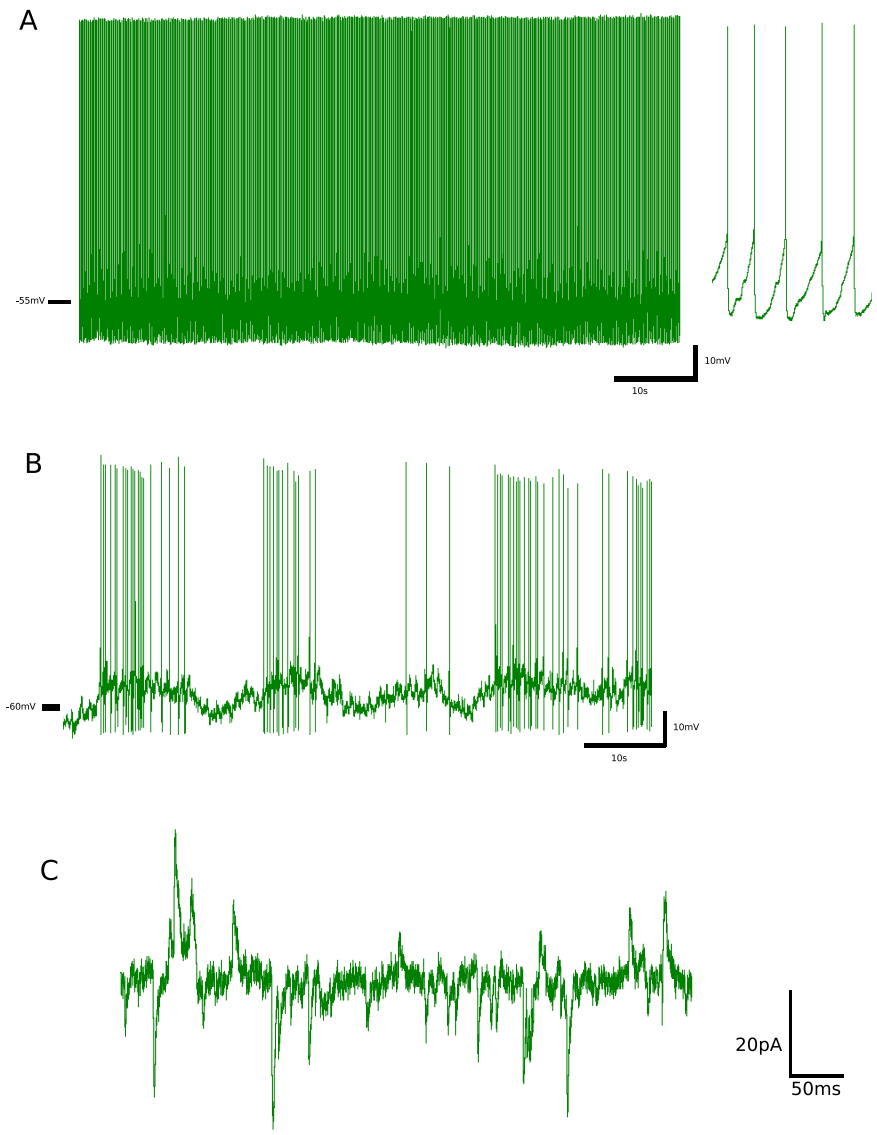

Figure 4.4 Further illustrations of CRH-Cre x TdTomato cell properties
Example whole cell current clamp traces from cells in 10mM glucose, with differing action potential firing profiles
A Tonically active cell, inset blown up part of trace to show action potential profile
B Cell exhibiting bursting pattern of activity
C Illustration of excitatory and inhibitory post synaptic currents in voltage clamp, cell held at -65mV

4.4.1.2 Comparing baseline characteristics in 10mM or 2.5mM glucose

The same data was also obtained from cells with 2.5mM glucose as their baseline solution (n=10), which more closely represents likely physiological levels in the brain tissue. The results of the comparison between the intrinsic properties of CRH neurons with baseline glucose of 10mM and 2.5mM is shown in Table 4.4. The only parameters where statistically significant differences were observed were action potential (AP) amplitude and after-hyperpolarisation (AHP) amplitude.

In order to examine whether the difference in AHP amplitude had an effect on other cell properties, the current-firing frequency relationship was plotted for cells patched in 10mM glucose compared to those in 2.5mM glucose. Cells in 2.5mM glucose were in fact less likely to fire action potentials in response to any given current injection, compared to those in 10mM glucose (data not shown). This is the opposite effect to what might have been predicted based on the larger AHP amplitude in 10mM glucose, and suggests that the larger AHP seen in 10mM glucose, whilst statistically significant, may not result in a relevant biological effect.

Table 4.4 Cell properties in 2.5mmol glucose (n=10) compared to 10mmol glucose (n=20)

	2.5mMglucose	**10mMglucose**	**P value**
Resting Potential (mV)	-53±2.2	-52±0.9	0.66
Threshold (mV)	-43±2.1	-39±1.0	0.08
AP Amplitude (mV)	31.81±3.5	39.90±2.1	0.04
AP duration (ms)	2.73±0.3	3.02±0.2	0.46
AHP amplitude (ms)	-15.39±0.8	-20.08±1.2	0.02
AHP duration (ms)	52.5±8.9	61.65±7.1	0.45
AP frequency (Hz)	7.07±1.3	6.9±0.7	0.93
Input resistance (MΩ)	704.4±39.1	751.6±50.1	0.55
Time constant (ms)	18.3±1.6	21.6±1.4	0.16
Capacitance (pF)	26.0±1.7	30.7±2.7	0.27

4.4.3 Initial electrophysiological evidence for glucose sensitivity in PVN CRH neurons

4.4.3.1 Defining cell responses and spatial locations

A priori, neurons were arbitrarily classified on the basis of their potential responses to glucose. Neurons increasing their firing frequency by >30% on transitioning to a low glucose solution were defined as glucose inhibited (GI). Neurons that decreased their firing frequency by >30% when stepped to low glucose were labelled glucose excited (GE). The remaining neurons were classified as non-responsive to glucose (NR).

It was possible to identify the approximate location of cells recorded within the PVN. In general, each mouse brain gave rise to 2 or occasionally 3 slices containing PVN cells. Slices were marked on one edge to indicate left and right, allowing orientation in the bath that preserved the rostro-caudal orientation of each slice, and kept in rostro-caudal order. It was therefore possible to distinguish rostro-caudal levels between slices. In addition, it was possible to state whether cells were located ventrally or dorsally within the PVN.

4.4.3.2 Effect of a step from baseline 10mM to a hypoglycaemic perfusate

The majority of cells (59/68) were observed to fire spontaneous action potentials, as described in Table 4.4. (mean resting potential -52±0.9mV, mean AP frequency 6.9±0.7, n=20). An outlier subset of cells (9/68) were also identified; these did not fire action potentials at rest and were significantly more hyperpolarised (-85±5.36mV). This smaller subset of 'silent' cells will be discussed in more detail in section 4.4.3.4.

23 neurons from the main, spontaneously active group were maintained throughout the entire protocol to provide interpretable data including a low glucose step and washout. Of these, 35% fitted the criteria for being glucose excited neurons, and 8% were glucose inhibited. The remainder (57%) were not responsive to glucose (Figure 4.5). The thresholds described in section 4.4.3.1 appear to appropriately delineate three distinct populations with regard to their change in AP frequency in response to glucose (Figure 4.5B). The GE responses were large (5.6±1.5Hz in 10mM glucose falling to 1.1±0.66Hz in 2.5mM glucose, n= 8) and reversible in 7/8 recordings. In 4/8 cells the GE response was

repeatable as shown in Figure 4.5C. GI responses were also reversible in 2/2 cells, with a change in AP frequency of 1.7-5.0 rising to 6.2-7.4Hz (range).

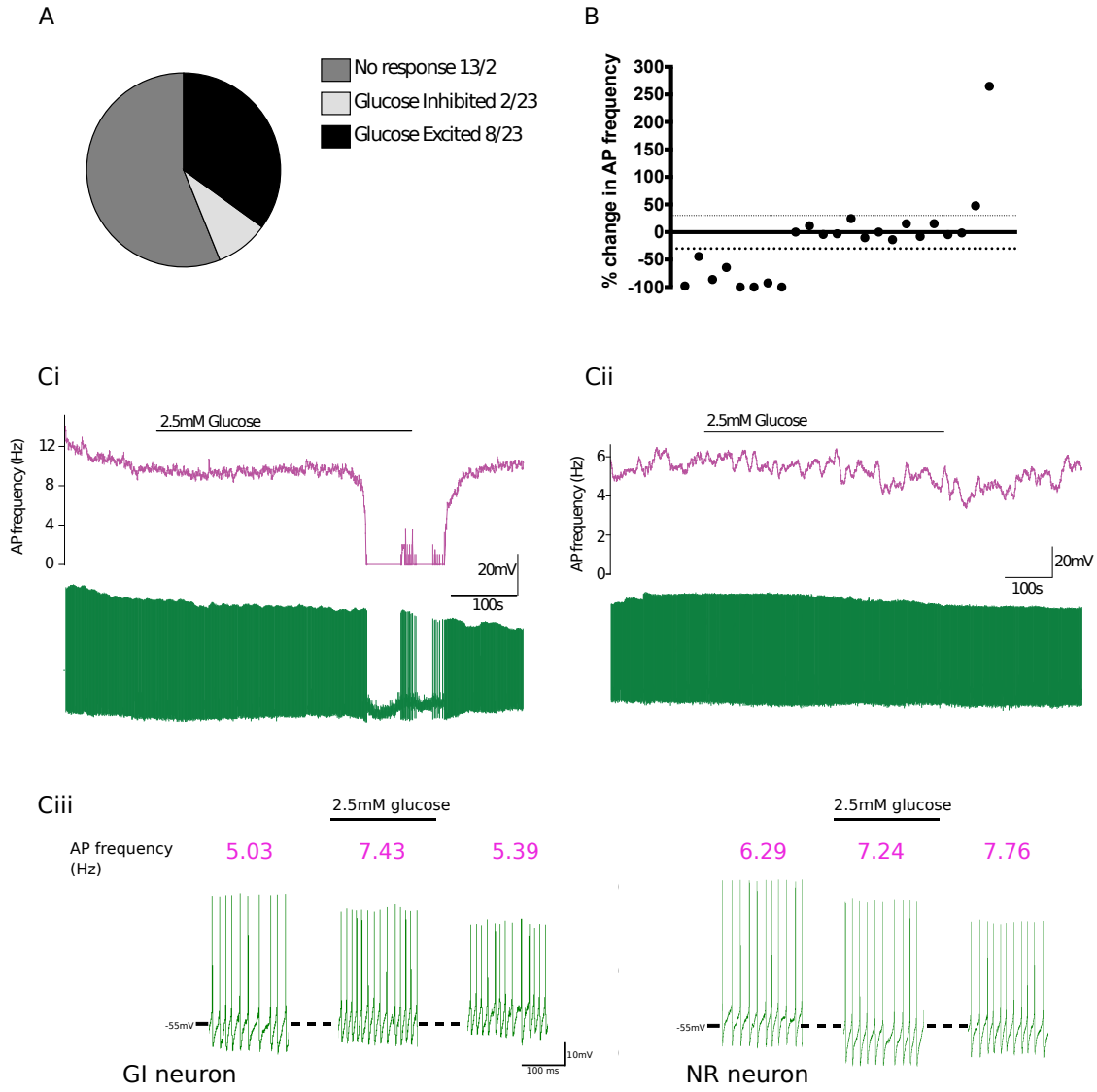

Figure 4.5 Initial electrophysiological evidence for glucose sensitivity in CRH neurons in the PVN

A Classification of 23 neurons according to a response to a step from 10mM to 2.5mM glucose

B Graph to show cut off levels for categorisation of neurons. Lines at +30% and -30%

C Examples of i) glucose excited (GE), ii) non responsive and iii) glucose inhibited (GI) neurons

4.4.3.3 Difficulties with stability of recordings in slices obtained in 2.5mM glucose

The initial experimental plan was to go on to investigate the responses of cells following slicing in 2.5mM glucose, with a step to 0.5mM. This would more closely replicate physiological levels of recorded in brain tissue (Silver and Erecinska, 1994b). However, cutting in 2.5mM glucose produced slices in which it was challenging to establish stable recordings. Gigaohm seals were more difficult to achieve and cells did not often remain stable in the whole cell configuration. It did not prove possible to obtain stable recordings for long durations in most of the neurons patched. From the few cells recorded in 2.5mM glucose with steps to 0.5mM glucose, 2 GE and 4 NR neurons were observed, with recordings appearing comparable to those seen in 10mM glucose (Figure 4.6). GI neurons were not observed in this group, which is unsurprising given the small sample size.

The rest of the electrophysiological data obtained and presented here uses slices cut and maintained in 10mM glucose, with steps to 2.5mM glucose, which (whilst not physiological) is in line with the levels used in previous studies and did allow data collection with a much higher degree of consistency.

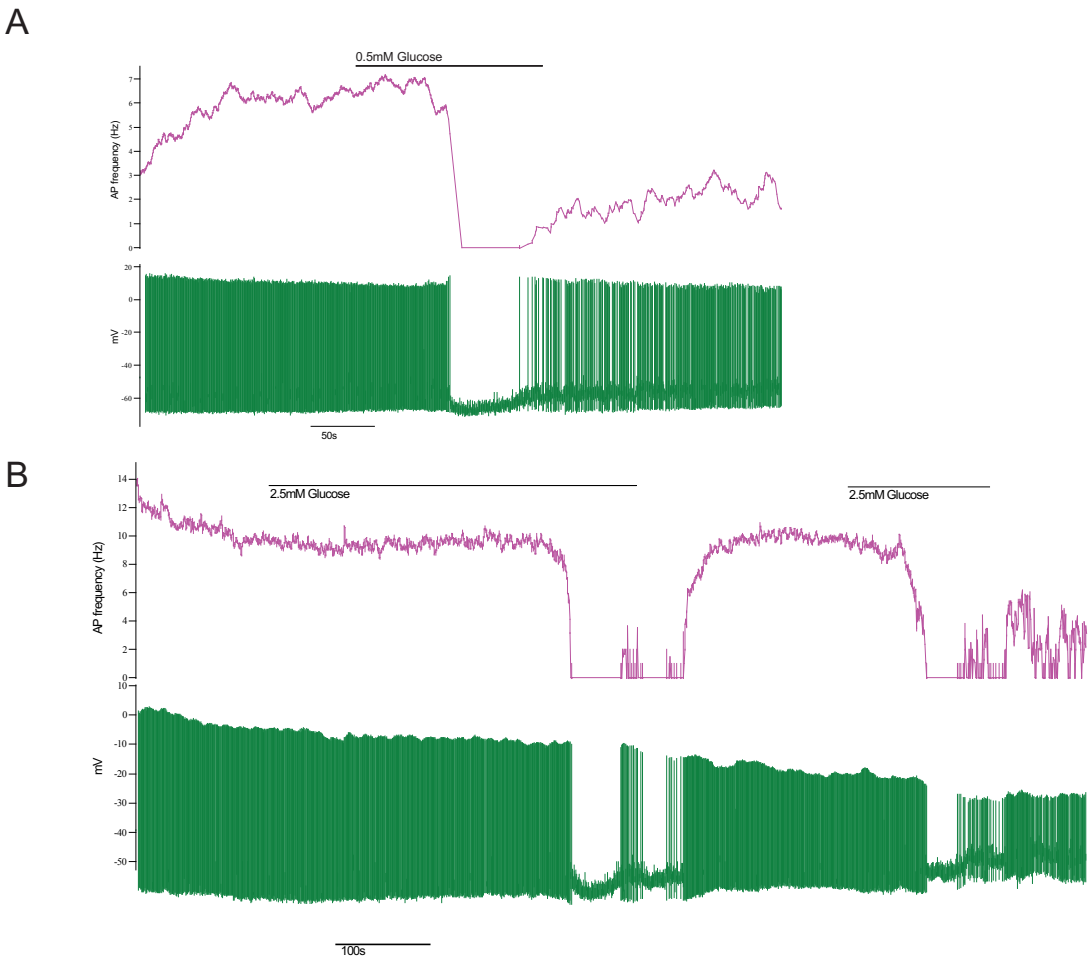

Figure 4.6 Glucose excited cells seen in 2.5mM and 10mM glucose

A Spontaneously active CRH neuron strongly and reversibly inhibited in response to a change of solutions from 2.5mM to 0.5mM glucose.

B Example of a comparable response to a change of solutions from 10mM to 2.5mM glucose.

Top panel indicates action potential frequency, lower panel displays whole cell current clamp trace. Bar indicating application of low glucose solution commences from time that solution first reaches bubble trap. There will be a short delay before arrival at the bath.

4.4.3.4 A subgroup of 'silent' neurons was observed which did not fire action potentials at rest and depolarised in response to a low glucose step

An outlier subset of PVN CRH neurons with distinctive cell properties was also identified in 10mM glucose (9/68, 13%). These cells were silent at rest and were significantly more hyperpolarised (-85 ± 5.4mV, n=7). In addition, they had lower input resistances, and a slightly higher capacitance, which would be consistent with the idea that they were larger neurons (Figure 4.7). This subgroup was largely found in more caudal slices of the PVN and tended to be located ventrally within the PVN. 4 cells were challenged with a low glucose step to 2.5mM glucose. All became more depolarised (change in membrane potential +13.4 ± 2.74 mV) and one cell began firing spontaneously suggesting that these are glucose inhibited neurons (Figure 4.8). None of these neurons were exposed to TTX.

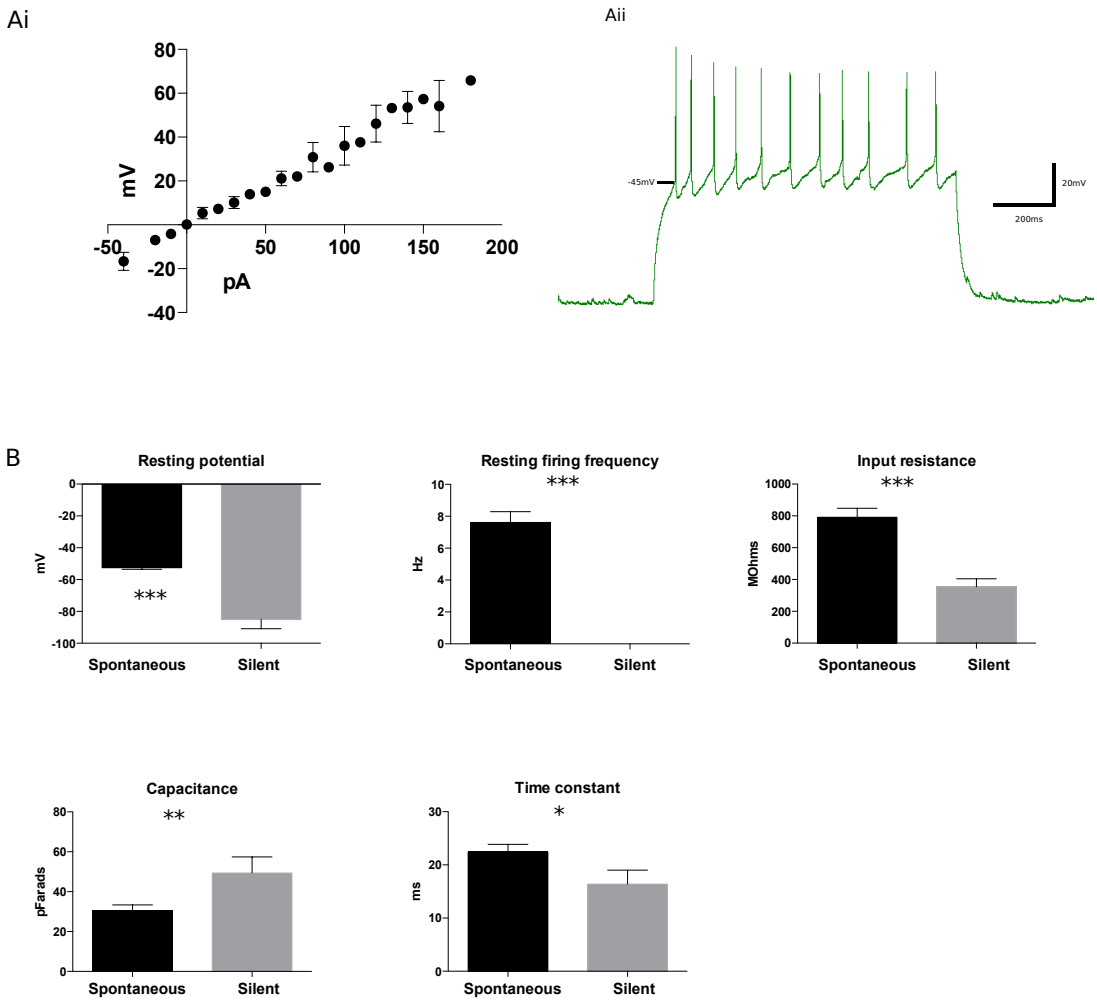

Figure 4.7 A second population of silent neurons with differing properties from the main spontaneously active subgroup

Ai) Current voltage relationships for 'silent' neurons, which do not fire action potentials at rest and are a small minority ii) example of voltage response of a neuron to 150pA current injection showing that these cells can still fire healthy action potentials

B Comparison of cell properties of silent neurons with previously described spontaneous subgroup (n=20 spontaneous, n=7 silent, ***=p<0.001, **=p<0.01, *=p<0.05, unpaired t-test)

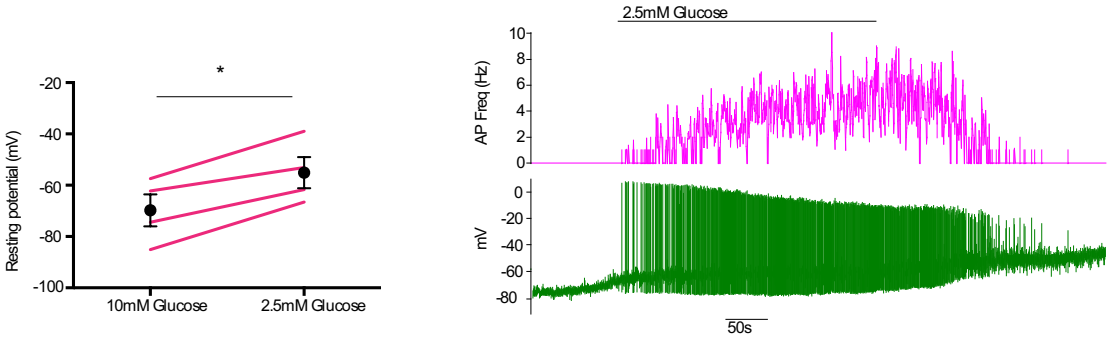

Figure 4.8 Responses of 'silent' neurons to a low glucose step
A Significant depolarisation seen in all cells where a step from 10mM to 2.5mM glucose solution was applied (n=4, $p<0.05$, paired t-test)
B Example cell which depolarises and increases firing frequency in low glucose (n=1; further 3 cells depolarised but did not fire)

4.4.4 Electrophysiological investigation of the anatomically distinct neuronal population projecting to NTS/DMX

One possibility was that the silent neurons might represent a pre-autonomic population. In an attempt to investigate this further, 8 CRH x Td mice, aged 6-12 weeks received brainstem injections to the NTS/DMX of the CAV-CMV-eGFP virus with the aim of retrogradely transducing the pre-autonomic PVN CRH neurons. Their brains were subsequently sliced for electrophysiology (after 2-4 weeks). As expected, retrogradely transduced eGFP positive neurons were observed, predominantly localised in the posterior part of the PVN, but there were relatively few of these in each slice, and even fewer which were also showing red fluorescence indicating CRH. Increasing the incubation time following injection did not increase the number of cells observed. Despite repeated attempts it was not possible to make stable recordings from any of these cells, and so no further conclusions could be drawn.

4.4.5 The effect of TTX on glucose responses

It is not possible to tell from the data presented thus far whether the neurons responding to glucose were directly sensing a change in glucose levels, or were responding to inputs from neurons in other areas within the slice- for example, VMN neurons which are known to be glucose sensitive (and would be expected to be contained in a coronal slice through the PVN). The effect of the same glucose step in the presence of TTX (to prevent action potential propagation and hence remove synaptic inputs) was therefore investigated. TTX was effective in blocking spontaneous action potentials in the majority of cells to which is was applied (12/17, 70%) (Figure 4.9A). 5 cells exhibited wide based spiking activity at a lower frequency- an appearance consistent with a calcium spikes (Figure 4.9 C). TTX had no effect on the resting potential Figure 4.9B). The protocol used to investigate the effect of TTX involved an initial control low glucose step, washout and subsequent application of TTX. Following this a second low glucose step in the presence of TTX was applied. Interestingly, regardless of the response of the same cells in the absence of TTX, 8/10 neurons depolarized when stepped to low glucose in the presence of TTX (Figure 4.10). Of these 8, 7 had a step to low glucose prior to perfusion with TTX. 5 were NR, 1GE and 1GI in

the absence of TTX. The final 2 neurons, which hyperpolarised in the presence of TTX, were both NR prior to application of TTX.

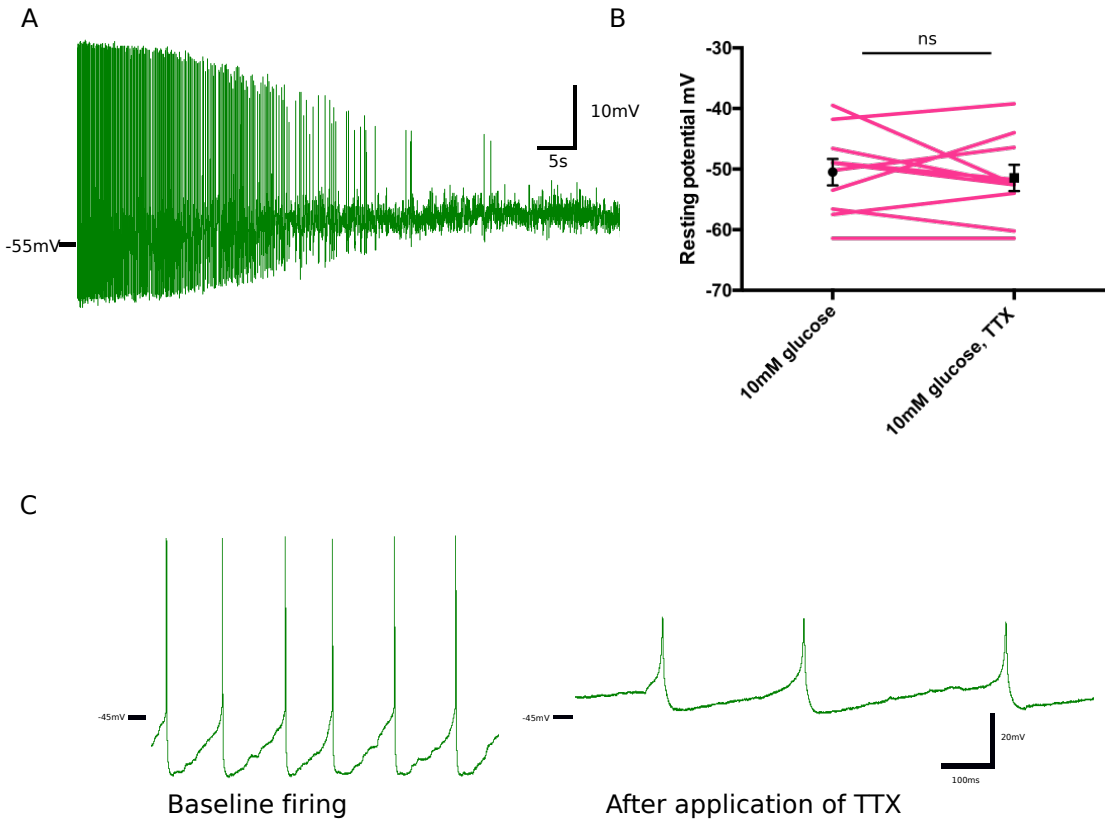

Figure 4.9 Effect of TTX on CRH PVN neurons in current clamp
A Example trace showing cessation of action potentials after TTX application
B TTX has no significant effect on the resting potential of this group of neurons. Graph shows mean and SEM as well as individual neuronal responses (n=10, p=0.64, paired t-test)
C A few cells exhibited persistent firing prior to and in the presence of TTX. Slower time course and smaller amplitude in TTX is suggestive of voltage gated calcium channels

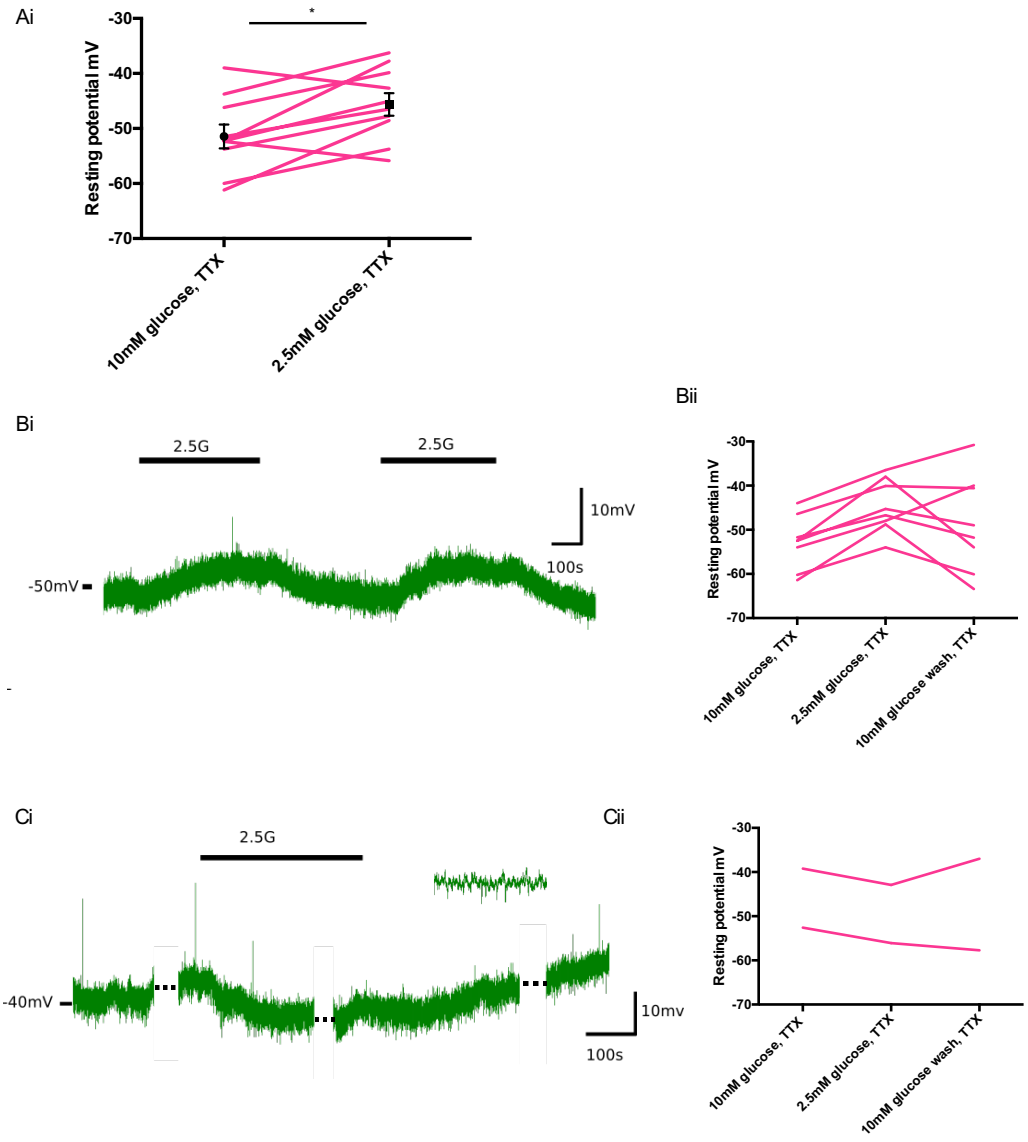

Figure 4.10 The majority of CRH neurons depolarise in response to a step from 10mM to 2.5mM glucose in the presence of TTX

Ai) A step to 2.5mM glucose in the presence of TTX resulting in a significant depolarisation. Graph shows mean and SEM as well as individual neuronal responses (n=10, p=0.012, paired t-test)

Bi) example trace of neuron which depolarised

Bii) individual changes in resting potential for all depolarising neurons, washout effect also shown (-54.5±2mV in 10mM glucose, -46.4±2mV in 2.5mM glucose, p=0.0003, paired t-test)

Ci)Example trace of neuron which hyperpolarised. Inset, zoomed in section to show mini excitatory post synaptic potentials. Gaps in trace at times of current injections

Cii) as for Bii) but showing those neurons which hyperpolarised.

4.4.6 A calcium imaging strategy to characterise glucose sensing properties of PVN CRH neurons

The electrophysiological data presented thus far suggests a proportion of CRH neurons are glucose sensitive. However, it was challenging and time consuming to collect the data; in part this reflects the fact that only a small subset of the neurons are glucose responsive (35% GE and 8% GI). To potentially obtain a higher throughput of data, investigate responses with steps from 2.5 to 0.5mM glucose, and in addition collect more spatial information about where within the PVN responsive cells might be found, a second set of experiments were carried out utilising calcium imaging in slices, using CRH x GCaMP6f mice.

As mentioned in the introduction, GCaMP6f is visible but not highly fluorescent in neurons with low levels of calcium (most neurons will have resting levels of 50-100nm (Berridge et al., 2000)). It is therefore difficult to identify non-responsive neurons, which could artificially amplify the numbers of responsive cells. A strategy to identify non-responsive neurons was employed- after performing low glucose steps and washouts, the slices were subsequently perfused with a high potassium solution to depolarize and increase calcium in all GCaMP6f containing neurons. This depolarisation typically revealed a much larger number of neurons and this data was used to inform ROI selection during analysis offline.

4.4.6.1 Specificity of GCaMP6f expression in the CRH x GCaMP6f mouse strain

A CRH x GCaMP6f homozygous mouse was bred successfully, as shown in Figure 4.11A. Unfortunately, it became apparent on imaging that expression of GCaMP6f in the CRH x GCaMP6f homozygous strain was off target, with high levels of expression throughout the forebrain (Figure 4.11B and C). Indeed, expression of GCaMP6f was so widespread that these off-target animals could be identified using a fluorescent light source and goggles, (excitation 440-460nm, emission 500nm longpass (Nightsea Dual Fluorescent Protein Flashlight, MA, USA)) when viewing the freshly dissected brain, as shown in figure 4.11B. This strategy was, therefore, abandoned and heterozygous CRH x GCaMP6f animals were used for all subsequent calcium imaging. These animals clearly expressed GCaMP6f in a circumscribed manner, which recapitulated that observed in

CRH x TdTomato mice. Expression of GCaMPf in heterozygous CRH x GCaMP6f mice in the PVN is demonstrated in Figure 4.11D.

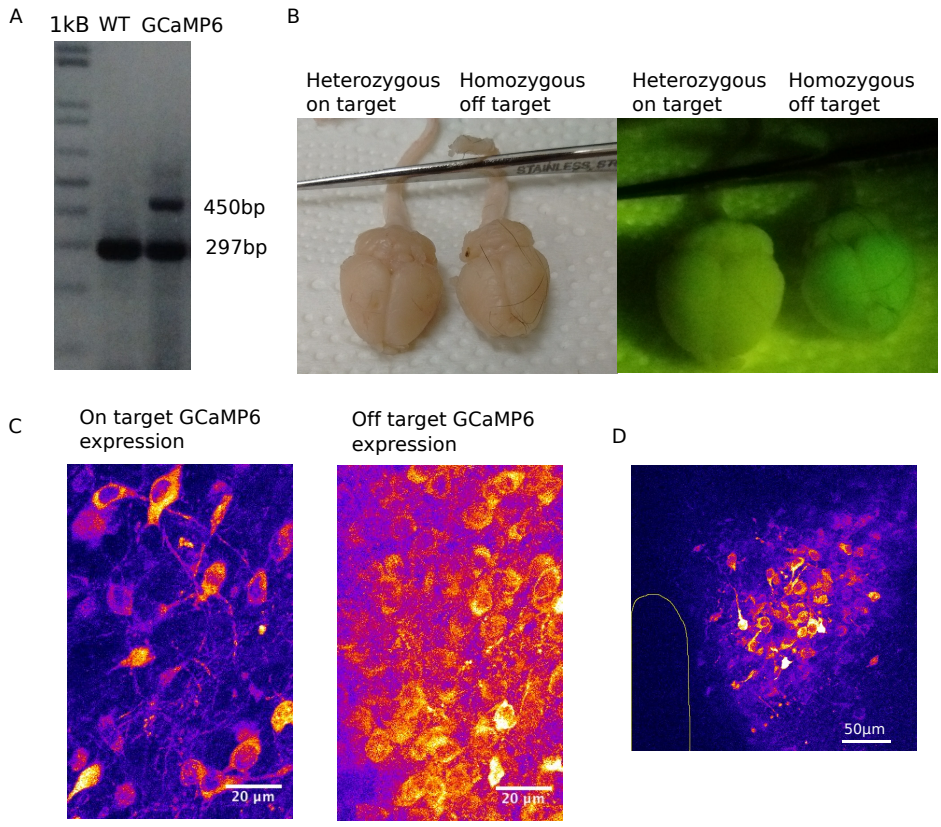

Figure 4.11 Inconsistent expression of GCaMP6f in mice bred from parents with both GCaMP6f and CRH-ires-Cre present in each parent

A Example of genotyping of GCaMP6f. WT band 297bp, mutant band 450bp

B Macroscopic demonstration of off target expression. The left-hand brain in each image expressed GCaMP6f under the control of the CRH promotor. The right-hand brain is from an off-target mouse and can be seen to fluoresce by the naked eye using Nightsea Lightsource and goggles (right hand image)

C Example images from calcium imaging (60X objective) in the periventricular region after application of high potassium to depolarise cells and increase their calcium signal. A much larger number of cells are visible in the image from the off-target mouse on the right.

D On target expression of GCaMP6f in the PVN in a mouse bred from a CRH-ires-Cre homozygous female and a GCaMP6f heterozygous male after application of high potassium as for C

4.4.6.2 Establishing recording and thresholding protocols

Small numbers of bright cells were readily visible in the PVN using epifluorescent microscopy, and this facilitated identification of relevant areas i.e. the PVN for 2-photon imaging. Some of these cells were likely to be undergoing necrosis, and fewer were observed deeper in the slice (consistent with the surface cells being more damaged by slicing). 2-photon imaging was therefore performed in a z-plane deeper than the surface of the slice to avoid the majority of these cells. A wide range of levels of baseline fluorescence were observed across cells. Therefore, each recording was normalised to its own baseline (lowest 5% of values) to allow reliable identification of relevant signals and thresholding (for more details of the data processing pipeline, see methods section 2.8). A baseline period of 200-400 seconds was recorded for each slice prior to any change in the perfusate. In order to assign neurons to GI and GE categories, a threshold of >3 standard deviations from the mean of the final 100 seconds of the baseline was chosen. For more details on thresholding, again see methods chapter 2 section 2.8.

On perfusion with low glucose for ~400s, a subset of cells responded with an increase (GI) or decrease (GE) in fluorescence which was taken as corresponding to an increase or decrease in intracellular calcium ((Grienberger and Konnerth, 2012) Figure 4.12 A,B). The majority of neurons had calcium signals which did not change until potassium was applied to depolarise all cells (NR). Examples are shown in Figure 4.12 C. A further subset were 'spontaneously active' (SA) with marked fluctuations in their fluorescence (calcium levels) but not responsive to changes in glucose (Figure 4.12 D).

The size of response was calculated differently for GI and GE neurons, as the profile of the calcium signal change was very different for the 2 groups. For more details please refer to the methods section 2.8. For GE neurons, a rolling mean of 40 seconds (20 images) was obtained for each time point from the raw data. The peak value during the baseline prior to changing the perfusate was calculated, and the trough value of the response to the low glucose solution was also obtained. The data was then normalised to the baseline by calculating (response-baseline)/baseline. For GI neurons, many responses were spiking in nature rather than slow rises in calcium level. This made a similar approach, or indeed calculation of area under the curve of limited value, as

values were small, and differences were not numerically significant between groups evens for cells that markedly changed their behaviour. Instead, the time spent with calcium levels greater than 3 standard deviations above the mean was calculated for each baseline and experimental period, and is expressed out of a maximum time of 450 seconds (the time spent in low glucose).

Images were acquired at 0.5Hz for the majority of the calcium experiments presented here. A single slice was imaged at a higher frequency (5Hz). Examples GI traces from this experiment are shown in Figure 4.14D. The gaps in the recording were necessary to maintain a manageable file size. It can be seen that response is still easily identified. However, the increased frequency of imaging did not reveal any further detail with regard to calcium transients, suggesting that 0.5Hz is a reasonable frequency for data acquisition for these experiments.

To enable comparison with previous electrophysiological data, 4 slices were cut and maintained in 10mmol glucose with steps to 2.5mM glucose. 30 GI and 9 GE cells were observed. Overall the response to the first application of 2.5mM glucose was greater than that to the second with regard to the number of neurons observed to respond (Figure 4.13 A). There was no statistically significant change in the size of the second response when compared to the first for either GI or GE neurons (Figure 4.13 B). Both spiking and slow rising responses were observed amongst GI cells (for examples see figure 4.12 A). 59.3% of GI cells had spiking responses, 40.7% exhibited slow calcium rises

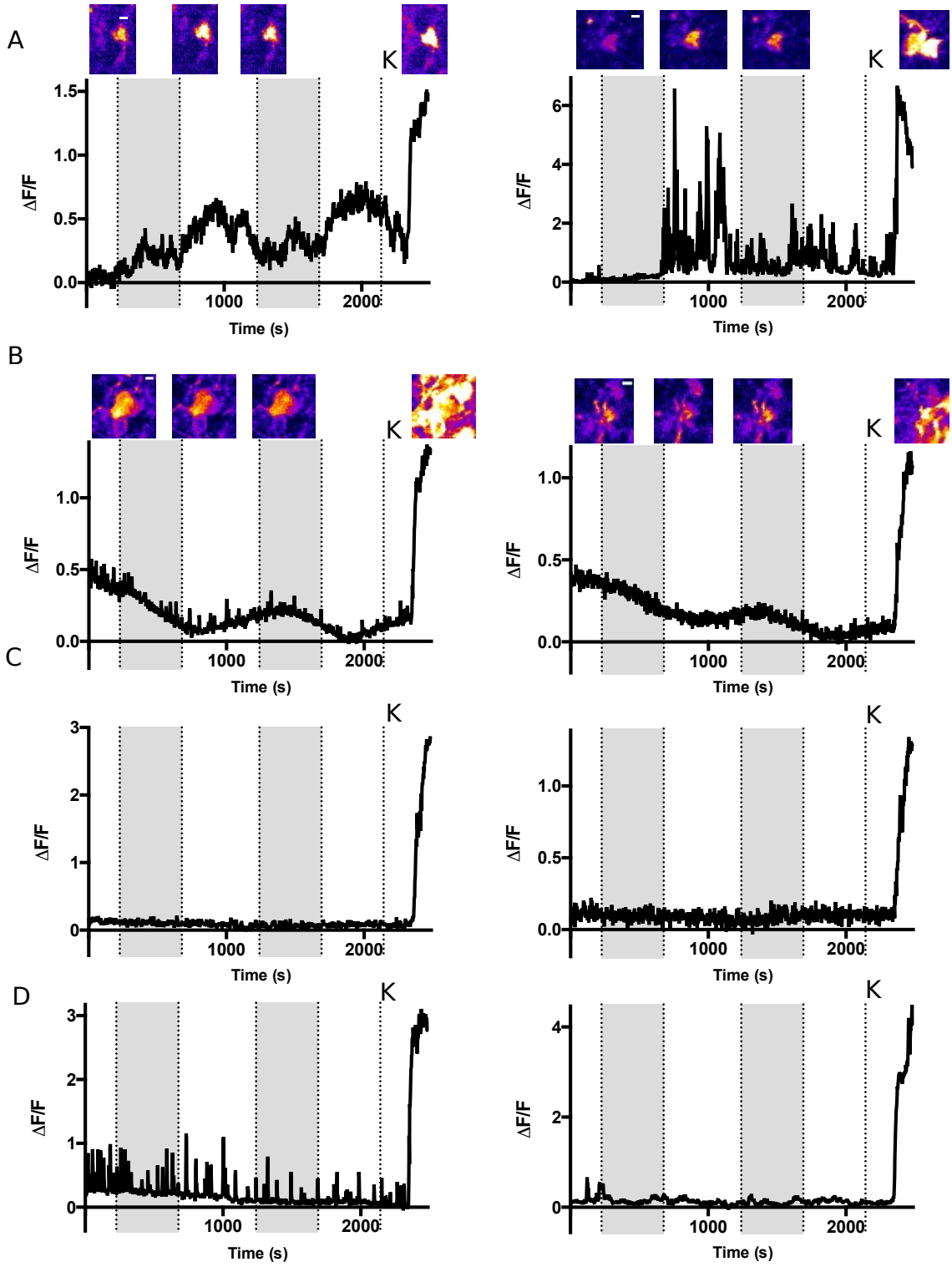
A
B
C
D
K
ΔF/F
Time (s)
1000
2000

Figure 4.12 Example traces for the 4 possible categories of CRH x GCaMP6f neuron observed using calcium imaging

A Glucose inhibited (GI), showing increased calcium after exposure to 0.5mM glucose
B Glucose excited (GE), showing decreased calcium after exposure to 0.5mM glucose
C Non-responsive (NR); changes in glucose had no effect
D Spontaneously active (SA); changes in calcium levels not associated with glucose changes
All data from CRH neurons in a single slice of paraventricular hypothalamus, cut and maintained in 2.5mM glucose. Steps down to 0.5mM glucose are indicated by the shaded areas of the graphs. A high potassium solution was applied at the final dotted line K
Inset images of GI and GE cells are averages of 10 images around time points 112s (baseline), 788s (0.5mM glucose), 1238s (washout) and 2464s (potassium response). White scale bars are 10microns

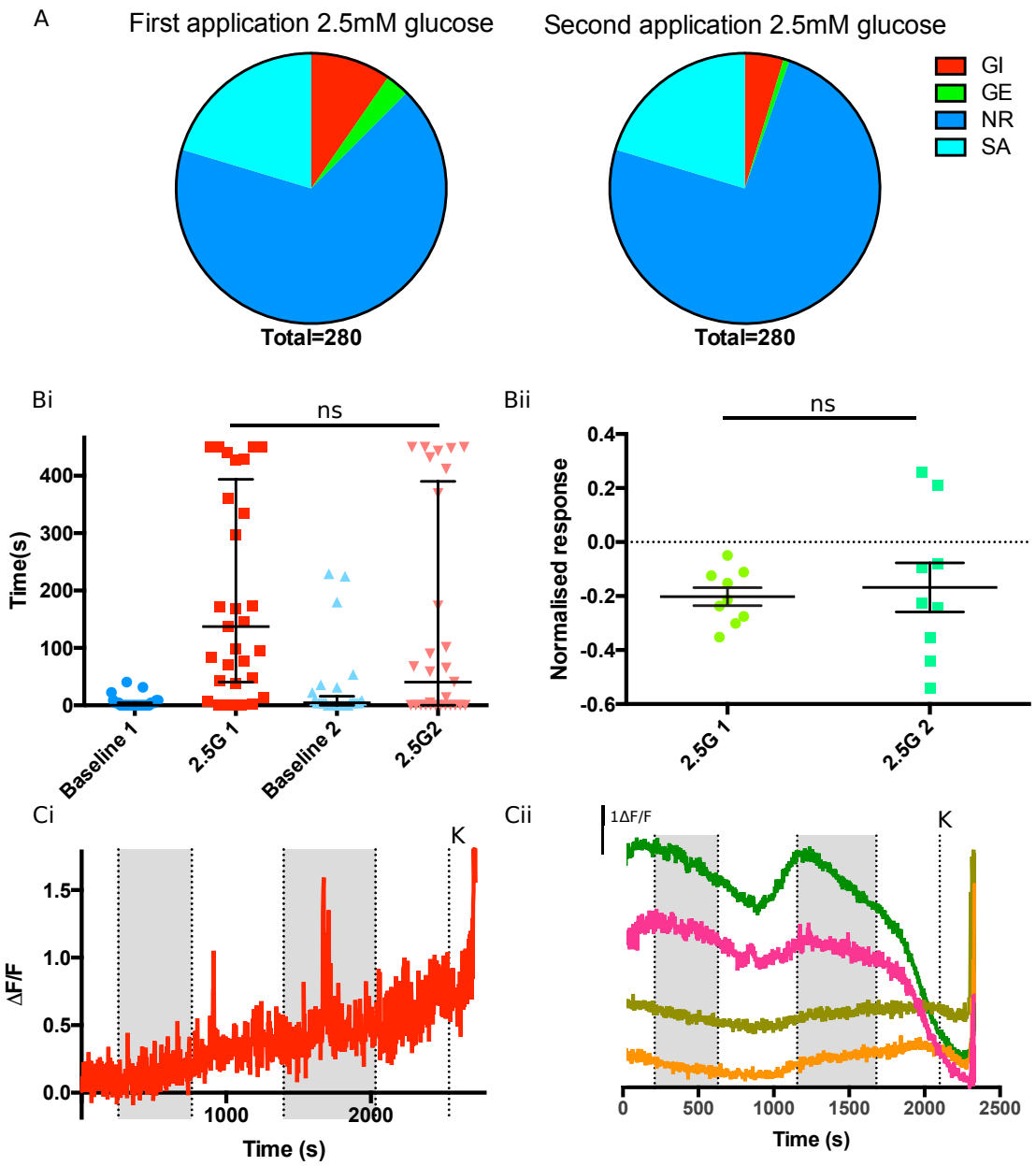
A
First application 2.5mM glucose
Second application 2.5mM glucose
GI
GE
NR
SA
Total=280
Total=280
Bi
ns
Time(s)
400
300
200
100
0
Baseline 1
2.5G 1
Baseline 2
2.5G2
Bii
ns
Normalised response
0.4
0.2
0.0
-0.2
-0.4
-0.6
2.5G 1
2.5G 2
Ci
K
ΔF/F
1.5
1.0
0.5
0.0
1000
2000
Time (s)
Cii
1ΔF/F
K
0
500
1000
1500
2000
2500
Time (s)

Figure 4.13 Calcium responses of CRH PVN neurons following steps from 10mM glucose to 2.5mM glucose

A Categorisation of neurons following a first and second step to 2.5mM glucose. Fewer cells respond to a second application of low glucose (Chi square value 8.942, p=0.0341)
B There is no change in the size of the response of GI (i) or GE (ii) cells to a second application of low glucose compared to the first (GI-Friedman test with Dunn's multiple comparisons, GE paired t-test)
C Example calcium traces for i) a GI cell and ii) a group of 4 GE cells (all from a single slice). Perfusion with low (2.5mM) glucose is indicated by shading in grey. Application of a high potassium solution occurs at the final vertical line (K)
Data from 4 slices, 2mice, 70±23.3 cells per slice. Data presented as median and IQR for GI, mean and SEM for GE

4.4.6.3 Comparison of recordings made in 10mM and 2.5mM glucose

Having established an imaging and processing protocol, slices were next cut in 2.5mM glucose and recorded following a step to 0.5mM glucose. Imaging was straightforward and there was no appreciable deterioration in cell health compared to slices obtained in 10mM glucose (as assessed by number of fluorescent cells per slice, stability of fluorescence and number of very bright (presumed necrotic) cells seen). Again, both spiking calcium responses and slower rises were observed in the GI population, with similar proportions to those seen in the 10mM slices (39.1% spiking, 60.1% slow rise). A similar pattern of responses to a first and second application of low glucose was seen to that observed for slices in 10mM glucose with fewer cells responding to a second application of low glucose (Figure 4.14A). However, in these conditions the size of both GI and GE responses were smaller after the second application of low glucose compared to the first (Figure 4.14B). Slicing and recording in 2.5mM glucose increased the numbers of GI and GE cells seen compared to 10mM (Chi-square 46.52, $p<0.0001$, Figure 4.15B). There was no significant change in the size of the first GI or GE response observed comparing cells in 10mM glucose with cells in 2.5mM (Figure 4.15C).

In this larger dataset, the question of whether cells could be pre-identified as, for example, GE, on the basis of their initial levels of fluorescence was raised. The hypothesis was that GE cells would have a higher baseline fluorescence (raw) compared to GI and NR cells in the same slice, due to their higher activity levels in baseline glucose (leading to elevated intracellular calcium). This was broadly correct, as shown in Figure 4.16 and suggests that GE cells do generally have an increased baseline firing rate compared to GI or NR cells. However, it did not hold true for every cell or indeed every slice, as is apparent from Figure 4.16C. This approach was not useful practically in pre-identifying GE cells, as some cells with very high baseline levels of fluorescence were in fact undergoing cell death, and it was not possible to differentiate these from possible GE cells at baseline.

Having established slicing in 2.5mM glucose with healthy appearing slices and performed an initial comparison with 10mM glucose slices, all subsequent data presented here uses 2.5mM glucose as a baseline level with steps to 0.5mM glucose to further investigate glucose sensing in CRH neurons.

4.4.6.4 Location of responsive cells within the PVN

It was possible to record precisely where each responsive cell was within each imaged slice, and also to estimate the rostro-caudal location of each slice with reference to the mouse brain atlas. These data are presented for the 2.5mM glucose slices in Figure 4.17. It appears that GE cells are primarily located more rostrally, whilst GI cells are found throughout the rostro-caudal extent of the PVN. GI neurons also appear to be more generally found at the edges of the CRH population, whilst GE neurons are located more centrally.

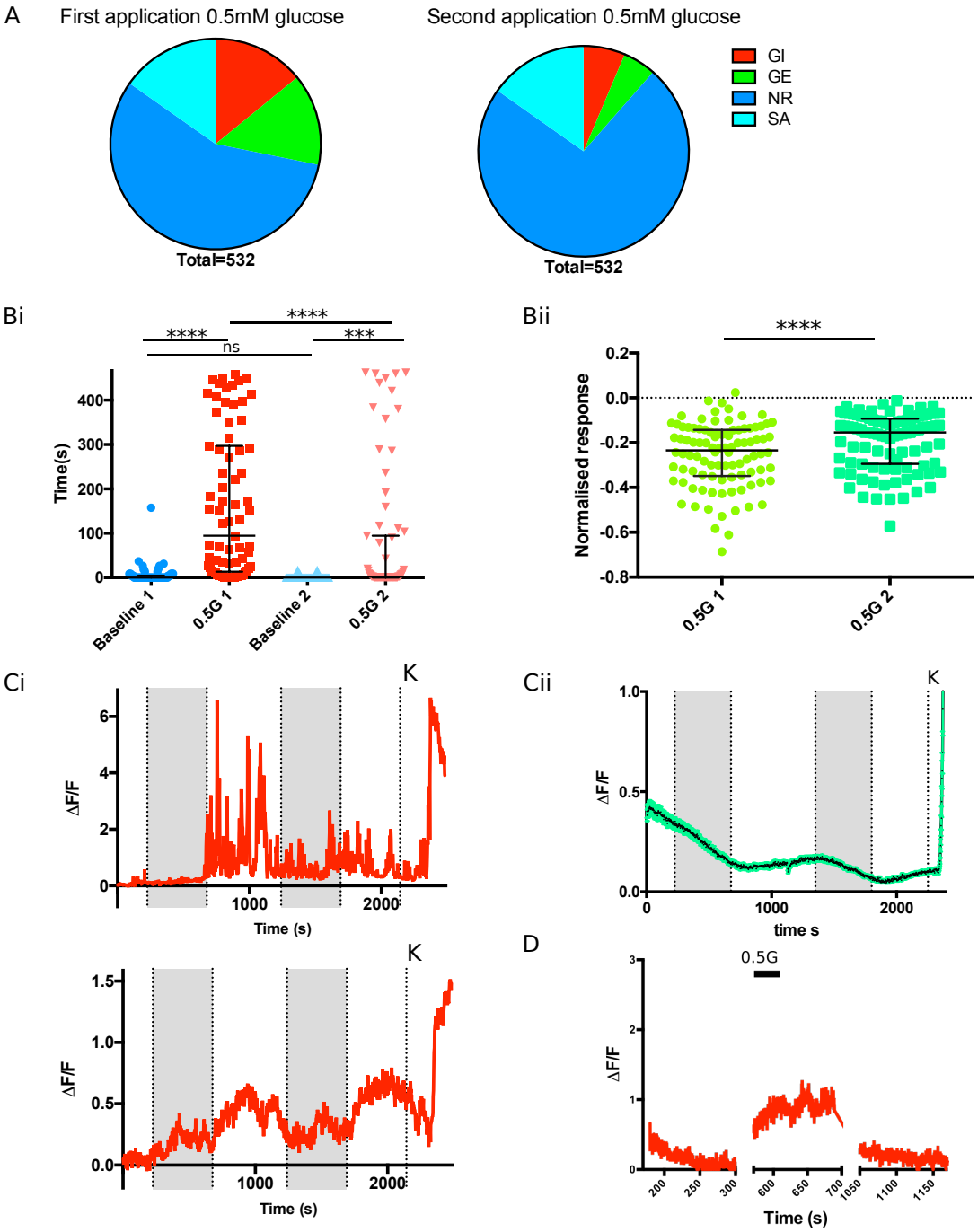
A
First application 0.5mM glucose
Second application 0.5mM glucose
GI
GE
NR
SA
Total=532
Total=532
Bi
****
****
***
ns
Time(s)
Baseline 1
0.5G 1
Baseline 2
0.5G 2
Bii
****
Normalised response
0.5G 1
0.5G 2
Ci
K
ΔF/F
Time (s)
K
ΔF/F
Time (s)
Cii
K
ΔF/F
time s
D
0.5G
ΔF/F
Time (s)

Figure 4.14 Calcium responses of CRH PVN neurons following steps from 2.5mM glucose to 0.5mM glucose

A Categorisation of neurons following a first and second step to 0.5mM glucose. Fewer cells respond to a second application of low glucose (Chi square value 8.942, p=0.0341)
B The size of the response of both GI (i) and GE (ii) cells is smaller following a second application of low glucose (Wilcoxon matched pairs signed rank test for GE, Friedman test with Dunn's multiple comparisons for GI, ****p<0.0001)
C Example calcium traces for i) a GI cell and ii) a group of 51 GE cells (all from a single slice), mean (black) and SEM (green) of the recordings shown. Perfusion with low (2.5mmol) glucose is indicated by shading in grey. Application of a high potassium solution occurs at the final vertical line (K)
D Example cell recorded at 5Hz rather than 0.5Hz. Gaps in recording due to file size limitations.
Data obtained from 3 mice, 5 slices, 106.4 ±28.7cells/slice. Data presented as median and IQR

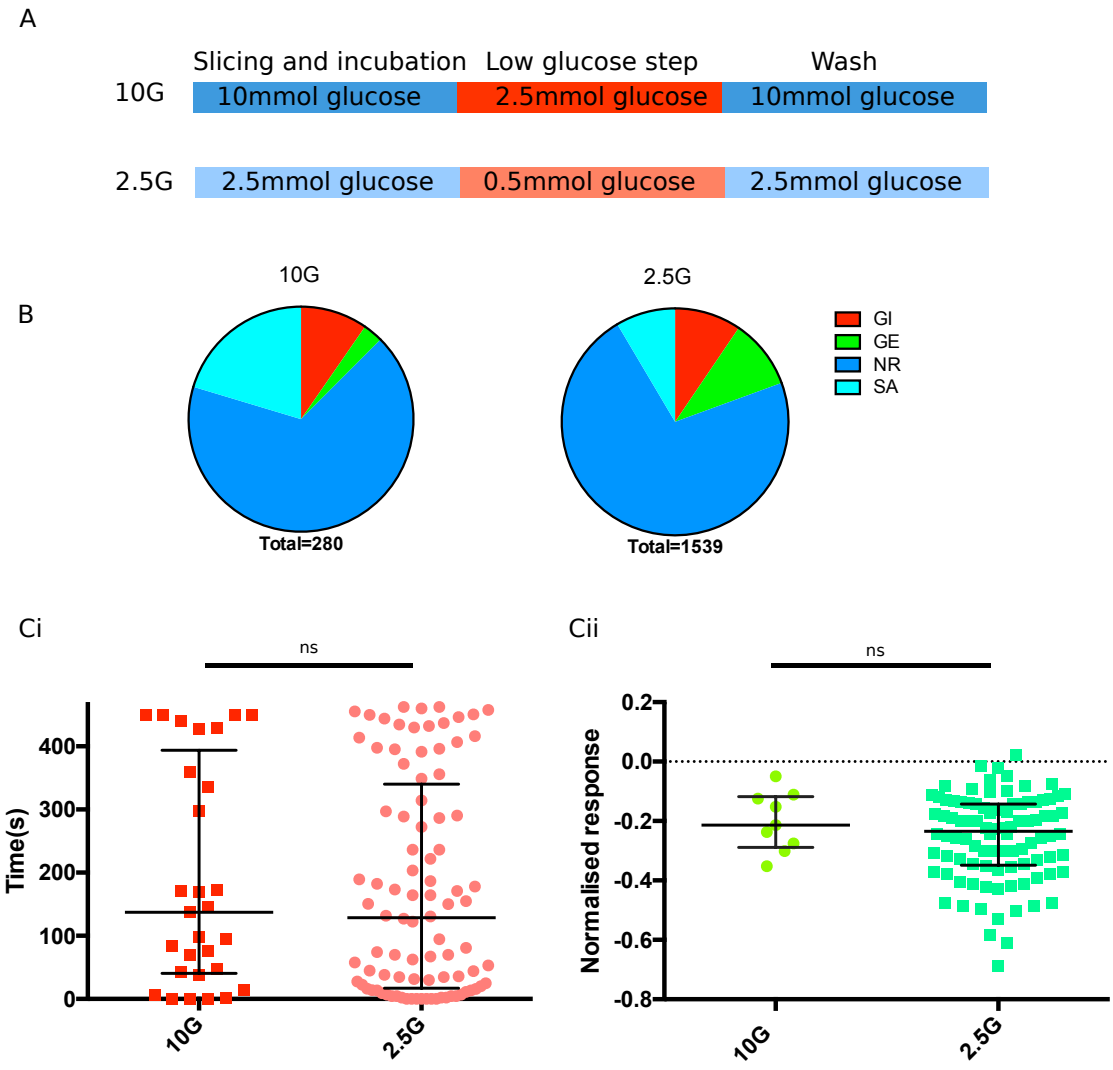

Figure 4.15 Comparison of CRH PVN cell responses to a low glucose step for cells cut and maintained in 2.5mM glucose compared to 10mM glucose

A Protocol for each group outlining glucose concentrations used

B Pie charts illustrating the distribution of cell responses for each population. There is an increase in GE cells and a decrease in SA cells in the 2.5mM glucose group (Chi square=46.52, $p<0.0001$)

Ci) There is no change in the size of the GI response seen between the 2 groups ii)There is no change in the size of the GE response seen between the 2 groups (Mann Whitney U test). Data shown as median and IQR

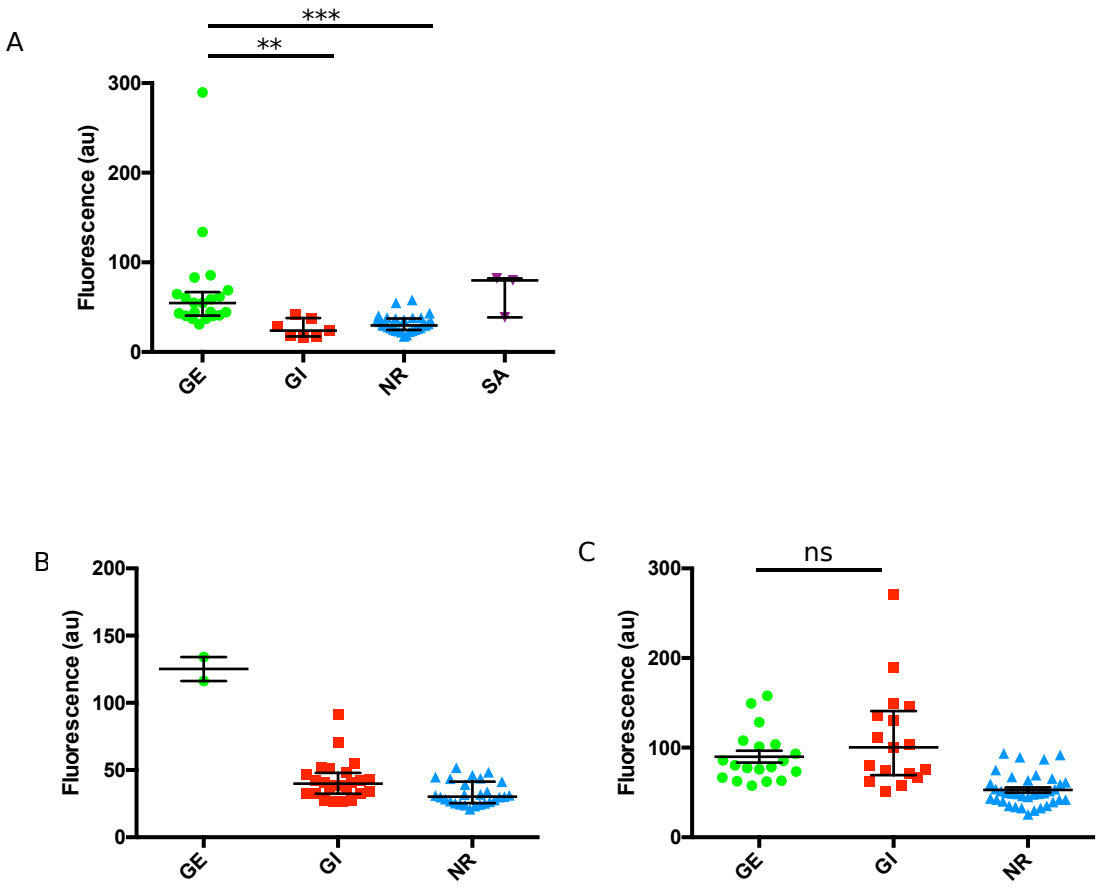

Figure 4.16 Baseline fluorescence in the raw data is indicative but not reliably predictive of response to low glucose

Examples of the mean raw fluorescence of the baseline (first 90seconds). Data is shown for individual slices as there is interslice variation between the maximum and minimum fluorescence levels.

A In the majority of slices, GE neurons, on average, have significantly higher baseline fluorescence than GI or NR. Spontaneously active cells are not distinguishable from GE cells on the basis of their baseline fluorescence (Kruskal Wallis test with Dunn's multiple comparisons, all comparisons not shown on the graph are ns)

B Some slices have very few GE neurons

C A slice in which the mean baseline fluorescence appeared similar for GI and GE neurons (Kruskal Wallis test with Dunn's multiple comparisons)

Data presented as median and IQR

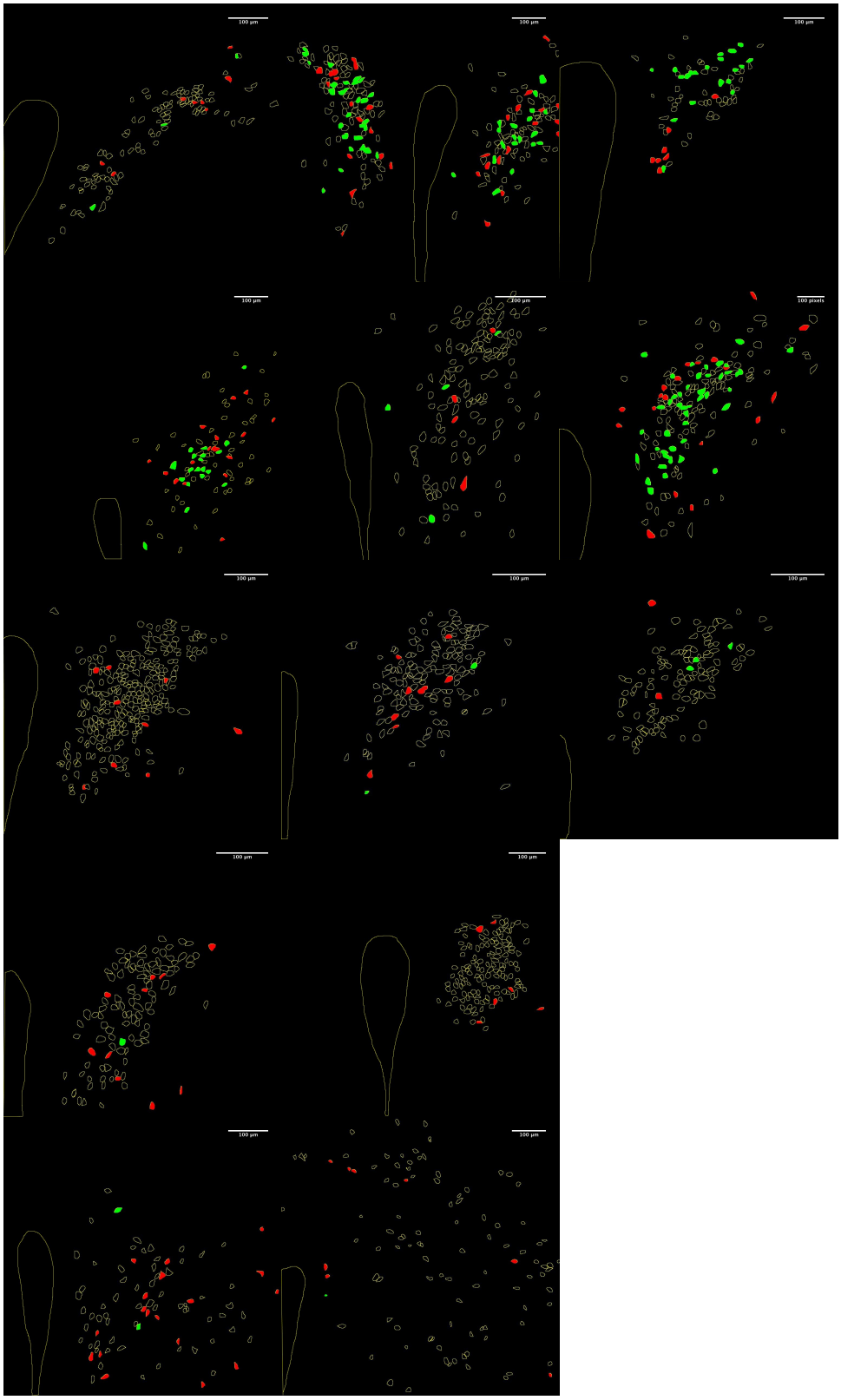
-0.58
-0.7
-0.82
-0.94
-1.06

Figure 4.17 Spatial distribution of GI and GE cells after a step from 2.5mM to 0.5mM glucose

Images are arranged rostral to caudal, GI neurons are red, GE green. Approximate bregma values are indicated on the left.
Data obtained from 8 mice, 1-3 slices per mouse.

4.4.6.5 Potential double labelling strategy- to use TdTomato to pre-identify CRH neurons for calcium imaging using GCaMP6

As a strategy to improve the ability to initially identify all CRH neurons, triple transgenic mice expressing both GCaMP6 and TdTomato under the control of CRH-Cre were bred. However, calcium imaging experiments carried out using these animals did not show any responses to glucose. The filter sets on the 2-photon microscope do not fully segregate the green and red signals (see Figure 4.18). This is particularly relevant given that the TdTomato signal is very bright, and the GCaMP6f fluorescence is dim, especially in quiescent cells. Even a small amount of bleed through of TdTomato into the GFP channel leads to problems with signal: noise in the data (given that the GCaMPf signal at basal levels of calcium was relatively small). The need to image 2 channels for each Z-plane or stack also led to a reduction in the temporal resolution of the images. This approach was therefore not pursued.

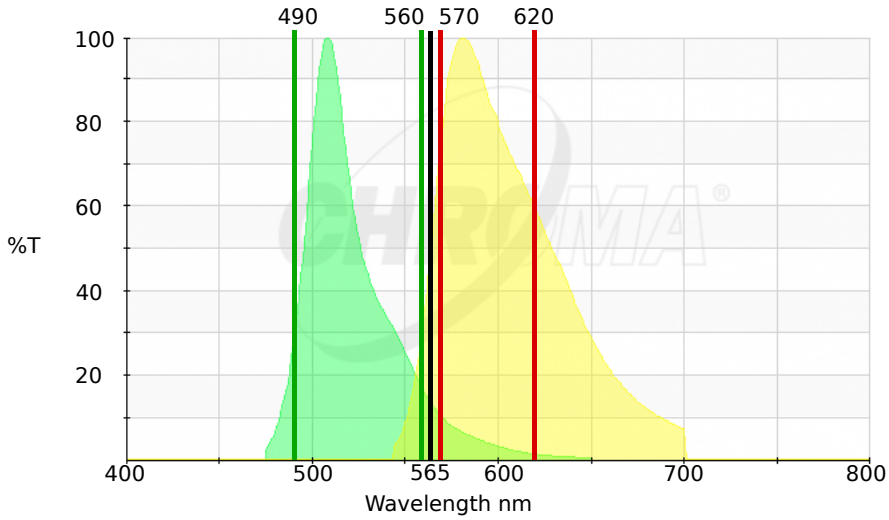

Figure 4.18 Emission spectra for TdTomato and GFP (GCaMP6F) are not fully segregated using the filters on the 2-photon microscope
Graph superimposing emission spectra and filter sets (derived from Chroma spectra viewer). There is overlapping of the emission spectra in both the green and red filters. %T is percentage of light transmitted at that wavelength

4.5 Discussion

These data present the first evidence for glucose sensing in specific subsets of CRH neurons within the PVN. GI and GE responsive neurons were identified responding to a reduction in extracellular glucose, using both whole cell patch clamp electrophysiology and calcium imaging techniques. This discussion will examine in more detail the effects observed using each technique, whilst considering these findings in the wider context of glucose sensing within the hypothalamus.

4.5.1 Electrophysiological properties of CRH neurons

Initial data obtained in 10mM glucose demonstrated some comparable cell properties to those previously reported for this neuronal population (Wamsteeker Cusulin et al., 2013). It is notable that the slicing methods used in this paper were somewhat different to that used here, with 25mM glucose present in the slicing aCSF used by Wamsteeker Cusulin et al., compared to 10mM here. However, the external and internal solutions used during patch clamping were otherwise comparable, and the data collected here made reference to this study protocols and data presented by the Wamsteeker group to facilitate comparisons. The previously reported input resistance (933±19.8 MΩ) is higher than that reported here (752+/-50.1MΩ), and the IV relationship appears similar (near linear relationship from -20 to +20pA). The cells recorded from here fire at a higher frequency following the same current injection, which may be partially explained by the differing holding potentials (-80mV for Wamsteeker et al. (2013), -70mV here). Of interest, when cells are held at negative resting potentials, frequent EPSPs and some IPSPs can be observed, suggesting that these neurons receive significant inputs from elsewhere in the slice. This aligns with the report by Wamsteeker et al. of $GABA_A$, NMDA and AMPA synaptic inputs onto CRH neurons.

The data presented here expands on that already published, in particular providing information about the intrinsic firing frequencies and resting potentials of CRH neurons. It is interesting to note that cells sliced and maintained in 10mM glucose appeared to have very similar cell properties to those sliced and maintained in 2.5mM glucose. The observation of a second subset of neurons with markedly differing cell properties is a new finding, not previously reported. Given that Wamsteeker et al. patched primarily in

the mid PVN, it is unsurprising that they did not observe these cells, which were found in the posterior PVN.

Previous reports of cell properties in rat PVN neurons have noted a difference in the morphology of the action potential profile in response to current injection in pre-autonomic cells compared to neurosecretory cells. In particular, the presence of a low threshold spike (LTS) in pre-autonomic cells has been considered as a significant identifying marker of these neurons. This property is thought to be due to T-type calcium channels in pre-autonomic rat neurons. It is not known whether mouse pre-autonomic and neurosecretory neurons can be similarly differentiated. As previously discussed, the mouse PVN differs significantly in anatomical structure compared to the rat. Spike morphologies suggestive of LTS were not observed in any of the cells patched here and there was no evidence of rebound spiking after hyperpolarising pulses (another marker of T-type conductances). However, on application of TTX, some cells (5/17, 30%) did maintain wide based spiking, suggestive of voltage gated calcium channels, likely L, N or R-type. More investigation of this phenomenon would be required to draw any firm conclusions in the mouse.

4.5.2 Glucose sensitivity- evidence for intrinsic glucose sensing from electrophysiological recordings

Both GI and GE neurons were observed in response to a step to a lower glucose perfusate. The subsets of responsive neurons were relatively small, with 35% of neurons GE and 8% GI in the main electrophysiology dataset, with steps from 10 to 2.5mM glucose. A further group of silent neurons were all GI (4/4 neurons depolarised after a step from 10 to 2.5mM glucose). Although it proved difficult to achieve stable recordings in lower levels of glucose, those recording which were made appeared similar in their responses to a step from 2.5 to 0.5mM glucose. These data can be compared with the evidence published by Melnick et al. (2011), regarding glucose sensing in the PVN. That paper initially examined responses to steps in glucose from 10mM to 2.5mM as described here. However, they saw no effect at these levels. They did observe GI (24%) and GE (26%) cells when glucose was stepped from 10 to 0.2mM, but this was only seen in cells which had properties suggestive of pre-autonomic neurons, as outlined in section 4.5.1 above.

In the data presented here, relatively long periods of perfusion in low glucose were required before a response was observed. Figure 5.3 provides examples of GE responses. It can be seen that perfusion for around 5 minutes in 2.5mM glucose occurs, before a fall in action potential frequency is evident (5.3B). Several possible explanations exist for this delay. Firstly, there will be a delay from the time that the perfusion is switched due to delay in exchanging the medium in the chamber. The perfusion system ran at 2-3ml/minute in both electrophysiology and calcium imaging experiments. The chamber used in electrophysiological recordings is relatively large, especially compared to that used for calcium imaging (~1ml for electrophysiology, ~0.5ml for calcium imaging), and so it could be expected that this delay will be longer under these conditions. In addition, the mechanism by which cells sense changes in glucose may add to a delay to response. If glucose is required to enter cells and be metabolised to effect a response, this will lead to a delay. Finally, if signalling were from other cells in the slice, rather than intrinsic signalling, this might also contribute to a delayed effect.

Interestingly, a second step to 2.5mM glucose results in a more rapid response. A shorter delay to response is also seen with a step from 2.5 to 0.5mM glucose (Figure5.3A). This seems likely to be due to a more rapid fall to a low glucose level within the slice, reaching the cell's threshold for activation faster. An alternative cause of this effect would be that the cell has already been metabolically activated by the first stimulus and so is more sensitive to a second stimulus. However, the counter argument to this is that not every cell responds a second time.

4.5.2.1 Effect of TTX on glucose responses in patch clamp recordings

In patch clamp recordings, TTX had a clear effect in removing action potential spiking, but no significant effect on the resting potential of cells. As previously mentioned, a few cells were observed to continue to spike, presumably due to calcium channels, but these were not stepped to low glucose and are not included in subsequent analysis. It was notable that the majority of neurons responded to a step to low glucose in the presence of TTX by depolarising. This may suggest that the majority of CRH neurons are intrinsically glucose inhibited. This was of particular interest as GI neurons were not frequently seen in the absence of TTX. This could imply that these neurons are being

synaptically inhibited by neurons elsewhere in the slice, and are therefore only revealed when these inputs are removed.

4.5.3 Glucose sensitivity- evidence from calcium imaging

Both GI and GE responses were observed in CRH neurons in PVN slices using GCaMP6f calcium imaging, both in slices cut in 10mM and 2.5mM glucose. This technique has not previously been used in the investigation of glucose sensing (in vitro or in vivo). Some but not all neurons were able to respond reversibly and repeatably to perfusion with low glucose. GI neurons were present in roughly equal numbers to GE in many slices (9% of cells GE and 9% GI after slicing in 2.5mM glucose), and overall more GI and fewer GE cells were observed than was the case during electrophysiological experiments, where 8% of cells were GI and 35% GE. It is possible that this could be due to differences in the ease of patching different CRH neurons, preselecting for GE and NR cells. Another explanation could be related to the relatively high firing rate seen in many neurons in whole cell patch clamp. When looking for evidence of excitation, it may be easier to detect this when a cell is firing slowly or is silent than with a baseline AP frequency of 6-7Hz.

The data presented here using calcium imaging is novel in its use of a genetically coded calcium indicator, GCaMP6f, in hypothalamic cell subtypes to identify changes in calcium in response to a low glucose stimulus. Initial validation using the same conditions as in the electrophysiological experiments shows that it is indeed possible to detect responses to low glucose using this mode of calcium imaging in slices. As previously noted, both GI and GE responses could be detected. The resting calcium levels of a CRH neuron are unknown. The high action potential frequencies recorded in many CRH PVN neurons during patch clamp recordings suggest that some cells might be expected to have relatively high resting calcium levels.

GI responses as observed in calcium experiments are readily understood- the cell becomes more active, resulting in calcium influx and possibly release from intracellular stores, leading to increased binding of GCaMP6f and increased fluorescence. The changes observed in GE neurons require a little more thought. If these cells are already active at baseline, possibly with relatively high calcium levels, one needs to consider

what changes in fluorescence would result from a reduction in activity. Essentially, with falling calcium levels, the binding of GCaMP6f will be reduced and fluorescence will fall. However, the kinetics of this effect must be considered. The tau off for GCaMP6f is 400ms, as compared to a tau on of 74ms (Chen et al., 2013). Therefore, the delay before a reduction in calcium will result in a fall in fluorescence will be considerably longer than for the onset of activation. This should not be a major issue for the data collected here, as the imaging frequency is 0.5Hz, so 5 half-lives of GCAMP6f decay can pass between acquiring one image and the next. This point has been considered in some work by Otis and colleagues, covered in the extended data of their publication, where the effect of inducing and then pausing action potentials was examined, recording the decay in fluorescence during a pause in action potentials compared to a hyperpolarisation without action potentials (Otis et al., 2017). They showed that a fall in action potential firing is needed to generate a reduction in fluorescence, and that pauses in firing of 3 seconds can be tracked as a fall in fluorescence, with the magnitude of the fall in fluorescence being linearly related to the action potential frequency prior to the pause. Sternson and colleagues also present data when cells become less active in response to feeding, using GCaMP6f in awake mice, and again, observe similar falls in calcium sensitive fluorescence after exposure to a stimulus (Betley et al., 2015). This study imaged cells in vivo, and so no comparison could be made to AP frequency. As described in section 4.4.6.3, GE neurons were found to tend to have higher raw baseline fluorescence when compared to GI and NR cells. This lends support to the hypothesis that these cells have higher activity levels in 2.5mM glucose when compared to GI and NR cells.

In addition, it is of interest to consider what happens to the fluorescence in a tonically firing cell. GCaMP6f is widely used to identify events due to small numbers of action potentials in cells with low frequency spiking patterns and the focus is on extrapolating fluorescence signals to infer events due to 1 or a small cluster of action potentials. However, in the data presented here, at least some of the cells are likely to be firing at very much higher rates, and in this case the fluorescence signal should read out at a steady state for a given firing frequency, with changes in fluorescence due to changes in AP frequency occurring over a slower time-course.

4.5.4 Do calcium levels represent neuronal activity?

The measurement of calcium levels as a valid indication of neuronal activity is widely accepted (Grienberger and Konnerth, 2012). Calcium signalling has been demonstrated as a trigger for a very wide range of neuronal events, including exocytosis at pre-synaptic terminals, generation of action potentials post synaptically, nuclear calcium rises related to transcription and apoptosis. In particular, calcium is an appealing molecule for imaging because the change in calcium levels in response to activation is very large, and the time course is relatively slow in comparison to changes in cell membrane potentials. In addition, because changes in calcium levels occur within the cytoplasm, or a sub-compartment of the cell, they are more readily imaged than small changes in membrane potential, only affecting the cell membrane. There are some caveats which should be considered when employing calcium imaging as a technique to investigate neuronal activity. The most important is that an assumption is being made that levels of fluorescence within the cell reflect calcium levels, and that these in turn represent the level of activity of the cell, which is more directly measured in electrophysiological recordings. GECIs have been extensively investigated and validated in multiple modalities, and have been shown to robustly reflect neuronal activity across species from drosophila to primates, in vitro and in vivo, and in soma, dendrites and subcellular compartments (Grienberger and Konnerth, 2012, Badura et al., 2014, Grynkiewicz et al., 1985). Much of the current debate in the field revolves around which is the best choice of GECI for the desired experiment, rather than whether to use a GECI.

4.5.5 Advantages and disadvantages of calcium imaging compared to patch clamping

Calcium imaging was initially frequently used in conjunction with patch clamp electrophysiology in the literature, as the micropipette offered a means of introducing the calcium indicator into the cell. The advent of, firstly, acetoxymethyl (AM) esters of small molecule calcium indicators, and subsequently GECIs, which can be delivered via viral vectors or expressed in genetically modified mouse lines, allows the imaging of multiple cells in a single experiment. This offers several attractive advantages over electrophysiology for the investigation of glucose sensing. The ability to collect data from multiple cells in one experiment and to gain more information about the spatial

distribution of responsive cells are important considerations. Additionally, calcium imaging is potentially less invasive to the cells involved than whole cell patch clamp. No dialysis of the cytoplasm occurs and there is no physical disruption to the cells. Finally, this method can allow multiple imaging sessions when carried out in vivo.

It is more complex to directly influence the activity of the cells being imaged, although combination with an optogenetic technique could achieve this. A great deal of information can be obtained from voltage or current steps in a patch clamped neuron, which is not available from calcium imaging. In addition, there is always a trade-off between spatial and temporal resolution, which can be viewed as an advantage or disadvantage, depending on the question being asked. In order to image a larger number of cells, the temporal resolution for each cell must fall.

4.5.6 Optimisation of calcium imaging

The experiments presented here did not aim to simply recapitulate the results seen in the electrophysiological section (i.e. of action potential discharge). Rather, the intent was to capture slower calcium events. Given that the timescale of responses to low glucose seen in electrophysiological studies occurred over 100-200s, it seemed that 0.5Hz would be an adequate temporal resolution. One experiment was performed here at 5Hz, and this did not reveal further information than those performed at 0.5Hz. Therefore, this appears to be a suitable time course.

Several experiments were performed to establish which objectives were most suitable for imaging in slices. A 60X (Nikon)and a 40X (Olympus) objective were both tried, with imaging through a z-stack of 15-24 planes. However, this greatly increased the time interval between acquisition of sequential images, from 2.1s for a single z-plane to 11-20s for a stack. In addition, this setup was more sensitive to drift, especially in the z-plane, and 4-dimensional registration is much more challenging to achieve. Overall, temporal and spatial resolution was improved by using a 16X objective and a single z-plane of around 1-2µm.

Two major problems with the breeding of CRH x GCaMP6f mice were experienced during optimisation of calcium imaging in this thesis. Firstly, the breeding of double

homozygous CRH x GCaMP6f mice resulted in widespread expression of GCaMP6f, which was no longer linked to CRH expression. It is known that having a Cre recombinase and a reporter gene present in the germline can lead to spontaneous recombination events during gametogenesis (Morrison and Munzberg, 2012, Schmidt-Supprian and Rajewsky, 2007, Weng et al., 2008), and it seems likely that this is what occurred here. The commonest cause of this is recombination of the floxed reporter gene in germline cells, due to transient expression of Cre recombinase during development. Subsequent to this, all offspring will have reporter gene expressed in a non-specific fashion. The germline recombination event can occur in males only, females only, or both, and is dependent on the gene under which Cre recombinase is expressed. The most straightforward way to avoid this is to avoid breeding with animals which have Cre recombinase and the floxed reporter both present, and this was the solution adopted here.

The second problem which arose was in the development of a mouse line co-expressing GCaMP6f and TdTomato in offspring, as a means of identifying all of the GCaMP6f neurons by expressing a second, non-calcium dependent fluorescent protein. A more complex breeding strategy was planned to express GCaMP6f (calcium sensitive reporter protein) AND TdTomato (standard reporter protein) under the control of the CRH-ires-Cre line. This involved the breeding of a CRH-Cre x GCaMP6f mouse, to cross with a homozygous TdTomato animal to gain all three genes in the offspring. The TdTomato and GCaMP6f genes were not introduced into a single breeding animal, as they are both inserted at the same locus (ROSASor 2.6) and there is therefore a high chance of recombination which could lead to deletion or silencing of one or both reporter genes.

As described in section 4.4.6.5, this approach, whilst intuitively attractive, did not prove successful, as responsive cells were not found using GCaMP6f imaging. Problems with overlap of TdTomato and GCaMP6f signal have already been described in the results section, and essentially the signal to noise was much less favourable in the presence of TdTomato. In addition, there was a loss of temporal resolution due to the need to image 2 channels. It was also apparent that some neurons expressed only one fluorescent protein at a level which could be seen on imaging, rather than both, which further reduces the value of having a double fluorescent signal. It is unclear why this

should occur. Both GCaMP6f and TdTomato are present at the same locus (ROSASor 2.6), although they are on separate chromosomes as the mice are bred as heterozygotes. However, there could be an issue with chromosome inactivation, or a recombination event in some neurons. It is also possible that both genes are being expressed, but with one at a much higher level than the other. This approach was therefore abandoned.

4.5.7 Spatial location of GI neurons is suggestive of a pre-autonomic population

The small subset of 'silent' neurons observed during whole cell patch clamp experiments were of interest in a number of ways. Clearly, the fact that the majority depolarised in response to a low glucose step, (i.e. GI) was of interest. It was notable that these cells appear to have lower input resistances and may be larger (based on their capacitance). Their location in more posterior areas of the PVN was suggestive that these cells could be pre-autonomic. Melnick and colleagues report low firing frequencies more similar to these neurons, in the range 0.2-0.5Hz, in their pre-autonomic cell population (Melnick et al., 2011). However, no low threshold spike activity (characteristic of pre-autonomic neurons in the rat, see also section 4.5.1) was observed in the neurons patched here.

Calcium imaging data could be translated into more precise information on where cells were located within the PVN as well as their responses. Of interest, GI neurons predominated in more caudal sections, and scattered in the periphery of the PVN, whilst GE neurons tended to be found more rostrally and centrally. This information is of interest as it can give clues as to the underlying mechanisms and connectivity of subgroups of neurons. For example, the GE neurons of the VMN are largely found in the ventrolateral part, which is thought to be a key mediator of metabolic regulation and body weight (King, 2006). The mouse PVN is a much less stereotyped nucleus than the rat, and so it is more difficult to infer possible functions from anatomy (Biag et al., 2012). However, the posterior location of many GI neurons is suggestive that at least some of these may be part of the brainstem projecting pre-autonomic population.

Attempts to record in whole cell patch clamp from an anatomically defined pre-autonomic population using retrograde tracing from the NTS were unsuccessful. This was partially due to the scarcity of retrogradely transduced neurons visible in the fresh

slice. In addition, it was challenging to identify 'truly' green eGFP$^+$ neurons as the brighter red (TdTomato$^+$) cells were also visible in the green channel, although it was possible to distinguish these by their colour. It is extremely difficult to circumvent this problem for direct microscopy even using alternative filters, as TdTomato fluorescence remains bright in comparison to eGFP even at the extremes of its excitation and emission spectra, and if a filter is chosen to exclude it, eGFP fluorescence is also significantly reduced.

One method which could overcome these problems would be to use a Cre dependent vector in a retrograde virus, injected into brainstem areas of a CRH-Cre mouse without TdTomato. In this case, all visible fluorescent neurons identified in the PVN would be both CRH positive and brainstem projecting, without the need for co-localisation. A potentially higher transduction yield might also result from the opposite strategy, injecting a Cre recombinase vector in a retrograde virus into the brainstem of a reporter mouse. Either of these methods could be a useful alternative strategy for the future.

4.5.8 Consideration of physiological glucose levels

4.5.8.1 Electrophysiology

Although few cells were recorded here in 2.5mM glucose, with steps to 0.5mM, the fact that their properties and responses appear broadly similar to those in 10mM glucose suggests that at least some of the observed responses in CRH neurons can still operate at physiological levels. It seems highly unlikely that CRH neurons in the PVN would ever be exposed to levels of glucose of 10mM. However, it is interesting to note that the majority of responses observed in the initial datasets, with synaptic inputs intact, were GE, and that these responses were seen at much lower frequency, if at all, in the presence of TTX which would abolish synaptic inputs. This is significant given that cells responding to high and low levels of glucose have been reported in other parts of the hypothalamus, in particular the VMN. Both high glucose excited (HGE) and high glucose inhibited (HGI) neurons, responding to steps from 10 to 0.5mM glucose, have been described in the VMN, where BBB is thought to be deficient and experience extracellular levels of glucose that are close to blood levels of glucose (Fioramonti et al., 2004). It is therefore possible that HGE or HGI neurons could synapse onto the PVN CRH neurons recorded here to cause some of the responses seen.

4.5.8.2 Calcium

Calcium imaging provided a high throughput and effective means of collecting data from slices cut in 2.5mM glucose. This was valuable as steps from 2.5mM glucose to 0.5mM are much more likely to represent the glucose levels experienced by PVN cells in vivo. Glucose responses were clearly present under these conditions, and indeed there was an increase in the numbers of GE neurons observed compared to slices cut in 10mM glucose with steps to 2.5mM. This is an important finding as it suggests that moving glucose concentrations into the normal physiological range allows more cells to respond, likely to be due to examining effects in a situation where the sensing processes are not saturated.

4.5.9 Summary

Overall, the data presented here provides initial evidence of a glucose sensitive population of CRH PVN neurons, with a GI population which persists in the presence of TTX. This suggests that at least some GI neurons in this population are intrinsically sensing glucose. Further investigation of this population will be presented in the next chapter.

Chapter 5 A subset of CRH PVN neurons intrinsically sense a fall in glucose, and this is dependent on glucose metabolism.

5.1 Introduction

This chapter continues from the previous work to characterise the glucose sensitive CRH cells within the PVN. The focus is on intrinsic versus synaptically-mediated glucose sensing, and on the mechanisms of glucose sensing. The introduction summarises what is currently known about mechanisms of glucose sensing in the central nervous system, and also discusses what inputs the PVN receives from other glucose sensing regions. Glucose sensing by non-neuronal cells will also be considered.

5.1.1 Mechanisms of glucose sensing in the CNS- glucose excited cells

The cardinal peripheral glucose sensor is the pancreatic beta cell, which utilises an ATP-sensitive potassium channel to respond to changes in blood glucose. Glucose enters the beta cell via low affinity GLUT-2 transporters and is metabolised by glucokinase, generating ATP. ATP in turn binds to K_{ATP} channels, causing them to close. This reduces potassium conductance across the cell membrane, depolarising the cell, and leading to generation of action potentials, calcium influx and insulin release (Ashcroft and Rorsman, 2004). This elegant system links the extracellular glucose level to the degree of depolarisation of the cell, and thus to insulin release. Early thinking on glucose sensing within the CNS drew parallels with peripheral nervous system and this has been reviewed extensively in the context of glucose sensing in the CNS (Burdakov et al., 2005b, Routh, 2002).

Glucokinase, GLUT2 and the subunits of the K_{ATP} channel (Kir6.2 and SUR1) are all widely expressed in glucose sensing areas of the CNS (Kang et al., 2004, Lynch et al., 2000, Stanley et al., 2013). In particular, there is evidence that GE VMN neurons use glucokinase (Dunn-Meynell et al., 2002, Kang et al., 2006) and K_{ATP} channels (Ashford et al., 1990a, Song et al., 2001, Kang et al., 2006) to respond to changes in glucose. Glucose sensing neurons of the dorsal vagal complex have also been shown to utilise glucokinase (Balfour et al., 2006). However, this is unlikely to be the only mechanism of

glucose sensing in the CNS. Not all GE cells express glucokinase, GLUT-2 and K_{ATP} channels, and they can also be found in cells which are not glucose sensing (Kang et al., 2004, Lynch et al., 2000). In addition, measurement of ATP levels in glucose sensing cells in the hypothalamus, whilst elevating glucose, failed to show any change in ATP (Ainscow et al., 2002). Studies exploiting K_{ATP} channel mutations have also been informative. In the Kir6.2 global knockout mouse, there is indeed loss of VMN glucose excitation (Miki 2001). However, the same mouse had preserved GE neurons in the ARC (Fioramonti et al., 2004). Investigations using a GM mouse with a mutation in the K_{ATP} channel that renders it insensitive to ATP have shown that POMC neurons have an altered glucose sensitivity (Parton et al., 2007). However, in both the Kir6.2 knockout and the mutated K_{ATP} channel mouse lines the baseline firing and excitability of the cells was significantly different from that seen in native neurons, and it is very difficult to unpick how much of the observed effects were due to this alteration rather than to a direct effect on glucose sensing.

Alternative potential contributors towards intrinsic glucose sensing in glucose excited neurons are summarised in table 5.1. In addition, it is important to note that more than one mechanism could be operating in any one cell. It is also likely that the whole milieu in which any glucose sensing cell exists will also be important (for example, many glucose sensing cells also express receptors for insulin, leptin and other molecules which inform overall metabolic state)(Canabal et al., 2007b, Cotero and Routh, 2009, Flak et al., 2014, Roland and Moenter, 2011, Santiago et al., 2016).

With regard to the PVN, Melnick et al. (2011), report that glibenclamide or tolbutamide (K_{ATP} channel blockers) had no effect on GE currents evoked by a step to low glucose. In addition, the KATP activators diazoxide (SUR1) and chromakialin (SUR2) did not evoke any significant change in membrane potential or conductance. Immunohistochemistry for SUR1 (a component of the K_{ATP} channel) in the PVN did not convincingly demonstrate fluorescence at primary antibody concentrations which did result in bright fluorescence in the VMN and ARC, areas known to express SUR1. Melnick et al. suggest that either a potassium leak channel or a chloride conductance is involved in GE cell glucose sensing in the PVN. Alternative candidates for PVN GE responses might include the sweet taste

receptors, which have been shown to be expressed in both PVN and ARC (Ren et al., 2009).

Table 5.1 Potential mechanisms contributing to glucose sensing in the hypothalamus

Potential mechanism	Neurochemical phenotype	References
AMPK	POMC GnRH	(Claret et al., 2007) (Beall et al., 2012b, Roland and Moenter, 2011)
Sodium glucose co-transporters	VMN (25% of GE neurons express) Unknown (hypothalamic cell culture)	(Kang et al., 2004) (O'Malley et al., 2006)
Non-specific cation channel (Could include TRP, SGLTs)	Pre autonomic PVN GnRH ARC	(Melnick et al., 2011) (Roland and Moenter, 2011) (Fioramonti et al., 2004)
Sweet taste receptors	Expressed in PVN and ARC	(Ren et al., 2009)
Reactive oxygen species	ARC. Possibly POMC	(Pauliina Markkula et al., 2016, Leloup et al., 2006)

AMPK- 5' adenosine monophosphate-activated kinase, TRP-transient receptor potential channel , SGLT- sodium glucose co-transporters, GnRH- gonadotrophin releasing hormone

5.1.2 Mechanisms of glucose sensing in the CNS- Glucose inhibited cells

Less is understood about the mechanisms which may operate in GI cells. Vanessa Routh and colleagues have extensively investigated mechanisms by which VMN GI neurons may respond to glucose and suggest a model in which glucose metabolism leads to decreased AMPK activity, NO generation, increased cGMP levels, and opening of a chloride channel (possibly a member of the CFTR family), leading to hyperpolarisation of the cell (Canabal et al., 2007b, Dunn-Meynell et al., 2002, Kang et al., 2006, Kang et al., 2004, Murphy et al., 2009a) summarised in (Zhou et al., 2018). CFTR channels have also been implicated in the glucose inhibited ARC neurons (Fioramonti et al., 2007). AMPK could also operate via other means to alter cell excitability via phosphorylation of additional membrane and cytosolic proteins (Song et al., 2001) and is also know to alter gene transcription via CREB co-activation by CRTC2 (Lerner et al., 2009). With regard to the PVN, AMPK is expressed in PVN neurons and hypoglycaemia has been shown to result in activation of AMPK in the PVN and the VMN, but not in other parts of the

hypothalamus (Han et al., 2005). However, mechanisms of glucose sensing in GI neurons of the PVN have not been previously investigated.

Denis Burdakov and colleagues (Gonzalez et al., 2009) have investigated the mechanisms by which orexin neurons in the lateral hypothalamus are inhibited by glucose, and suggest a very different mechanism for these cells, independent of metabolism. A series of experiments demonstrated that some non-metabolisable sugars such as 2-deoxyglucose could elicit the same response as glucose in these cells (Gonzalez et al., 2008), and that inhibition of glucokinase had no effect. In addition, glucose or an analogue needed to be applied to the external cell membrane to cause a response. The channel responsible for hyperpolarisation of these cells appears to be a potassium 'leak-like' channel. However, the sensor linking the change in glucose to the potassium channel is thus far unknown.

Other putative mechanisms for GI neurons include reduction in activity of Na-K-ATPase at the cell membrane leading to depolarisation (Oomura et al., 1974, Silver and Erecinska, 1994b), and the concept of voltage induced inactivation of sodium channels as a result of K_{ATP} channels closing and causing prolonged depolarisation (Burdakov and Lesage, 2010, Gromada et al., 2004). Generation of reactive oxygen species has also been identified as a potential mediator of glucose sensing in the central nervous system, (Pauliina Markkula et al., 2016).

5.1.3 Mechanisms of glucose sensing in the CNS- Non-neuronal cells

Neurons are not the only cells in the CNS which are capable of responding to changes in their environment. It is clear that glial cells in general are much more active in signalling locally than originally thought (Araque et al., 2001). Indeed, re-expressing GLUT-2 in astrocytes restored glucagon responses to hypoglycaemia in global GLUT-2 knock out mice (Marty et al., 2005). Neither TTX nor fast synaptic blockade will have any effect to block signalling from glial cells, astrocytes or tanycytes. Astrocytes store glucose as glycogen, and release lactate into the surrounding interstitium. A recent bioarchiv preprint reported increases in AMPK activation and lactate release in response to hypoglycaemia in primary human astrocyte cultures and an astrocytoma cell line (Weightman Potter et al., 2018). Lactate can be taken up via monocarboxylase

transporters on neuronal cell membranes and converted to pyruvate, generating ATP (Kang et al., 2004, Magistretti et al., 1999). These transporters are present at relatively high levels within the hypothalamus, and may provide an additional means of signalling metabolic state, which could operate in GI and GE neurons (Ainscow et al., 2002, Pierre et al., 2000). This mechanism could provide an alternative means of inactivating K_{ATP} channels and depolarising GE neurons, independent of glucokinase and GLUT transporters.

Tanycytes lining the third ventricle have also been shown to be able to respond to glucose application in vitro (Frayling et al., 2011). These cells extend processes into the surrounding neuronal tissue and could therefore signal to neurons in their locality. Both lactate and ATP have been suggested as potential signalling molecules from tanycytes to neurons (Frayling et al., 2011, Elizondo-Vega et al., 2015).

5.1.4 Investigating whether cell metabolism is involved in glucose sensing

The commonest method by which this question is address is by examining the effect of a non-metabolisable sugar in place of glucose. 2-deoxyglucose (2-DG) is a glucose analogue which is transported by most glucose transporters, and is metabolised by hexokinase to form 2DG-6-phosphate, which cannot then leave the cell or be further metabolised. This results in inhibition of hexokinase and glucoisomerase, depleting ATP (Wick et al., 1957). It is commonly used intracerebroventricularly, to mimic localised hypoglycaemia in vivo (Marty et al., 2005, Sanders and Ritter, 2000) and has also been used in vitro in patch clamp experiments to examine the role of metabolism in glucose sensing cells (Lamy et al., 2014, Gonzalez et al., 2008). Gonzalez et al. were able to show that GI orexin neurons in the LH responded to increases in 2-DG in the same way as they did glucose, suggesting a metabolism independent mechanism was operating in these neurons. Lamy et al. examined GI neurons in the NTS (expressing GLUT-2), and suggest that glucose metabolism was required in these cells, as perfusion with 2-DG in the presence of 5mM glucose caused similar responses to a step to 0.5mM glucose.

5.1.5 Synaptic inputs to the PVN from glucose sensing areas

This topic has already been covered in some detail in the general introduction (Chapter 1 section 1.8.2). The focus here will be on which nuclei with known intrinsic glucose

sensing properties could provide inputs to CRH neurons of the PVN during in vitro slice experiments.

The hypothalamus is a key glucose sensing area and there are a number of candidate areas surrounding the PVN which could be contributing to the responses to glucose reported in chapter 4. In particular this is relevant to the GE responses, which were largely abolished by TTX in electrophysiological recordings and so are likely to be synaptically-mediated. If a coronal section, around 300microns thick through the PVN is considered, then the VMN, ARC, DMN and LH are all potentially included in the slice, and all are recognised to contain glucose sensing neurons (Burdakov et al., 2005b, Otgon-Uul et al., 2016, Fioramonti et al., 2004). In addition, all these areas are known to send processes to synapse onto neurons of the PVN (Larsen et al., 1994). Figure 5.1 provides a summary. The preoptic area is the other hypothalamic area which has been identified as containing glucose sensing neurons and having connections to the PVN, but this seems an unlikely candidate as it is situated very anteriorly in the hypothalamus, and so would not be in the slice.

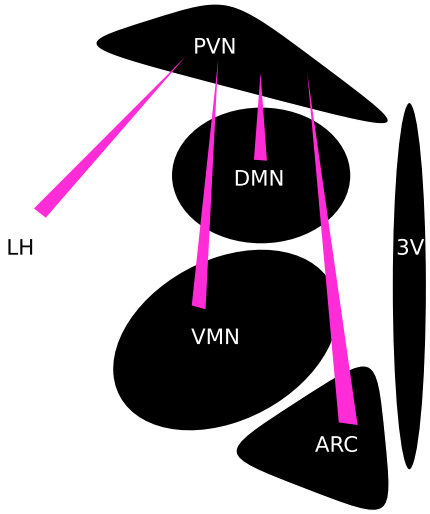

Figure 5.1 Potential nuclei containing glucose sensing populations in a coronal slice which could synaptically influence CRH PVN neurons in response to a low glucose step

- **LH:** As described in section 4.1.4, orexin neurons of the LH are glucose inhibited. It is also known that orexin expressing neurons send processes into the PVN (Sakurai et al., 1998) and that these projections can affect a range of PVN functions including autonomic regulation, food intake and metabolism, (Edwards et al., 1999) and PVN neuron excitability (orexin neurons appear to be excitatory in the PVN) (Samson et al., 2002, Ferguson et al., 2008). Additional glucose sensing populations within the LH are the NPY subgroup (Marston et al., 2011), and MCH neurons (GE, (Burdakov et al., 2005a)). The effects of NPY and MCH neuronal inputs on the PVN are not known.
- **ARC:** POMC and AgRP neurons are well recognised PVN projecting populations, and these pathways are of key importance in modulation of feeding behaviour via the MC4R, with melanocortin activating this receptor and AgRP inhibiting it. Glucose sensing has been demonstrated in ARC neurons, although some controversy exists as to whether the POMC neurons are glucose sensing, or responding to other neurons. Ibrahim et al. (2003) reported that 80% of POMC neurons in slices from mice were GE, but did not investigate whether this was an intrinsic effect or via synaptic inputs. Increased glucose levels have been shown to cause increased α-melanocyte-stimulating hormone release in hypothalamic slices in vitro, but again the effect may be indirect (Parton et al., 2007). Reports by Wang et al. (2004) in rats and Fioramonti et al. (2007) using mice have not found any evidence for direct glucose sensing by POMC neurons of the ARC. It is likely based on these findings that POMC neurons are indirectly glucose responsive (Fioramonti et al., 2017).

  AgRP/NPY neurons have been shown to directly sense glucose, with 40% found to be GI (Fioramonti et al., 2007). GI AgRP neurons are sensitised by fasting (Murphy et al., 2009b). This population is less likely to be able to act on PVN CRH neurons to give a GE response, unless an interneuron is involved.

  GE neurons are certainly present in the ARC, and would be good candidates to act on CRH PVN GE neurons, but the cell subtypes remain unknown (Fioramonti et al., 2007).
- **VMN:** This is a key glucose sensing area which has been extensively investigated (Routh, 2003). Again, projections to the PVN have been demonstrated (Larsen

et al., 1994). This region has been of particular interest with regard to responses to hypoglycaemia, and is known to contain intrinsic glucose inhibited and glucose excited neurons. Modulation of the thresholds of GI neurons following recurrent hypoglycaemia has been described for this region (Routh, 2003, Song and Routh, 2006).

- **DMN:** GABAergic neurons of the DMN have been described as exhibiting both GI and GE responses (Otgon-Uul et al., 2016). Again, this nucleus is known to connect to the PVN as described in the same paper.

5.2 Hypotheses

- PVN CRH neurons are intrinsically glucose sensing
- Glucose sensing is dependent on glucose metabolism in CRH neurons of the PVN

5.3 Aims

- Use tetrodotoxin to block action potentials and test whether glucose sensitivity is intrinsic to CRH neurons
- Investigate effect of pharmacological synaptic blockade on glucose responses in CRH PVN neurons
- Examine effect of applying 2-DG as a non-metabolizable glucose analogue

5.4 Results

5.4.1 Is glucose responsivity intrinsic to CRH PVN neurons or a function of synaptic drives from elsewhere in the coronal slice?

5.4.1.1 Effect of TTX on glucose responses during calcium imaging

Having seen a significant change in glucose responsiveness to a primarily GI population when using TTX in electrophysiological experiments, it was logical to proceed to perform the same experiment using calcium imaging, to examine whether this phenomenon could also be seen using calcium levels as an indicator of cell activity. After application of 0.5mM glucose in the presence of TTX, GI neurons were readily observed, and were possibly more numerous than in the control group, suggesting that these cells do not require sodium dependent action potential firing to generate a calcium response to low glucose, and that these responses are unlikely to be synaptically-mediated (Figure 5.2

A,B). However, in contrast the number of GE neurons was significantly decreased (Figure 5.2 A). The size of the GI and GE responses were not affected by TTX (Figure 5.2 D). The morphology of the GI responses was altered, with 76.9% of responses now appearing slow rising (39.1% in control population), and 23.1% spiking (60.1% in control populations) ($p<0.0001$, Fishers exact test compared to GI cells from 2.5mM glucose control population).

TTX in itself resulted in a small but significant reduction in calcium levels when measured across the whole population (Figure 5.2 Ci), as would be expected for an agent which blocks sodium dependent action potentials (so reducing influx across the membrane) and also synaptic transmission. This effect was also observed in the small population of GE cells which were still identifiable in the presence of TTX (Figure 5.2 Cii). TTX had no effect on calcium levels in the larger population of GI neurons, which is what would be expected if this cell population were not firing action potentials in the presence of 2.5mM glucose (Figure 5.2 Ciii). TTX was observed to slow the onset of effect of a high potassium solution (360.0±31.0s from start of perfusion with high potassium to start of response, compared to 95.0±10.7s in control cells), again as would be expected on blocking sodium dependent action potentials (Figure 5.2 B).

The location of GI and GE cells in the presence of TTX was similar to that seen in control slices. However, more GE cells were found caudally in the presence of TTX. The GI cells appeared to be spread more generally through the CRH neurons of the PVN, rather than primarily in the periphery of the CRH population (Figure 5.3). This could be due to removal of inhibitory inputs in the presence of TTX revealing a more widespread GI population.

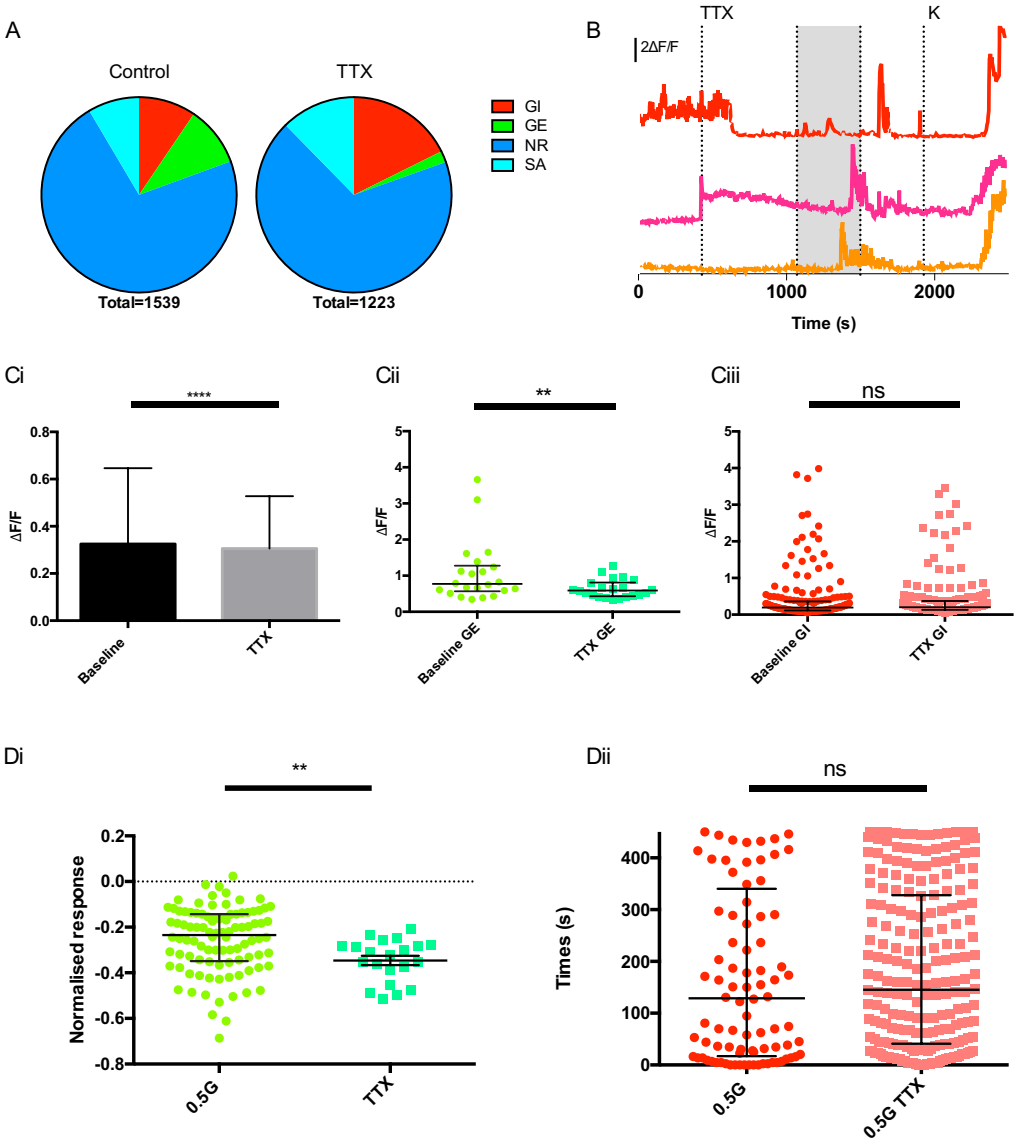
A
Control
TTX
GI
GE
NR
SA
Total=1539
Total=1223
B
TTX
K
2ΔF/F
0
1000
2000
Time (s)
Ci
****
ΔF/F
Baseline
TTX
Cii
**
ΔF/F
Baseline GE
TTX GE
Ciii
ns
ΔF/F
Baseline GI
TTX GI
Di
**
Normalised response
0.5G
TTX
Dii
ns
Times (s)
0.5G
0.5G TTX

Figure 5.2 Effect of TTX on CRH PVN neurons

A Comparison of responses to 0.5mM glucose step in the presence of TTX and control. Significant reduction in number of GE cells seen (Chi-square 115.6, $p<0.0001$)

B Examples of 3 GI cells in the presence of TTX. TTX applied at first vertical line, shaded area represents perfusion with 0.5mM glucose, high potassium applied at final vertical line (K)

C Effect of TTX alone on calcium levels prior to a step to 0.5mmol glucose. i) all cells, ****$p<0.0001$, n=1101 ii) GE cells only, **$p=0.0015$, n=22cells, iii) GI cells only, no significant change in calcium levels, n=198cells. Wilcoxon matched pairs signed rank.

D Effect of TTX on the size of responses to step to 0.5mM glucose compared to control. i) GE effect size is significantly increased, $p=0.0015$, Mann-Whitney U ii) GI effect size, no significant difference, Mann Whitney U.

TTX data obtained from 4 mice, 11 slices, 111.2 ±16.0 cells/slice. Data presented as median and IQR

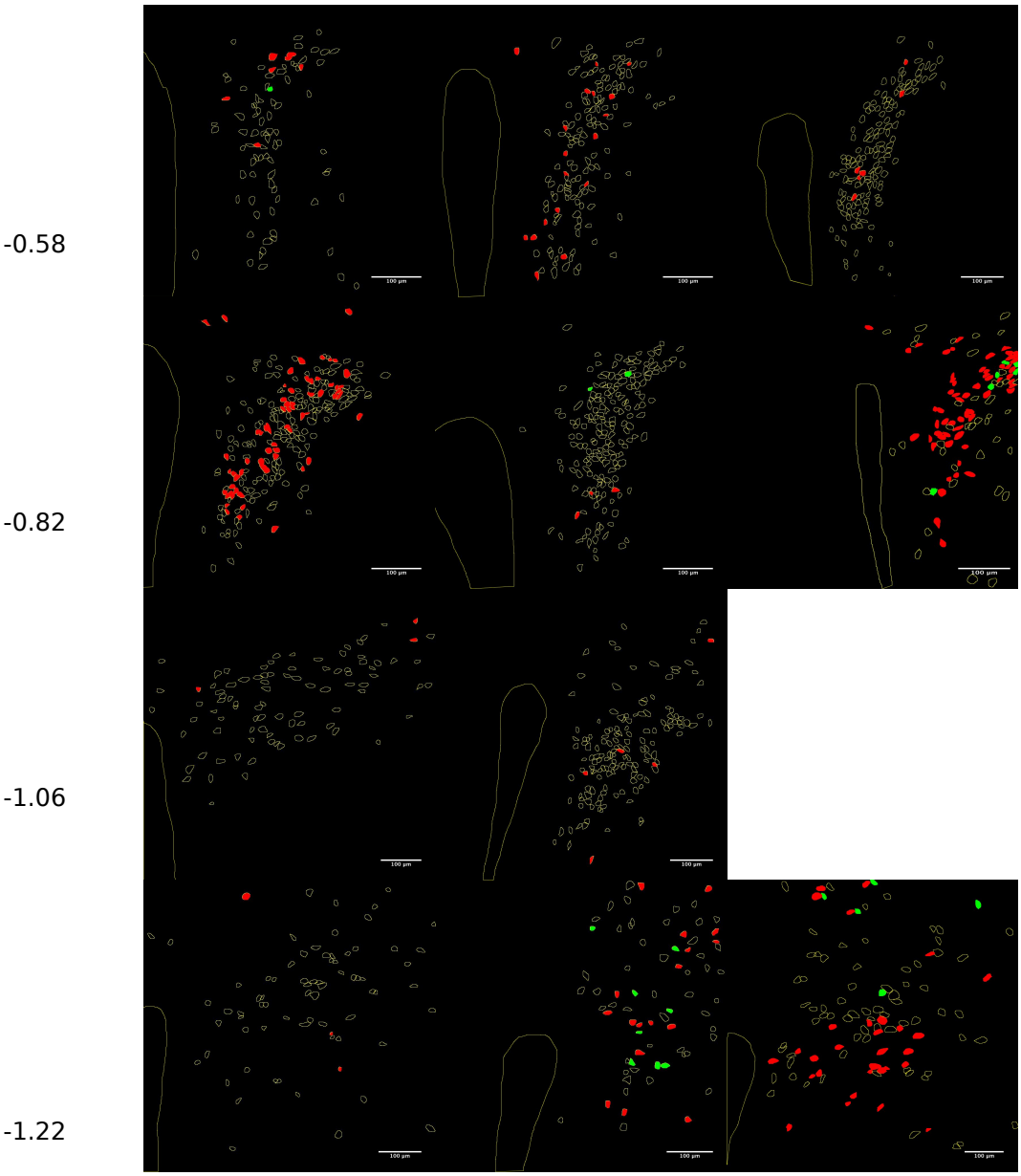

Figure 5.3 Spatial distribution of GI and GE cells after a step from 2.5mM to 0.5mM glucose in the presence of TTX

Images are arranged rostral to caudal, GI neurons are red, GE green. Approximate Bregma values are indicated on the left.

5.4.1.2 Effect of excitatory synaptic blockade on glucose responses

Having established that TTX ablates and/or reduces GE responses, but not GI, the effect of blocking excitatory fast glutamatergic synaptic inputs was investigated using a cocktail of 50μM D-AP5 (NMDA antagonist) and 10μM CNQX (AMPA/kainate receptor antagonist). For this series of experiments, the glucose responsiveness as assessed with GCaMP6f imaging of each slice was first assessed in the absence of synaptic blockade, and subsequently after application of D-AP5/CNQX. Data is therefore presented as repeated measures comparing each neuron's response within the same slice, and group responses are also compared to the effects seen after the *second* application of 0.5mmol glucose in control slices (as the second response was significantly different to the first). The effect of D-AP5/CNQX in itself on basal GCaMP6f fluorescence was subtle in most cells. The median effect for the entire cell population was no change in calcium sensitive fluorescence following application of D-AP5/CNQX, and this was also the case for the GI subgroup (Figure 5.4 A and Bi). The GE subgroup showed a significant reduction in fluorescence, which would fit with the concept that these cells are receiving significant synaptic inputs, which are causing them to fire spontaneously (Figure 5.4 Bii).

As for TTX, the overall effect of D-AP5/CNQX was to abolish the responses of GE neurons, whilst leaving the GI response largely intact (Figure 5.5). The size of the GI response appears to be slightly smaller after application of D-AP5/CNQX, when compared within the same cell (Figure 5.5 Ci). However, this effect had also been observed after a second application of 0.5mM glucose in control cells (Figure 4.14). If the GI response in D-AP5/CNQX is compared to the second application of glucose in GI cells in control slices, then there is no significant difference in response size (Figure 5.5 Cii). This indicates that there is no overall effect of D-AP5/CNQX on GI neurons, either with regard to the number of responsive cells or the size of response- suggesting that this response is not dependent on fast excitatory glutamatergic synaptic transmission.

The GI cells observed in the presence of D-AP5/CNQX were scattered throughout the rostro-caudal extent of the PVN, in a similar fashion to that seen for the TTX experiment (Figure 5.6).

Chapter 5 A subset of CRH PVN neurons intrinsically sense a fall in glucose, and this is dependent on glucose metabolism.

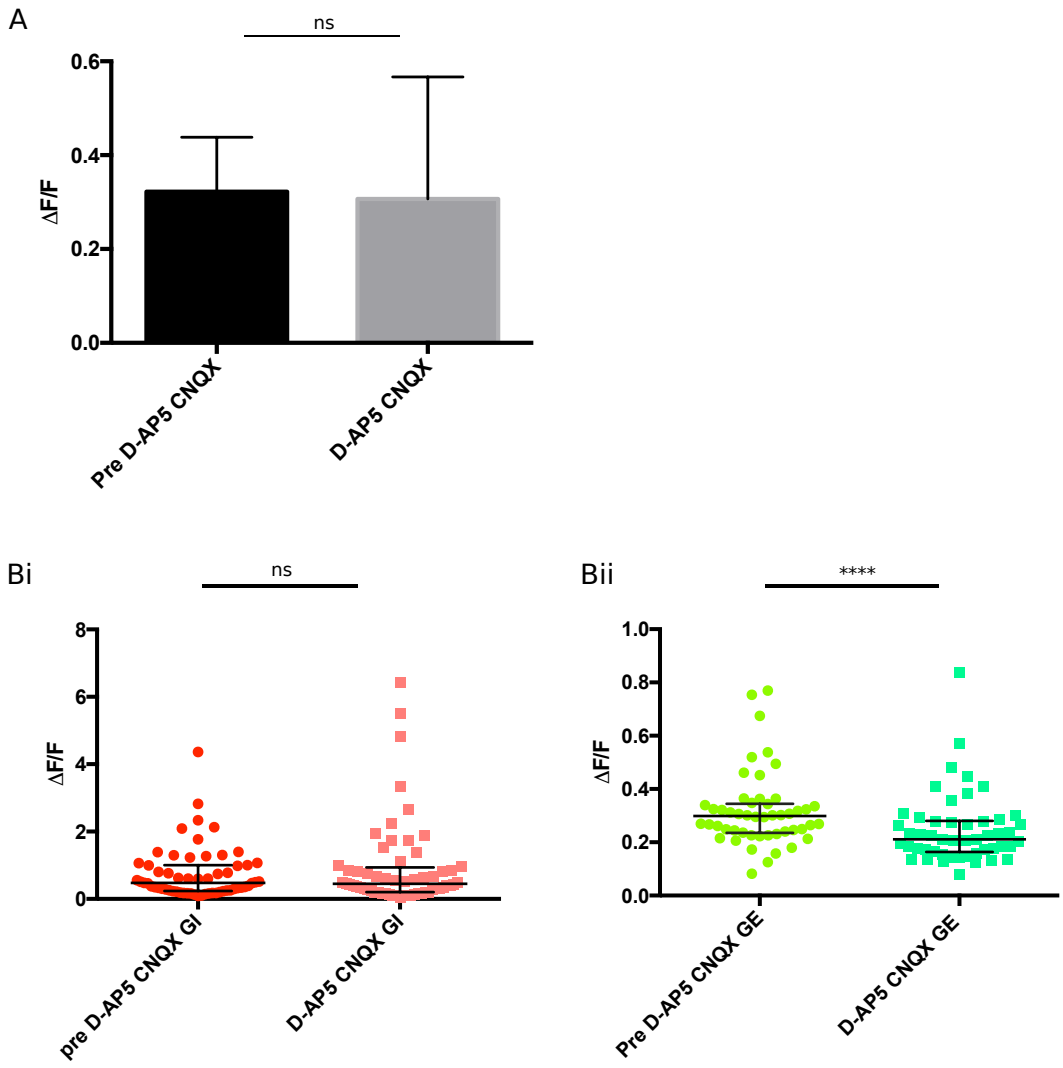

Figure 5.4 Effect of D-AP5/CNQX on calcium levels

A Overall effect of D-AP5/CNQX on calcium levels for all cells. There is no significant change in mean calcium levels (Wilcoxon paired signed rank, n=720)

B D-AP5/CNQX has no effect on mean calcium levels for the GI subgroups of cells (Wilcoxon paired signed rank, ns, n=60). There is a significant decrease in mean calcium levels for the GE subgroup of cells (Wilcoxon paired signed rank, $p<0.0001$, n=50)

Data obtained from 3 mice, 5 slices, 144±30.4 cells/slice. Data shown as median and IQR.

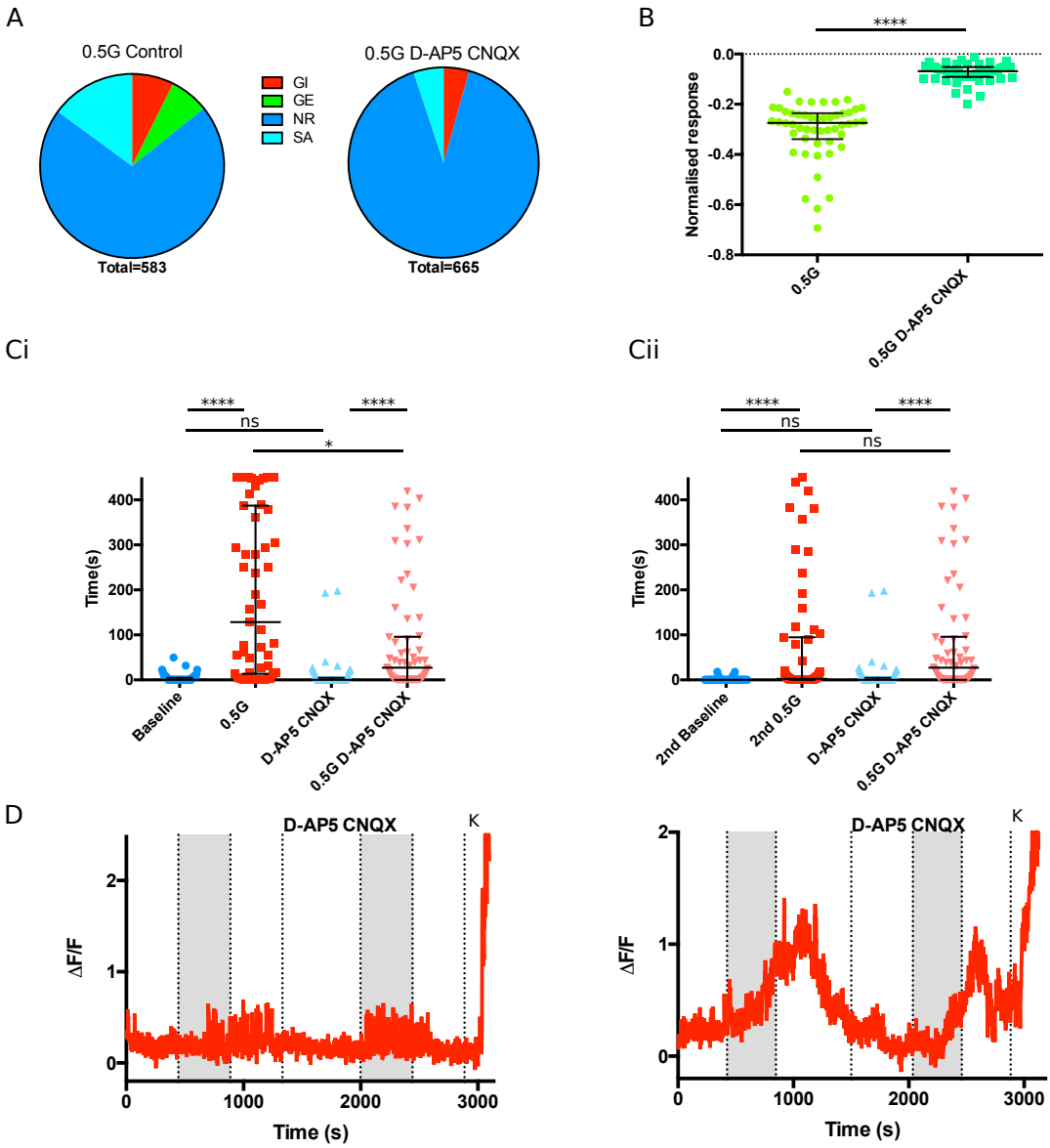
A
0.5G Control
0.5G D-AP5 CNQX
GI
GE
NR
SA
Total=583
Total=665
B
****
Normalised response
0.0
-0.2
-0.4
-0.6
-0.8
0.5G
0.5G D-AP5 CNQX
Ci
Cii
****
ns
*
Time(s)
400
300
200
100
0
Baseline
0.5G
D-AP5 CNQX
0.5G D-AP5 CNQX
2nd Baseline
2nd 0.5G
D
D-AP5 CNQX
K
ΔF/F
2
1
0
0
1000
2000
3000
Time (s)

Figure 5.5 Effect of excitatory synaptic blockade on responses to low glucose in CRH PVN cells

A Cell population responses to a step to low glucose in presence of D-AP5/CNQX compared to control population. GE responses no longer present in D-AP5/CNQX (Chi square 96.16, $p<0.0001$)

B Population of GE neurons identified prior to application of D-AP5/CNQX no longer show any calcium response to low glucose in presence of D-AP5/CNQX, (Wilcoxon paired signed rank, $p<0.0001$, $n=50$)

Ci) GI responses are reduced in size but not ablated in presence of D-AP5/CNQX. ii) the size of GI response is not significantly different to the size of response seen after second application of low glucose in control cells. (Kruskal Wallis test with Dunn's multiple comparisons)

D Example calcium traces showing GI cells responding to low glucose before and after synaptic blockade. D-AP5/CNQX applied at 3rd vertical line, shaded grey areas represent application of low glucose, high potassium solution applied at final vertical line K.

Data for D-AP5/CNQX from 3 mice, 4 slices, 166.3±25.5 cells/slice. Data shown as median and IQR

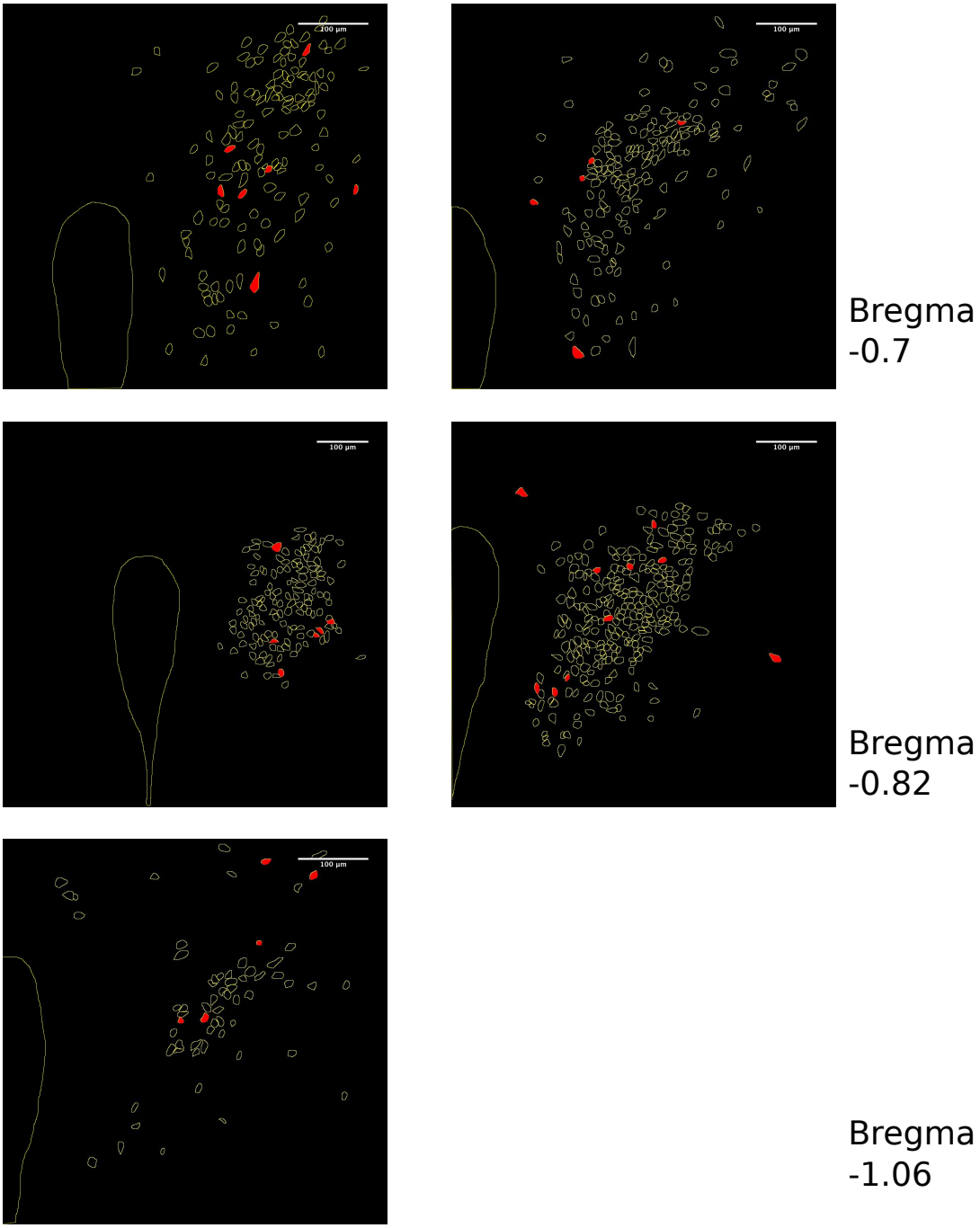

Figure 5.6 Spatial distribution of GI and GE cells after a step from 2.5mmol to 0.5mmol glucose in the presence of synaptic blockade
Images are arranged rostral to caudal, GI neurons are red, GE green. Approximate bregma values are indicated.

5.4.1.3 Effect of excitatory and inhibitory synaptic blockade (EISB)

A further set of slices were exposed to a cocktail of CNQX, D-AP5 and in addition 100μM picrotoxin ($GABA_A$ antagonist) to block inhibitory inputs in addition to excitatory inputs (Figure 5.7). Again, this was a 2-exposure protocol, with low glucose applied before and after EISB. GI responses were preserved in the presence of D-AP5, CNQX and picrotoxin. The slices exhibited a smaller population of GI and GE neurons prior to application of EISB compared to the control slices (Chi square 96.24, $p<0.0001$, Figure 5.7A). In particular only 5 cells in total were identified as GE, and essentially this means that the effect on GE responses cannot be commented on using this dataset. There was a reduction in the size of the GI response after EISB compared to the response seen in the same slice prior to EISB (Figure 5.7Ci). There was no change in the size of GI responses in the presence of EISB compared to a second application of 0.5mM glucose in control slices (Figure 5.7C ii).

The effect of EISB itself was to cause an average decrease in calcium levels across all cells (0.58(0.36-0.93) to 0.43(0.27-0.98), median and IQR, Wilcoxon signed rank $p<0.0001$, $n=444$), which was also observed in the GI subgroup (Figure 5.7B). The spatial distribution of responsive cells in this experiment was similar to that for D-AP5/CNQX and to TTX, although far fewer cells were observed to respond (data not shown).

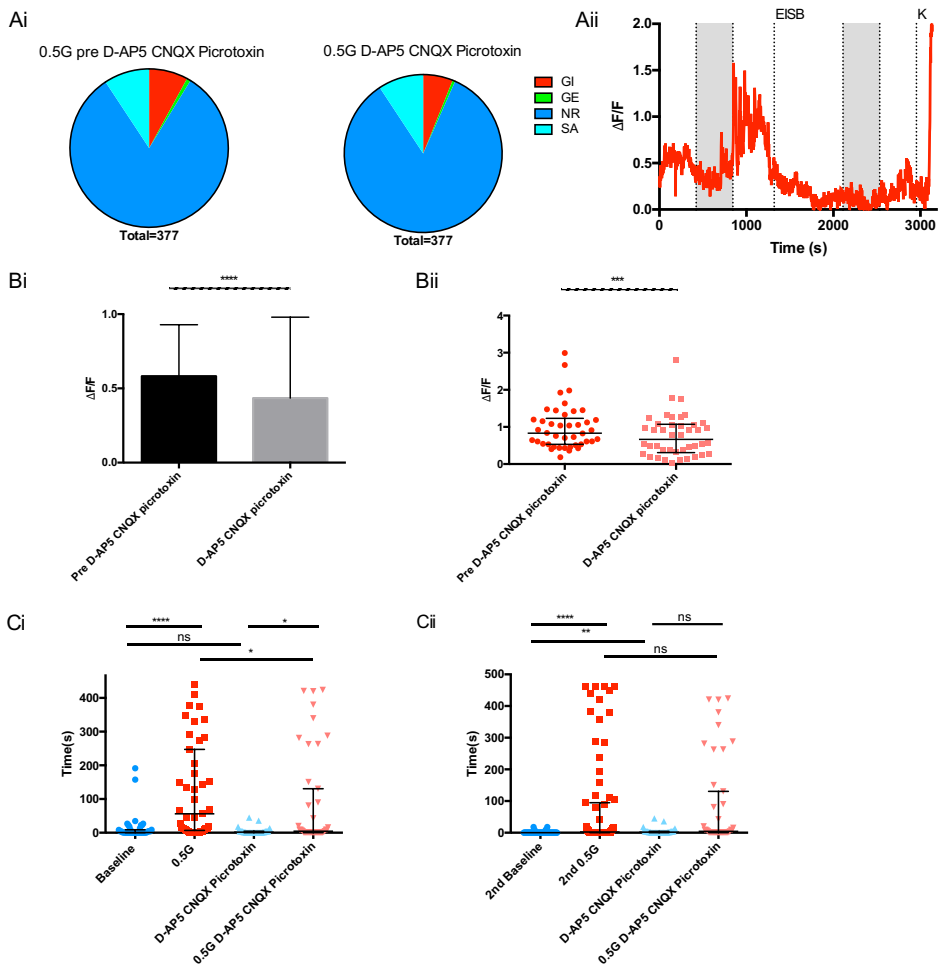

Figure 5.7 Effect of inhibitory and excitatory synaptic blockade (EISB) on responses to 0.5mmol glucose in CRH PVN cells

Ai) GI cells are present both before and after application of EISB (Chi square 1.227, ns). The numbers of GE cells are very small in this data set (5 in total)

Aii) Example cell responding to 0.5mM glucose in absence and presence of EISB.

B EISB application reduces median calcium sensitive fluorescence i) on all cells, ii) on GI subgroup (Wilcoxon signed rank, ****p<0.0001, ***p=0.0006)

C There is a reduction in the size of the GI response in the presence of EISB when comparing responses within the same slice (i). There is no significant change in the size of response compared a second application of 0.5mM glucose in control slices (ii) (Kruskall Wallis test with Dunn's multiple comparisons)

Data obtained from 2 mice, 4 slices, 94.3±15.2cells/slice. Data displayed as median and IQR

5.4.2 Glucose sensitivity and glucose metabolism

The protocols used so far have been designed to examine the effect of a step from a baseline level of glucose representative of levels in a fed animal to a level which would be expected during significant hypoglycaemia. If sensing this change in glucose does not depend on metabolism, then replacing 2.5mM glucose with a combination of 2mM 2-DG and 0.5mM glucose will not have any effect on glucose responsive cells (so long as 2-DG is a substrate for the transporter or sensor which usually carries/detects glucose). If, however, sensing requires metabolism, then this combination will if anything show an enhanced effect because of the ATP depleting effect of 2DG. In this experimental protocol, 2-DG and 0.5mM glucose were applied twice with washout being performed in between, similar to the initial protocol where steps from 2.5mM glucose to 0.5mM were performed twice.

GI and GE responses were maintained in the presence of 2-DG (Figure 5.8), there was even some expansion of the number of GI cells. Interestingly, the size of both the GI and GE responses was reduced on first application of 0.5mM glucose plus 2-DG when compared to control slices with 0.5mM glucose alone. However, the second response was larger compared to the first where 2-DG was present in the case of the GE cells. This might suggest an accumulation of the effect of 2-DG over time. This experiment suggests that both the GE and GI responses depend on metabolism.

There was no change in the spatial locations of responsive cells with 2DG compared to control or TTX groups (data not shown).

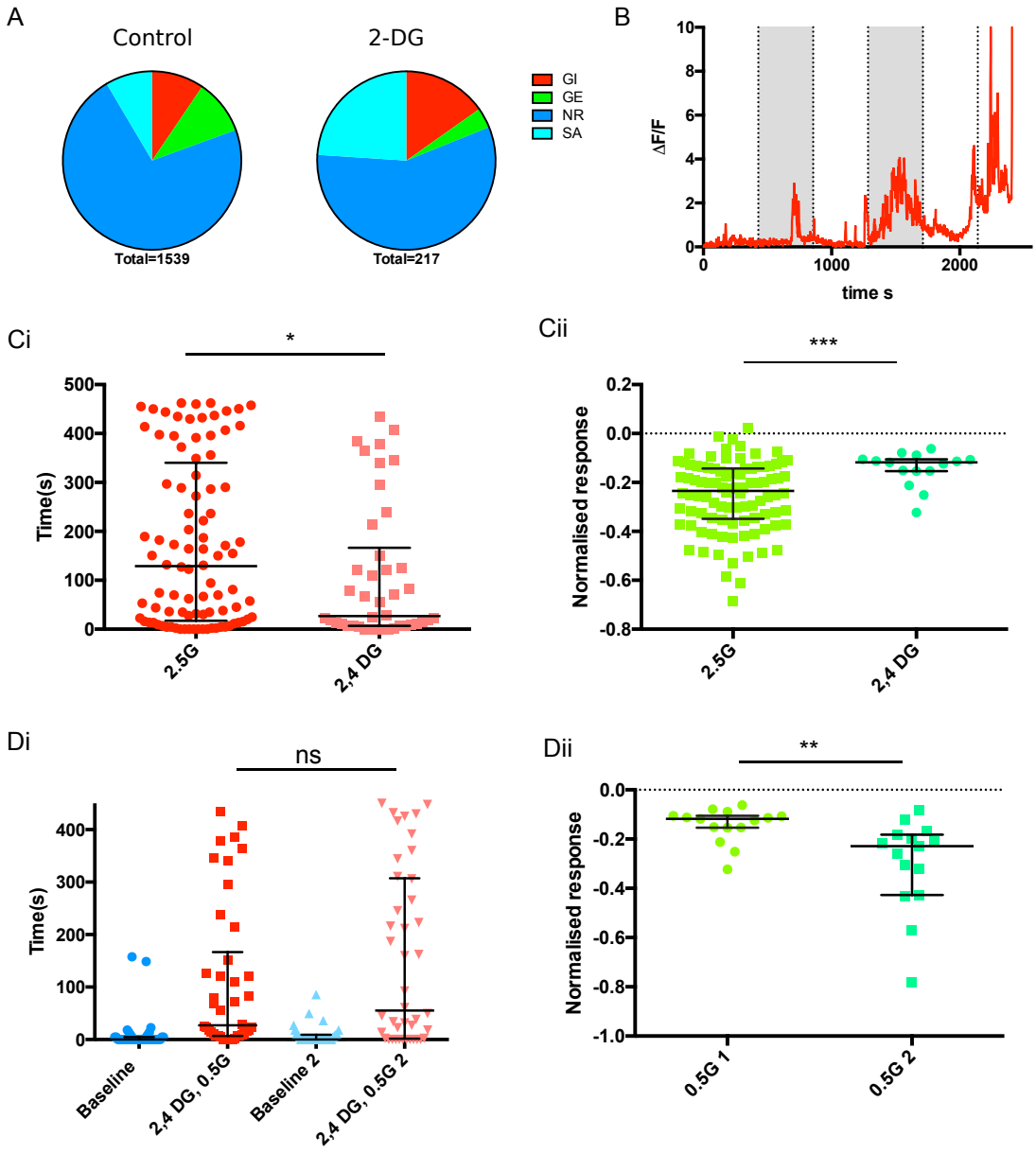

Figure 5.8 Application of 2-DG expands number of GI cells observed in CRH PVN cells
A Proportion of GI, GE, NR and SA cells observed in presence of 2mM 2DG with 0.5mM glucose compared to control slices. Chi square=63.82, p<0.0001
B Example GI cell responding in presence of 2-DG throughout. Shaded areas- 0.5mM glucose, final dotted line- application of high potassium
C Size of the GI response (i) and GE response (ii) both reduced compared to control responses. GI * p=0.0241, GE *** p=0.0007, Mann Whitney test
D Size of the second response to application of 2-DG significantly larger than size of first response in GE but not GI cells. i) GI cells ns Friedman test with Dunn's multiple comparisons. ii) GE cells, ** p=0.0026, Wilcoxon matched pairs signed rank
Data obtained from 2 mice, 4 slices, 54.25 ± 13.7cells/slice. All data displayed as median and IQR

5.5 Discussion

5.5.1 Intrinsic glucose sensing by a subgroup of PVN CRH neurons; evidence from TTX experiments

The defining aspect of a glucose sensing neuron is that it should be intrinsically able to respond to changes in glucose. Clearly, synaptic inputs can result in cells appearing to be glucose sensing, where they are in fact responding to glucose sensing via synaptic input from the primary GI or GE neuron. The hypothalamus is richly supplied with glucose sensing populations (LH, VMN, ARC, DMN, PVN, PO), and many of these could maintain synaptic inputs to the PVN in 300micron thick slice as discussed in section 5.1.5. It was therefore important to examine the effect of glucose on CRH neurons in the absence of such inputs. TTX was chosen as the simplest method to reduce/remove all synaptic inputs, by blocking voltage gated sodium channels necessary for the transmission of action potentials required to trigger synaptic release.

The calcium imaging data collected in the presence of TTX supports and enhances the findings from patch clamping. These data were collected at lower glucose levels than in patch clamping. Here, GI responses were preserved in the presence of TTX compared to control cells, and very few GE cells were observed in TTX. This would fit with the hypothesis that a proportion of CRH PVN cells have intrinsic GI responses (~20% based on the TTX data). This could represent a means by which the intrinsic excitability of the neurons in question could be modulated by the glucose status of the local environment.

The reduction in numbers of GE neurons compared to control slices implies that the majority (if not all) of these neurons are synaptically activated, and not directly sensing glucose.

5.5.2 Intrinsic glucose sensing by a subgroup of PVN CRH neurons; Evidence from synaptic blockade experiments

In all cases involving synaptic blockade, GI responses are maintained. This confirms a novel population of intrinsically glucose sensing GI CRH PVN neurons, which has not previously been identified. Given the known roles of CRH at the top of the ACTH-cortisol axis, and in addition the newly identified autonomic projections from CRH PVN neurons,

these cells are well positioned to be involved in the counter-regulatory response to hypoglycaemia.

One further possibility should not be discounted. Although TTX and synaptic blockade remove neuronal inputs from these cells, it is still possible that non-neuronal cell signalling could be responsible for the effects seen. A local glucose sensing astrocyte population could release glucose or lactate onto the CRH PVN GI cells, for example (Leloup et al., 2016). However, this is true of almost all of the previous studies of intrinsic glucose sensing neurons within the CNS, as few experiments are carried out in conditions which would block non-neuronal inputs. It is also unlikely to alter the overall implications of this finding significantly. If GI CRH PVN cells are in fact the first order downstream neuron of the 'true' glucose sensing cells, they remain important and specific effector cells in the response to hypoglycaemia, and would still be attractive for further investigation and indeed as potential future therapeutic targets.

The finding that the GE responses to glucose amongst CRH PVN neurons are abolished by TTX and excitatory synaptic blockade indicates that these cells are not in fact intrinsically glucose sensing but are responding to synaptic inputs from other glucose sensing cells within the slice. As described in section 5.1, there are a wide range of possible candidate populations which could fulfil this role. Depending on whether any synaptic connection is direct, or involves an interneuron and on whether the primary sensing neuron is itself excitatory or inhibitory, either GE or GI cells from elsewhere in the slice could be involved as outlined in section 5.1.5.

5.5.3 Metabolism is necessary for both GE and GI responses

The 2-DG experiment suggests that metabolism is necessary for both GE and GI responses within the CRH PVN neurons. A non-metabolism dependent cell population would have shown no effect with the switch from 2.5mM glucose to a combination of 2mM 2DG and 0.5mM glucose. The fact that the second response to application of 2-DG was larger than the first is also supportive of this interpretation of the data as 2-DG is likely to accumulate in cells and cause increasing metabolic effects with time.

Further confirmatory work would be helpful to explore these findings. Repeating the experiment in the presence of TTX or synaptic blockade would remove the possibility of inputs from elsewhere in the slice confusing the issue, and allow a focus on the GI CRH PVN neurons. A step from 0.5mM glucose to 0.5mM glucose plus 2-DG would be expected to show lack of inhibition by glucose in GI cells. Logical experiments beyond this would be to examine the effect of pharmacological blockade/activation of glucokinase or AMPK and then downstream candidate molecules previously identified as important in glucose sensing cells.

GE responses are also preserved in CRH PVN neurons in the presence of 2-DG. This suggests that metabolism is necessary for the glucose sensing population acting on GE CRH PVN cells. LH GI neurons sense glucose independent of metabolism, which would make a LH input much less likely. Essentially, every other GI and GE population in the hypothalamus remains a potential candidate. Further investigation might be possible using alternative slicing strategies to anatomically remove individual hypothalamic nuclei from the slice and examine the effect of this on CRH PVN responses. Alternatively, pharmacological investigation based on known mechanisms of glucose sensing in other glucose sensing populations could provide clues as to identity of the upstream glucose sensing population.

5.5.4 Effect of TTX or synaptic blockers on PVN CRH neuronal calcium levels.

The effect of TTX prior to a low glucose step on calcium levels in these experiments was interesting. The effect on individual cells was very variable, with some cells showing large falls in fluorescence whilst many others showed little or no change or indeed slight rises. The effect seen might be expected to depend on the balance of excitatory and inhibitory inputs onto each individual cell. In the overall cell population, there was a small fall in fluorescence after application of TTX. This would fit with the concept that many of these cells receive overall excitatory inputs, and that blocking these would result in a fall in calcium levels. The GE neurons showed responses similar to the overall group. This would also fit with the idea that these neurons are spontaneously active, and are reducing their activity in the presence of TTX. However, the GI neurons did not as a group exhibit a significant fall in fluorescence. This might suggest that these cells

receive a differing set of inputs to the population as a whole, or that their basal firing rates are lower (or indeed that these neurons are quiescent in 2.5mM glucose).

The effect of excitatory blockade alone was not significant in the whole cell population, or in the GI subgroup. D-AP5/CNQX did result in a median decrease in fluorescence in the GE subgroup, suggestive of blockade of excitatory synaptic inputs to these neurons. This would fit with the effect seen with TTX, adding to the evidence that these neurons are tonically active, and driven by excitatory inputs. PVN cells receive extensive excitatory inputs from elsewhere in the hypothalamus, and the primary inhibitory inputs are from a surrounding 'shell' of GABA releasing axons, often from cells within the PVN itself including CRH neurons (Ramot et al., 2017, Roland and Sawchenko, 1993). It is important to note that some of the excitatory inputs are in fact thought to synapse onto the inhibitory shell rather than directly onto PVN neurons (Herman et al., 2003). This might explain why in the majority of cells no direct effect was seen on application of excitatory blockade- the removal of direct inputs and those acting via the inhibitory shell could balance one another out to no overall effect.

Combined excitatory and inhibitory blockade caused a decrease in fluorescence in the whole neuronal population in a similar fashion to TTX. This would be consistent, as combined excitatory/inhibitory blockade or TTX should result in removal of rapid action potential dependent synaptic inputs in a similar manner. However, additional modulation of synaptic inputs may be being blocked by TTX compared to combined excitatory/inhibitory blockade. Examples would include the effects of CRH itself on local receptors, MC4 receptor effects, vasopressin and oxytocin receptors.

5.5.5 Summary

This chapter presents the evidence for a novel population of GI neurons which express CRH and are situated in the PVN. Experiments using 2-DG suggest that metabolism of glucose is important for glucose sensing in this new population. In addition, a further subgroup of CRH PVN GE neurons are indirectly modulated by synaptic inputs from elsewhere in the hypothalamus, with potential primary glucose sensing candidates including neurons in the LH, VMN, DMN or ARC, or indeed the newly identified CRH GI PVN neurons.

Chapter 6 CRH-Cre neurons have a role to play in the response to recurrent hypoglycaemia

6.1 Introduction

This chapter describes models of insulin induced hypoglycaemia (IIH) and HAAF in humans, rats and mice, with their advantages and disadvantages. Data from mouse models of both single and recurrent episodes of hypoglycaemia are presented. The CRH x Td mouse is used in the single hypoglycaemia model to demonstrate neuronal activation as evidenced by cfos expression in the hypothalamus. Finally, CRH x GCaMP6f mice are exposed to recurrent hypoglycaemia and data are presented showing the responses of the subsequent acute slices to low glucose using calcium imaging.

6.1.1 Models of hypoglycaemia and autonomic failure in human and animal models

The development of HAAF was described in the introductory chapter. As established there, the mechanisms underlying this phenomenon remain poorly understood. In order to gain a better understanding, reliable models of HAAF are needed, both in humans and in animals (Tkacs and Thompson, 2006).

6.1.1.1 Human models of HAAF

HAAF has been produced under controlled conditions in both diabetic subjects and healthy volunteers. In most cases, following an overnight fast, a hyper-insulinaemic glucose clamp technique is used, with insulin and glucose being infused into an indwelling cannula in one arm. Glucose infusion is used in addition to insulin to allow much tighter control of glucose levels and ensure that the subject does not become excessively hypoglycaemic. Repeated sampling of blood is performed from a cannula in the other arm. By warming the sample hand/arm, 'arterialised' venous blood can be sampled, as warmth opens up additional capillary beds, bypassing metabolically active tissue. A range of durations and depths of hypoglycaemia have been induced using this technique. Information on the hormonal response provoked by a given level of hypoglycaemia can be obtained from blood sample assays. In addition, questionnaires can be used to gain an understanding of the subject's experience of neurogenic and

neuroglycopenic symptoms of hypoglycaemia (Senthilkumaran et al., 2016). Some studies report that after a single hypoglycaemic episode a degree of HAAF can develop (Heller and Cryer, 1991), whilst others suggest 2 or 3 prior episodes are required (Davis et al., 1996, Moheet et al., 2014). Healthy volunteers have been reliably shown to exhibit all the canonical features of HAAF (Senthilkumaran et al., 2016), even though they would not experience this degree of hypoglycaemia outside the test arena.

Diabetic subjects are in some ways a more appropriate subject group for investigation as they are the patients suffering the adverse sequelae. A range of protocols with differing frequencies and depth of hypoglycaemia have been described (Dagogo-Jack et al., 1993, Rattarasarn et al., 1994, Lingenfelser et al., 1993). However, it is challenging to control for degree of prior glycaemic control, and especially to recruit a group who do not already have any degree of HAAF. For this reason, in many cases healthy volunteers have been preferred.

The major limitation of human studies is that it is not possible to study neuronal activity or the underlying mechanisms with the same level of resolution, and possible interventions are limited. Imaging has provided some insights, but to gain a greater understanding of underlying mechanisms, models, particularly in rodents, have been developed. In addition, this provides the potential for use of genetic modification, analysis of gene expression, activation/inactivation of brain areas/systems and indeed the production of more severe degrees of hypoglycaemia than would be deemed acceptable in a human subject (Senthilkumaran et al., 2016).

6.1.1.2 Rat models of HAAF

A number of rat models of HAAF have been reported in the literature. The route of administration of insulin varies, with some groups using subcutaneous insulin (Sanders et al., 2006, Orban et al., 2015) and others i.p insulin (Flanagan et al., 2003, McCrimmon et al., 2005) to induce hypoglycaemia. There has been a move towards chronic cannulation of the internal jugular for insulin (and sometimes additional glucose) infusion, with blood samples being withdrawn either from an arterial cannula (Herzog et al., 2008, Al-Noori et al., 2008, Evans et al., 2001), or by repeated tail tip (de Vries et al., 2004). Chronic cannulation allows a similar degree of control of hypoglycaemia to that

achieved in human subjects. It also reduces stress due to restraint and pain from injection. However, a degree of technical skill is required to prepare the animals. Repeated sampling is generally not a significant issue. An adult rat's blood volume is approximately 25mL (64mL/kg, 400g rat), and 15% total blood volume is suggested as a maximum to withdraw over a 28 day period if the animal is to recover, which is equivalent to 3.84mL (nc3rs, 2018b). Terminal samples are unrestricted. In some cases, replacement of blood samples with donor rat blood has been used to allow larger samples to be taken (Evans et al., 2003).

Effects similar to those seen in humans have been reported in rat models of recurrent hypoglycaemia. Between one (Kang et al., 2008, Tkacs et al., 2005) and four (Orban et al., 2014, Herzog et al., 2008) prior hypoglycaemic episodes have been reported to be required to produce a hormonal profile consistent with HAAF. Of note, some studies do not see a fall in epinephrine levels in recurrent hypoglycaemia animals compared to single hypoglycaemia (Figlewicz et al., 2002, Paranjape and Briski, 2005). However, as we will discuss in more detail below, it is difficult to unpick the effect of restraint and intervention stress from the stress evoked by the study conditions and this may be a confounding factor.

Clearly, it is advantageous to be able to sample tissue for either imaging, recording or analysis of gene expression following induction of HAAF and this is the major advantage of a rat model. However, because of the lack of verbal report it is not possible to gain information regarding neurogenic or neuroglycopenic symptoms as in the human. In addition, very few rat models with genetic modifications are available. Potentially interesting transgenic rats might include the CHAT-CRE, TH-Cre and TPH2-CreERT2 strains, which express Cre recombinase under the control of cholinergic, adrenergic/noradrenergic (Witten et al., 2011) and serotonergic (Weber et al., 2011) cells respectively. A CRH-Cre transgenic rat has been developed, using a BAC (Pomrenze et al., 2015). However, although expression of Cre recombinase was observed in the amygdala and parts of the BNST, no expression was found in the paraventricular hypothalamus in this strain, so this would not be of use to investigate CRH PVN neurons. In the future, it seems likely that a larger number of relevant models will become

available, using the newer gene editing toolkits, for example CRISPR (Li et al., 2013), TALEN (Tesson et al., 2011) and zinc finger nucleases (Geurts et al., 2009).

6.1.1.3 Mouse models of HAAF

The very wide range of transgenic and knock in mouse models available make developing a mouse model of HAAF very attractive. However, there are a number of important considerations which have made this a challenging prospect.

Firstly, technically obtaining blood samples which provide useful information from an animal which has a circulating volume of around 1.5mL (58.5mL/kg, 25g mouse) is challenging. Clearly the number and volume of samples must be limited, with the limit for an animal which is to recover being 15% of total blood volume over 28 days (0.21mL) (nc3rs, 2018a). Even with a terminal procedure, the maximum blood sample that could be obtained is the total blood volume or less. This reduces the amount of information that can be gathered, particularly with regard to hormonal levels which tend to require larger blood volumes. For example, the glucagon RIA used here requires 100µL of plasma or serum for a single time point, which is equivalent to approximately 180µL of blood.

Secondly, mice as a prey animal species are extremely easy to stress, simply by handling or indeed any change in their housing and environmental conditions. This is especially problematic for measuring epinephrine and norepinephrine levels. Anaesthesia can be used but induces a different range of stressors, and has been shown to alter the response to hypoglycaemia (Ayala et al., 2010). This, as well as the fact that only a small number of samples can be taken from any one animal, may explain why no publication has yet been able to show blunting of the epinephrine response to hypoglycaemia in a mouse model (Senthilkumaran et al., 2016).

There is also the question of how to induce hypoglycaemia. A single i.p injection of insulin is probably the most commonly used method for a single hypoglycaemic episode, and is widely used to perform an insulin tolerance test in mice (Dearden and Balthasar, 2014, Ayala et al., 2010). A dose of 2-2.5units/kg of a fast-acting insulin such as Actrapid or Humulin S is commonly used (Poplawski et al., 2011, Dearden and Balthasar, 2014).

However, it is more challenging to reliably induce hypoglycaemia repeatedly as required to induce HAAF. Poplawski and colleagues used i.p insulin at 2.5units/kg to induce HAAF, with tail tip blood glucose (2011). Potentially chronic cannulation is more attractive, as it allows use of an insulin (± glucose) infusion to induce controlled hypoglycaemia, and this was used by Jacobson et al. (2006b, 2006a). However, cannulation in the mouse is technically challenging. In addition, infusion of i.v fluids into a very small circulating volume without significant dilution effects is required. The limitations already mentioned for blood sampling are also an important consideration, even with a tightly controlled infusion. Glucose control may be less tight as there are limits to the frequency at which measurements can be safely taken.

Neither an i.p nor an i.v approach induced a fall in epinephrine levels back towards baseline levels in publications in mice to date, but both techniques did show falls in cortisol and glucagon, as would be expected in HAAF. A review by Senthilkumaran et al. therefore concludes that until a loss of the epinephrine elevation is seen in a mouse model, it cannot be reasonably concluded that a mouse model of HAAF exists (Senthilkumaran et al., 2016). However, it is very difficult to unpick the effect of hypoglycaemia and other stressors on mouse epinephrine levels. It is clear that it is possible to reliably induce recurrent hypoglycaemic episodes in mice, using either i.p or i.v insulin, and that using these methods an attenuation of both the glucagon and cortisol response to hypoglycaemia can be produced which would be consistent with the development of HAAF.

6.1.2 cfos as a marker of neuronal activation

CFos is an immediate early gene which has been widely used as a marker of neuronal activation in a wide range of studies, both in vitro and in vivo (Kovacs, 1998, Hoffman et al., 1993). It was first described in 1984 (Greenberg and Ziff, 1984), and it encodes a 55kDa protein, with a short half-life of around 2hours. cfos interacts with cjun and other members of the jun family to form the AP-1 transcription factor. CFos mRNA is measurable within minutes of an acute stimulus, and peaks at 30-60mins. cfos protein levels peak 1-3hours after the onset of a stimulus. Activation of CFos transcription is mediated by both a CRE (cAMP response element) and SRE (serum response element) sited in the promotor region of the CFos gene. This allows a range of different forms of

activation of a neuron to initiate CFos transcription, including rises in PKA, CAM kinase IV, PKC and other MAP kinases (Kovacs, 1998).

cfos acts as a transcription factor in concert with other members of the immediate early gene family including cjun. It is known to target AP-1 promotor regions, and was initially identified as a proto-oncogene in the periphery, causing transcription of genes involved in initiating cell division amongst other roles. The downstream targets of cfos in the brain, where very little mitosis occurs, are less well understood, although cfos is known to activate transcription of genes including cytokines, growth factors, stress signals and oncogenes (Alberini, 2009). The primary value of cfos in the brain has been as a marker of neuronal activation, allowing functional mapping of anatomical areas within the brain which are activated by an acute stimulus. An important caveat in the use of cfos for this purpose is that cfos will only identify cells that become activated by a stimulus. Cells which are inhibited cannot be identified. There is also a threshold that must be reached to induce cfos, and additional cells may be activated subthreshold and so not identified. In addition, cfos is not a specific marker, and it is possible that unidentified events could induce cfos in the same time frame as the experimental stimulus. Therefore, careful choice of control groups is required.

Several previous studies in rats have reported increased cfos labelling in a range of hypothalamic areas following a single episode of hypoglycaemia, including in the PVN (Ao et al., 2005, Al-Noori et al., 2008, Evans et al., 2001, Niimi et al., 1995). Interestingly, the VMN, which is believed to be a key area in the response to hypoglycaemia (McCrimmon, 2009), does not exhibit an elevation in cfos under the same conditions (Niimi et al., 1995). Some studies have gone on to show a reduction in cfos expression in the PVN, and also the DMN and arcuate nucleus, following recurrent hypoglycaemia when compared to a single hypoglycaemic episode (Al-Noori et al., 2008, Evans et al., 2001). Several equivalent studies have been performed in mice, and show similar patterns of cfos after insulin induced hypoglycaemia in the PVN (Tamaki et al., 1995, Diggs-Andrews et al., 2010).

There have been few attempts to define neuronal subtypes which show elevated cfos and other early genes in response to hypoglycaemia within hypothalamic areas. Al-

Noori et al. (2008) examined the expression of fosB in CRH, TRH, vasopressin and oxytocin neurons in the PVN after recurrent hypoglycaemia. fosB is a slower onset transcription factor, which is activated after recurrent hypoglycaemia to a greater extent than after single hypoglycaemia. They showed that around 30% of the fosB expressing cells were CRH positive. This may be an underestimate of the CRH positive proportion, as the animals were not colchicine treated. None of the other 3 neuronal subtypes examined (TRH, vasopressin and oxytocin) co-localised with fosB. Equivalent work has not been performed for cfos and neuronal subtypes in mice or rats.

Importantly, cfos expression can be produced in the PVN in response to a wide range of other acute stimuli, including restraint, osmotic stress, fear, pain and immobilisation (Kovacs, 1998). It is therefore important to design experiments to minimise confounds and improve the signal to noise of the cfos expression to allow effects of the intervention to be detected. Stress must be minimised as far as possible, and control groups must be designed to reproduce those effects which cannot be minimised, and which are not part of the intended stimulus.

6.2 Hypotheses

- CRH neurons are activated by a single episode of hypoglycaemia as indicated by cfos expression
- The counterregulatory response is blunted in a mouse model of recurrent hypoglycaemia
- Recurrent hypoglycaemia reduces the numbers of glucose responsive CRH PVN neurons

6.3 Aims

- Develop a mouse model of IIH
- Seek evidence of neuronal activation (using cfos) following single hypoglycaemia
- Develop a mouse model of recurrent hypoglycaemia and HAAF
- Assess whether glucagon and corticosterone levels fall after recurrent hypoglycaemia compared to single hypoglycaemia

- Examine effect of recurrent hypoglycaemia on glucose sensing in CRH PVN neurons in vitro using calcium imaging

6.4 Results

6.4.1 Developing a mouse model of insulin induced hypoglycaemia

A insulin dose finding pilot experiment was carried out in male CRH x TdTomato mice as shown in table 6.1. A dose of 2units/kg i.p Humulin S was sufficient in to induce hypoglycaemia in 50% of mice (5/10) (blood glucose <4mM). 2.5units/kg induced more consistent hypoglycaemia (4/4, 100%). 2.5units/kg was therefore used for induction of hypoglycaemia.

Table 6.1 Insulin dose finding in CRH x TdTomato male mice

Dose (units/kg)	**1.5**	**2**	**2.5**
Blood glucose at 30minutes mM (Mean ± SEM)	6.5± 0.8 n=4	4.5 ± 0.6 n=10	3.3 ± 0.2 n=4

This dose of insulin was then used in a protocol to induce single hypoglycaemia (SH), as summarised in figure 6.1. A control group (CT) of mice were handled in exactly the same manner as the hypoglycaemia group, but received i.p saline rather than insulin. The resulting blood glucose measurements are summarised in figure 6.2, with a significant fall in blood glucose levels in the SH at 30 minutes compared to CT. All SH animals had glucose levels below the defined threshold for hypoglycaemia (4mM) at 30 minutes.

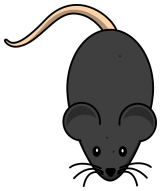

6-12 weeks. Male. C57Bl6 strain
For cfos, CRHXTdTomato

Day 1-7 Habituation period: once daily scruff and IP saline

Day 8

House individually
Tail tip and baseline blood glucose
IP insulin (or saline control) 2.5U/kg (=5µl/g)

Wait 30minutes

Check blood glucose (from tail tip)

Wait 2hours
Terminal anaesthesia and
check blood glucose
Perfuse/fix with formalin
Collect brain for cfos

Figure 6.1 Single hypoglycaemia protocol

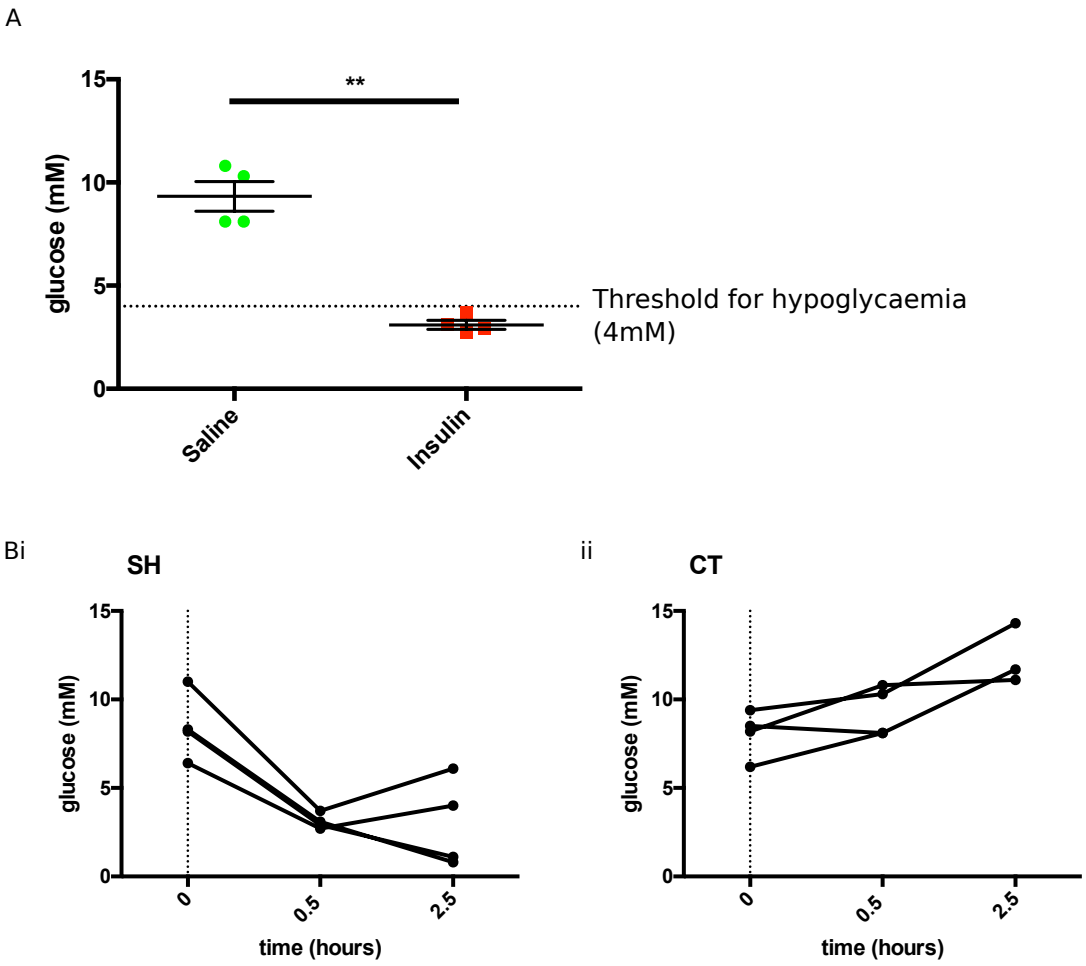

Figure 6.2 Glucose levels for single hypoglycaemia protocol mice
Blood glucose levels measured from tail tip blood samples for mice subsequently used for cfos immunohistochemistry. n=4 per group
A Blood glucose 0.5 hours after a single IP injection of insulin (SH group) or saline (CT group) p=0.0019, unpaired t-test
B Blood glucose at time 0, 0.5 and 2.5 hours after IP insulin (SH group, i) or saline (CT group, ii)

6.4.2 Activation of PVN CRH neurons in a mouse model of IIH

Mouse brains were processed for cfos IHC to look for evidence of PVN-CRH neuronal activation in response to hypoglycaemia, after undergoing the protocol described in section 6.4.1. cfos expression in the PVN is markedly increased after a single episode of IIH, when compared to a saline injected control (Fig 6.3A, n=4 for each group). Co-localisation of cfos and Tdtomato showed that 84% of CRH neurons are activated in response to IIH compared to 30% in the control group (Figure 6.3B, Figure 6.4B). Interestingly, there appeared to be a correlation between blood sugar level at 30 minutes post injection and cfos cell count as shown in figure 6.4A. Co-localisation in the posterior part of the PVN was also examined, as this area is thought to be the site of projections to autonomic areas (Biag et al., 2012), but in these sections no difference between levels of expression of cfos was observed, either in the PVH in total or in CRH neurons (Figure 6.3C).

As a control experiment, a second series of slices from the same animals was double labelled for oxytocin and cfos using IHC (Figure 6.5). There was no increase in cfos expression in oxytocin expressing neurons in the PVN when comparing SH and CT groups (5 ± 2.5 cells, n=3 for SH vs 0 ± 0, n=4 for CT, unpaired t-test ns, Figure 6.6). There was a significant increase in cfos expression for all cells in the PVN (124 ± 14, n=3 for SH vs 18 ± 5.6, n=4 for CT, unpaired t-test p=0.01). There was no difference in the numbers of oxytocin neurons between the 2 groups (19 ± 3, n=3 for SH vs 24 ± 5.6, n=4 for CT, unpaired t-test ns).

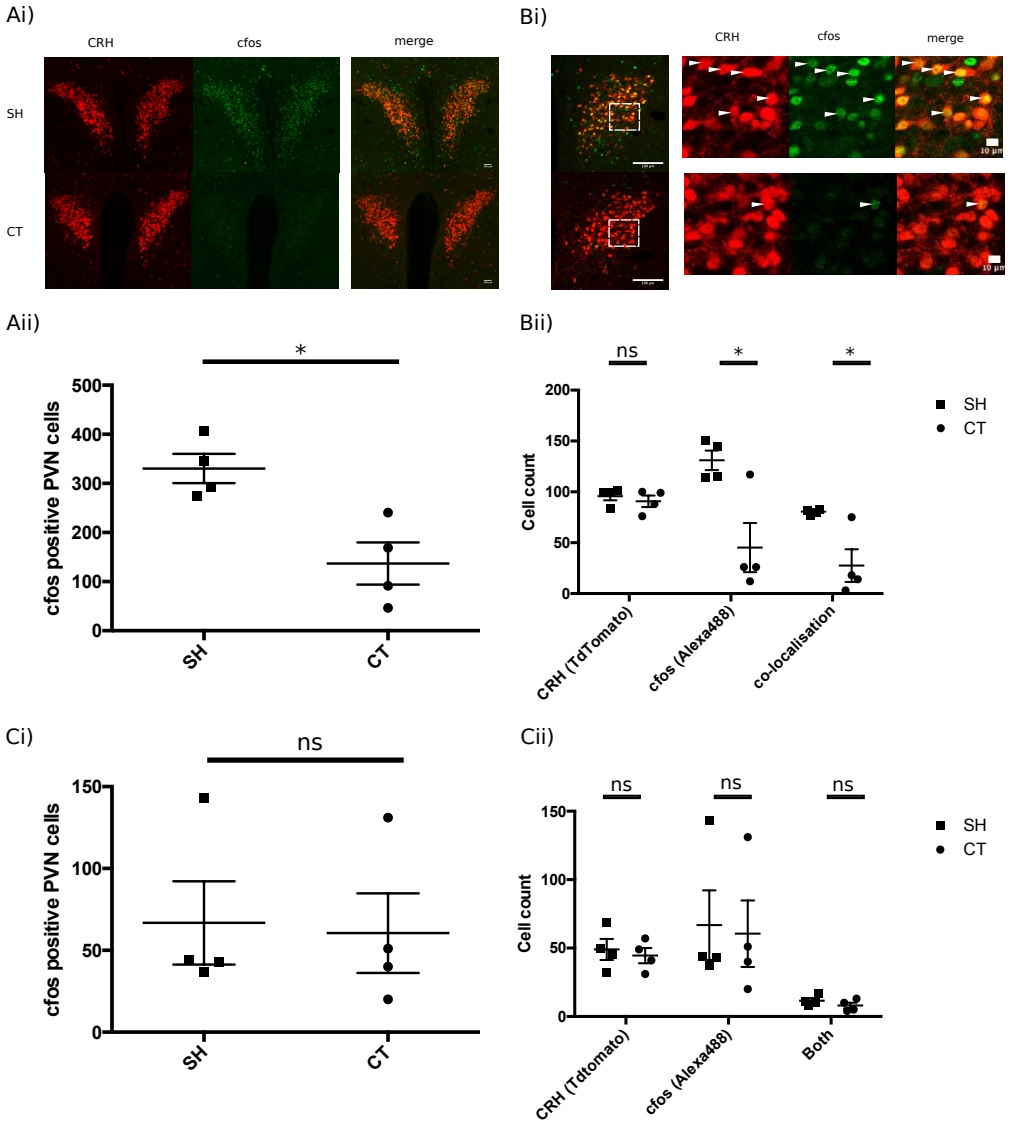

Figure 6.3 CRH neuronal activation by hypoglycaemia: cfos expression after a single episode of insulin induced hypoglycaemia

A i) Representative images after immunohistochemistry for cfos in mid PVN ii) cells counts, one slice per animal, n=4 for each group. Mean SEM and data spread shown
B i) Confocal images of hemi PVN and associated high power images (single z plane) to show co-localisation of CRH (TdTomato positive) and cfos positive neurons ii) manual cells counts, one slice per animal, n=4 for each group *=p<0.05
C i) cfos cell counts in a single posterior PVN slice for each animal, ii) co-localisation of CRH and cfos in the posterior PVN, no significant difference between the 2 groups was found

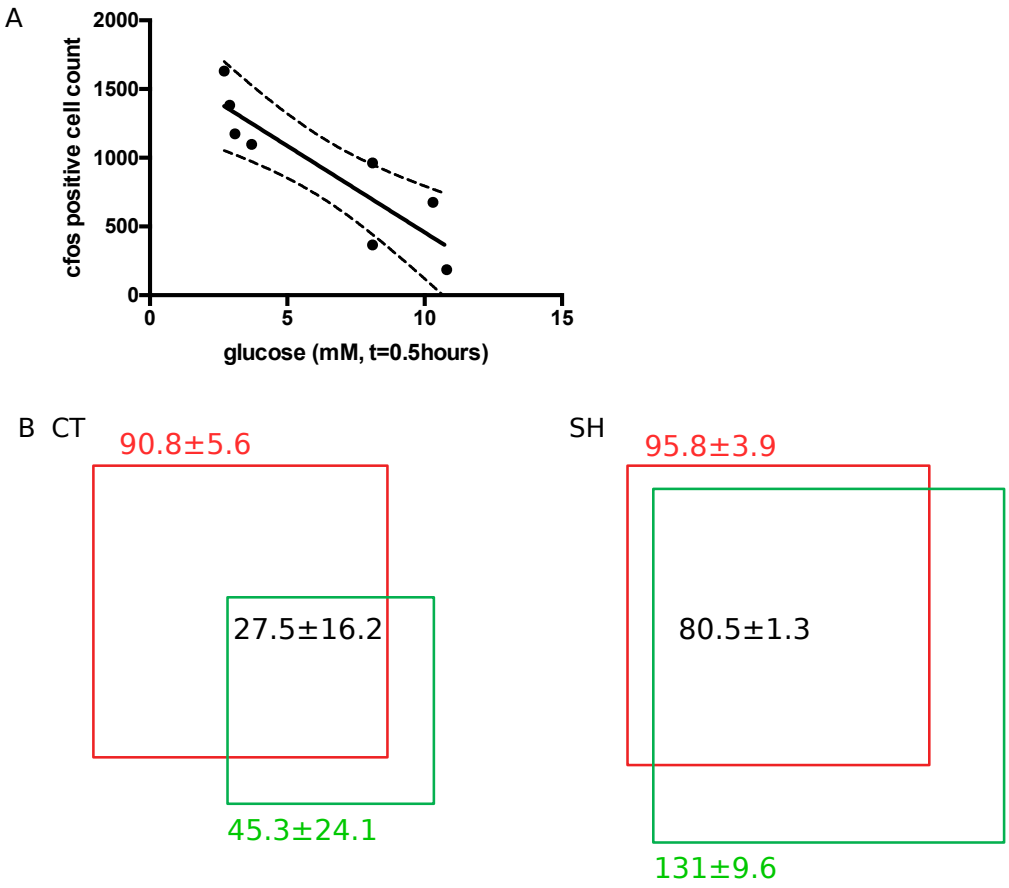

Figure 6.4 Additional cfos information

A Correlation between blood glucose measurement 0.5 hours after i.p injection of insulin or saline and cfos positive cell counts. Line of best fit and 95% confidence intervals plotted, R square= 0.776

B Diagram to show effect of SH vs CT on induction of a cfos population which is largely co-localised with CRH. Red box=CRH neurons, green=cfos, numbers are mean ± SEM of cells counted for CRH (red), cfos (green) and both (black) in the SH group

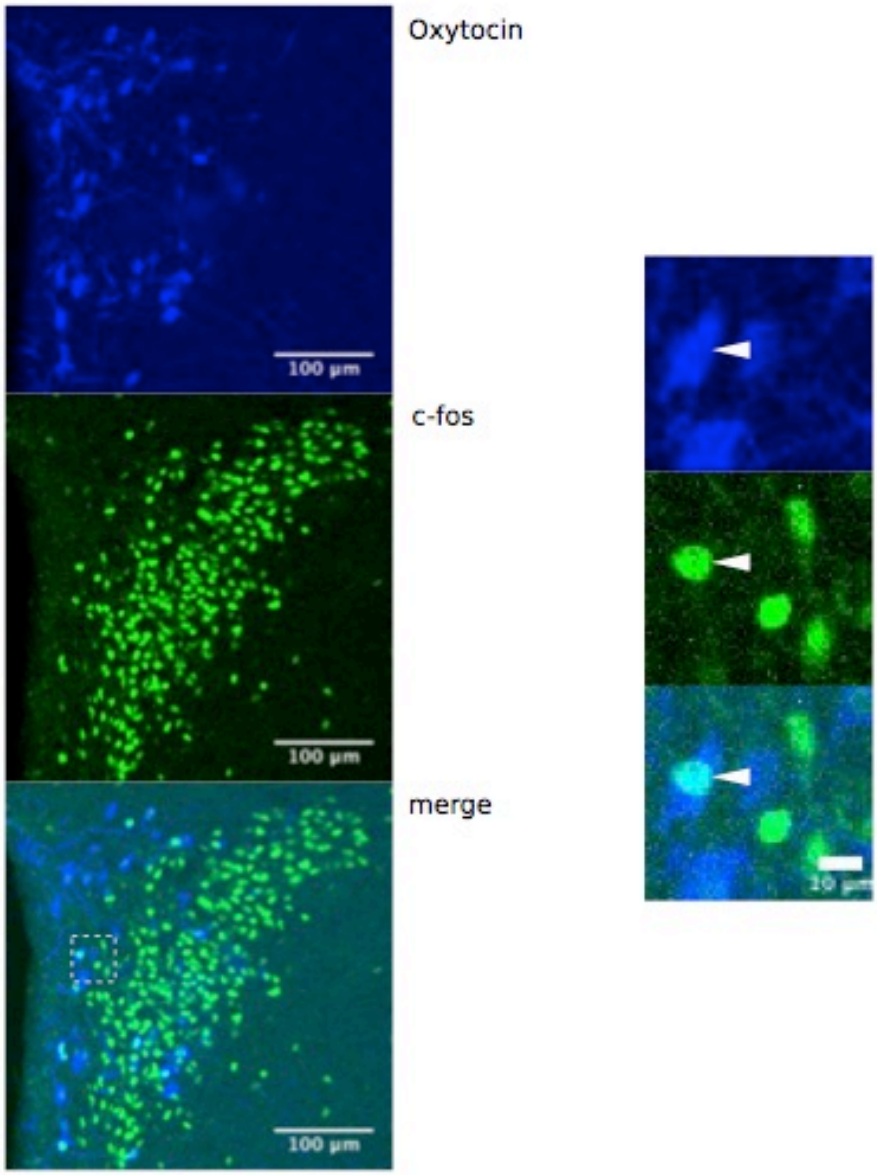

Figure 6.5 Images to show oxytocin staining from a SH mouse from the same cohort as the cfos CRH colocalisation

A Image of hemi PVN, blue is Alexa 405 secondary antibody (oxytocin), green is Alexa 488 secondary antibody (cfos)

B Zoomed in to show colocalisation of oxytocin and cfos in 1/4 oxytocin neurons in the field of view (white arrows)

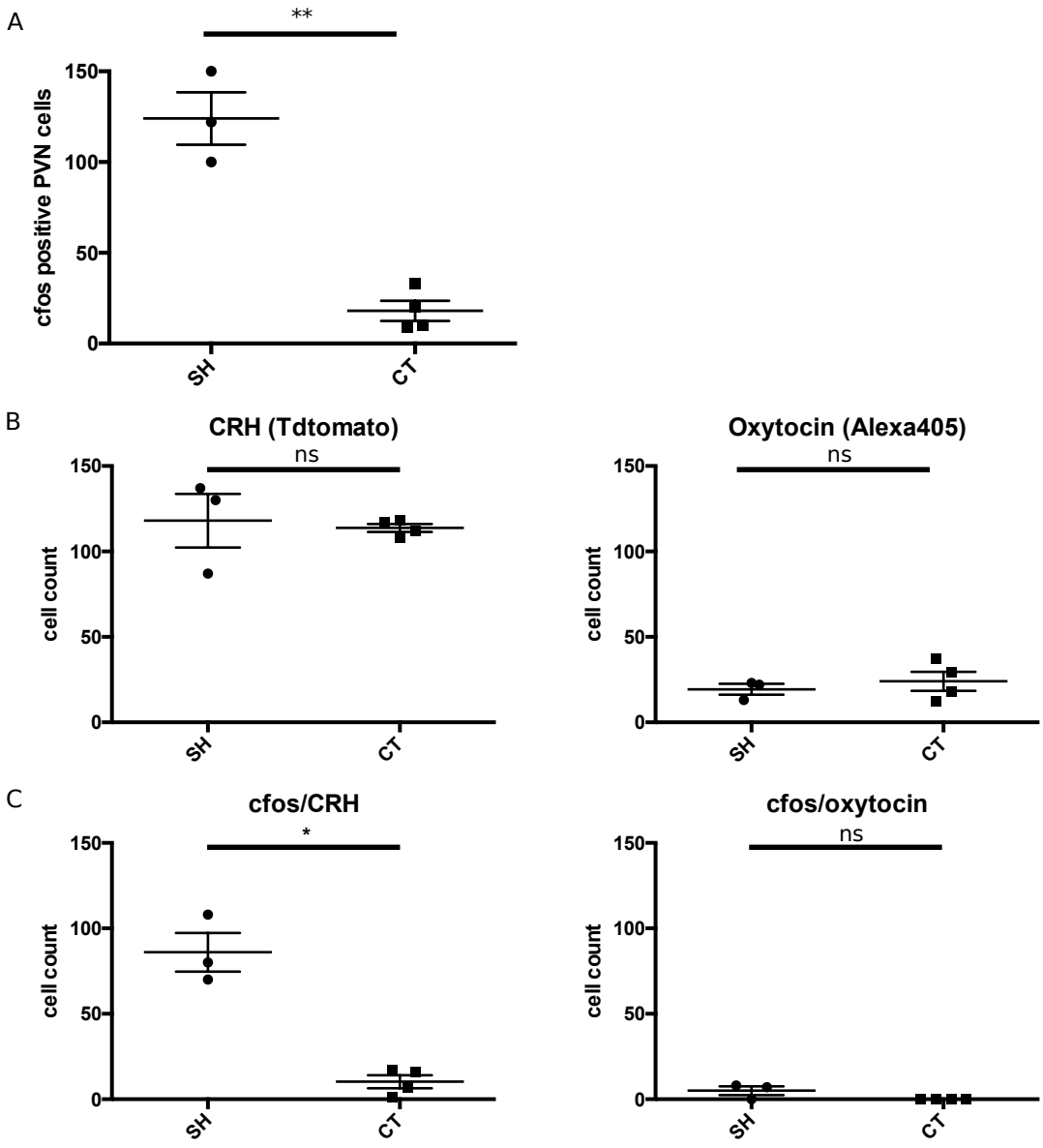

Figure 6.6 Cfos, oxytocin and CRH cell counts in PVN following single episode of hypoglycaemia compared to control saline injection

A Cfos cell counts are significantly increased in SH mice compared to CT (p=0.01)
B No significant difference in CRH or oxytocin cell counts
C Significant increase in cfos positive CRH neurons in SH group compared to CT (p=0.0142) n=3 for SH group, n=4 for CT group, unpaired t-tests

6.4.3 Development of a recurrent IIH model to investigate HAAF in mice.

Having successfully induced single hypoglycaemia, a model of recurrent IIH (RH) was developed as outlined in Figure 6.7. A rapid acting insulin was used (Lispro), with the aim of achieving more rapid onset of hypoglycaemia compared to Humulin S. A 20% lower insulin dose was used for this protocol than the SH protocol above reflecting concern that the mice would need to be able to recover from 4 sequential episodes of hypoglycaemia. Hypoglycaemia of <2mM was relatively uncommon (observed in 17.5% of 40 hypoglycaemic episodes) and was successfully treated with i.p glucose (20% solution). No animals in the experimental groups were observed to experience seizures or became comatose.

Initial samples were collected from a cohort of mice to assess for evidence of HAAF. 24 male mice aged 12-20 weeks were used, all on a CRH-ires-Cre C57Bl6 background. Glucose levels recorded for the cohort showed that hypoglycaemia was achieved following 75% of insulin injections (summarised in Figure 6.8A). Glucagon and cortisol levels were assessed using radioimmunoassay (Figure 6.8B).

Elevation of both glucagon and corticostreone was seen after single hypoglycaemia when compared to control mice. There was a trend towards elevation in glucagon above control levels in the RH group, however, this did not reach statistical significance. It was notable that the SH group showed very variable glucagon levels, and that higher glucagon levels were observed in mice with lesser severity of hypoglycaemia in the SH group, which is counterintuitive (Figure 6.9C). However, the lines of best fit for the RH and SH groups of mice were not significantly non-zero in either direction. Elevation of corticosterone levels in the RH group was observed, compared to control, with no significant difference from the SH group.

A

C57Bl6 strain, CRHXAi95D
Male (for RIA) Female (for calcium imaging)
6-12 weeks

Day 1

House individually

Fast for 2 hours
(from 8am for am episode, from 1pm for pm episode)

Tail tip for baseline blood glucose
IP insulin 2U/kg (or saline 4µl/g)

Wait 30 minutes

Tail tip for blood glucose
Refeed

If <2mmol, IP 20% glucose 3µl/g

Recover for minimum of 2 hours
(10:45-12:45 for am episode, overnight for pm episode)

Day 2

As day 1

Teminal anaesthesia and collect blood for RIA

Day 3

Terminal anaesthesia and remove brain for in vitro calcium imaging

B

	am	pm	am	pm
RH	Insulin	Insulin	Insulin	Insulin
SH	Saline	Saline	Saline	Insulin
CT	Saline	Saline	Saline	Saline

Figure 6.7 Recurrent hypoglycaemia protocol
A Scheme of work over 3 days
B Table to show i.p injections received by recurrent hypoglycaemia (RH), single hypoglycaemia (SH) and control (CT) mice respectively

A

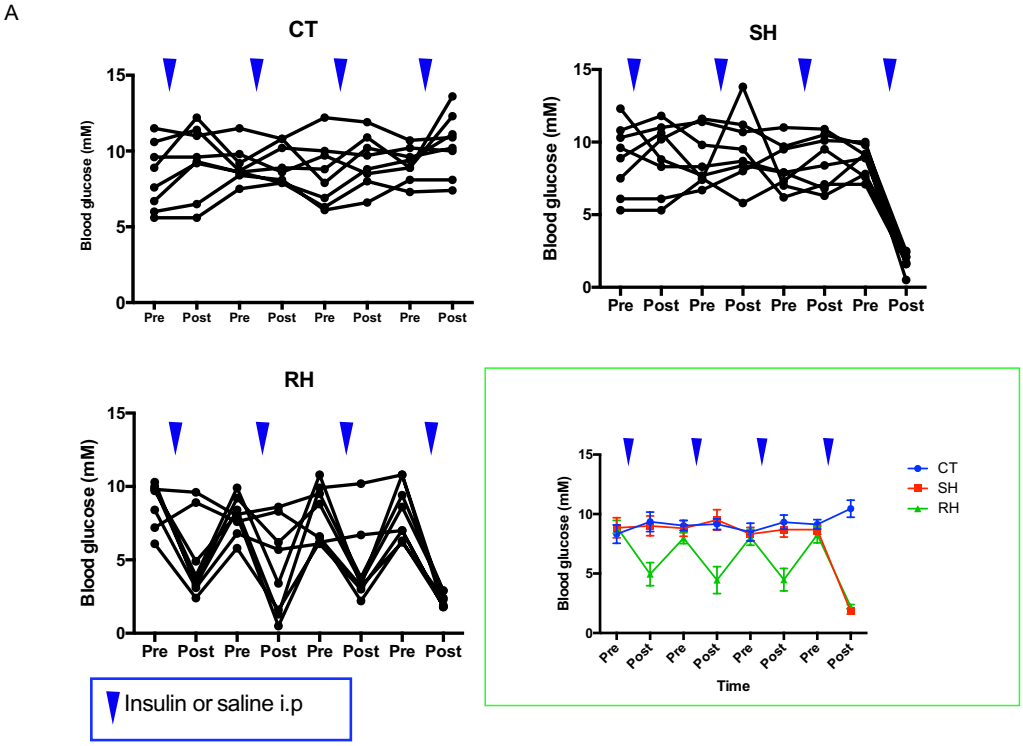
CT
SH
RH
Blood glucose (mM)
15
10
5
0
Pre Post Pre Post Pre Post Pre Post
Insulin or saline i.p
CT
SH
RH
Time

Bi

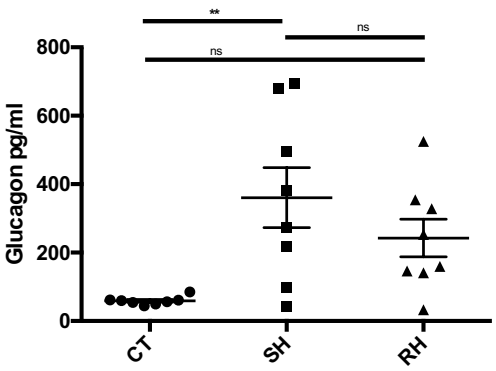
Glucagon pg/ml
800
600
400
200
0
**
ns
ns
CT
SH
RH

Bii

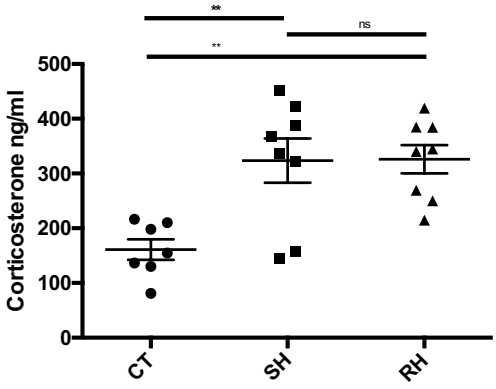
Corticosterone ng/ml
500
400
300
200
100
0
**
**
ns
CT
SH
RH

Figure 6.8 Glucose, glucagon and corticosterone levels after RH protocol
A Glucose levels for cohort of mice subsequently used for glucagon and corticosterone RIAs. Glucose levels for individual mice shown, followed by a summary graph (in green box) showing the mean and SEM for RH, SH and CT groups
Bi) Glucagon levels in CT, SH and RH treated mice n=7-8 per group. p=0.0066, one way ANOVA with Sidak's multiple comparisons test. **CT vs SH. No significant difference between CT and RH or RH and SH groups.
Bii) Corticosterone levels in same groups, n=7-8 per group. p=0.0016, one way ANOVA with Sidak's multiple comparisons test. ** CT vs SH and CT vs RH. No significant difference between SH and RH

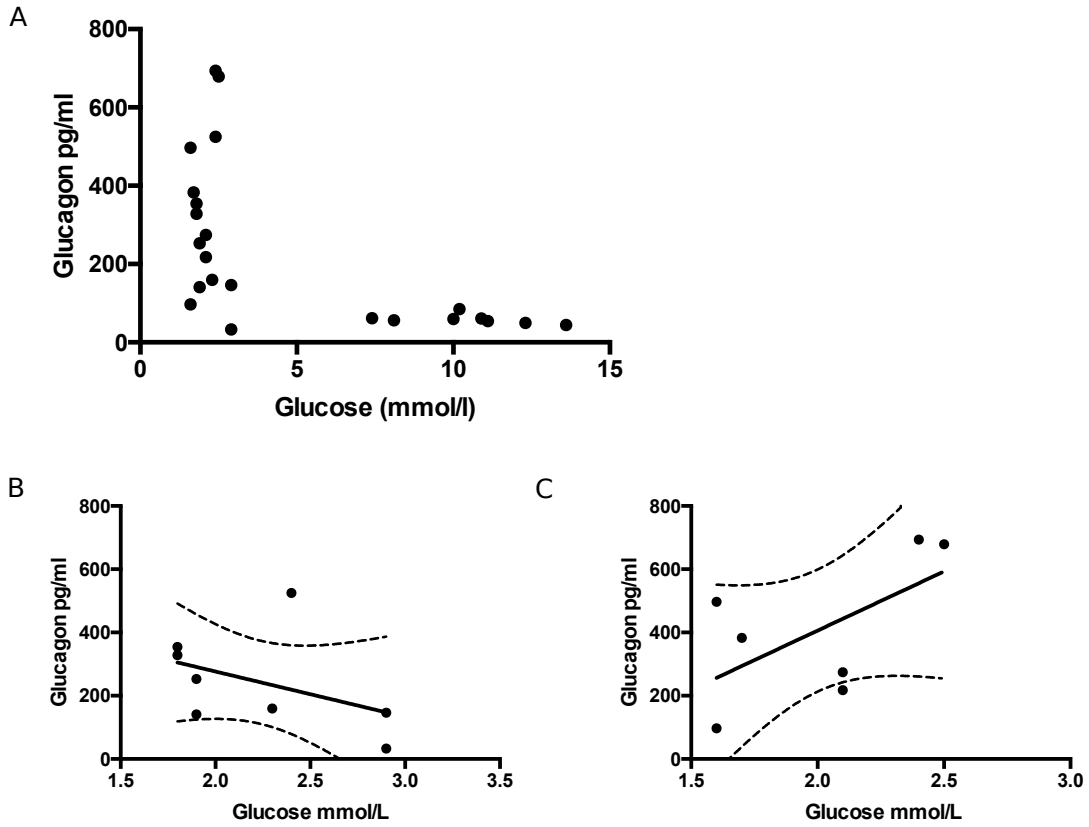

Figure 6.9 Relationship between glucose and glucagon levels following RH protocol.
A Glucose and glucagon levels just prior to perfusion for all animals used in the RH protocol for RIA- SH, RH and CT n=23
B Glucose and glucagon levels in RH group, with line of best fit and 95% confidence intervals. R square= 0.1840, ns
C Glucose and glucagon levels in SH with line of best fit and 95% confidence intervals. R square=0.3732, ns

6.4.4 Effect of recurrent hypoglycaemia on subsequent glucose sensing in CRH PVN neurons

A further 6 CRH x GCamp6f female mice aged 6-9 weeks were subjected to the same recurrent hypoglycaemia protocol, with 3 animals injected with insulin and 3 matched controls receiving saline injections in place of insulin. The insulin injected group of animals achieved very consistent hypoglycaemia over four episodes, and their glucose levels are summarised in table 6.2.

Table 6.2 Glucose levels in mice exposed to recurrent hypoglycaemia (RH) or saline (CT) prior to slicing for calcium imaging

Mouse	Blood glucose 1 (mM)	Blood glucose 2 (mM)	Blood glucose 3 (mM)	Blood glucose 4 (mM)
RH1	2.4	1.5	2.1	1.3
RH2	2.3	1.9	3.5	2.1
RH3	3.6	1.6	2.5	3.3
CT1	7.4	8.5	9.6	7.8
CT2	6.9	5.8	5.8	6.5
CT3	7.7	6.9	6.1	6.3

On the third day, the animals were culled, and acute brain slices cut as detailed in the methods section 2.7.1. Slices were imaged with two repeated steps from 2.5mM glucose to 0.5mM glucose using the same protocol as developed in chapter 4 (section 4.4.6.3). The results were not as predicted. There was in fact a substantial expansion of the number of both GI and GE neurons in the RH group compared to control (for GI 11% RH, 4.5% CT, and for GE, 6.8% RH, 3.7% CT, Chi square 17.08, p=0.0007), as shown in Figure 6.10A. It was also notable that the numbers of responsive cells in the CT group were smaller than observed in comparable experiments without antecedent i.p injections (4.5% of cells GI, 3.7% of cells GE in the CT group here, 9.5% GI and 9.9% GE in the 2.5mM glucose baseline group). There was no difference in the size of the GI or GE responses between the 2 groups on the first application of glucose (Figure 6.10B, Mann-Whitney test, ns).

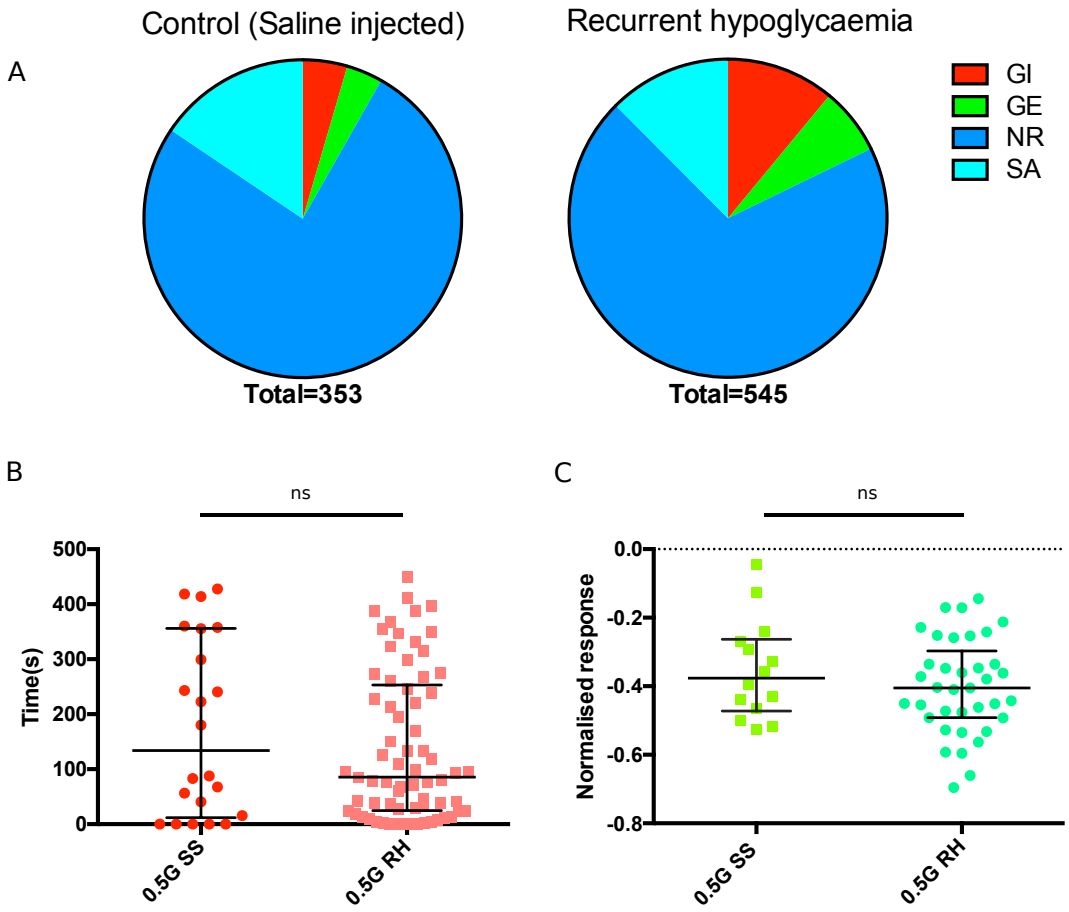

Figure 6.10 Effect of recurrent hypoglycaemia on glucose sensing as observed using calcium imaging

A There is a significant increase in the numbers of GI and GE cells identified in the RH group compared to control (Chi square 17.08, p=0.0007)

B There is no significant difference in the size of the GI response between the 2 groups (Mann Whitney test)

C There is no significant difference in the size of the GE response between the 2 groups (Mann Whitney test)

Data obtained from 3 mice in each group. RH 6 slices, 90.8 ± 23.4cells/slice, Control 5 slices, 70.8±16.6cells/slice. Data shown as median and IQR

6.5 Discussion

6.5.1 A mouse model of insulin induced hypoglycaemia

Single hypoglycaemic episodes were successfully induced in mice, using i.p insulin injections at 2.5units/kg. This is a relatively simple model, and has been used extensively in the published literature to assess insulin tolerance (Dearden and Balthasar, 2014, Ayala et al., 2010). The SH cohorts reliably responded to a single i.p insulin injection by lowering their glucose to <4mmol/L after 30 minutes, and remaining stable without significant sequelae over the next 2 hours prior to perfusion. This appears to be a good model for a single hypoglycaemic episode.

6.5.2 A mouse model of recurrent hypoglycaemia

Developing a recurrent hypoglycaemia protocol proved more challenging. In particular, occasionally a mouse fails to become hypoglycaemic following an insulin injection, possibly due to injection into bowel or bladder, rather than intraperitoneal. The failure of mice to become hypoglycaemic can be seen in the data for the RH group of mice used to assess glucagon and corticosterone levels, where several mice experienced 3 or even just 2 out of an intended 4 hypoglycaemic episodes. In addition, the RH mice need monitoring to identify any which become excessively hypoglycaemic. Injection of i.p glucose (20%) in mice with blood glucose measured as <2mM was used to ensure full recovery from the episode, allowing continuation of the RH protocol. This was required in 17.5% of hypoglycaemic episodes. It was however difficult to manage 2 episodes of hypoglycaemia per day for large numbers of animals. Where animals are to be used for in vitro work following the protocol, and only 2-3 are required at any one time, this is straightforward. However, for samples for RIA (or IHC), where 4-6 animals in each group are needed, a limit of 6 animals for each iteration of the protocol was employed, with repeats over subsequent days/weeks. This introduced the potential for increased variation between batches of animals.

It is possible that this model could be improved by extending the intervals between hypoglycaemic episodes to once every 24 hours. This has been described previously in one mouse model of recurrent hypoglycaemia (Poplawski et al., 2011). The initial protocol used here was based on a rat protocol (Al-Noori et al., 2008). A number of

other rat models successfully use once daily insulin injections to induce HAAF (Herzog et al., 2008, Orban et al., 2014). This could also make it more practical to give animals a slightly higher dose of 2.5units/kg insulin and still allow them sufficient recovery time. This could be explored in future work. Part of the appeal of a 2 day protocol was the option to readily extend the protocol on day 3 for example to in vitro electrophysiology or calcium imaging, but this is only of value if the model is successful in reliably inducing recurrent episodes of hypoglycaemia. It is also possible that more reliable and repeatable hypoglycaemic episodes could be achieved using chronic cannulation and a hyperinsulinaemic clamp, which would result in more controlled hypoglycaemia and remove variability due to the site of injection of insulin compared to i.p injection. This has been reported by one group in mice (Jacobson et al., 2006a, Jacobson et al., 2006b) and requires a significant investment in technical expertise, as well as a possible increase in the stress experienced by the animals.

6.5.3 Difficulties with finding evidence for hypoglycaemia induced autonomic failure in a RH model in mice

HAAF has been demonstrated in both humans and rodents, as evidenced by failure to elevate counterregulatory hormones including glucagon, cortisol/corticosterone, epinephrine, norepinephrine and growth hormone (Senthilkumaran et al., 2016). This is discussed in some detail in the introduction to this chapter, section 6.1.1. It is important to note that not all models of HAAF recapitulate the full profile of counterregulatory hormone failure. For example, i.v insulin administration by Figlewicz et al. (2002) did not result in significant attenuation of epinephrine rises following recurrent hypoglycaemia in their rat model. A similar effect was seen in the paper by Paranjape et al. (2005) using s.c insulin in rats.

The model used here showed a clear increase in both corticosterone and glucagon following a single episode of hypoglycaemia. There was no significant difference between control and RH glucagon levels, suggestive of a trend towards return of glucagon levels to baseline, but equally there was no significance difference between RH and SH levels, so the evidence for a failure of glucagon counterregulation is equivocal. There was no evidence of any form of HAAF as evidenced by corticosterone levels following recurrent hypoglycaemia, with corticosterone levels in SH and RH mice both

being significantly increased from baseline and no significant difference between the SH and RH groups.

There are several reasons why this may have occurred. Firstly, there are limits to the number of samples which can be taken for analysis of hormonal levels. In the model presented here, essentially a large volume of blood can only be taken at an end point in order to gain a large enough sample from the mouse without causing undue stress. Even in a cannulated mouse, where samples could be taken without restraint, the circulating blood volume would still limit the number of samples possible. Around 120µL of plasma is needed for each time point to perform a glucagon and corticosterone RIA. In terms of whole blood, this is likely to be around 200µL at each time point, or 10% of the total circulating blood volume. 2-3 samples of this size would almost certainly induce stress related to blood loss. In the rat and human models, sequential samples are routinely taken, and this makes it much more likely that a sample is taken at the optimal time point to see a difference in response for a given hormone. Indeed, frequently only one or 2 time points are observed to be significantly different in rodent models of hypoglycaemia (Evans et al., 2001, Jacobson et al., 2006a). It is therefore possible that if samples could be taken from a mouse at a different time point, or levels could be measured at several time points, an effect might be seen that is not apparent here.

In addition, there is the issue of the stress response of the mouse. It is widely recognised that mice do not acclimatise well to stressful stimuli even with extensive habituation. Previous baseline levels of corticosterone in the mouse have been reported as 16.1±1.8 µg/dL (Jacobson et al., 2006a), which aligns closely with the levels found in this study (16.9±1.8µg/dL in control animals). It is still entirely possible that the high corticosterone levels measured here could be partially a result of the stressful effects of repeated handling, changes to clean cages, fasting, and movement from their home room to an experimental room, masking any amelioration of the corticosterone response to recurrent hypoglycaemia compared to single hypoglycaemia.

However, this does not explain the findings for glucagon, as glucagon is not produced in response to stress. The recurrent hypoglycaemia group were not significantly different

when compared to controls. However, the levels measured were also not significantly different from those seen in the single hypoglycaemia group. In this case, the most striking thing was the variability in glucagon levels for the single hypoglycaemia group. Although the mean single hypoglycaemia glucagon response was high, the variation was very wide, and the highest glucagon levels were observed in the animal with the highest glucose levels in this group, where it might be expected that a lower glucose would result in higher glucagon levels. It is not clear why this was the case. There was not a clear correlation between glucose levels and glucagon levels in the mice used for this experiment, in either the RH or SH groups (Figure 6.9). One interesting paper examined glucagon levels in response to different degrees of hypoglycaemia in the mouse (Malmgren and Ahren, 2015). They compared the glucagon responses to a graded hyperinsulinaemic hypoglycaemic clamp with those observed following a simple i.p insulin tolerance test. There was good correlation between glucose levels and glucagon in the graded clamp, but very poor correlation for the ITT. This fits with the data presented here.

Overall, the RH model appears to require further optimisation. It is possible that the RIA results presented here are simply underpowered. This seems more likely in the case of glucagon, where there was a trend to a return of glucagon levels to baseline in the recurrent hypoglycaemia group. It is also possible that the corticosterone result is unclear due to significant noise from the stress of the protocol as a whole. A chronic cannulation approach to allow greater control of blood glucose would be helpful in establishing a more reliable model. In the small body of literature available for mouse models of RH, chronic cannulation and intravenous infusion of insulin was able to demonstrate reliable blunting of the glucagon and corticosterone response to hypoglycaemia in RH mice, although this was still not always the case for the epinephrine response (Jacobson et al., 2006b, Jacobson et al., 2006a).

Finally, it is reasonable to briefly question whether the mouse model of RH will look exactly like the rat or human model. Senthilkumaran and colleagues suggest that there has yet to be a valid model of HAAF in the mouse, as no group has been able to show a consistent return towards baseline of epinephrine levels in the recurrent hypoglycaemia group (Senthilkumaran et al., 2016). Some of the issues with obtaining valid epinephrine

levels in a mouse under any scenario were discussed briefly in the introduction to this chapter. We did not attempt to obtain epinephrine levels in this model, as there was no realistic prospect of obtaining stress free samples. Indeed, in some cases the epinephrine and norepinephrine levels reported in rat models of HAAF are inconsistent (Evans et al., 2001, Orban et al., 2014) or there is a failure to show blunting of the glucagon and corticosterone responses, although there is a fall in epinephrine (Tkacs et al., 2005). It is possible that a sufficiently useful mouse model of HAAF could be developed that shows consistent reduced levels of glucagon and corticosterone in recurrent hypoglycaemia compared to single hypoglycaemia, without necessarily causing blunting of epinephrine/norepinephrine levels.

6.5.4 cfos is increased in CRH neurons in IIH compared to control animals

cfos expression was increased in 84% of CRH neurons following insulin induced hypoglycaemia, compared to 30% of CRH neurons in the control group, a substantial increase. This effect has not been previously been demonstrated in CRH PVN neurons. The effect is not merely due to the stress of injection and handling, as the saline controls were treated exactly as the insulin receiving animals, and a significant difference between the groups is seen. The increase in cfos expression in the PVN has been previously been reported in rats for non-specific neurons after insulin induced hypoglycaemia (Niimi et al., 1995). In addition, this marker of neuronal activation is lost after recurrent episodes of hypoglycaemia (Evans et al., 2001).

It is not possible to make statements of certainty based on this experiment, with regard to what is causing the neuronal activation; the insulin directly, the hypoglycaemia directly, or indirect activation related to the overall response of the animal. In order to unpick the mechanism further, insulin injection as part of a normoglycaemic clamp could be used to test for a direct effect of insulin. Alternatively, 2,4 deoxyglucose injected intracerebroventricularly could be used to induce CNS hypoglycaemia, which would be of interest as the whole animal does not experience hypoglycaemia, and there is no use of insulin. However, this would still not answer the question as to whether the hypoglycaemia is directly activating the PVN, or whether activation is occurring via a set of pathways in the brain as a whole. For this, in vitro investigations could prove more valuable.

Interestingly, cfos activation was not observed in the most posterior PVN slices. This was surprising as it was predicted that these autonomic projecting areas might show strong activation. It is possible that activation occurred at sub threshold levels that were not detected here, or indeed that these neurons, similarly to VMN neurons (Niimi et al., 1995), are involved in responses to hypoglycaemia, but do not elevate cfos levels.

As a control experiment, oxytocin and cfos double immunohistochemistry was performed looking for evidence of cfos expression in oxytocin neurons in single hypoglycaemia mice as compared to control. There was no evidence of increased cfos in oxytocin neurons after single hypoglycaemia. Interestingly, one study had previously reported increases in cfos in oxytocin neurons in a rat model of insulin induced hypoglycaemia (Griffond et al 1994). However, the effect was only seen in around 18% of oxytocin neurons, and no other neuronal subtypes were examined. The data presented here fits more consistently with that reported by Niimi et al. (1995), who show an increase in cfos following insulin induced hypoglycaemia in the parvocellular part of the PVN, with much less cfos in the magnocellular areas.

The logical extension to this work would be to seek evidence of a reduction in cfos expression in RH mice as compared to SH. However, it would be preferable to examine this in an optimised model of HAAF in mice. The large number of animals that would be required to have sufficient power for an effect to be seen would be difficult to put through the current protocol in a consistent fashion. In addition, the stress of the recurrent hypoglycaemia procedure would be a confounding factor which could affect the cfos levels seen. A chronic cannulation model of recurrent hypoglycaemia in mice, as described by Jacobson and colleagues (Jacobson et al., 2006a), would be less stressful and more reliable in inducing hypoglycaemia. It is also possible that fewer episodes of hypoglycaemia could be sufficient. Just one prior hypoglycaemic episode was sufficient to induce a degree of HAAF in some studies in humans, rats and mice (Jacobson et al., 2006a, Heller and Cryer, 1991, Kang et al., 2008).

6.5.5 Effects of recurrent hypoglycaemia on the glucose sensing CRH PVN neurons

Slices from mice exposed to recurrent insulin induced hypoglycaemia as compared to saline injected controls showed an expansion of the numbers of GI and GE cells observed. This was counter to the hypothesis. The expectation was that RH would cause glucose sensing neurons to shift their threshold for glucose sensing, such that a lower level of glucose was required to elicit the same response. A left shift in threshold of activation would result in a contraction of the numbers of glucose sensing neurons observed when exposed to the same low glucose step. This has previously been reported for VMN glucose inhibited neurons (Song and Routh, 2006, Kang et al., 2008). The expansion reported here might suggest that these neurons are in fact being sensitised to low glucose by the previous exposure to hypoglycaemia, which has not previously been reported for a glucose sensing population after recurrent hypoglycaemia.

At this point, the potential outflow of glucose sensing CRH PVN neurons should be considered. The implied result of this finding would be that neurons would increase their release of CRH (and/or additional neurotransmitters) after hypoglycaemia in the context of recurrent hypoglycaemic episodes, compared to the response to a single hypoglycaemic episode. CRH mRNA levels were found to be raised after recurrent hypoglycaemia in previous work by Nina Balthasar (unpublished data). CRH is anorexigenic and raised levels of CRH have previously been implicated in the development of HAAF (Flanagan et al., 2003). The mechanism underlying this is unclear. CRH is known to cause hyperglycaemia via a brainstem effect, not dependent on either the pituitary or the adrenal medulla (adrenalectomy or hypophysectomy has no effect) (Brown et al., 1982). A further paper infused CRH chronically intracerebroventricularly, and showed that the effect of CRH waned over time, suggesting that chronic release of CRH causes desensitisation of the responsive neurons (Cunningham et al., 1988). The expansion of the glucose sensitive population, in particular the glucose inhibited population after RH, could therefore represent a mechanism by which RH could result in increased CRH release, and attenuated autonomic responses, contributing to HAAF. This mechanism could operate either via the pre-autonomic or neurosecretory outflow, but

previous work suggests that the pre-autonomic pathway is more likely (Brown et al., 1982, Flanagan et al., 2003).

With regard to the pre-autonomic CRH PVN population, it is not known what other neurotransmitter(s) these cells release. There is some evidence for a glutamatergic CRH PVN population (Zhao et al., 2017, Dabrowska et al., 2013). This would mean that RH results in increased release of glutamate as well as CRH in the brainstem, from synapses, which could activate the autonomic areas. This would not fit so well with a mechanism for inducing HAAF, unless inhibitory interneurons were involved. Other neurotransmitters have been described as co-released with CRH from the PVN, especially in the context of chronic stress, for example oxytocin and vasopressin (Dabrowska et al., 2013).

6.5.6 Summary

Overall, this chapter discusses the models used for HAAF, and presents a model of insulin induced hypoglycaemia in mice, which has been valuable to show evidence of PVH CRH neuronal activation after a single episode of hypoglycaemia. The challenges in extending this model to induce recurrent hypoglycaemia and in particular HAAF in the mouse are described. Finally, the effect of recurrent hypoglycaemia on subsequent responses to low glucose in acute slices in vitro is presented, followed by an outline of potential mechanisms for how this could contribute to the development of HAAF.

Chapter 7 General Discussion

7.1 Summary of findings and their relevance

This thesis used the CRH-ires-Cre mouse in combination with floxed reporter mice (TdTomato and GCaMP6f) and viral vectors including floxed mCherry to investigate the neuroanatomy and glucose responsiveness of CRH PVN neurons. A summary of the key findings with reference to the original hypotheses is presented below.

7.1.1 CRH PVN neurons make direct connections to autonomic areas of the brainstem

Evidence was presented in chapter 3 that this is indeed the case. A wide range of targets for CRH PVN neuronal projections were identified, with particular regions of interest including the NTS, DMX and ventrolateral medulla as well as the lateral PBN, the VTA, the PAG and sympathetic preganglionic neurons of the thoracic spinal cord. Catecholaminergic, serotoninergic and cholinergic neuronal targets were all identified. This represents an important and, in most cases, novel set of targets that may be engaged by the CRH PVN neurons in in response to a wide range of stressful stimuli including hypoglycaemia. The known reciprocal connections from many of these areas onto the PVN are also interesting, as this creates a direct feedback loop between the CRH neurons of the PVN and autonomic outflow areas of the brainstem.

7.1.2 CRH PVN neurons are glucose sensing

Chapters 4 and 5 present the first evidence of a novel subset of CRH PVN neurons that are directly glucose inhibited, with a mechanism which involves glucose metabolism. This is the first evidence that these neurons can sense the glycaemic state of the local milieu, in addition to receiving inputs from a wide range of other areas sensing glucose both locally (VMN, DMN, ARC, LH, PO) and from more distant sites (NTS, PBN via VMN, peripheral glucose sensors via the brainstem). The wide variety of areas which respond to a fall in glucose means that there are multiple levels of redundancy in the system- if any one glucose sensor fails, the event will still be detected. The presence of directly glucose sensitive neurons in the CRH PVN group, at the top of the HPA axis, further increases the biological security of the response to hypoglycaemia. In addition, the

ability to directly sense glucose could enable CRH PVN neurons to alter their intrinsic excitability in the context of the local fuel status in the PVN, and thus modulate the likelihood that activation and release of neurotransmitters from CRH PVN neurons to cause downstream effects will occur, following integration of the multitude of signals being received from elsewhere in the CNS and peripherally.

7.1.3 CRH PVN neurons are activated by hypoglycaemia

Cfos expression following insulin induced hypoglycaemia suggested that a much larger group of CRH PVN neurons (~84%) were activated in this whole animal model of hypoglycaemia. This matches with previous reports examining cfos in the PVN in rat models of hypoglycaemia. However, when compared to the numbers of CRH PVN neurons activated by low glucose in vitro (~10%) the population activated as evidenced by cfos expression is much larger. The two models are not truly comparable, however. In vivo hypoglycaemia induced by insulin was prolonged (75% of animals remained hypoglycaemic when perfused after 2.5hours) compared to transient hypoglycaemia in vitro (low glucose applied for ~400s at a time). There is a much greater degree of connectivity in vivo, and peripheral sensing mechanisms will also feed into the CNS. In addition, the in vivo model would be expected to activate a wide range of stress responses, both signalling via hormones and via neuronal activation of additional stress responsive regions. This would be expected to cause a much broader activation of CRH neurons of the PVN over time. The direct effect of insulin in vivo may also have had an impact.

7.1.4 CRH PVN neurons exhibit altered responses to glucose following exposure to recurrent hypoglycaemia

An expansion of the glucose inhibited PVN CRH population was observed following exposure of mice to recurrent episodes of hypoglycaemia, compared to control saline injected mice. Based on previous reports in the literature, it was expected that the opposite would be observed. This finding therefore rejects the initial hypothesis. However, given the potential for CRH in itself to cause some elements of HAAF, the finding becomes more explicable as discussed in chapter 6, section 6.5.5, leading to the generation of a new set of hypotheses. Overall, the expansion of the CRH PVN GI

population after RH could represent a novel mechanism whereby the sympatho-adrenal system is downregulated by CRH following recurrent hypoglycaemia, contributing to HAAF. A figure summarising the overall effect of the CRH PVN neurons is presented below (Figure 7.1).

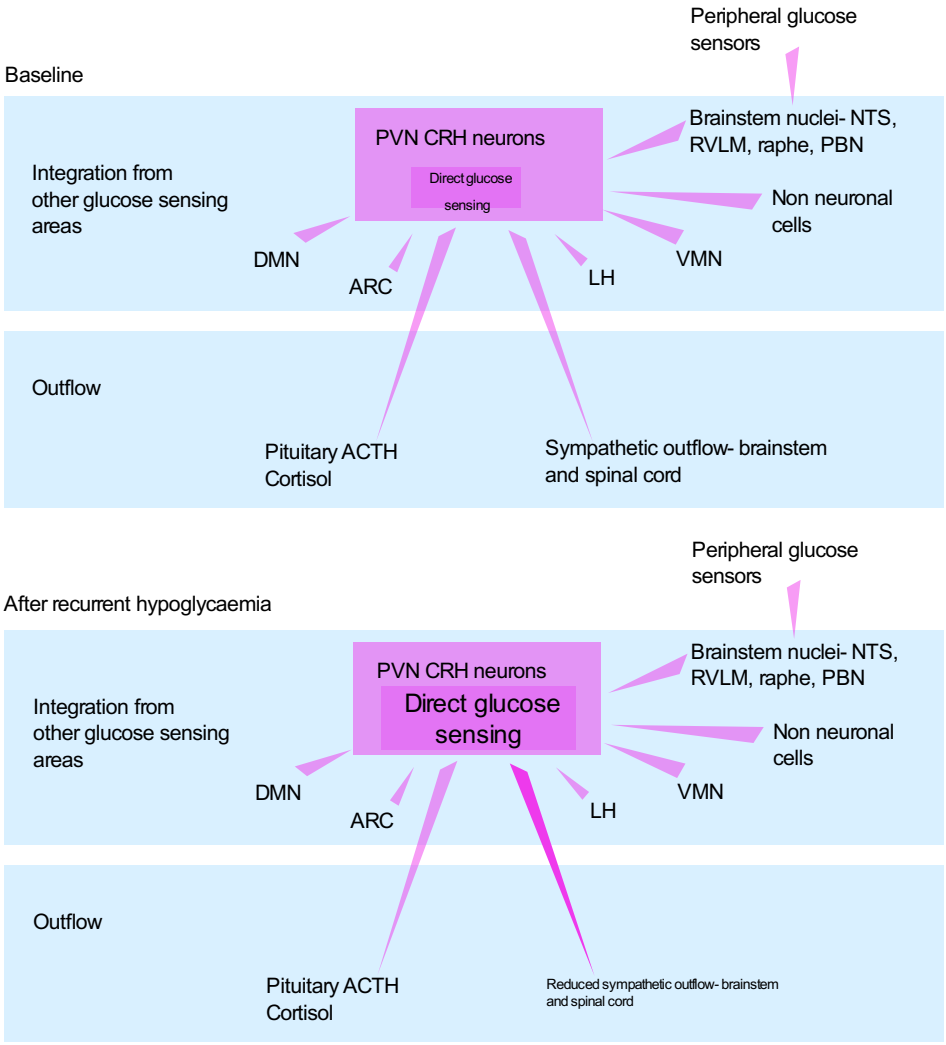

Figure 7.1 Proposed role of CRH PVN neurons in glucose sensing and counterregulatory response to hypoglycaemia

CRH PVN neurons, a subset of which directly sense glucose (indicated by inset dark pink box), are able to integrate information from a wide range of glucose sensing cells of central and peripheral origin, and respond with alterations of outflow both via the pituitary-adrenal axis and via modulation of sympathetic brainstem and spinal cord. Recurrent hypoglycaemia expands the number of glucose inhibited neurons, which are activated by hypoglycaemia.

7.2 Potential future work

7.2.1 Improvement to the RH model to generate robust activation of HAAF

As discussed in chapter 6, the RH model described in this thesis was effective in inducing recurrent episodes of hypoglycaemia in mice, with limited evidence of development of HAAF. Further optimisation of this model would be of great value in allowing investigation of the role of CRH PVN neurons in HAAF. Simple alterations could include lengthening the time course of the hypoglycaemic events to target one hypoglycaemic episode per day for 4 days. This could also potentially allow administration of an increased dose of insulin, which would induce hypoglycaemia more reliably. Use of chronic cannulation could also be explored to examine whether this resulted in more reliable hypoglycaemic episodes, and to reduce stress when sampling from animals. Finally, blood donation could be considered to allow increased sampling from test animals over time.

7.2.2 Anatomy of CRH PVN neuronal projections to the brainstem

A number of potential avenues to explore present themselves following on from the neuronal tracing work described here. Firstly, it would be of interest to confirm the neurotransmitter expression of the projections. It has been reported that glutamate is the main fast neurotransmitter released from CRH PVN neurons, and that GABA transmission is not seen in pre-autonomic PVN neurons. This could be explored further using VGAT and VGLUT antibodies in combination with anterograde tracing to examine expression of these transmitter specific transporter proteins at CRH PVN synapses in the brainstem. A second experiment would be to examine whether the neurosecretory CRH PVN populations and the pre-autonomic CRH PVN populations are overlapping, or segregated. One way to examine this would be to combine i.v fluorogold to label neurosecretory neurons (Markakis and Swanson, 1997, Biag et al., 2012) , and a retrograde tracing virus injected into known projection targets in the brainstem (for example NTS) and examine for overlap in cell bodies in the PVN.

Finally, the logical next steps would be to further characterise the CRH PVH pre-autonomic population functionally to assess their importance and role in responses to hypoglycaemia. This could involve in vitro work examining the responses of pre-labelled

pre autonomic CRH neurons to low glucose, in vivo imaging, and indeed functional manipulation of the labelled population using opto or pharmacogenetic approaches to examine the effect of activation or silencing of this neuronal population on whole animal physiology, and in particular the counterregulatory response to hypoglycaemia.

7.2.3 In vitro investigation of CRH PVN neurons

The calcium imaging technique using GCaMP6f opens a broad range of possible future experiments. Clearly, further investigation of the mechanisms of glucose sensing in the CRH neurons would be of interest, in particular to examine whether AMPK, cGMP and CFTRs are implicated in GI neurons. Identifying the synaptic inputs driving GE responses would also be interesting, and potentially could be carried out by altering the plane of slicing or dissecting out parts of the hypothalamus with potential inputs and examining the effect on glucose sensing. In addition, as mentioned in section 7.2.2, retrograde labelling of pre-autonomic CRH neurons with GCaMP6 could enable calcium imaging in this population to seek evidence of glucose sensing.

A potentially further very interesting experiment would be to simultaneously record in cell attached mode from CRH neurons whilst imaging their calcium levels. This would be of help to develop knowledge of how a rapidly firing cell behaves with regard to its calcium levels, in particular when neuronal activity is reduced.

A voltage clamp approach could provide valuable clues to the conductances that are being activated or inhibited in response to a low glucose step in vitro, which would aid further mechanistic investigation. The electrophysiological phenotypes of CRH PVN cells could also be investigated further. In particular, a closer examination using patch clamping to investigate whether pre-autonomic neurons in mice exhibit similar properties to those reported in rats would be of interest. LTS and rebound spiking after hyperpolarising pulses could be examined, to compare to the results reported for rats. In addition, the cells which maintain wide based spiking in the presence of TTX could be investigated further.

7.2.4 In vivo investigation of CRH PVN neurons

A range of potential in vivo investigations could follow on from the experiments presented here. It would be fascinating to implant a Graded index (GRIN) lens and image CRH neurons of the PVN responding to a hypoglycaemic event in vivo, either in an anaesthetised or an awake mouse. This could help to improve understanding of the discrepancy between the numbers of neurons observed to be activated after in vitro low glucose (~10%) and the activation after IIH (~84%). Additionally, the effect of intracerebroventricular 2-DG could be examined as an alternative method of introducing local hypoglycaemia without involvement of insulin.

A follow up experiment to the description of PVN inactivation using lignocaine causing defective counter-regulation (Evans et al., 2003) would be to target CRH neurons specifically in the PVN with an inhibitory DREADD via a viral vector. The effect of pharmacogenetically silencing this population on counter-regulation could then be examined.

A much more complex experiment would be to identify and functionally modify the responses of the specific GI subset of CRH PVN neurons. A combination of a viral injection of a FRT/Cre dependent DREADD (Sciolino et al., 2016) to the PVN of a genetically modified mouse with FLP under the control of the CRH promoter (available from JAX, strain no 031559 Crh-ires-FlpO) and Cre recombinase expressed in a activity dependent TRAP (Kawashima et al., 2013), combined with an episode of hypoglycaemia could be effective in isolating these neurons in a fashion that would allow their subsequent pharmacological reactivation. See figure 7.2 for a detailed summary of this proposed experiment.

7.3 Is HAAF still a relevant clinical problem in need of a solution?

Given the recent advances in diabetic care, in particular technological developments such as closed loop glucose monitoring and insulin pump technologies, it is reasonable to question the relevance of HAAF for diabetic patients now and in the future. Whilst insulin pump technology is becoming more widely used in high income countries (generally with manual glucose measurement and adjustment by the patient), it is still

by no means the default mode of insulin delivery. Closed loop systems, which automatically adjust insulin infusion in response to glucose measurements, have been extensively trialled in research settings (Hovorka et al., 2011, Kumareswaran et al., 2014, Thabit et al., 2014), but are only now becoming suitable for use in the home (Elleri et al., 2011, Hovorka, 2011, Hovorka et al., 2011). Commercially available systems are now entering the market. The first device to be licensed by the FDA, the MiniMed 670G (Medtronic, USA) was approved in 2016. This device has been reported to perform well over short periods (up to 3 months (Garg et al., 2017)) and is currently being trialled for home use over 6 months in a multicentre Australian study (de Bock et al., 2018, McAuley et al., 2018). These devices are clearly life changing, in particular in increasing the time spent in the target blood glucose range and avoiding hypoglycaemia, whilst reducing the time spent by patients managing their condition. However, patients still need to be highly motivated, and in particular to be made aware of how to manage the systems in cases where their insulin requirements will change, for example during illness, exercise and pregnancy. Not all diabetic patients would be suitable candidates for such devices in the near future.

The other factor that needs to be taken into account is the epidemiology of diabetes worldwide. The diabetes epidemic shows some early signs of plateauing in the USA (Gregg, 2017). However, diabetes continues to increase in prevalence, especially in low and middle income countries (Mathers and Loncar, 2006, Patterson et al., 2009). Patients are also living longer with diabetes, which makes it more likely that they will need insulin to manage their condition, and be at greater risk of developing HAAF. Many of these patients lack access to advanced technologies, even given sufficient motivation. Better understanding of the underlying mechanisms of HAAF, with the ultimate aim of developing simple pharmacological methods to prevent it, remains a potentially valuable research goal.

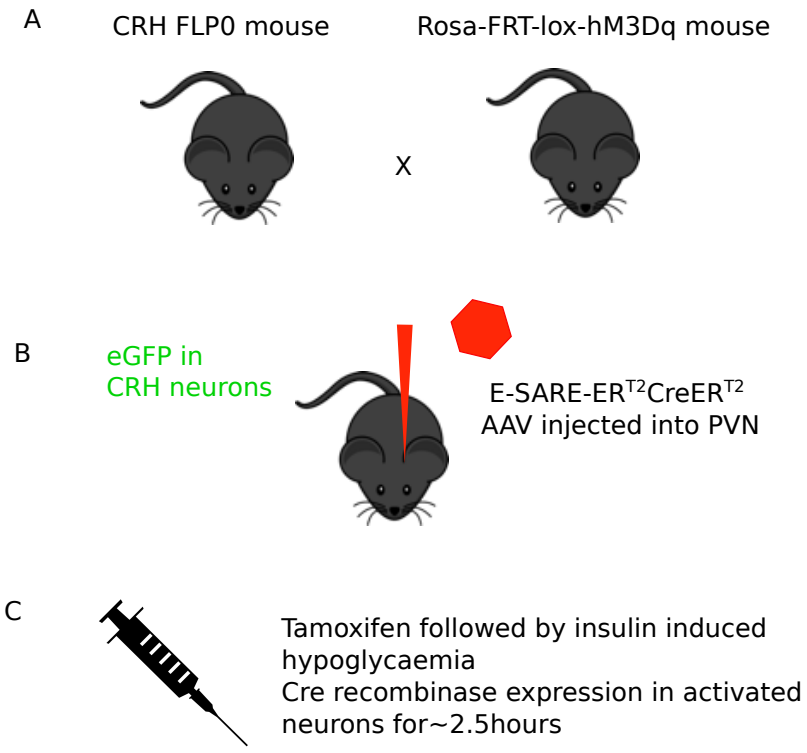

Figure 7.2 Potential future experiment to identify CRH PVN neurons which are activated by hypoglycaemia in vivo, and to target them functionally to investigate their effects on counterregulation.

A 2 transgenic mouse lines are required, i) CRH FLP0 (Jax stock no 031559, no publication, developed by B Sabatini, Harvard Medical School) which expresses FLP recombinase enzyme in CRH neurons and ii) Rosa-FRT-Lox-hM3Dq (Sciolino et al., 2016). The offspring of this cross will express eGFP in CRH neurons, but hM3Dq will remain inverted and will not be expressed

B Third transgene introduced to PVN alone as a viral (AAV) injection of E-SARE-ER^{T2}CreER^{T2} (Matsuda and Cepko, 2007, Kawashima et al., 2013)

C Tamoxifen administered, followed by insulin induced hypoglycaemia. Cre recombinase will be expressed in neurons activated during the ~2.5 hour time course following tamoxifen.

hM3Dq-mcherry will be expressed in neurons which were activated in the PVN AND express CRH. Can be identified (red fluorescence) and functionally activated using CNO.

Chapter 8 List of references

ABBOTT, N. J., PATABENDIGE, A. A., DOLMAN, D. E., YUSOF, S. R. & BEGLEY, D. J. 2010. Structure and function of the blood-brain barrier. *Neurobiol Dis,* 37**,** 13-25.

ADACHI, A., SHIMIZU, N., OOMURA, Y. & KOBASHI, M. 1984. Convergence of hepatoportal glucose-sensitive afferent signals to glucose-sensitive units within the nucleus of the solitary tract. *Neurosci Lett,* 46**,** 215-8.

AGUILERA, G. & LIU, Y. 2012. The molecular physiology of CRH neurons. *Frontiers in neuroendocrinology,* 33**,** 67-84.

AINSCOW, E. K., MIRSHAMSI, S., TANG, T., ASHFORD, M. L. & RUTTER, G. A. 2002. Dynamic imaging of free cytosolic ATP concentration during fuel sensing by rat hypothalamic neurones: evidence for ATP-independent control of ATP-sensitive K(+) channels. *J Physiol,* 544**,** 429-45.

AL-NOORI, S., SANDERS, N. M., TABORSKY, G. J., JR., WILKINSON, C. W., ZAVOSH, A., WEST, C., SANDERS, C. M. & FIGLEWICZ, D. P. 2008. Recurrent hypoglycemia alters hypothalamic expression of the regulatory proteins FosB and synaptophysin. *American journal of physiology. Regulatory, integrative and comparative physiology,* 295**,** R1446-54.

ALBANESE, C., HULIT, J., SAKAMAKI, T. & PESTELL, R. G. 2002. Recent advances in inducible expression in transgenic mice. *Semin Cell Dev Biol,* 13**,** 129-41.

ALBERINI, C. M. 2009. Transcription factors in long-term memory and synaptic plasticity. *Physiol Rev,* 89**,** 121-45.

ALLEN, K. V. & FRIER, B. M. 2003. Nocturnal hypoglycemia: clinical manifestations and therapeutic strategies toward prevention. *Endocr Pract,* 9**,** 530-43.

ALON, T., ZHOU, L., PEREZ, C. A., GARFIELD, A. S., FRIEDMAN, J. M. & HEISLER, L. K. 2009. Transgenic mice expressing green fluorescent protein under the control of the corticotropin-releasing hormone promoter. *Endocrinology,* 150**,** 5626-32.

ALVAREZ-GUISASOLA, F., YIN, D. D., NOCEA, G., QIU, Y. & MAVROS, P. 2010. Association of hypoglycemic symptoms with patients' rating of their health-related quality of life state: a cross sectional study. *Health Qual Life Outcomes,* 8**,** 86.

AMIEL, S. A., SHERWIN, R. S., SIMONSON, D. C. & TAMBORLANE, W. V. 1988. Effect of intensive insulin therapy on glycemic thresholds for counterregulatory hormone release. *Diabetes,* 37**,** 901-7.

ANAND, B. K., CHHINA, G. S., SHARMA, K. N., DUA, S. & SINGH, B. 1964. Activity of Single Neurons in the Hypothalamic Feeding Centers: Effect of Glucose. *The American journal of physiology,* 207**,** 1146-54.

AO, Y., WU, S., GO, V. L., TOY, N. & YANG, H. 2005. Maintaining euglycemia prevents insulin-induced Fos expression in brain autonomic regulatory circuits. *Pancreas,* 31**,** 142-7.

ARAQUE, A., CARMIGNOTO, G. & HAYDON, P. G. 2001. Dynamic signaling between astrocytes and neurons. *Annu Rev Physiol,* 63**,** 795-813.

ASHCROFT, F. & RORSMAN, P. 2004. Type 2 diabetes mellitus: not quite exciting enough? *Hum Mol Genet,* 13 Spec No 1**,** R21-31.

ASHFORD, M. L., BODEN, P. R. & TREHERNE, J. M. 1990a. Glucose-induced excitation of hypothalamic neurones is mediated by ATP-sensitive K+ channels. *Pflugers Arch,* 415**,** 479-83.

ASHFORD, M. L., BODEN, P. R. & TREHERNE, J. M. 1990b. Tolbutamide excites rat glucoreceptive ventromedial hypothalamic neurones by indirect inhibition of ATP-K+ channels. *Br J Pharmacol,* 101**,** 531-40.

ASVOLD, B. O., SAND, T., HESTAD, K. & BJORGAAS, M. R. 2010. Cognitive function in type 1 diabetic adults with early exposure to severe hypoglycemia: a 16-year follow-up study. *Diabetes Care,* 33**,** 1945-7.

ATLAS, A. M. B. C. 2011. Available: http://connectivity.brain-map.org/projection [Accessed 07.13.2018 2018].

AYALA, J. E., SAMUEL, V. T., MORTON, G. J., OBICI, S., CRONIGER, C. M., SHULMAN, G. I., WASSERMAN, D. H., MCGUINNESS, O. P. & CONSORTIUM, N. I. H. M. M. P. C. 2010. Standard operating procedures for describing and performing metabolic tests of glucose homeostasis in mice. *Dis Model Mech,* 3**,** 525-34.

BADURA, A., SUN, X. R., GIOVANNUCCI, A., LYNCH, L. A. & WANG, S. S. 2014. Fast calcium sensor proteins for monitoring neural activity. *Neurophotonics,* 1**,** 025008.

BALFOUR, R. H., HANSEN, A. M. & TRAPP, S. 2006. Neuronal responses to transient hypoglycaemia in the dorsal vagal complex of the rat brainstem. *J Physiol,* 570**,** 469-84.

BANARER, S., MCGREGOR, V. P. & CRYER, P. E. 2002. Intraislet hyperinsulinemia prevents the glucagon response to hypoglycemia despite an intact autonomic response. *Diabetes,* 51**,** 958-65.

BANTING FG, B. C., COLLIP JB, CAMPBELL WR, FLETCHER AA 1922. Pancreatic Extracts in the Treatment of Diabetes Mellitus. *Canadian Medical Association Journal,* 12**,** 141-146.

BARJA, F. & MATHISON, R. 1984. Sensory innervation of the rat portal vein and the hepatic artery. *J Auton Nerv Syst,* 10**,** 117-25.

BEALL, C., ASHFORD, M. L. & MCCRIMMON, R. J. 2012a. The physiology and pathophysiology of the neural control of the counterregulatory response. *American journal of physiology. Regulatory, integrative and comparative physiology,* 302**,** R215-23.

BEALL, C., HAMILTON, D. L., GALLAGHER, J., LOGIE, L., WRIGHT, K., SOUTAR, M. P., DADAK, S., ASHFORD, F. B., HAYTHORNE, E., DU, Q., JOVANOVIC, A., MCCRIMMON, R. J. & ASHFORD, M. L. 2012b. Mouse hypothalamic GT1-7 cells demonstrate AMPK-dependent intrinsic glucose-sensing behaviour. *Diabetologia,* 55**,** 2432-44.

BEHBEHANI, M. M. 1995. Functional characteristics of the midbrain periaqueductal gray. *Prog Neurobiol,* 46**,** 575-605.

BENFORD, H., BOLBOREA, M., POLLATZEK, E., LOSSOW, K., HERMANS-BORGMEYER, I., LIU, B., MEYERHOF, W., KASPAROV, S. & DALE, N. 2017. A sweet taste receptor-dependent mechanism of glucosensing in hypothalamic tanycytes. *Glia,* 65**,** 773-789.

BERKENBOSCH, F. & TILDERS, F. J. 1988. Effect of axonal transport blockade on corticotropin-releasing factor immunoreactivity in the median eminence of intact and adrenalectomized rats: relationship between depletion rate and secretory activity. *Brain Res,* 442**,** 312-20.

BERNARD, C. & TRIPIER, A. 1858. *Leçons sur la physiologie et la pathologie du système nerveux publié par le Dr A. Tripier,* Paris, J.-B. Baillière et fils.

BERRIDGE, M. J., LIPP, P. & BOOTMAN, M. D. 2000. The versatility and universality of calcium signalling. *Nat Rev Mol Cell Biol,* 1**,** 11-21.

BETLEY, J. N., XU, S., CAO, Z. F. H., GONG, R., MAGNUS, C. J., YU, Y. & STERNSON, S. M. 2015. Neurons for hunger and thirst transmit a negative-valence teaching signal. *Nature,* 521**,** 180-185.

BIAG, J., HUANG, Y., GOU, L., HINTIRYAN, H., ASKARINAM, A., HAHN, J. D., TOGA, A. W. & DONG, H. W. 2012. Cyto- and chemoarchitecture of the hypothalamic paraventricular nucleus in the C57BL/6J male mouse: a study of immunostaining and multiple fluorescent tract tracing. *The Journal of comparative neurology,* 520**,** 6-33.

BIGGERS, D. W., MYERS, S. R., NEAL, D., STINSON, R., COOPER, N. B., JASPAN, J. B., WILLIAMS, P. E., CHERRINGTON, A. D. & FRIZZELL, R. T. 1989. Role of brain in counterregulation of insulin-induced hypoglycemia in dogs. *Diabetes,* 38**,** 7-16.

BIN-JALIAH, I., MASKELL, P. D. & KUMAR, P. 2004. Indirect sensing of insulin-induced hypoglycaemia by the carotid body in the rat. *J Physiol,* 556**,** 255-66.

BLOOM, F. E., BATTENBERG, E. L., RIVIER, J. & VALE, W. 1982. Corticotropin releasing factor (CRF): immunoreactive neurones and fibers in rat hypothalamus. *Regulatory peptides,* 4**,** 43-8.

BORG, M. A., SHERWIN, R. S., BORG, W. P., TAMBORLANE, W. V. & SHULMAN, G. I. 1997. Local ventromedial hypothalamus glucose perfusion blocks counterregulation during systemic hypoglycemia in awake rats. *J Clin Invest,* 99**,** 361-5.

BORG, W. P., SHERWIN, R. S., DURING, M. J., BORG, M. A. & SHULMAN, G. I. 1995. Local ventromedial hypothalamus glucopenia triggers counterregulatory hormone release. *Diabetes,* 44**,** 180-4.

BOUMEZBEUR, F., PETERSEN, K. F., CLINE, G. W., MASON, G. F., BEHAR, K. L., SHULMAN, G. I. & ROTHMAN, D. L. 2010. The contribution of blood lactate to brain energy metabolism in humans measured by dynamic 13C nuclear magnetic resonance spectroscopy. *J Neurosci,* 30**,** 13983-91.

BOYLE, P. J., KEMPERS, S. F., O'CONNOR, A. M. & NAGY, R. J. 1995. Brain glucose uptake and unawareness of hypoglycemia in patients with insulin-dependent diabetes mellitus. *N Engl J Med,* 333**,** 1726-31.

BOYLE, P. J., NAGY, R. J., O'CONNOR, A. M., KEMPERS, S. F., YEO, R. A. & QUALLS, C. 1994. Adaptation in brain glucose uptake following recurrent hypoglycemia. *Proc Natl Acad Sci U S A,* 91**,** 9352-6.

BOYLE, P. J., SCHWARTZ, N. S., SHAH, S. D., CLUTTER, W. E. & CRYER, P. E. 1988. Plasma glucose concentrations at the onset of hypoglycemic symptoms in patients with poorly controlled diabetes and in nondiabetics. *N Engl J Med,* 318**,** 1487-92.

BROWN, A. M. 2004. Brain glycogen re-awakened. *J Neurochem,* 89**,** 537-52.

BROWN, M. R., FISHER, L. A., SPIESS, J., RIVIER, C., RIVIER, J. & VALE, W. 1982. Corticotropin-releasing factor: actions on the sympathetic nervous system and metabolism. *Endocrinology,* 111**,** 928-31.

BRU, T., SALINAS, S. & KREMER, E. J. 2010. An update on canine adenovirus type 2 and its vectors. *Viruses,* 2**,** 2134-53.

BUIJS, R. M. 1978. Intra- and extrahypothalamic vasopressin and oxytocin pathways in the rat. Pathways to the limbic system, medulla oblongata and spinal cord. *Cell Tissue Res,* 192**,** 423-35.

BURCELIN, R., DOLCI, W. & THORENS, B. 2000. Glucose sensing by the hepatoportal sensor is GLUT2-dependent: in vivo analysis in GLUT2-null mice. *Diabetes,* 49**,** 1643-8.

BURDAKOV, D., GERASIMENKO, O. & VERKHRATSKY, A. 2005a. Physiological changes in glucose differentially modulate the excitability of hypothalamic melanin-concentrating hormone and orexin neurons in situ. *J Neurosci,* 25**,** 2429-33.

BURDAKOV, D. & LESAGE, F. 2010. Glucose-induced inhibition: how many ionic mechanisms? *Acta Physiol (Oxf),* 198**,** 295-301.

BURDAKOV, D., LUCKMAN, S. M. & VERKHRATSKY, A. 2005b. Glucose-sensing neurons of the hypothalamus. *Philos Trans R Soc Lond B Biol Sci,* 360**,** 2227-35.

CANABAL, D. D., POTIAN, J. G., DURAN, R. G., MCARDLE, J. J. & ROUTH, V. H. 2007a. Hyperglycemia impairs glucose and insulin regulation of nitric oxide production in glucose-inhibited neurons in the ventromedial hypothalamus. *Am J Physiol Regul Integr Comp Physiol,* 293**,** R592-600.

CANABAL, D. D., SONG, Z., POTIAN, J. G., BEUVE, A., MCARDLE, J. J. & ROUTH, V. H. 2007b. Glucose, insulin, and leptin signaling pathways modulate nitric oxide synthesis in glucose-inhibited neurons in the ventromedial hypothalamus. *Am J Physiol Regul Integr Comp Physiol,* 292**,** R1418-28.

CAPRIO, S., GERETY, G., TAMBORLANE, W. V., JONES, T., DIAMOND, M., JACOB, R. & SHERWIN, R. S. 1991. Opiate blockade enhances hypoglycemic counterregulation in normal and insulin-dependent diabetic subjects. *Am J Physiol,* 260**,** E852-8.

CAREY, M., GOSPIN, R., GOYAL, A., TOMUTA, N., SANDU, O., MBANYA, A., LONTCHI-YIMAGOU, E., HULKOWER, R., SHAMOON, H., GABRIELY, I. & HAWKINS, M. 2017. Opioid Receptor Activation Impairs Hypoglycemic Counterregulation in Humans. *Diabetes,* 66**,** 2764-2773.

CERRITELLI, S., HIRSCHBERG, S., HILL, R., BALTHASAR, N. & PICKERING, A. E. 2016. Activation of Brainstem Pro-opiomelanocortin Neurons Produces Opioidergic Analgesia, Bradycardia and Bradypnoea. *PLoS One,* 11**,** e0153187.

CHEN, T. W., WARDILL, T. J., SUN, Y., PULVER, S. R., RENNINGER, S. L., BAOHAN, A., SCHREITER, E. R., KERR, R. A., ORGER, M. B., JAYARAMAN, V., LOOGER, L. L., SVOBODA, K. & KIM, D. S. 2013. Ultrasensitive fluorescent proteins for imaging neuronal activity. *Nature,* 499**,** 295-300.

CHEN, Y., MOLET, J., GUNN, B. G., RESSLER, K. & BARAM, T. Z. 2015. Diversity of Reporter Expression Patterns in Transgenic Mouse Lines Targeting Corticotropin-Releasing Hormone-Expressing Neurons. *Endocrinology,* 156**,** 4769-80.

CHENG, J. T., LIU, I. M., KUO, D. H. & LIN, M. T. 2001. Stimulatory effect of phenylephrine on the secretion of beta-endorphin from rat adrenal medulla in vitro. *Auton Neurosci,* 93**,** 31-5.

CHENG, J. T., LIU, I. M., TZENG, T. F., TSAI, C. C. & LAI, T. Y. 2002. Plasma glucose-lowering effect of beta-endorphin in streptozotocin-induced diabetic rats. *Horm Metab Res,* 34**,** 570-6.

CHOI, I. Y., SEAQUIST, E. R. & GRUETTER, R. 2003. Effect of hypoglycemia on brain glycogen metabolism in vivo. *J Neurosci Res,* 72**,** 25-32.

CHOUDHARY, P., RAMASAMY, S., GREEN, L., GALLEN, G., PENDER, S., BRACKENRIDGE, A., AMIEL, S. A. & PICKUP, J. C. 2013. Real-time continuous glucose monitoring significantly reduces severe hypoglycemia in hypoglycemia-unaware patients with type 1 diabetes. *Diabetes Care,* 36**,** 4160-2.

CLARET, M., SMITH, M. A., BATTERHAM, R. L., SELMAN, C., CHOUDHURY, A. I., FRYER, L. G., CLEMENTS, M., AL-QASSAB, H., HEFFRON, H., XU, A. W., SPEAKMAN, J. R., BARSH, G. S., VIOLLET, B., VAULONT, S., ASHFORD, M. L., CARLING, D. &

WITHERS, D. J. 2007. AMPK is essential for energy homeostasis regulation and glucose sensing by POMC and AgRP neurons. *J Clin Invest,* 117**,** 2325-36.

COLL, A. P., FAROOQI, I. S., CHALLIS, B. G., YEO, G. S. & O'RAHILLY, S. 2004. Proopiomelanocortin and energy balance: insights from human and murine genetics. *J Clin Endocrinol Metab,* 89**,** 2557-62.

COTERO, V. E. & ROUTH, V. H. 2009. Insulin blunts the response of glucose-excited neurons in the ventrolateral-ventromedial hypothalamic nucleus to decreased glucose. *Am J Physiol Endocrinol Metab,* 296**,** E1101-9.

CRYER, P. E. 1997a. Hierarchy of physiological responses to hypoglycemia: relevance to clinical hypoglycemia in type I (insulin dependent) diabetes mellitus. *Horm Metab Res,* 29**,** 92-6.

CRYER, P. E. 1997b. *Hypoglycemia : pathophysiology, diagnosis, and treatment,* New York ; Oxford, Oxford University Press.

CRYER, P. E. 2001. Hypoglycemia-associated autonomic failure in diabetes. *American journal of physiology. Endocrinology and metabolism,* 281**,** E1115-21.

CRYER, P. E. 2004. Diverse causes of hypoglycemia-associated autonomic failure in diabetes. *The New England journal of medicine,* 350**,** 2272-9.

CRYER, P. E. 2005. Mechanisms of hypoglycemia-associated autonomic failure and its component syndromes in diabetes. *Diabetes,* 54**,** 3592-601.

CRYER, P. E., DAVIS, S. N. & SHAMOON, H. 2003. Hypoglycemia in diabetes. *Diabetes Care,* 26**,** 1902-12.

CUNNINGHAM, E. T., JR. & SAWCHENKO, P. E. 1988. Anatomical specificity of noradrenergic inputs to the paraventricular and supraoptic nuclei of the rat hypothalamus. *The Journal of comparative neurology,* 274**,** 60-76.

CUNNINGHAM, J. J., MEARA, P. A., LEE, R. Y. & BODE, H. H. 1988. Chronic intracerebroventricular CRF infusion attenuates ACTH-corticosterone release. *Am J Physiol,* 255**,** E213-7.

DABROWSKA, J., HAZRA, R., GUO, J. D., DEWITT, S. & RAINNIE, D. G. 2013. Central CRF neurons are not created equal: phenotypic differences in CRF-containing neurons of the rat paraventricular hypothalamus and the bed nucleus of the stria terminalis. *Frontiers in neuroscience,* 7**,** 156.

DAGOGO-JACK, S., RATTARASARN, C. & CRYER, P. E. 1994. Reversal of hypoglycemia unawareness, but not defective glucose counterregulation, in IDDM. *Diabetes,* 43**,** 1426-34.

DAGOGO-JACK, S. E., CRAFT, S. & CRYER, P. E. 1993. Hypoglycemia-associated autonomic failure in insulin-dependent diabetes mellitus. Recent antecedent hypoglycemia reduces autonomic responses to, symptoms of, and defense against subsequent hypoglycemia. *J Clin Invest,* 91**,** 819-28.

DAVIS, M. R. & SHAMOON, H. 1991. Counterregulatory adaptation to recurrent hypoglycemia in normal humans. *J Clin Endocrinol Metab,* 73**,** 995-1001.

DAVIS, S. N., SHAVERS, C., COSTA, F. & MOSQUEDA-GARCIA, R. 1996. Role of cortisol in the pathogenesis of deficient counterregulation after antecedent hypoglycemia in normal humans. *J Clin Invest,* 98**,** 680-91.

DAVIS, S. N., SHAVERS, C., DAVIS, B. & COSTA, F. 1997. Prevention of an increase in plasma cortisol during hypoglycemia preserves subsequent counterregulatory responses. *J Clin Invest,* 100**,** 429-38.

DE BOCK, M., MCAULEY, S. A., ABRAHAM, M. B., SMITH, G., NICHOLAS, J., AMBLER, G. R., CAMERON, F. J., FAIRCHILD, J. M., KING, B. R., GEELHOED, E. A., DAVIS, E. A., O'NEAL, D. N., JONES, T. W. & AUSTRALIAN, J. C.-L. R. G. 2018. Effect of 6

months hybrid closed-loop insulin delivery in young people with type 1 diabetes: a randomised controlled trial protocol. *BMJ Open,* 8**,** e020275.

DE FEYTER, H. M., MASON, G. F., SHULMAN, G. I., ROTHMAN, D. L. & PETERSEN, K. F. 2013. Increased brain lactate concentrations without increased lactate oxidation during hypoglycemia in type 1 diabetic individuals. *Diabetes,* 62**,** 3075-80.

DE GALAN, B. E., TACK, C. J., WILLEMSEN, J. J., SWEEP, C. G., SMITS, P. & LENDERS, J. W. 2004. Plasma metanephrine levels are decreased in type 1 diabetic patients with a severely impaired epinephrine response to hypoglycemia, indicating reduced adrenomedullary stores of epinephrine. *J Clin Endocrinol Metab,* 89**,** 2057-61.

DE VRIES, M. G., ARSENEAU, L. M., LAWSON, M. E. & BEVERLY, J. L. 2003. Extracellular glucose in rat ventromedial hypothalamus during acute and recurrent hypoglycemia. *Diabetes,* 52**,** 2767-73.

DE VRIES, M. G., LAWSON, M. A. & BEVERLY, J. L. 2004. Dissociation of hypothalamic noradrenergic activity and sympathoadrenal responses to recurrent hypoglycemia. *Am J Physiol Regul Integr Comp Physiol,* 286**,** R910-5.

DEARDEN, L. & BALTHASAR, N. 2014. Sexual dimorphism in offspring glucose-sensitive hypothalamic gene expression and physiological responses to maternal high-fat diet feeding. *Endocrinology,* 155**,** 2144-54.

DELAERE, F., DUCHAMPT, A., MOUNIEN, L., SEYER, P., DURAFFOURD, C., ZITOUN, C., THORENS, B. & MITHIEUX, G. 2012. The role of sodium-coupled glucose co-transporter 3 in the satiety effect of portal glucose sensing. *Mol Metab,* 2**,** 47-53.

DERMITZAKI, E., GRAVANIS, A., VENIHAKI, M., STOURNARAS, C. & MARGIORIS, A. N. 2001. Opioids suppress basal and nicotine-induced catecholamine secretion via a stabilizing effect on actin filaments. *Endocrinology,* 142**,** 2022-31.

DEROSA, M. A. & CRYER, P. E. 2004. Hypoglycemia and the sympathoadrenal system: neurogenic symptoms are largely the result of sympathetic neural, rather than adrenomedullary, activation. *Am J Physiol Endocrinol Metab,* 287**,** E32-41.

DESOUZA, C., SALAZAR, H., CHEONG, B., MURGO, J. & FONSECA, V. 2003. Association of hypoglycemia and cardiac ischemia: a study based on continuous monitoring. *Diabetes Care,* 26**,** 1485-9.

DIABETESUK. 2017. *Diabetes Prevalence 2017* [Online]. Available: https://www.diabetes.org.uk/professionals/position-statements-reports/statistics/diabetes-prevalence-2017 [Accessed June 30 2017].

DIGGS-ANDREWS, K. A., ZHANG, X., SONG, Z., DAPHNA-IKEN, D., ROUTH, V. H. & FISHER, S. J. 2010. Brain insulin action regulates hypothalamic glucose sensing and the counterregulatory response to hypoglycemia. *Diabetes,* 59**,** 2271-80.

DIROCCO, R. J. & GRILL, H. J. 1979. The forebrain is not essential for sympathoadrenal hyperglycemic response to glucoprivation. *Science,* 204**,** 1112-4.

DONOVAN, C. M. & WATTS, A. G. 2014. Peripheral and central glucose sensing in hypoglycemic detection. *Physiology (Bethesda),* 29**,** 314-24.

DOYLE, A., MCGARRY, M. P., LEE, N. A. & LEE, J. J. 2012. The construction of transgenic and gene knockout/knockin mouse models of human disease. *Transgenic Res,* 21**,** 327-49.

DUNN-MEYNELL, A. A., ROUTH, V. H., KANG, L., GASPERS, L. & LEVIN, B. E. 2002. Glucokinase is the likely mediator of glucosensing in both glucose-excited and glucose-inhibited central neurons. *Diabetes,* 51**,** 2056-65.

DUNN-MEYNELL, A. A., SANDERS, N. M., COMPTON, D., BECKER, T. C., EIKI, J., ZHANG, B. B. & LEVIN, B. E. 2009. Relationship among brain and blood glucose levels and spontaneous and glucoprivic feeding. *J Neurosci,* 29**,** 7015-22.

EDWARDS, C. M., ABUSNANA, S., SUNTER, D., MURPHY, K. G., GHATEI, M. A. & BLOOM, S. R. 1999. The effect of the orexins on food intake: comparison with neuropeptide Y, melanin-concentrating hormone and galanin. *J Endocrinol,* 160**,** R7-12.

ELIAVA, M., MELCHIOR, M., KNOBLOCH-BOLLMANN, H. S., WAHIS, J., DA SILVA GOUVEIA, M., TANG, Y., CIOBANU, A. C., TRIANA DEL RIO, R., ROTH, L. C., ALTHAMMER, F., CHAVANT, V., GOUMON, Y., GRUBER, T., PETIT-DEMOULIERE, N., BUSNELLI, M., CHINI, B., TAN, L. L., MITRE, M., FROEMKE, R. C., CHAO, M. V., GIESE, G., SPRENGEL, R., KUNER, R., POISBEAU, P., SEEBURG, P. H., STOOP, R., CHARLET, A. & GRINEVICH, V. 2016. A New Population of Parvocellular Oxytocin Neurons Controlling Magnocellular Neuron Activity and Inflammatory Pain Processing. *Neuron,* 89**,** 1291-1304.

ELIZONDO-VEGA, R., CORTES-CAMPOS, C., BARAHONA, M. J., OYARCE, K. A., CARRIL, C. A. & GARCIA-ROBLES, M. A. 2015. The role of tanycytes in hypothalamic glucosensing. *J Cell Mol Med,* 19**,** 1471-82.

ELLERI, D., DUNGER, D. B. & HOVORKA, R. 2011. Closed-loop insulin delivery for treatment of type 1 diabetes. *BMC Med,* 9**,** 120.

EVANS, M. L., MCCRIMMON, R. J., FLANAGAN, D. E., KESHAVARZ, T., FAN, X., MCNAY, E. C., JACOB, R. J. & SHERWIN, R. S. 2004. Hypothalamic ATP-sensitive K + channels play a key role in sensing hypoglycemia and triggering counterregulatory epinephrine and glucagon responses. *Diabetes,* 53**,** 2542-51.

EVANS, S. B., WILKINSON, C. W., BENTSON, K., GRONBECK, P., ZAVOSH, A. & FIGLEWICZ, D. P. 2001. PVN activation is suppressed by repeated hypoglycemia but not antecedent corticosterone in the rat. *American journal of physiology. Regulatory, integrative and comparative physiology,* 281**,** R1426-36.

EVANS, S. B., WILKINSON, C. W., GRONBECK, P., BENNETT, J. L., TABORSKY, G. J., JR. & FIGLEWICZ, D. P. 2003. Inactivation of the PVN during hypoglycemia partially simulates hypoglycemia-associated autonomic failure. *American journal of physiology. Regulatory, integrative and comparative physiology,* 284**,** R57-65.

FEIL, D. G. & POGACH, L. M. 2014. Cognitive impairment is a major risk factor for serious hypoglycaemia; public health intervention is warranted. *Evid Based Med,* 19**,** 77.

FEINKOHL, I., AUNG, P. P., KELLER, M., ROBERTSON, C. M., MORLING, J. R., MCLACHLAN, S., DEARY, I. J., FRIER, B. M., STRACHAN, M. W., PRICE, J. F. & EDINBURGH TYPE 2 DIABETES STUDY, I. 2014. Severe hypoglycemia and cognitive decline in older people with type 2 diabetes: the Edinburgh type 2 diabetes study. *Diabetes Care,* 37**,** 507-15.

FENNO, L., YIZHAR, O. & DEISSEROTH, K. 2011. The development and application of optogenetics. *Annu Rev Neurosci,* 34**,** 389-412.

FERGUSON, A. V., LATCHFORD, K. J. & SAMSON, W. K. 2008. The paraventricular nucleus of the hypothalamus - a potential target for integrative treatment of autonomic dysfunction. *Expert opinion on therapeutic targets,* 12**,** 717-27.

FIGLEWICZ, D. P., VAN DIJK, G., WILKINSON, C. W., GRONBECK, P., HIGGINS, M. & ZAVOSH, A. 2002. Effects of repetitive hypoglycemia on neuroendocrine response and brain tyrosine hydroxylase activity in the rat. *Stress,* 5**,** 217-26.

FIORAMONTI, X., CHRETIEN, C., LELOUP, C. & PENICAUD, L. 2017. Recent Advances in the Cellular and Molecular Mechanisms of Hypothalamic Neuronal Glucose Detection. *Front Physiol,* 8**,** 875.

FIORAMONTI, X., CONTIE, S., SONG, Z., ROUTH, V. H., LORSIGNOL, A. & PENICAUD, L. 2007. Characterization of glucosensing neuron subpopulations in the arcuate nucleus: integration in neuropeptide Y and pro-opio melanocortin networks? *Diabetes,* 56**,** 1219-27.

FIORAMONTI, X., LORSIGNOL, A., TAUPIGNON, A. & PENICAUD, L. 2004. A new ATP-sensitive K+ channel-independent mechanism is involved in glucose-excited neurons of mouse arcuate nucleus. *Diabetes,* 53**,** 2767-75.

FISHER SJ, D.-I. D., PEREZ R, OLORUNTOBA O, KAHN CR 2005. Hypoglycemia dependent insulin mediated autonomic failure (Abstract). *Diabetes,* 54**,** A70.

FLAK, J. N., PATTERSON, C. M., GARFIELD, A. S., D'AGOSTINO, G., GOFORTH, P. B., SUTTON, A. K., MALEC, P. A., WONG, J. T., GERMANI, M., JONES, J. C., RAJALA, M., SATIN, L., RHODES, C. J., OLSON, D. P., KENNEDY, R. T., HEISLER, L. K. & MYERS, M. G., JR. 2014. Leptin-inhibited PBN neurons enhance responses to hypoglycemia in negative energy balance. *Nat Neurosci,* 17**,** 1744-1750.

FLANAGAN, D. E., KESHAVARZ, T., EVANS, M. L., FLANAGAN, S., FAN, X., JACOB, R. J. & SHERWIN, R. S. 2003. Role of corticotrophin-releasing hormone in the impairment of counterregulatory responses to hypoglycemia. *Diabetes,* 52**,** 605-13.

FLOYD, N. S., KEAY, K. A., ARIAS, C. M., SAWCHENKO, P. E. & BANDLER, R. 1996. Projections from the ventrolateral periaqueductal gray to endocrine regulatory subdivisions of the paraventricular nucleus of the hypothalamus in the rat. *Neurosci Lett,* 220**,** 105-8.

FRAYLING, C., BRITTON, R. & DALE, N. 2011. ATP-mediated glucosensing by hypothalamic tanycytes. *J Physiol,* 589**,** 2275-86.

FRIER, B. M. 2009. The incidence and impact of hypoglycemia in type 1 and type 2 diabetes. *International Diabetes Monitor***,** 210-218.

FRIER, B. M. 2014. Hypoglycaemia in diabetes mellitus: epidemiology and clinical implications. *Nat Rev Endocrinol*.

FUJITA, S., BOHLAND, M., SANCHEZ-WATTS, G., WATTS, A. G. & DONOVAN, C. M. 2007. Hypoglycemic detection at the portal vein is mediated by capsaicin-sensitive primary sensory neurons. *Am J Physiol Endocrinol Metab,* 293**,** E96-E101.

FUJITA, S. & DONOVAN, C. M. 2005. Celiac-superior mesenteric ganglionectomy, but not vagotomy, suppresses the sympathoadrenal response to insulin-induced hypoglycemia. *Diabetes,* 54**,** 3258-64.

FUNAHASHI, M. & ADACHI, A. 1993. Glucose-responsive neurons exist within the area postrema of the rat: in vitro study on the isolated slice preparation. *Brain Res Bull,* 32**,** 531-5.

GARFIELD, A. S., SHAH, B. P., MADARA, J. C., BURKE, L. K., PATTERSON, C. M., FLAK, J., NEVE, R. L., EVANS, M. L., LOWELL, B. B., MYERS, M. G., JR. & HEISLER, L. K. 2014. A parabrachial-hypothalamic cholecystokinin neurocircuit controls counterregulatory responses to hypoglycemia. *Cell Metab,* 20**,** 1030-7.

GARG, S. K., WEINZIMER, S. A., TAMBORLANE, W. V., BUCKINGHAM, B. A., BODE, B. W., BAILEY, T. S., BRAZG, R. L., ILANY, J., SLOVER, R. H., ANDERSON, S. M., BERGENSTAL, R. M., GROSMAN, B., ROY, A., CORDERO, T. L., SHIN, J., LEE, S. W. & KAUFMAN, F. R. 2017. Glucose Outcomes with the In-Home Use of a Hybrid

Closed-Loop Insulin Delivery System in Adolescents and Adults with Type 1 Diabetes. *Diabetes Technol Ther,* 19**,** 155-163.

GEERLING, J. C., SHIN, J. W., CHIMENTI, P. C. & LOEWY, A. D. 2010. Paraventricular hypothalamic nucleus: axonal projections to the brainstem. *J Comp Neurol,* 518**,** 1460-99.

GEURTS, A. M., COST, G. J., FREYVERT, Y., ZEITLER, B., MILLER, J. C., CHOI, V. M., JENKINS, S. S., WOOD, A., CUI, X., MENG, X., VINCENT, A., LAM, S., MICHALKIEWICZ, M., SCHILLING, R., FOECKLER, J., KALLOWAY, S., WEILER, H., MENORET, S., ANEGON, I., DAVIS, G. D., ZHANG, L., REBAR, E. J., GREGORY, P. D., URNOV, F. D., JACOB, H. J. & BUELOW, R. 2009. Knockout rats via embryo microinjection of zinc-finger nucleases. *Science,* 325**,** 433.

GONZALEZ, J. A., JENSEN, L. T., FUGGER, L. & BURDAKOV, D. 2008. Metabolism-independent sugar sensing in central orexin neurons. *Diabetes,* 57**,** 2569-76.

GONZALEZ, J. A., REIMANN, F. & BURDAKOV, D. 2009. Dissociation between sensing and metabolism of glucose in sugar sensing neurones. *The Journal of physiology,* 587**,** 41-8.

GREENBERG, M. E. & ZIFF, E. B. 1984. Stimulation of 3T3 cells induces transcription of the c-fos proto-oncogene. *Nature,* 311**,** 433-8.

GREGG, E. W. 2017. The Changing Tides of the Type 2 Diabetes Epidemic-Smooth Sailing or Troubled Waters Ahead? Kelly West Award Lecture 2016. *Diabetes Care,* 40**,** 1289-1297.

GRIENBERGER, C. & KONNERTH, A. 2012. Imaging calcium in neurons. *Neuron,* 73**,** 862-85.

GRIFFIN, G. D., FERRI-KOLWICZ, S. L., REYES, B. A., VAN BOCKSTAELE, E. J. & FLANAGAN-CATO, L. M. 2010. Ovarian hormone-induced reorganization of oxytocin-labeled dendrites and synapses lateral to the hypothalamic ventromedial nucleus in female rats. *J Comp Neurol,* 518**,** 4531-45.

GRISSOM, N. & BHATNAGAR, S. 2009. Habituation to repeated stress: get used to it. *Neurobiol Learn Mem,* 92**,** 215-24.

GROMADA, J., MA, X., HOY, M., BOKVIST, K., SALEHI, A., BERGGREN, P. O. & RORSMAN, P. 2004. ATP-sensitive K+ channel-dependent regulation of glucagon release and electrical activity by glucose in wild-type and SUR1-/- mouse alpha-cells. *Diabetes,* 53 Suppl 3**,** S181-9.

GRYNKIEWICZ, G., POENIE, M. & TSIEN, R. Y. 1985. A new generation of Ca2+ indicators with greatly improved fluorescence properties. *J Biol Chem,* 260**,** 3440-50.

GUAN, H. Z., DONG, J., JIANG, Z. Y. & CHEN, X. 2017. alpha-MSH Influences the Excitability of Feeding-Related Neurons in the Hypothalamus and Dorsal Vagal Complex of Rats. *Biomed Res Int,* 2017**,** 2034691.

HAN, S. M., NAMKOONG, C., JANG, P. G., PARK, I. S., HONG, S. W., KATAKAMI, H., CHUN, S., KIM, S. W., PARK, J. Y., LEE, K. U. & KIM, M. S. 2005. Hypothalamic AMP-activated protein kinase mediates counter-regulatory responses to hypoglycaemia in rats. *Diabetologia,* 48**,** 2170-8.

HARRIS, G. W. 1955. Neural Control of The Pituitary Gland. *MONOGRAPHS OF THE PHYSIOLOGICAL SOCIETY***,** 298.

HARRIS, J. A., HIROKAWA, K. E., SORENSEN, S. A., GU, H., MILLS, M., NG, L. L., BOHN, P., MORTRUD, M., OUELLETTE, B., KIDNEY, J., SMITH, K. A., DANG, C., SUNKIN, S., BERNARD, A., OH, S. W., MADISEN, L. & ZENG, H. 2014. Anatomical characterization of Cre driver mice for neural circuit mapping and manipulation. *Front Neural Circuits,* 8**,** 76.

HELLER, S. R. & CRYER, P. E. 1991. Reduced neuroendocrine and symptomatic responses to subsequent hypoglycemia after 1 episode of hypoglycemia in nondiabetic humans. *Diabetes,* 40**,** 223-6.

HENCKENS, M. J., DEUSSING, J. M. & CHEN, A. 2016. Region-specific roles of the corticotropin-releasing factor-urocortin system in stress. *Nat Rev Neurosci,* 17**,** 636-51.

HERMAN, J. P. & CULLINAN, W. E. 1997. Neurocircuitry of stress: central control of the hypothalamo-pituitary-adrenocortical axis. *Trends in neurosciences,* 20**,** 78-84.

HERMAN, J. P., FIGUEIREDO, H., MUELLER, N. K., ULRICH-LAI, Y., OSTRANDER, M. M., CHOI, D. C. & CULLINAN, W. E. 2003. Central mechanisms of stress integration: hierarchical circuitry controlling hypothalamo-pituitary-adrenocortical responsiveness. *Frontiers in neuroendocrinology,* 24**,** 151-80.

HERZOG, R. I., CHAN, O., YU, S., DZIURA, J., MCNAY, E. C. & SHERWIN, R. S. 2008. Effect of acute and recurrent hypoglycemia on changes in brain glycogen concentration. *Endocrinology,* 149**,** 1499-504.

HEVENER, A. L., BERGMAN, R. N. & DONOVAN, C. M. 1997. Novel glucosensor for hypoglycemic detection localized to the portal vein. *Diabetes,* 46**,** 1521-5.

HICKEY, L., LI, Y., FYSON, S. J., WATSON, T. C., PERRINS, R., HEWINSON, J., TESCHEMACHER, A. G., FURUE, H., LUMB, B. M. & PICKERING, A. E. 2014. Optoactivation of locus ceruleus neurons evokes bidirectional changes in thermal nociception in rats. *J Neurosci,* 34**,** 4148-60.

HILL, J. W. 2012. PVN pathways controlling energy homeostasis. *Indian journal of endocrinology and metabolism,* 16**,** S627-36.

HOFFMAN, G. E., SMITH, M. S. & VERBALIS, J. G. 1993. c-Fos and related immediate early gene products as markers of activity in neuroendocrine systems. *Frontiers in neuroendocrinology,* 14**,** 173-213.

HOSOYA, Y., SUGIURA, Y., OKADO, N., LOEWY, A. D. & KOHNO, K. 1991. Descending input from the hypothalamic paraventricular nucleus to sympathetic preganglionic neurons in the rat. *Experimental brain research,* 85**,** 10-20.

HOVORKA, R. 2011. Closed-loop insulin delivery: from bench to clinical practice. *Nat Rev Endocrinol,* 7**,** 385-95.

HOVORKA, R., KUMARESWARAN, K., HARRIS, J., ALLEN, J. M., ELLERI, D., XING, D., KOLLMAN, C., NODALE, M., MURPHY, H. R., DUNGER, D. B., AMIEL, S. A., HELLER, S. R., WILINSKA, M. E. & EVANS, M. L. 2011. Overnight closed loop insulin delivery (artificial pancreas) in adults with type 1 diabetes: crossover randomised controlled studies. *BMJ,* 342**,** d1855.

IBRAHIM, N., BOSCH, M. A., SMART, J. L., QIU, J., RUBINSTEIN, M., RONNEKLEIV, O. K., LOW, M. J. & KELLY, M. J. 2003. Hypothalamic proopiomelanocortin neurons are glucose responsive and express K(ATP) channels. *Endocrinology,* 144**,** 1331-40.

INKSTER, B. & FRIER, B. M. 2013. Diabetes and driving. *Diabetes Obes Metab,* 15**,** 775-83.

INOUYE, K. E., CHAN, O., YUE, J. T., MATTHEWS, S. G. & VRANIC, M. 2005. Effects of diabetes and recurrent hypoglycemia on the regulation of the sympathoadrenal system and hypothalamo-pituitary-adrenal axis. *Am J Physiol Endocrinol Metab,* 288**,** E422-9.

IXART, G., SIAUD, P., BARBANEL, G., MEKAOUCHE, M., GIVALOIS, L. & ASSENMACHER, I. 1993. Circadian variations in the amplitude of corticotropin-releasing hormone 41 (CRH41) episodic release measured in vivo in male rats: correlations with diurnal fluctuations in hypothalamic and median eminence CRH41 contents. *J Biol Rhythms,* 8**,** 297-309.

JACOBSON, L., ANSARI, T. & MCGUINNESS, O. P. 2006a. Counterregulatory deficits occur within 24 h of a single hypoglycemic episode in conscious, unrestrained, chronically cannulated mice. *Am J Physiol Endocrinol Metab,* 290**,** E678-84.

JACOBSON, L., ANSARI, T., POTTS, J. & MCGUINNESS, O. P. 2006b. Glucocorticoid-deficient corticotropin-releasing hormone knockout mice maintain glucose requirements but not autonomic responses during repeated hypoglycemia. *American journal of physiology. Endocrinology and metabolism,* 291**,** E15-22.

JANSEN, A. S., WESSENDORF, M. W. & LOEWY, A. D. 1995. Transneuronal labeling of CNS neuropeptide and monoamine neurons after pseudorabies virus injections into the stellate ganglion. *Brain Res,* 683**,** 1-24.

JORDAN, S. D., KONNER, A. C. & BRUNING, J. C. 2010. Sensing the fuels: glucose and lipid signaling in the CNS controlling energy homeostasis. *Cell Mol Life Sci,* 67**,** 3255-73.

JUNYENT, F. & KREMER, E. J. 2015. CAV-2--why a canine virus is a neurobiologist's best friend. *Curr Opin Pharmacol,* 24**,** 86-93.

KANG, L., DUNN-MEYNELL, A. A., ROUTH, V. H., GASPERS, L. D., NAGATA, Y., NISHIMURA, T., EIKI, J., ZHANG, B. B. & LEVIN, B. E. 2006. Glucokinase is a critical regulator of ventromedial hypothalamic neuronal glucosensing. *Diabetes,* 55**,** 412-20.

KANG, L., ROUTH, V. H., KUZHIKANDATHIL, E. V., GASPERS, L. D. & LEVIN, B. E. 2004. Physiological and molecular characteristics of rat hypothalamic ventromedial nucleus glucosensing neurons. *Diabetes,* 53**,** 549-59.

KANG, L., SANDERS, N. M., DUNN-MEYNELL, A. A., GASPERS, L. D., ROUTH, V. H., THOMAS, A. P. & LEVIN, B. E. 2008. Prior hypoglycemia enhances glucose responsiveness in some ventromedial hypothalamic glucosensing neurons. *Am J Physiol Regul Integr Comp Physiol,* 294**,** R784-92.

KANT, G. J., BUNNELL, B. N., MOUGEY, E. H., PENNINGTON, L. L. & MEYERHOFF, J. L. 1983. Effects of repeated stress on pituitary cyclic AMP, and plasma prolactin, corticosterone and growth hormone in male rats. *Pharmacol Biochem Behav,* 18**,** 967-71.

KANTOR, B., BAILEY, R. M., WIMBERLY, K., KALBURGI, S. N. & GRAY, S. J. 2014. Methods for gene transfer to the central nervous system. *Adv Genet,* 87**,** 125-97.

KARNANI, M. M., SZABO, G., ERDELYI, F. & BURDAKOV, D. 2013. Lateral hypothalamic GAD65 neurons are spontaneously firing and distinct from orexin- and melanin-concentrating hormone neurons. *J Physiol,* 591**,** 933-53.

KAWASHIMA, T., KITAMURA, K., SUZUKI, K., NONAKA, M., KAMIJO, S., TAKEMOTO-KIMURA, S., KANO, M., OKUNO, H., OHKI, K. & BITO, H. 2013. Functional labeling of neurons and their projections using the synthetic activity-dependent promoter E-SARE. *Nat Methods,* 10**,** 889-95.

KEIM, K. L. & SIGG, E. B. 1976. Physiological and biochemical concomitants of restraint stress in rats. *Pharmacol Biochem Behav,* 4**,** 289-97.

KING, B. M. 2006. The rise, fall, and resurrection of the ventromedial hypothalamus in the regulation of feeding behavior and body weight. *Physiol Behav,* 87**,** 221-44.

KING, C. M. & HENTGES, S. T. 2011. Relative number and distribution of murine hypothalamic proopiomelanocortin neurons innervating distinct target sites. *PLoS One,* 6**,** e25864.

KLEMENT, J., MERGELKUHL, B., BORN, J., LEHNERT, H. & HALLSCHMID, M. 2014. Role of gamma-aminobutyric acid signalling in the attenuation of counter-regulatory hormonal responses after antecedent hypoglycaemia in healthy men. *Diabetes Obes Metab*.

KOBASHI, M. & ADACHI, A. 1995. Chemosensitivity of neurons in the dorsal motor nucleus of the vagus that responded to portal infusion of hypertonic saline in rats. *Brain Res Bull,* 38**,** 11-5.

KOBLINGER, K., FUZESI, T., EJDRYGIEWICZ, J., KRAJACIC, A., BAINS, J. S. & WHELAN, P. J. 2014. Characterization of A11 neurons projecting to the spinal cord of mice. *PLoS One,* 9**,** e109636.

KONG, D., TONG, Q., YE, C., KODA, S., FULLER, P. M., KRASHES, M. J., VONG, L., RAY, R. S., OLSON, D. P. & LOWELL, B. B. 2012. GABAergic RIP-Cre neurons in the arcuate nucleus selectively regulate energy expenditure. *Cell,* 151**,** 645-57.

KOUTCHEROV, Y., MAI, J. K., ASHWELL, K. W. & PAXINOS, G. 2000. Organization of the human paraventricular hypothalamic nucleus. *J Comp Neurol,* 423**,** 299-318.

KOVACS, K. J. 1998. c-Fos as a transcription factor: a stressful (re)view from a functional map. *Neurochem Int,* 33**,** 287-97.

KRUKOFF, T. L., HARRIS, K. H. & JHAMANDAS, J. H. 1993. Efferent projections from the parabrachial nucleus demonstrated with the anterograde tracer Phaseolus vulgaris leucoagglutinin. *Brain Res Bull,* 30**,** 163-72.

KUMAGAI, A. K., KANG, Y. S., BOADO, R. J. & PARDRIDGE, W. M. 1995. Upregulation of blood-brain barrier GLUT1 glucose transporter protein and mRNA in experimental chronic hypoglycemia. *Diabetes,* 44**,** 1399-404.

KUMARESWARAN, K., THABIT, H., LEELARATHNA, L., CALDWELL, K., ELLERI, D., ALLEN, J. M., NODALE, M., WILINSKA, M. E., EVANS, M. L. & HOVORKA, R. 2014. Feasibility of closed-loop insulin delivery in type 2 diabetes: a randomized controlled study. *Diabetes Care,* 37**,** 1198-203.

LAING, S. P., SWERDLOW, A. J., SLATER, S. D., BOTHA, J. L., BURDEN, A. C., WAUGH, N. R., SMITH, A. W., HILL, R. D., BINGLEY, P. J., PATTERSON, C. C., QIAO, Z. & KEEN, H. 1999. The British Diabetic Association Cohort Study, II: cause-specific mortality in patients with insulin-treated diabetes mellitus. *Diabet Med,* 16**,** 466-71.

LAMARCHE, L., YAMAGUCHI, N. & PERONNET, F. 1996. Selective hypoglycemia in the liver induces adrenomedullary counterregulatory response. *Am J Physiol,* 270**,** R1307-16.

LAMY, C. M., SANNO, H., LABOUEBE, G., PICARD, A., MAGNAN, C., CHATTON, J. Y. & THORENS, B. 2014. Hypoglycemia-Activated GLUT2 Neurons of the Nucleus Tractus Solitarius Stimulate Vagal Activity and Glucagon Secretion. *Cell metabolism,* 19**,** 527-38.

LARSEN, P. J., HAY-SCHMIDT, A. & MIKKELSEN, J. D. 1994. Efferent connections from the lateral hypothalamic region and the lateral preoptic area to the hypothalamic paraventricular nucleus of the rat. *J Comp Neurol,* 342**,** 299-319.

LEE, C. Y., DALLERAC, G., EZAN, P., ANDEROVA, M. & ROUACH, N. 2016. Glucose Tightly Controls Morphological and Functional Properties of Astrocytes. *Front Aging Neurosci,* 8**,** 82.

LEELARATHNA, L., LITTLE, S. A., WALKINSHAW, E., TAN, H. K., LUBINA-SOLOMON, A., KUMARESWARAN, K., LANE, A. P., CHADWICK, T., MARSHALL, S. M., SPEIGHT, J., FLANAGAN, D., HELLER, S. R., SHAW, J. A. & EVANS, M. L. 2013. Restoration of self-awareness of hypoglycemia in adults with long-standing type 1 diabetes: hyperinsulinemic-hypoglycemic clamp substudy results from the HypoCOMPaSS trial. *Diabetes Care,* 36**,** 4063-70.

LELOUP, C., ALLARD, C., CARNEIRO, L., FIORAMONTI, X., COLLINS, S. & PENICAUD, L. 2016. Glucose and hypothalamic astrocytes: More than a fueling role? *Neuroscience,* 323**,** 110-20.

LELOUP, C., MAGNAN, C., BENANI, A., BONNET, E., ALQUIER, T., OFFER, G., CARRIERE, A., PERIQUET, A., FERNANDEZ, Y., KTORZA, A., CASTEILLA, L. & PENICAUD, L. 2006. Mitochondrial reactive oxygen species are required for hypothalamic glucose sensing. *Diabetes,* 55**,** 2084-90.

LERNER, R. G., DEPATIE, C., RUTTER, G. A., SCREATON, R. A. & BALTHASAR, N. 2009. A role for the CREB co-activator CRTC2 in the hypothalamic mechanisms linking glucose sensing with gene regulation. *EMBO reports,* 10**,** 1175-81.

LEU, J., CUI, M. H., SHAMOON, H. & GABRIELY, I. 2009. Hypoglycemia-associated autonomic failure is prevented by opioid receptor blockade. *J Clin Endocrinol Metab,* 94**,** 3372-80.

LI, W., TENG, F., LI, T. & ZHOU, Q. 2013. Simultaneous generation and germline transmission of multiple gene mutations in rat using CRISPR-Cas systems. *Nat Biotechnol,* 31**,** 684-6.

LI, Y., HICKEY, L., PERRINS, R., WERLEN, E., PATEL, A. A., HIRSCHBERG, S., JONES, M. W., SALINAS, S., KREMER, E. J. & PICKERING, A. E. 2016. Retrograde optogenetic characterization of the pontospinal module of the locus coeruleus with a canine adenoviral vector. *Brain Res,* 1641**,** 274-90.

LINGENFELSER, T., RENN, W., SOMMERWERCK, U., JUNG, M. F., BUETTNER, U. W., ZAISER-KASCHEL, H., KASCHEL, R., EGGSTEIN, M. & JAKOBER, B. 1993. Compromised hormonal counterregulation, symptom awareness, and neurophysiological function after recurrent short-term episodes of insulin-induced hypoglycemia in IDDM patients. *Diabetes,* 42**,** 610-8.

LIPOSITS, Z., PAULL, W. K., SETALO, G. & VIGH, S. 1985. Evidence for local corticotropin releasing factor (CRF)-immunoreactive neuronal circuits in the paraventricular nucleus of the rat hypothalamus. An electron microscopic immunohistochemical analysis. *Histochemistry,* 83**,** 5-16.

LUITEN, P. G., TER HORST, G. J., KARST, H. & STEFFENS, A. B. 1985. The course of paraventricular hypothalamic efferents to autonomic structures in medulla and spinal cord. *Brain Res,* 329**,** 374-8.

LUNDKVIST, J., BERNE, C., BOLINDER, B. & JONSSON, L. 2005. The economic and quality of life impact of hypoglycemia. *Eur J Health Econ,* 6**,** 197-202.

LUTHER, J. A., DAFTARY, S. S., BOUDABA, C., GOULD, G. C., HALMOS, K. C. & TASKER, J. G. 2002. Neurosecretory and non-neurosecretory parvocellular neurones of the hypothalamic paraventricular nucleus express distinct electrophysiological properties. *J Neuroendocrinol,* 14**,** 929-32.

LYNCH, R. M., TOMPKINS, L. S., BROOKS, H. L., DUNN-MEYNELL, A. A. & LEVIN, B. E. 2000. Localization of glucokinase gene expression in the rat brain. *Diabetes,* 49**,** 693-700.

MADDEN, C. J., STOCKER, S. D. & SVED, A. F. 2006. Attenuation of homeostatic responses to hypotension and glucoprivation after destruction of catecholaminergic rostral ventrolateral medulla neurons. *Am J Physiol Regul Integr Comp Physiol,* 291**,** R751-9.

MADISEN, L., GARNER, A. R., SHIMAOKA, D., CHUONG, A. S., KLAPOETKE, N. C., LI, L., VAN DER BOURG, A., NIINO, Y., EGOLF, L., MONETTI, C., GU, H., MILLS, M., CHENG, A., TASIC, B., NGUYEN, T. N., SUNKIN, S. M., BENUCCI, A., NAGY, A., MIYAWAKI, A., HELMCHEN, F., EMPSON, R. M., KNOPFEL, T., BOYDEN, E. S., REID, R. C., CARANDINI, M. & ZENG, H. 2015. Transgenic mice for intersectional targeting of neural sensors and effectors with high specificity and performance. *Neuron,* 85**,** 942-58.

MADISEN, L., ZWINGMAN, T. A., SUNKIN, S. M., OH, S. W., ZARIWALA, H. A., GU, H., NG, L. L., PALMITER, R. D., HAWRYLYCZ, M. J., JONES, A. R., LEIN, E. S. & ZENG, H. 2010. A robust and high-throughput Cre reporting and characterization system for the whole mouse brain. *Nat Neurosci,* 13**,** 133-40.

MAGISTRETTI, P. J., PELLERIN, L., ROTHMAN, D. L. & SHULMAN, R. G. 1999. Energy on demand. *Science,* 283**,** 496-7.

MALMGREN, S. & AHREN, B. 2015. Deciphering the Hypoglycemic Glucagon Response: Development of a Graded Hyperinsulinemic Hypoglycemic Clamp Technique in Female Mice. *Endocrinology,* 156**,** 3866-71.

MANSOUR, A., FOX, C. A., BURKE, S., MENG, F., THOMPSON, R. C., AKIL, H. & WATSON, S. J. 1994. Mu, delta, and kappa opioid receptor mRNA expression in the rat CNS: an in situ hybridization study. *J Comp Neurol,* 350**,** 412-38.

MARAN, A., CREPALDI, C., TRUPIANI, S., LUCCA, T., JORI, E., MACDONALD, I. A., TIENGO, A., AVOGARO, A. & DEL PRATO, S. 2000. Brain function rescue effect of lactate following hypoglycaemia is not an adaptation process in both normal and type I diabetic subjects. *Diabetologia,* 43**,** 733-41.

MARKAKIS, E. A. & SWANSON, L. W. 1997. Spatiotemporal patterns of secretomotor neuron generation in the parvicellular neuroendocrine system. *Brain Res Brain Res Rev,* 24**,** 255-91.

MARSTON, O. J., HURST, P., EVANS, M. L., BURDAKOV, D. I. & HEISLER, L. K. 2011. Neuropeptide Y cells represent a distinct glucose-sensing population in the lateral hypothalamus. *Endocrinology,* 152**,** 4046-52.

MARTY, N., DALLAPORTA, M., FORETZ, M., EMERY, M., TARUSSIO, D., BADY, I., BINNERT, C., BEERMANN, F. & THORENS, B. 2005. Regulation of glucagon secretion by glucose transporter type 2 (glut2) and astrocyte-dependent glucose sensors. *J Clin Invest,* 115**,** 3545-53.

MASON, G. F., PETERSEN, K. F., LEBON, V., ROTHMAN, D. L. & SHULMAN, G. I. 2006. Increased brain monocarboxylic acid transport and utilization in type 1 diabetes. *Diabetes,* 55**,** 929-34.

MATHERS, C. D. & LONCAR, D. 2006. Projections of global mortality and burden of disease from 2002 to 2030. *PLoS Med,* 3**,** e442.

MATSUDA, T. & CEPKO, C. L. 2007. Controlled expression of transgenes introduced by in vivo electroporation. *Proc Natl Acad Sci U S A,* 104**,** 1027-32.

MATVEYENKO, A. V. & DONOVAN, C. M. 2006. Metabolic sensors mediate hypoglycemic detection at the portal vein. *Diabetes,* 55**,** 1276-82.

MATYKA, K., EVANS, M., LOMAS, J., CRANSTON, I., MACDONALD, I. & AMIEL, S. A. 1997. Altered hierarchy of protective responses against severe hypoglycemia in normal aging in healthy men. *Diabetes Care,* 20**,** 135-41.

MAYER, J. 1955. Regulation of energy intake and the body weight: the glucostatic theory and the lipostatic hypothesis. *Ann N Y Acad Sci,* 63**,** 15-43.

MCAULEY, S. A., DE BOCK, M. I., SUNDARARAJAN, V., LEE, M. H., PALDUS, B., AMBLER, G. R., BACH, L. A., BURT, M. G., CAMERON, F. J., CLARKE, P. M., COHEN, N. D., COLMAN, P. G., DAVIS, E. A., FAIRCHILD, J. M., HENDRIECKX, C., HOLMES-WALKER, D. J., HORSBURGH, J. C., JENKINS, A. J., KAYE, J., KEECH, A. C., KING, B. R., KUMARESWARAN, K., MACISAAC, R. J., MCCALLUM, R. W., NICHOLAS, J. A., SIMS, C., SPEIGHT, J., STRANKS, S. N., TRAWLEY, S., WARD, G. M., VOGRIN, S., JONES, T. W. & O'NEAL, D. N. 2018. Effect of 6 months of hybrid closed-loop insulin delivery in adults with type 1 diabetes: a randomised controlled trial protocol. *BMJ Open,* 8**,** e020274.

MCCALL, J. G., AL-HASANI, R., SIUDA, E. R., HONG, D. Y., NORRIS, A. J., FORD, C. P. & BRUCHAS, M. R. 2015. CRH Engagement of the Locus Coeruleus Noradrenergic System Mediates Stress-Induced Anxiety. *Neuron,* 87**,** 605-20.

MCCLUNG, C. A., ULERY, P. G., PERROTTI, L. I., ZACHARIOU, V., BERTON, O. & NESTLER, E. J. 2004. DeltaFosB: a molecular switch for long-term adaptation in the brain. *Brain research. Molecular brain research,* 132**,** 146-54.

MCCRIMMON, R. 2009. Glucose sensing during hypoglycemia: lessons from the lab. *Diabetes care,* 32**,** 1357-63.

MCCRIMMON, R. J. 2011. The response to hypoglycemia: a role for the opioid system? *J Clin Endocrinol Metab,* 96**,** 3357-9.

MCCRIMMON, R. J., EVANS, M. L., FAN, X., MCNAY, E. C., CHAN, O., DING, Y., ZHU, W., GRAM, D. X. & SHERWIN, R. S. 2005. Activation of ATP-sensitive K+ channels in the ventromedial hypothalamus amplifies counterregulatory hormone responses to hypoglycemia in normal and recurrently hypoglycemic rats. *Diabetes,* 54**,** 3169-74.

MCCRIMMON, R. J., FAN, X., DING, Y., ZHU, W., JACOB, R. J. & SHERWIN, R. S. 2004. Potential role for AMP-activated protein kinase in hypoglycemia sensing in the ventromedial hypothalamus. *Diabetes,* 53**,** 1953-8.

MCCRIMMON, R. J., FRIER, B. M. & DEARY, I. J. 1999. Appraisal of mood and personality during hypoglycaemia in human subjects. *Physiol Behav,* 67**,** 27-33.

MCCRIMMON RJ, M. E., CHAN O, FAN X, CATHERINE YW, SHERWIN RS 2005. Role of CRH-2 receptor in the ventromedial hypothalamus in modulating

counterregulatory responses to hypoglycemia (Abstract). *Diabetes,* 54**,** A26.

MCCRIMMON, R. J., SONG, Z., CHENG, H., MCNAY, E. C., WEIKART-YECKEL, C., FAN, X., ROUTH, V. H. & SHERWIN, R. S. 2006. Corticotrophin-releasing factor receptors within the ventromedial hypothalamus regulate hypoglycemia-induced hormonal counterregulation. *The Journal of clinical investigation,* 116**,** 1723-30.

MCDOUGAL, D. H., HERMANN, G. E. & ROGERS, R. C. 2013. Astrocytes in the nucleus of the solitary tract are activated by low glucose or glucoprivation: evidence for glial involvement in glucose homeostasis. *Front Neurosci,* 7**,** 249.

MCGREGOR, V. P., BANARER, S. & CRYER, P. E. 2002. Elevated endogenous cortisol reduces autonomic neuroendocrine and symptom responses to subsequent hypoglycemia. *Am J Physiol Endocrinol Metab,* 282**,** E770-7.

MCLELLAN, M. A., ROSENTHAL, N. A. & PINTO, A. R. 2017. Cre-loxP-Mediated Recombination: General Principles and Experimental Considerations. *Curr Protoc Mouse Biol,* 7**,** 1-12.

MCNAY, E. C. & GOLD, P. E. 2001. Age-related differences in hippocampal extracellular fluid glucose concentration during behavioral testing and following systemic glucose administration. *J Gerontol A Biol Sci Med Sci,* 56**,** B66-71.

MECAWI, A. S., VILHENA-FRANCO, T., ARAUJO, I. G., REIS, L. C., ELIAS, L. L. & ANTUNES-RODRIGUES, J. 2011. Estradiol potentiates hypothalamic vasopressin and oxytocin neuron activation and hormonal secretion induced by hypovolemic shock. *Am J Physiol Regul Integr Comp Physiol,* 301**,** R905-15.

MELNICK, I., PRONCHUK, N., COWLEY, M. A., GROVE, K. L. & COLMERS, W. F. 2007. Developmental switch in neuropeptide Y and melanocortin effects in the paraventricular nucleus of the hypothalamus. *Neuron,* 56**,** 1103-15.

MELNICK, I. V., PRICE, C. J. & COLMERS, W. F. 2011. Glucosensing in parvocellular neurons of the rat hypothalamic paraventricular nucleus. *The European journal of neuroscience,* 34**,** 272-82.

MIMEE, A. & FERGUSON, A. V. 2015. Glycemic state regulates melanocortin, but not nesfatin-1, responsiveness of glucose-sensing neurons in the nucleus of the solitary tract. *Am J Physiol Regul Integr Comp Physiol,* 308**,** R690-9.

MIYAWAKI, A., LLOPIS, J., HEIM, R., MCCAFFERY, J. M., ADAMS, J. A., IKURA, M. & TSIEN, R. Y. 1997. Fluorescent indicators for Ca2+ based on green fluorescent proteins and calmodulin. *Nature,* 388**,** 882-7.

MOBBS, C. V., KOW, L. M. & YANG, X. J. 2001. Brain glucose-sensing mechanisms: ubiquitous silencing by aglycemia vs. hypothalamic neuroendocrine responses. *Am J Physiol Endocrinol Metab,* 281**,** E649-54.

MOHEET, A., KUMAR, A., EBERLY, L. E., KIM, J., ROBERTS, R. & SEAQUIST, E. R. 2014. Hypoglycemia-associated autonomic failure in healthy humans: comparison of two vs three periods of hypoglycemia on hypoglycemia-induced counterregulatory and symptom response 5 days later. *J Clin Endocrinol Metab,* 99**,** 664-70.

MOKAN, M., MITRAKOU, A., VENEMAN, T., RYAN, C., KORYTKOWSKI, M., CRYER, P. & GERICH, J. 1994. Hypoglycemia unawareness in IDDM. *Diabetes Care,* 17**,** 1397-403.

MORALES, J. & SCHNEIDER, D. 2014. Hypoglycemia. *Am J Med,* 127**,** S17-24.

MORRISON, C. D. & MUNZBERG, H. 2012. Capricious Cre: the devil is in the details. *Endocrinology,* 153**,** 1005-7.

MUECKLER, M. & THORENS, B. 2013. The SLC2 (GLUT) family of membrane transporters. *Mol Aspects Med,* 34**,** 121-38.

MUROYA, S., YADA, T., SHIODA, S. & TAKIGAWA, M. 1999. Glucose-sensitive neurons in the rat arcuate nucleus contain neuropeptide Y. *Neurosci Lett,* 264**,** 113-6.

MURPHY, B. A., FAKIRA, K. A., SONG, Z., BEUVE, A. & ROUTH, V. H. 2009a. AMP-activated protein kinase and nitric oxide regulate the glucose sensitivity of ventromedial hypothalamic glucose-inhibited neurons. *Am J Physiol Cell Physiol,* 297**,** C750-8.

MURPHY, B. A., FIORAMONTI, X., JOCHNOWITZ, N., FAKIRA, K., GAGEN, K., CONTIE, S., LORSIGNOL, A., PENICAUD, L., MARTIN, W. J. & ROUTH, V. H. 2009b. Fasting enhances the response of arcuate neuropeptide Y-glucose-inhibited neurons to decreased extracellular glucose. *Am J Physiol Cell Physiol,* 296**,** C746-56.

NAGAI, T., YAMADA, S., TOMINAGA, T., ICHIKAWA, M. & MIYAWAKI, A. 2004. Expanded dynamic range of fluorescent indicators for Ca(2+) by circularly permuted yellow fluorescent proteins. *Proc Natl Acad Sci U S A,* 101**,** 10554-9.

NAIK, S., BELFORT-DEAGUIAR, R., SEJLING, A. S., SZEPIETOWSKA, B. & SHERWIN, R. S. 2017. Evaluation of the counter-regulatory responses to hypoglycaemia in patients with type 1 diabetes during opiate receptor blockade with naltrexone. *Diabetes Obes Metab,* 19**,** 615-621.

NAKAO, K., NAKAI, Y., JINGAMI, H., OKI, S., FUKATA, J. & IMURA, H. 1979. Substantial rise of plasma beta-endorphin levels after insulin-induced hypoglycemia in human subjects. *J Clin Endocrinol Metab,* 49**,** 838-41.

NASSI, J. J., CEPKO, C. L., BORN, R. T. & BEIER, K. T. 2015. Neuroanatomy goes viral! *Front Neuroanat,* 9**,** 80.

NC3RS, N. C. F. T. R., REFINEMENT AND REDUCTION OF ANIMALS IN RESEARCH. 2018a. *Blood sampling mouse decision tree* [Online]. Available:

https://www.nc3rs.org.uk/mouse-decision-tree-blood-sampling [Accessed 10 July 2018].

NC3RS, N. C. F. T. R., REFINEMENT AND REDUCTION OF ANIMALS IN RESEARCH. 2018b. *Blood sampling rat decision tree* [Online]. Available: https://www.nc3rs.org.uk/rat-decision-tree-blood-sampling [Accessed 10 July 2018].

NEHER, E. 1995. The use of fura-2 for estimating Ca buffers and Ca fluxes. *Neuropharmacology,* 34**,** 1423-42.

NIIJIMA, A. 1989. Neural mechanisms in the control of blood glucose concentration. *J Nutr,* 119**,** 833-40.

NIIMI, M., SATO, M., TAMAKI, M., WADA, Y., TAKAHARA, J. & KAWANISHI, K. 1995. Induction of Fos protein in the rat hypothalamus elicited by insulin-induced hypoglycemia. *Neurosci Res,* 23**,** 361-4.

NURSE, C. A. 2005. Neurotransmission and neuromodulation in the chemosensory carotid body. *Auton Neurosci,* 120**,** 1-9.

O'MALLEY, D., REIMANN, F., SIMPSON, A. K. & GRIBBLE, F. M. 2006. Sodium-coupled glucose cotransporters contribute to hypothalamic glucose sensing. *Diabetes,* 55**,** 3381-6.

OH, S. W., HARRIS, J. A., NG, L., WINSLOW, B., CAIN, N., MIHALAS, S., WANG, Q., LAU, C., KUAN, L., HENRY, A. M., MORTRUD, M. T., OUELLETTE, B., NGUYEN, T. N., SORENSEN, S. A., SLAUGHTERBECK, C. R., WAKEMAN, W., LI, Y., FENG, D., HO, A., NICHOLAS, E., HIROKAWA, K. E., BOHN, P., JOINES, K. M., PENG, H., HAWRYLYCZ, M. J., PHILLIPS, J. W., HOHMANN, J. G., WOHNOUTKA, P., GERFEN, C. R., KOCH, C., BERNARD, A., DANG, C., JONES, A. R. & ZENG, H. 2014. A mesoscale connectome of the mouse brain. *Nature,* 508**,** 207-14.

OOMURA, Y., KIMURA, K., OOYAMA, H., MAENO, T., IKI, M. & KUNIYOSHI, M. 1964. Reciprocal Activities of the Ventromedial and Lateral Hypothalamic Areas of Cats. *Science,* 143**,** 484-5.

OOMURA, Y., ONO, T., OOYAMA, H. & WAYNER, M. J. 1969. Glucose and osmosensitive neurones of the rat hypothalamus. *Nature,* 222**,** 282-4.

OOMURA, Y., OOYAMA, H., SUGIMORI, M., NAKAMURA, T. & YAMADA, Y. 1974. Glucose inhibition of the glucose-sensitive neurone in the rat lateral hypothalamus. *Nature,* 247**,** 284-6.

ORBAN, B. O., ROUTH, V. H., LEVIN, B. E. & BERLIN, J. R. 2014. Direct effects of recurrent hypoglycaemia on adrenal catecholamine release. *Diab Vasc Dis Res*.

ORBAN, B. O., ROUTH, V. H., LEVIN, B. E. & BERLIN, J. R. 2015. Direct effects of recurrent hypoglycaemia on adrenal catecholamine release. *Diab Vasc Dis Res,* 12**,** 2-12.

OTGON-UUL, Z., SUYAMA, S., ONODERA, H. & YADA, T. 2016. Optogenetic activation of leptin- and glucose-regulated GABAergic neurons in dorsomedial hypothalamus promotes food intake via inhibitory synaptic transmission to paraventricular nucleus of hypothalamus. *Mol Metab,* 5**,** 709-15.

OTIS, J. M., NAMBOODIRI, V. M., MATAN, A. M., VOETS, E. S., MOHORN, E. P., KOSYK, O., MCHENRY, J. A., ROBINSON, J. E., RESENDEZ, S. L., ROSSI, M. A. & STUBER, G. D. 2017. Prefrontal cortex output circuits guide reward seeking through divergent cue encoding. *Nature,* 543**,** 103-107.

PADILLA, S. L., REEF, D. & ZELTSER, L. M. 2012. Defining POMC neurons using transgenic reagents: impact of transient Pomc expression in diverse immature neuronal populations. *Endocrinology,* 153**,** 1219-31.

PAGE, K. A., SEO, D., BELFORT-DEAGUIAR, R., LACADIE, C., DZUIRA, J., NAIK, S., AMARNATH, S., CONSTABLE, R. T., SHERWIN, R. S. & SINHA, R. 2011. Circulating glucose levels modulate neural control of desire for high-calorie foods in humans. *J Clin Invest,* 121**,** 4161-9.

PARANJAPE, S. A. & BRISKI, K. P. 2005. Recurrent insulin-induced hypoglycemia causes site-specific patterns of habituation or amplification of CNS neuronal genomic activation. *Neuroscience,* 130**,** 957-70.

PAREDES, R. M., ETZLER, J. C., WATTS, L. T., ZHENG, W. & LECHLEITER, J. D. 2008. Chemical calcium indicators. *Methods,* 46**,** 143-51.

PARTON, L. E., YE, C. P., COPPARI, R., ENRIORI, P. J., CHOI, B., ZHANG, C. Y., XU, C., VIANNA, C. R., BALTHASAR, N., LEE, C. E., ELMQUIST, J. K., COWLEY, M. A. & LOWELL, B. B. 2007. Glucose sensing by POMC neurons regulates glucose homeostasis and is impaired in obesity. *Nature,* 449**,** 228-32.

PATCHING, S. G. 2017. Glucose Transporters at the Blood-Brain Barrier: Function, Regulation and Gateways for Drug Delivery. *Mol Neurobiol,* 54**,** 1046-1077.

PATTERSON, C. C., DAHLQUIST, G. G., GYURUS, E., GREEN, A., SOLTESZ, G. & GROUP, E. S. 2009. Incidence trends for childhood type 1 diabetes in Europe during 1989-2003 and predicted new cases 2005-20: a multicentre prospective registration study. *Lancet,* 373**,** 2027-33.

PAULIINA MARKKULA, S., LYONS, D., YUEH, C. Y., RICHES, C., HURST, P., FIELDING, B., HEISLER, L. K. & EVANS, M. L. 2016. Intracerebroventricular Catalase Reduces Hepatic Insulin Sensitivity and Increases Responses to Hypoglycemia in Rats. *Endocrinology,* 157**,** 4669-4676.

PAULSON, J. C. & MCCLURE, W. O. 1975. Inhibition of axoplasmic transport by colchicine, podophyllotoxin, and vinblastine: an effect on microtubules. *Ann N Y Acad Sci,* 253**,** 517-27.

PEDERSEN-BJERGAARD, U., PRAMMING, S., HELLER, S. R., WALLACE, T. M., RASMUSSEN, A. K., JORGENSEN, H. V., MATTHEWS, D. R., HOUGAARD, P. & THORSTEINSSON, B. 2004. Severe hypoglycaemia in 1076 adult patients with type 1 diabetes: influence of risk markers and selection. *Diabetes Metab Res Rev,* 20**,** 479-86.

PELLERIN, L. & MAGISTRETTI, P. J. 1994. Glutamate uptake into astrocytes stimulates aerobic glycolysis: a mechanism coupling neuronal activity to glucose utilization. *Proc Natl Acad Sci U S A,* 91**,** 10625-9.

PELLERIN, L. & MAGISTRETTI, P. J. 2012. Sweet sixteen for ANLS. *J Cereb Blood Flow Metab,* 32**,** 1152-66.

PIERRE, K., PELLERIN, L., DEBERNARDI, R., RIEDERER, B. M. & MAGISTRETTI, P. J. 2000. Cell-specific localization of monocarboxylate transporters, MCT1 and MCT2, in the adult mouse brain revealed by double immunohistochemical labeling and confocal microscopy. *Neuroscience,* 100**,** 617-27.

POMRENZE, M. B., MILLAN, E. Z., HOPF, F. W., KEIFLIN, R., MAIYA, R., BLASIO, A., DADGAR, J., KHARAZIA, V., DE GUGLIELMO, G., CRAWFORD, E., JANAK, P. H., GEORGE, O., RICE, K. C. & MESSING, R. O. 2015. A Transgenic Rat for Investigating the Anatomy and Function of Corticotrophin Releasing Factor Circuits. *Front Neurosci,* 9**,** 487.

POPLAWSKI, M. M., MASTAITIS, J. W. & MOBBS, C. V. 2011. Naloxone, but not valsartan, preserves responses to hypoglycemia after antecedent hypoglycemia: role of metabolic reprogramming in counterregulatory failure. *Diabetes,* 60**,** 39-46.

RAJU, B., MCGREGOR, V. P. & CRYER, P. E. 2003. Cortisol elevations comparable to those that occur during hypoglycemia do not cause hypoglycemia-associated autonomic failure. *Diabetes,* 52**,** 2083-9.

RAMOT, A., JIANG, Z., TIAN, J. B., NAHUM, T., KUPERMAN, Y., JUSTICE, N. & CHEN, A. 2017. Hypothalamic CRFR1 is essential for HPA axis regulation following chronic stress. *Nat Neurosci,* 20**,** 385-388.

RATTARASARN, C., DAGOGO-JACK, S., ZACHWIEJA, J. J. & CRYER, P. E. 1994. Hypoglycemia-induced autonomic failure in IDDM is specific for stimulus of hypoglycemia and is not attributable to prior autonomic activation. *Diabetes,* 43**,** 809-18.

REN, X., ZHOU, L., TERWILLIGER, R., NEWTON, S. S. & DE ARAUJO, I. E. 2009. Sweet taste signaling functions as a hypothalamic glucose sensor. *Front Integr Neurosci,* 3**,** 12.

RHO, J. H. & SWANSON, L. W. 1989. A morphometric analysis of functionally defined subpopulations of neurons in the paraventricular nucleus of the rat with observations on the effects of colchicine. *The Journal of neuroscience : the official journal of the Society for Neuroscience,* 9**,** 1375-88.

RITTER, S., BUGARITH, K. & DINH, T. T. 2001. Immunotoxic destruction of distinct catecholamine subgroups produces selective impairment of glucoregulatory responses and neuronal activation. *J Comp Neurol,* 432**,** 197-216.

RITTER, S., DINH, T. T. & ZHANG, Y. 2000. Localization of hindbrain glucoreceptive sites controlling food intake and blood glucose. *Brain Res,* 856**,** 37-47.

RIVIER, C. 2001. Relative importance of nitric oxide and carbon monoxide in regulating the ACTH response to immune and non-immune signals. *Stress,* 4**,** 13-24.

RIVIER, C. 2002. Role of nitric oxide and carbon monoxide in modulating the activity of the rodent hypothalamic-pituitary-adrenal axis. *Front Horm Res,* 29**,** 15-49.

ROBINSON, R. T., HARRIS, N. D., IRELAND, R. H., LEE, S., NEWMAN, C. & HELLER, S. R. 2003. Mechanisms of abnormal cardiac repolarization during insulin-induced hypoglycemia. *Diabetes,* 52**,** 1469-74.

ROLAND, A. V. & MOENTER, S. M. 2011. Glucosensing by GnRH neurons: inhibition by androgens and involvement of AMP-activated protein kinase. *Mol Endocrinol,* 25**,** 847-58.

ROLAND, B. L. & SAWCHENKO, P. E. 1993. Local origins of some GABAergic projections to the paraventricular and supraoptic nuclei of the hypothalamus in the rat. *J Comp Neurol,* 332**,** 123-43.

ROUTH, V. H. 2002. Glucose-sensing neurons: are they physiologically relevant? *Physiol Behav,* 76**,** 403-13.

ROUTH, V. H. 2003. Glucosensing neurons in the ventromedial hypothalamic nucleus (VMN) and hypoglycemia-associated autonomic failure (HAAF). *Diabetes/metabolism research and reviews,* 19**,** 348-56.

SABERI, M., BOHLAND, M. & DONOVAN, C. M. 2008. The locus for hypoglycemic detection shifts with the rate of fall in glycemia: the role of portal-superior mesenteric vein glucose sensing. *Diabetes,* 57**,** 1380-6.

SAKURAI, T., AMEMIYA, A., ISHII, M., MATSUZAKI, I., CHEMELLI, R. M., TANAKA, H., WILLIAMS, S. C., RICHARSON, J. A., KOZLOWSKI, G. P., WILSON, S., ARCH, J. R., BUCKINGHAM, R. E., HAYNES, A. C., CARR, S. A., ANNAN, R. S., MCNULTY, D. E., LIU, W. S., TERRETT, J. A., ELSHOURBAGY, N. A., BERGSMA, D. J. & YANAGISAWA, M. 1998. Orexins and orexin receptors: a family of hypothalamic neuropeptides

and G protein-coupled receptors that regulate feeding behavior. *Cell,* 92**,** 1 page following 696.

SAMSON, W. K., TAYLOR, M. M., FOLLWELL, M. & FERGUSON, A. V. 2002. Orexin actions in hypothalamic paraventricular nucleus: physiological consequences and cellular correlates. *Regul Pept,* 104**,** 97-103.

SANDERS, N. M., FIGLEWICZ, D. P., TABORSKY, G. J., JR., WILKINSON, C. W., DAUMEN, W. & LEVIN, B. E. 2006. Feeding and neuroendocrine responses after recurrent insulin-induced hypoglycemia. *Physiol Behav,* 87**,** 700-6.

SANDERS, N. M. & RITTER, S. 2000. Repeated 2-deoxy-D-glucose-induced glucoprivation attenuates Fos expression and glucoregulatory responses during subsequent glucoprivation. *Diabetes,* 49**,** 1865-74.

SANTIAGO, A. M., CLEGG, D. J. & ROUTH, V. H. 2016. Ventromedial hypothalamic glucose sensing and glucose homeostasis vary throughout the estrous cycle. *Physiol Behav,* 167**,** 248-254.

SAPER, C. B., LOEWY, A. D., SWANSON, L. W. & COWAN, W. M. 1976. Direct hypothalamo-autonomic connections. *Brain Res,* 117**,** 305-12.

SAWCHENKO, P. E. 1987a. Evidence for differential regulation of corticotropin-releasing factor and vasopressin immunoreactivities in parvocellular neurosecretory and autonomic-related projections of the paraventricular nucleus. *Brain Res,* 437**,** 253-63.

SAWCHENKO, P. E. 1987b. Evidence for differential regulation of corticotropin-releasing factor and vasopressin immunoreactivities in parvocellular neurosecretory and autonomic-related projections of the paraventricular nucleus. *Brain research,* 437**,** 253-63.

SAWCHENKO, P. E. & SWANSON, L. W. 1982. Immunohistochemical identification of neurons in the paraventricular nucleus of the hypothalamus that project to the medulla or to the spinal cord in the rat. *The Journal of comparative neurology,* 205**,** 260-72.

SAWCHENKO, P. E. & SWANSON, L. W. 1983. The organization of forebrain afferents to the paraventricular and supraoptic nuclei of the rat. *J Comp Neurol,* 218**,** 121-44.

SAWCHENKO, P. E. & SWANSON, L. W. 1985. Localization, colocalization, and plasticity of corticotropin-releasing factor immunoreactivity in rat brain. *Fed Proc,* 44**,** 221-7.

SAWCHENKO, P. E., SWANSON, L. W., STEINBUSCH, H. W. & VERHOFSTAD, A. A. 1983. The distribution and cells of origin of serotonergic inputs to the paraventricular and supraoptic nuclei of the rat. *Brain Res,* 277**,** 355-60.

SAWCHENKO, P. E., SWANSON, L. W. & VALE, W. W. 1984a. Co-expression of corticotropin-releasing factor and vasopressin immunoreactivity in parvocellular neurosecretory neurons of the adrenalectomized rat. *Proc Natl Acad Sci U S A,* 81**,** 1883-7.

SAWCHENKO, P. E., SWANSON, L. W. & VALE, W. W. 1984b. Corticotropin-releasing factor: co-expression within distinct subsets of oxytocin-, vasopressin-, and neurotensin-immunoreactive neurons in the hypothalamus of the male rat. *J Neurosci,* 4**,** 1118-29.

SCHADT, J. C. & LUDBROOK, J. 1991. Hemodynamic and neurohumoral responses to acute hypovolemia in conscious mammals. *Am J Physiol,* 260**,** H305-18.

SCHINDELIN, J., ARGANDA-CARRERAS, I., FRISE, E., KAYNIG, V., LONGAIR, M., PIETZSCH, T., PREIBISCH, S., RUEDEN, C., SAALFELD, S., SCHMID, B., TINEVEZ, J. Y., WHITE,

D. J., HARTENSTEIN, V., ELICEIRI, K., TOMANCAK, P. & CARDONA, A. 2012. Fiji: an open-source platform for biological-image analysis. *Nat Methods,* 9**,** 676-82.

SCHMIDT-SUPPRIAN, M. & RAJEWSKY, K. 2007. Vagaries of conditional gene targeting. *Nat Immunol,* 8**,** 665-8.

SCHNEIDER, C. A., RASBAND, W. S. & ELICEIRI, K. W. 2012. NIH Image to ImageJ: 25 years of image analysis. *Nat Methods,* 9**,** 671-5.

SCIOLINO, N. R., PLUMMER, N. W., CHEN, Y. W., ALEXANDER, G. M., ROBERTSON, S. D., DUDEK, S. M., MCELLIGOTT, Z. A. & JENSEN, P. 2016. Recombinase-Dependent Mouse Lines for Chemogenetic Activation of Genetically Defined Cell Types. *Cell Rep,* 15**,** 2563-73.

SEDBAZAR, U., AYUSH, E. A., MAEJIMA, Y. & YADA, T. 2014. Neuropeptide Y and alpha-melanocyte-stimulating hormone reciprocally regulate nesfatin-1 neurons in the paraventricular nucleus of the hypothalamus. *Neuroreport,* 25**,** 1453-8.

SEGEL, S. A., FANELLI, C. G., DENCE, C. S., MARKHAM, J., VIDEEN, T. O., PARAMORE, D. S., POWERS, W. J. & CRYER, P. E. 2001. Blood-to-brain glucose transport, cerebral glucose metabolism, and cerebral blood flow are not increased after hypoglycemia. *Diabetes,* 50**,** 1911-7.

SENTHILKUMARAN, M., ZHOU, X. F. & BOBROVSKAYA, L. 2016. Challenges in Modelling Hypoglycaemia-Associated Autonomic Failure: A Review of Human and Animal Studies. *Int J Endocrinol,* 2016**,** 9801640.

SERVICE, F. J. 1995. Hypoglycemia. *Med Clin North Am,* 79**,** 1-8.

SERVICE, F. J., MCMAHON, M. M., O'BRIEN, P. C. & BALLARD, D. J. 1991. Functioning insulinoma--incidence, recurrence, and long-term survival of patients: a 60-year study. *Mayo Clin Proc,* 66**,** 711-9.

SHIMIZU, N., OOMURA, Y., NOVIN, D., GRIJALVA, C. V. & COOPER, P. H. 1983. Functional correlations between lateral hypothalamic glucose-sensitive neurons and hepatic portal glucose-sensitive units in rat. *Brain Res,* 265**,** 49-54.

SHIRAISHI, T., OOMURA, Y., SASAKI, K. & WAYNER, M. J. 2000. Effects of leptin and orexin-A on food intake and feeding related hypothalamic neurons. *Physiol Behav,* 71**,** 251-61.

SILVER, I. A. & ERECINSKA, M. 1994a. Extracellular glucose concentration in mammalian brain: continuous monitoring of changes during increased neuronal activity and upon limitation in oxygen supply in normo-, hypo-, and hyperglycemic animals. *J Neurosci,* 14**,** 5068-76.

SILVER, I. A. & ERECINSKA, M. 1994b. Extracellular glucose concentration in mammalian brain: continuous monitoring of changes during increased neuronal activity and upon limitation in oxygen supply in normo-, hypo-, and hyperglycemic animals. *The Journal of neuroscience : the official journal of the Society for Neuroscience,* 14**,** 5068-76.

SIMMONS, D. M. & SWANSON, L. W. 2009. Comparison of the spatial distribution of seven types of neuroendocrine neurons in the rat paraventricular nucleus: toward a global 3D model. *The Journal of comparative neurology,* 516**,** 423-41.

SIMPSON, I. A., VANNUCCI, S. J. & MAHER, F. 1994. Glucose transporters in mammalian brain. *Biochem Soc Trans,* 22**,** 671-5.

SONG, Z., LEVIN, B. E., MCARDLE, J. J., BAKHOS, N. & ROUTH, V. H. 2001. Convergence of pre- and postsynaptic influences on glucosensing neurons in the ventromedial hypothalamic nucleus. *Diabetes,* 50**,** 2673-81.

SONG, Z. & ROUTH, V. H. 2006. Recurrent hypoglycemia reduces the glucose sensitivity of glucose-inhibited neurons in the ventromedial hypothalamus nucleus.

American journal of physiology. Regulatory, integrative and comparative physiology, 291**,** R1283-7.

STANLEY, S., DOMINGOS, A. I., KELLY, L., GARFIELD, A., DAMANPOUR, S., HEISLER, L. & FRIEDMAN, J. 2013. Profiling of Glucose-Sensing Neurons Reveals that GHRH Neurons Are Activated by Hypoglycemia. *Cell Metab,* 18**,** 596-607.

STANLEY, S., PINTO, S., SEGAL, J., PEREZ, C. A., VIALE, A., DEFALCO, J., CAI, X., HEISLER, L. K. & FRIEDMAN, J. M. 2010. Identification of neuronal subpopulations that project from hypothalamus to both liver and adipose tissue polysynaptically. *Proc Natl Acad Sci U S A,* 107**,** 7024-9.

STEINBUSCH, L., LABOUEBE, G. & THORENS, B. 2015. Brain glucose sensing in homeostatic and hedonic regulation. *Trends Endocrinol Metab,* 26**,** 455-66.

STEINMETZ, N. A., BUETFERING, C., LECOQ, J., LEE, C. R., PETERS, A. J., JACOBS, E. A. K., COEN, P., OLLERENSHAW, D. R., VALLEY, M. T., DE VRIES, S. E. J., GARRETT, M., ZHUANG, J., GROBLEWSKI, P. A., MANAVI, S., MILES, J., WHITE, C., LEE, E., GRIFFIN, F., LARKIN, J. D., ROLL, K., CROSS, S., NGUYEN, T. V., LARSEN, R., PENDERGRAFT, J., DAIGLE, T., TASIC, B., THOMPSON, C. L., WATERS, J., OLSEN, S., MARGOLIS, D. J., ZENG, H., HAUSSER, M., CARANDINI, M. & HARRIS, K. D. 2017. Aberrant Cortical Activity in Multiple GCaMP6-Expressing Transgenic Mouse Lines. *eNeuro,* 4.

STERN, J. E. 2015. Neuroendocrine-autonomic integration in the paraventricular nucleus: novel roles for dendritically released neuropeptides. *J Neuroendocrinol,* 27**,** 487-97.

STERNSON, S. M. & ROTH, B. L. 2014. Chemogenetic tools to interrogate brain functions. *Annu Rev Neurosci,* 37**,** 387-407.

SUDA, T., SATO, Y., SUMITOMO, T., NAKANO, Y., TOZAWA, F., IWAI, I., YAMADA, M. & DEMURA, H. 1992. Beta-endorphin inhibits hypoglycemia-induced gene expression of corticotropin-releasing factor in the rat hypothalamus. *Endocrinology,* 130**,** 1325-30.

SUH, S. W., BERGHER, J. P., ANDERSON, C. M., TREADWAY, J. L., FOSGERAU, K. & SWANSON, R. A. 2007. Astrocyte glycogen sustains neuronal activity during hypoglycemia: studies with the glycogen phosphorylase inhibitor CP-316,819 ([R-R*,S*]-5-chloro-N-[2-hydroxy-3-(methoxymethylamino)-3-oxo-1-(phenylmethyl)pro pyl]-1H-indole-2-carboxamide). *J Pharmacol Exp Ther,* 321**,** 45-50.

SUTTON, A. K., PEI, H., BURNETT, K. H., MYERS, M. G., JR., RHODES, C. J. & OLSON, D. P. 2014. Control of food intake and energy expenditure by Nos1 neurons of the paraventricular hypothalamus. *J Neurosci,* 34**,** 15306-18.

SVOBODA, K. & YASUDA, R. 2006. Principles of two-photon excitation microscopy and its applications to neuroscience. *Neuron,* 50**,** 823-39.

SWANSON, L. W., SAWCHENKO, P. E. & LIND, R. W. 1986. Regulation of multiple peptides in CRF parvocellular neurosecretory neurons: implications for the stress response. *Progress in brain research,* 68**,** 169-90.

SWANSON, L. W., SAWCHENKO, P. E., LIND, R. W. & RHO, J. H. 1987. The CRH motoneuron: differential peptide regulation in neurons with possible synaptic, paracrine, and endocrine outputs. *Annals of the New York Academy of Sciences,* 512**,** 12-23.

SWANSON, L. W., SAWCHENKO, P. E., RIVIER, J. & VALE, W. W. 1983. Organization of ovine corticotropin-releasing factor immunoreactive cells and fibers in the rat brain: an immunohistochemical study. *Neuroendocrinology,* 36**,** 165-86.

TAMAKI, M., SATO, M., NIIMI, M. & TAKAHARA, J. 1995. Resistance of growth hormone secretion to hypoglycemia in the mouse. *J Neuroendocrinol,* 7**,** 371-6.

TANIGUCHI, H., HE, M., WU, P., KIM, S., PAIK, R., SUGINO, K., KVITSIANI, D., FU, Y., LU, J., LIN, Y., MIYOSHI, G., SHIMA, Y., FISHELL, G., NELSON, S. B. & HUANG, Z. J. 2011. A resource of Cre driver lines for genetic targeting of GABAergic neurons in cerebral cortex. *Neuron,* 71**,** 995-1013.

TASKER, J. G. & DUDEK, F. E. 1991. Electrophysiological properties of neurones in the region of the paraventricular nucleus in slices of rat hypothalamus. *J Physiol,* 434**,** 271-93.

TATTERSALL, R. B. & GILL, G. V. 1991. Unexplained deaths of type 1 diabetic patients. *Diabet Med,* 8**,** 49-58.

TESSON, L., USAL, C., MENORET, S., LEUNG, E., NILES, B. J., REMY, S., SANTIAGO, Y., VINCENT, A. I., MENG, X., ZHANG, L., GREGORY, P. D., ANEGON, I. & COST, G. J. 2011. Knockout rats generated by embryo microinjection of TALENs. *Nat Biotechnol,* 29**,** 695-6.

THABIT, H., LUBINA-SOLOMON, A., STADLER, M., LEELARATHNA, L., WALKINSHAW, E., PERNET, A., ALLEN, J. M., IQBAL, A., CHOUDHARY, P., KUMARESWARAN, K., NODALE, M., NISBET, C., WILINSKA, M. E., BARNARD, K. D., DUNGER, D. B., HELLER, S. R., AMIEL, S. A., EVANS, M. L. & HOVORKA, R. 2014. Home use of closed-loop insulin delivery for overnight glucose control in adults with type 1 diabetes: a 4-week, multicentre, randomised crossover study. *Lancet Diabetes Endocrinol,* 2**,** 701-9.

TIBALDI, J. M. 2012. Evolution of insulin development: focus on key parameters. *Advances in therapy,* 29**,** 590-619.

TIEDEMANN, L. J., SCHMID, S. M., HETTEL, J., GIESEN, K., FRANCKE, P., BUCHEL, C. & BRASSEN, S. 2017. Central insulin modulates food valuation via mesolimbic pathways. *Nat Commun,* 8**,** 16052.

TKACS, N. C., PAN, Y., RAGHUPATHI, R., DUNN-MEYNELL, A. A. & LEVIN, B. E. 2005. Cortical Fluoro-Jade staining and blunted adrenomedullary response to hypoglycemia after noncoma hypoglycemia in rats. *J Cereb Blood Flow Metab,* 25**,** 1645-55.

TKACS, N. C. & THOMPSON, H. J. 2006. From bedside to bench and back again: research issues in animal models of human disease. *Biological research for nursing,* 8**,** 78-88.

TODA, C., KIM, J. D., IMPELLIZZERI, D., CUZZOCREA, S., LIU, Z. W. & DIANO, S. 2016. UCP2 Regulates Mitochondrial Fission and Ventromedial Nucleus Control of Glucose Responsiveness. *Cell,* 164**,** 872-83.

TONON, M. C., LANFRAY, D., CASTEL, H., VAUDRY, H. & MORIN, F. 2013. Hypothalamic glucose-sensing: role of Glia-to-neuron signaling. *Horm Metab Res,* 45**,** 955-9.

TOWLER, D. A., HAVLIN, C. E., CRAFT, S. & CRYER, P. 1993. Mechanism of awareness of hypoglycemia. Perception of neurogenic (predominantly cholinergic) rather than neuroglycopenic symptoms. *Diabetes,* 42**,** 1791-8.

TSAI, V. W., MANANDHAR, R., JORGENSEN, S. B., LEE-NG, K. K., ZHANG, H. P., MARQUIS, C. P., JIANG, L., HUSAINI, Y., LIN, S., SAINSBURY, A., SAWCHENKO, P. E., BROWN, D. A. & BREIT, S. N. 2014. The anorectic actions of the TGFbeta cytokine MIC-1/GDF15 require an intact brainstem area postrema and nucleus of the solitary tract. *PLoS One,* 9**,** e100370.

TSENG, Q., DUCHEMIN-PELLETIER, E., DESHIERE, A., BALLAND, M., GUILLOU, H., FILHOL, O. & THERY, M. 2012. Spatial organization of the extracellular matrix regulates cell-cell junction positioning. *Proc Natl Acad Sci U S A,* 109**,** 1506-11.

TSIEN, R. Y. 1980. New calcium indicators and buffers with high selectivity against magnesium and protons: design, synthesis, and properties of prototype structures. *Biochemistry,* 19**,** 2396-404.

U.K.HYPOGLYCAEMIASTUDYGROUP 2007. Risk of hypoglycaemia in types 1 and 2 diabetes: effects of treatment modalities and their duration. *Diabetologia,* 50**,** 1140-7.

VALE, W., SPIESS, J., RIVIER, C. & RIVIER, J. 1981. Characterization of a 41-residue ovine hypothalamic peptide that stimulates secretion of corticotropin and beta-endorphin. *Science,* 213**,** 1394-7.

VAN DEN POL, A. N. 1982. The magnocellular and parvocellular paraventricular nucleus of rat: intrinsic organization. *J Comp Neurol,* 206**,** 317-45.

VAN DEN TOP, M., ZHAO, F. Y., VIRIYAPONG, R., MICHAEL, N. J., MUNDER, A. C., PRYOR, J. T., RENAUD, L. P. & SPANSWICK, D. 2017. The impact of ageing, fasting and high-fat diet on central and peripheral glucose tolerance and glucose-sensing neural networks in the arcuate nucleus. *J Neuroendocrinol,* 29.

VAZIRANI, R. P., FIORAMONTI, X. & ROUTH, V. H. 2013. Membrane potential dye imaging of ventromedial hypothalamus neurons from adult mice to study glucose sensing. *J Vis Exp*.

VELE, S., MILMAN, S., SHAMOON, H. & GABRIELY, I. 2011. Opioid receptor blockade improves hypoglycemia-associated autonomic failure in type 1 diabetes mellitus. *J Clin Endocrinol Metab,* 96**,** 3424-31.

VENEMAN, T., MITRAKOU, A., MOKAN, M., CRYER, P. & GERICH, J. 1994. Effect of hyperketonemia and hyperlacticacidemia on symptoms, cognitive dysfunction, and counterregulatory hormone responses during hypoglycemia in normal humans. *Diabetes,* 43**,** 1311-7.

WALKER, J. N., RAMRACHEYA, R., ZHANG, Q., JOHNSON, P. R., BRAUN, M. & RORSMAN, P. 2011. Regulation of glucagon secretion by glucose: paracrine, intrinsic or both? *Diabetes Obes Metab,* 13 Suppl 1**,** 95-105.

WAMSTEEKER CUSULIN, J. I., FUZESI, T., WATTS, A. G. & BAINS, J. S. 2013. Characterization of Corticotropin-Releasing Hormone neurons in the Paraventricular Nucleus of the Hypothalamus of Crh-IRES-Cre Mutant Mice. *PloS one,* 8**,** e64943.

WANG, F., FLANAGAN, J., SU, N., WANG, L. C., BUI, S., NIELSON, A., WU, X., VO, H. T., MA, X. J. & LUO, Y. 2012. RNAscope: a novel in situ RNA analysis platform for formalin-fixed, paraffin-embedded tissues. *J Mol Diagn,* 14**,** 22-9.

WANG, R., LIU, X., HENTGES, S. T., DUNN-MEYNELL, A. A., LEVIN, B. E., WANG, W. & ROUTH, V. H. 2004. The regulation of glucose-excited neurons in the hypothalamic arcuate nucleus by glucose and feeding-relevant peptides. *Diabetes,* 53**,** 1959-65.

WANG, Y., KRUSHEL, L. A. & EDELMAN, G. M. 1996. Targeted DNA recombination in vivo using an adenovirus carrying the cre recombinase gene. *Proc Natl Acad Sci U S A,* 93**,** 3932-6.

WARREN, R. E. & FRIER, B. M. 2005. Hypoglycaemia and cognitive function. *Diabetes Obes Metab,* 7**,** 493-503.

WASSERMAN, D. H. 2009. Four grams of glucose. *Am J Physiol Endocrinol Metab,* 296**,** E11-21.

WATKINS, N. D., CORK, S. C. & PYNER, S. 2009. An immunohistochemical investigation of the relationship between neuronal nitric oxide synthase, GABA and presympathetic paraventricular neurons in the hypothalamus. *Neuroscience,* 159**,** 1079-88.

WATTS, A. G. & DONOVAN, C. M. 2010. Sweet talk in the brain: glucosensing, neural networks, and hypoglycemic counterregulation. *Front Neuroendocrinol,* 31**,** 32-43.

WATTS, A. G., TANIMURA, S. & SANCHEZ-WATTS, G. 2004. Corticotropin-releasing hormone and arginine vasopressin gene transcription in the hypothalamic paraventricular nucleus of unstressed rats: daily rhythms and their interactions with corticosterone. *Endocrinology,* 145**,** 529-40.

WEBER, T., SCHONIG, K., TEWS, B. & BARTSCH, D. 2011. Inducible gene manipulations in brain serotonergic neurons of transgenic rats. *PLoS One,* 6**,** e28283.

WEIGHTMAN POTTER, P. G., VLACHAKI WALKER, J. M., ROBB, J. L., CHILTON, J. K., WILLIAMSON, R., RANDALL, A. D., ELLACOTT, K. & BEALL, C. 2018. Human primary astrocytes increase basal fatty acid oxidation following recurrent low glucose to maintain intracellular nucleotide levels. *bioRxiv*.

WENG, D. Y., ZHANG, Y., HAYASHI, Y., KUAN, C. Y., LIU, C. Y., BABCOCK, G., WENG, W. L., SCHWEMBERGER, S. & KAO, W. W. 2008. Promiscuous recombination of LoxP alleles during gametogenesis in cornea Cre driver mice. *Mol Vis,* 14**,** 562-71.

WICK, A. N., DRURY, D. R., NAKADA, H. I. & WOLFE, J. B. 1957. Localization of the primary metabolic block produced by 2-deoxyglucose. *J Biol Chem,* 224**,** 963-9.

WIEGERS, E. C., ROOIJACKERS, H. M., TACK, C. J., GROENEWOUD, H., HEERSCHAP, A., DE GALAN, B. E. & VAN DER GRAAF, M. 2017. Effect of Exercise-Induced Lactate Elevation on Brain Lactate Levels During Hypoglycemia in Patients With Type 1 Diabetes and Impaired Awareness of Hypoglycemia. *Diabetes,* 66**,** 3105-3110.

WILD, D., VON MALTZAHN, R., BROHAN, E., CHRISTENSEN, T., CLAUSON, P. & GONDER-FREDERICK, L. 2007. A critical review of the literature on fear of hypoglycemia in diabetes: Implications for diabetes management and patient education. *Patient Educ Couns,* 68**,** 10-5.

WITTEN, I. B., STEINBERG, E. E., LEE, S. Y., DAVIDSON, T. J., ZALOCUSKY, K. A., BRODSKY, M., YIZHAR, O., CHO, S. L., GONG, S., RAMAKRISHNAN, C., STUBER, G. D., TYE, K. M., JANAK, P. H. & DEISSEROTH, K. 2011. Recombinase-driver rat lines: tools, techniques, and optogenetic application to dopamine-mediated reinforcement. *Neuron,* 72**,** 721-33.

YE, L., HAROON, M. A., SALINAS, A. & PAUKERT, M. 2017. Comparison of GCaMP3 and GCaMP6f for studying astrocyte Ca2+ dynamics in the awake mouse brain. *PLoS One,* 12**,** e0181113.

ZAMMITT, N. N., WARREN, R. E., DEARY, I. J. & FRIER, B. M. 2008. Delayed recovery of cognitive function following hypoglycemia in adults with type 1 diabetes: effect of impaired awareness of hypoglycemia. *Diabetes,* 57**,** 732-6.

ZHANG, C., PFAFF, D. W. & KOW, L. M. 1996. Functional analysis of opioid receptor subtypes in the ventromedial hypothalamic nucleus of the rat. *Eur J Pharmacol,* 308**,** 153-9.

ZHAO, Z., WANG, L., GAO, W., HU, F., ZHANG, J., REN, Y., LIN, R., FENG, Q., CHENG, M., JU, D., CHI, Q., WANG, D., SONG, S., LUO, M. & ZHAN, C. 2017. A Central Catecholaminergic Circuit Controls Blood Glucose Levels during Stress. *Neuron,* 95**,** 138-152 e5.

ZHENG, S. X., BOSCH, M. A. & RONNEKLEIV, O. K. 2005. mu-opioid receptor mRNA expression in identified hypothalamic neurons. *J Comp Neurol,* 487**,** 332-44.
ZHOU, C., TEEGALA, S. B., KHAN, B. A., GONZALEZ, C. & ROUTH, V. H. 2018. Hypoglycemia: Role of Hypothalamic Glucose-Inhibited (GI) Neurons in Detection and Correction. *Front Physiol,* 9**,** 192.